THE
PHYSICAL REVIEW
A Journal of Experimental and Theoretical Physics Established by E. L. Nichols in 1893
VOL. 51, NO. 10 MAY 15, 1937 SECOND SERIES

Inelastic Collision of Deuteron and Deuteron*

L. I. SCHIFF
Massachusetts Institute of Technology, Cambridge, Massachusetts
(Received February 13, 1937)

Certain symmetry properties of the two deuteron-deuteron reactions are developed in a rigorous manner, and are shown to require a distribution of the reaction products for moderate incident deuteron energies of the form $A(1+B\cos^2\theta)$ in the coordinate system in which the center of mass is at rest. This is shown to be in qualitative agreement with recent experimental data. The quantities A and B are evaluated approximately using a modification of Born's method and neglecting polarization of the deuterons; the quantitative discrepancies between theory and experiment are discussed. The theoretical relative yield from a "thick" deuterium target agrees well with the results of several experimenters; this quantity is influenced mainly by the Gamow factor, and is relatively independent of the details of the theory. The theoretical absolute yield is too large to agree with experiment.

INTRODUCTION

THE calculation of the transmutation function and angular distribution of the products of the reactions

$$H^2+H^2\rightarrow He^3+n, \quad (A)$$

$$H^2+H^2\rightarrow H^3+p \quad (B)$$

is of interest because of the recent experimental work[1] available for comparison with the predictions of the theory. The computations in this paper will be carried through using a potential between all pairs of particles of the form[2, 3]

$$V(r)=J(r)[(1-g)P^M+gP^H]$$
$$=J(r)P^M[1-\tfrac{1}{2}g+2g\boldsymbol{\sigma}_1\cdot\boldsymbol{\sigma}_2], \quad (1)$$

$$J(r)=De^{-4r/r_0}-2De^{-2r/r_0}, \quad (2)$$

in addition to the Coulomb repulsion between protons. We shall write all quantities in nuclear units of energy (506,000 ev) and of length (8.97×10^{-13} cm). A suitable value for r_0 which gives good agreement with experiment in computing a number of nuclear quantities[4, 5] is 0.3 (2.7×10^{-13} cm). Together with the value 4.35 (2.2 Mev) for the binding energy of the deuteron,[6] this fixes D at 71.2. Assuming that there is no bound singlet state of the deuteron, the elastic cross section 15 (12×10^{-24} cm^2) of protons for thermal neutrons[7] fixes the depth of the singlet unlike particle interaction at 28.9; so that $g=0.3$.

SYMMETRY PROPERTIES

In this section we shall present in a rigorous manner certain symmetry properties of the

* Preliminary report presented at the Cambridge meeting of the New England section of the American Physical Society, February 6, 1937.
[1] Kempton, Browne and Maasdorp, Proc. Roy. Soc. **A157**, 386 (1936); referred to here as KBM.
[2] Morse, Fisk and Schiff, Phys. Rev. **50**, 748 (1936).
[3] Breit and Feenberg, Phys. Rev. **50**, 850 (1936).
[4] Fisk, Schiff and Shockley, Phys. Rev. **50**, 1090 and 1191 (1936).
[5] Breit, Condon and Present, Phys. Rev. **50**, 825 (1936); Fisk and Morse, Phys. Rev. **51**, 54 (1937); Morse, Fisk and Schiff, Phys. Rev. **51**, 706 (1937).
[6] Feenberg and Share, Phys. Rev. **50**, 253 (1936).
[7] Amaldi and Fermi, Phys. Rev. **50**, 899 (1936).

problem that are important in predicting the angular distribution of the products. All equations refer to the coordinate system in which the center of mass is at rest (rest coordinate system).

Since the interactions are of the spin-dependent type, the initial state of reactions (A) and (B) describing two deuterons far apart must be an eigenstate of the operator $\boldsymbol{\mu}_1\cdot\boldsymbol{\mu}_2$ in order to remove degeneracy. Here $\boldsymbol{\mu}_1=\boldsymbol{\sigma}_1+\boldsymbol{\sigma}_2$, $\boldsymbol{\mu}_2=\boldsymbol{\sigma}_3+\boldsymbol{\sigma}_4$, where $\boldsymbol{\sigma}_1$ and $\boldsymbol{\sigma}_2$ are the spin operators of the two particles of deuteron 1, and $\boldsymbol{\sigma}_3$ and $\boldsymbol{\sigma}_4$ are the spin operators of the two particles of deuteron 2; particles 1 and 3, and particles 2 and 4, are alike. Since the deuterons are normally in triplet states, the spin parts of the eigenfunctions of $\boldsymbol{\mu}_1\cdot\boldsymbol{\mu}_2$ divide into singlet, triplet and quintet states which we denote by S_s, S_t and S_q, respectively. We shall mean by $(+--+)$ for example, that spin state in which the components of the spins of particles 1 and 4 have eigenvalues $+\frac{1}{2}$ along some arbitrary axis, and those of particles 2 and 3 have eigenvalues $-\frac{1}{2}$ along the same axis. Then

$$\begin{aligned}
S_s&=(1/\sqrt{3})[(++--)-\tfrac{1}{2}(+-+-)\\
&\quad-\tfrac{1}{2}(+--+)-\tfrac{1}{2}(-++-)\\
&\quad-\tfrac{1}{2}(-+-+)+(--++)],\\
S_t^1&=\tfrac{1}{2}[(+++-)+(++-+)\\
&\quad-(+-++)-(-+++)],\\
S_t^2&=(1/\sqrt{2})[(++--)-(--++)],\\
S_t^3&=\tfrac{1}{2}[(+---)+(-+--)\\
&\quad-(--+-)-(---+)],\\
S_q^1&=(++++),\\
S_q^2&=\tfrac{1}{2}[(+++-)+(++-+)\\
&\quad+(+-++)+(-+++)],\\
S_q^3&=(1/\sqrt{6})[(++--)+(+-+-)\\
&\quad+(+--+)+(-++-)\\
&\quad+(-+-+)+(--++)],\\
S_q^4&=\tfrac{1}{2}[(--+-)+(---+)\\
&\quad+(+---)+(-+--)],\\
S_q^5&=(----).
\end{aligned}\tag{3}$$

The final configuration in which we are interested will consist of a three-body system and a single particle (number 4, say) moving away from each other. Making the reasonable assumption that the three-body system (He^3 or H^3) is formed in its normal ^2S state, we can conveniently divide the final spin states when the reaction products are far apart into singlets and triplets. Denoting these by R_s and R_t, we obtain

$$\begin{aligned}
R_s&=\tfrac{1}{2}[(++--)-(-++-)\\
&\quad-(+--+)+(--++)],\\
R_t^1&=1/\sqrt{2}[(++-+)-(-+++)],\\
R_t^2&=\tfrac{1}{2}[(++--)-(-++-)\\
&\quad+(+--+)-(--++)],\\
R_t^3&=1/\sqrt{2}[(+---)-(--+-)].
\end{aligned}\tag{4}$$

The transition from initial to final state occurs under the influence of a perturbing energy whose most general form is

$$\begin{aligned}
M=A_0&+B_0\boldsymbol{\sigma}_1\cdot\boldsymbol{\sigma}_2+C_0\boldsymbol{\sigma}_1\cdot\boldsymbol{\sigma}_3+D_0\boldsymbol{\sigma}_1\cdot\boldsymbol{\sigma}_4\\
&+E_0\boldsymbol{\sigma}_2\cdot\boldsymbol{\sigma}_3+F_0\boldsymbol{\sigma}_2\cdot\boldsymbol{\sigma}_4+G_0\boldsymbol{\sigma}_3\cdot\boldsymbol{\sigma}_4,
\end{aligned}\tag{5}$$

where A_0, B_0, $\cdots G_0$ may be permuting functions of the space coordinates of the various particles. It is readily seen by direct expansion that all matrix elements of the form RMS vanish except

$$\begin{aligned}
R_sMS_s&=\sqrt{3}/2[A_0-\tfrac{3}{4}(C_0+F_0)\\
&\quad+\tfrac{1}{4}(B_0+G_0-D_0-E_0)],\\
R_tMS_t&=1/\sqrt{2}[A_0-\tfrac{3}{4}C_0\\
&\quad+\tfrac{1}{4}(B_0+F_0+G_0-D_0-E_0)],
\end{aligned}\tag{6}$$

where the R and S functions are any of those with the same subscript given in (3) and (4). Thus only singlet-singlet and triplet-triplet transitions can occur.

Now the Pauli principle requires that the wave function be antisymmetric in the interchange $1\rightarrow3$ and in the interchange $2\rightarrow4$. We therefore choose for our initial state wave function $\psi_i(1234)$, and our final state wave function $\psi_f(1234)$, forms that are symmetric in the interchange of the pair (12) with the pair (34). Then if we later make these antisymmetric in 2 and 4, say, we will have satisfied the Pauli principle. ψ_i always has the asymptotic form

$$\begin{aligned}
\psi_i(1234)&\underset{\rho\rightarrow\infty}{\longrightarrow}\phi_0(r_{12})\phi_0(r_{34})\\
&\quad\times\sum_l\chi_l(\rho)P_l(\cos\theta')S_l(1234).
\end{aligned}\tag{7}$$

Here, $\boldsymbol{\rho}$ is the coordinate joining the centers of mass of the two deuterons, θ' is the angle between the initial momentum vector $\mathbf{k}_0$ and $\boldsymbol{\rho}$, and ϕ_0 is the wave function for the (symmetric) normal state of the deuteron. Likewise, ψ_f has the asymptotic forms

$$\begin{aligned}
\psi_f(1234)&\underset{r_4\rightarrow\infty}{\longrightarrow}\psi_0(123)\sum_l F_l(r_4)P_l(\cos\theta_4)R_l(1234)\\
&\underset{r_2\rightarrow\infty}{\longrightarrow}\psi_0(134)\sum_l G_l(r_2)P_l(\cos\theta_2)R_l(1432).
\end{aligned}\tag{8}$$

Here, $\mathbf{r}_4$ is the coordinate joining the center of mass of (123) with 4, $\mathbf{r}_2$ the coordinate joining the center of mass of (143) with 2, θ_4 and θ_2 are the angles between $\mathbf{r}_4$ and $\mathbf{k}_0$ and between $\mathbf{r}_2$ and $\mathbf{k}_0$, respectively, and ψ_0 is the wave function for the (symmetric) normal state of the three-body system. In (7), the symmetry requirement [i.e., that ψ_i be symmetric in the interchange of the pair (12) with the pair (34)] and (3) show that $S_l=S_t$ for odd l, and that S_l is a linear combination of S_s and S_q for even l (except for $l=0$, when $S_0=S_s$; this is because the Pauli principle excludes a spherically symmetric quintet state). Again in (8), the symmetry requirement and (4) show that $F_l(r)=-G_l(r)$ for all l. Since (7) and (8) are symmetric in the interchange of the pair (12) with the pair (34), the final wave function which satisfies the Pauli principle has the asymptotic form for large r_4

$$\psi_f(1234)-\psi_f(1432)\sim 2\psi_0(123)\sum_l F_l(r_4)P_l(\cos\theta_4)R_l(1234). \quad (9)$$

To determine the R_l's, we note that the reactions (A) and (B) are generally thought to be radiationless; any radiation that is given off must be so weak that it seems very unlikely that the emission of photons can play an important part in the transitions. Therefore we can assume that total angular momentum is conserved; since total spin is conserved, it follows that orbital angular momentum (l value) is also conserved. The allowed transitions are then $^1S\rightarrow{}^1S$, $^3P\rightarrow{}^3P$, $^1D\rightarrow{}^1D$, $^3F\rightarrow{}^3F$, etc. Thus in the final states given by (9), $R_l=R_s$ for even l, and $R_l=R_t$ for odd l.

In (9) we can always put

$$|F_l(r_4)|=f_l(k_0,k)/r_4, \quad (10)$$

giving for the differential cross section in the rest coordinate system

$$I_0(\theta)=(2k/k_0)[2\sum_l f_l(k_0,k)P_l(\cos\theta)R_l(1234)]^2,$$
$$k^2=3(W+W_1)/2, \quad k_0^2=2W=W_0, \quad (11)$$

where $\mathbf{k}$ is the final momentum vector, and θ is the angle between $\mathbf{k}$ and $\mathbf{k}_0$. W is the kinetic energy of the incident deuterons in the rest coordinate system, W_0 this kinetic energy in the laboratory coordinate system, and W_1 is the energy given up in the reaction; the factor $3/2$ comes from a consideration of the reduced masses involved in the final state. The best values for W_1 appear to be[6] 6.26 for reaction (A), and 7.82 for reaction (B). The coefficient $(2k/k_0)$ in (11) is the ratio of the final neutron (or proton) velocity to the incident deuteron velocity. Because of the orthogonality of the R_l's for even l and the R_l's for odd l, (11) has the symmetry about 90° required by the general physical picture. If we restrict ourselves to incident deuteron energies small enough so that the contribution of the terms for $l\geqq 2$ can be neglected, (11) takes on the particularly simple form

$$I_0(\theta)=A(1+B\cos^2\theta),$$
$$A\equiv(8k/k_0)f_0^2(k_0,k),$$
$$B\equiv f_1^2(k_0,k)/f_0^2(k_0,k). \quad (12)$$

The total cross section then becomes

$$\sigma=4\pi A(1+B/3). \quad (13)$$

There will be an extra factor of 3 appearing in B which is due to the relative statistical weights of the P and S parts of the initial wave.

Results

The accurate evaluation of the various quantities appearing in (12) is very difficult. A modification of the Born approximation method has been used here; the details of the calculations will be omitted. We shall consider first under what circumstances we should expect the results to be reliable. The method is that outlined by Mott and Massey,[8] using for the approximate initial wave function that appears inside the integral, variational deuteron functions[4] times the solution in the Coulomb field,[9] rather than the simple plane wave as in Born's method. This neglects in the zero-order solution both the effect of the nonelectric field and the polarization of the deuterons at short distances. There is no doubt that both of these effects will be important in a quantitative evaluation of A and B, except perhaps at very high energies. But unless both can be accounted for, and it is not clear how this

[8] Mott and Massey, *Theory of Atomic Collisions*, p. 110.
[9] Reference 8, pp. 33 and 39.

can be done simply, the additional effort required by using a better initial state function connecting the two deuterons, without considering polarization, hardly seems worthwhile. Moreover, it seems possible that at low energies, the Coulomb repulsions might tend to keep the deuterons far enough apart so that the other shorter range effects would not play an important part.

The experimental results of KBM[1] (see their Figs. 6 and 11, which refer to the rest coordinate system) appear to be of the form (12). This is consistent with the theory presented here, since an estimate of the $l \geqq 2$ terms indicates that they should not come in strongly before about 2 Mev, giving a considerable factor of safety above the maximum of 0.2 Mev used by these experimenters. However, a theoretical evaluation of the quantity B in (12) shows that it is much too small: 0.03 from the theory as compared with 0.5 required by the KBM experiments. One might say that this discrepancy was due to the inaccuracy of the calculations, were it not for the following considerations. When one assumes that the departure from spherical symmetry in the final distribution is due to the $l=1$ part of the initial wave, it seems reasonable that such asymmetry should depend strongly on incident deuteron energy, and should be small until the classical distance of closest approach $1/k_0$ for angular momentum $h/2\pi$ is of the order of magnitude of the dimensions of the deuterons. The experiments, on the other hand, show a very marked asymmetry as low as 0.1 Mev, where $1/k_0$ is about ten times the deuteron "radius," and show practically no change in shape of the distribution when the energy is doubled. There is some possibility that more accurate calculation of B and its dependence on initial deuteron energy will remove these difficulties. If not, we may have to look for some way in which an appreciable final state $l=1$ wave can arise from an initial state $l=0$ wave, apparently without radiation; this would be necessary to make the magnitude of the final P wave independent of incident particle energy. Such a transition appears to be inexplicable, using nuclear interactions such as are in vogue at the present time.

Further experimental data on angle distribution have been obtained very recently by Neuert.[10] His results are in agreement with those of KBM over the range covered by the latter (0° to 90°). However, when his data are transformed to the rest coordinate system, the resulting distribution is not symmetrical about 90° within the indicated experimental error. That such symmetry exist is required by *any* reasonable theory (since there should be no distinction between incident and target deuterons in the rest coordinate system); indeed, this symmetry was used by KBM as one criterion for the validity of their results.

There seems to be no experimental evidence on the variation of total cross section with energy; such evidence would require the use of a very thin unbacked solid target or of a gas target. However, several experimenters have measured the *yield* from "thick" targets. The yield Y in neutrons (or protons) per incident deuteron is given by

$$Y=\int_0^{x_0} n(x)\sigma[E(x)]dx. \tag{14}$$

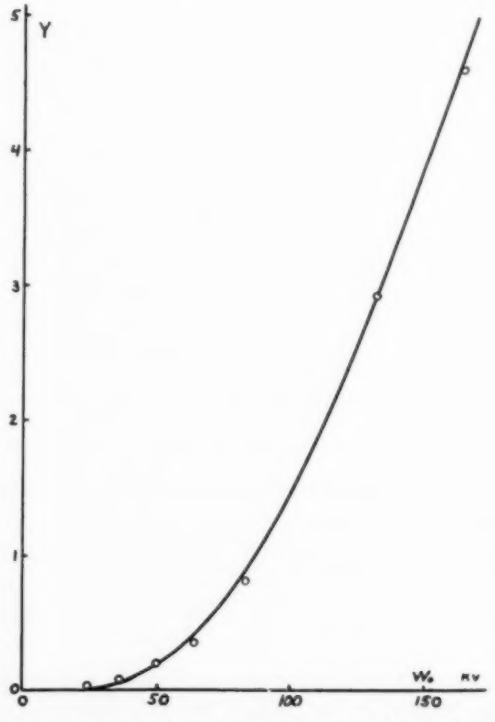

FIG. 1. Relative theoretical yield from infinitely thick target, with experimental points of reference 11. Low energy range, ordinate scale arbitrary.

[10] Neuert, Physik. Zeits. **38**, 122 (1937).

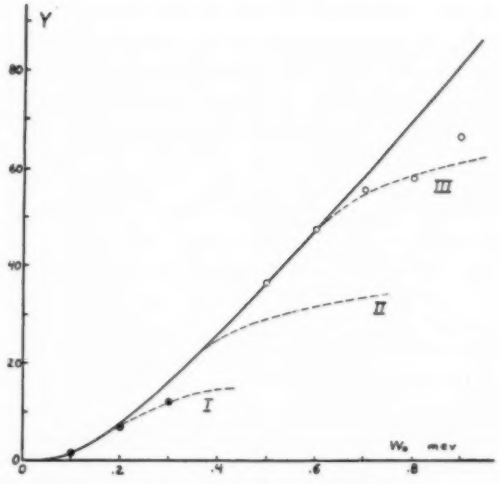

FIG. 2. Relative theoretical yield from infinitely thick target (solid line), with experimental points of references 12 and 13. Higher energy range, ordinate scale same as in Fig. 2. Dotted lines are for finite target thicknesses; I corresponds to thinnest target and III to thickest target. See reference 14.

Here, $n(x)$ is the number of deuterons per cc of target at the depth x below its surface, x_0 is the target thickness, and $E(x)$ is the energy of a deuteron of initial energy W_0 after it has penetrated a distance x into the target. (14) assumes quite reasonably that no deuterons are destroyed as the beam penetrates into the target (since deuterons, like protons and α-particles, have range properties), and that no emitted neutrons (or protons) are lost in coming out of the target. For definiteness in evaluating (14) we assume that $n(x)$ has the constant value n and that $E(x)=W_0-\beta x$. The linear relation between range and energy is a fairly good approximation for moderately small initial energies, by analogy with the range energy data for protons and α-particles. For a target thick enough to stop all the deuterons, (14) then becomes

$$Y=(n/\beta)\int_0^{W_0}\sigma(E)dE. \qquad (15)$$

n/β may be treated as an adjustable parameter, as far as relative yields are concerned. In Fig. 1, the computed curve of Y is plotted in arbitrary units, together with the low energy data of Oliphant, Harteck and Rutherford,[11] the points and the curve being fitted at 130 kv. The agreement is excellent. In Fig. 2 the data of Ladenburg and Roberts[12] and of Bonner and Brubaker,[13] for higher energies, are plotted to the same ordinate scale as Fig. 1, both being fitted to the curve at the lowest energy. When this is done, the theoretical yield at higher energies is too large in both cases. It seems plausible that the low energy deuterons (Fig. 1) are completely stopped in the thin layer of deuterium salt that constitutes the target, while the higher energy deuterons (Fig. 2) penetrate into the backing material where the only deuterium present is that driven in by the beam. The effect of this can be estimated by assigning a thickness x_0 to the deuterium salt layer, and performing the integration in (15) from $(W_0-\beta x_0)$ to W_0. The dotted curves in Fig. 2 correspond to $\beta x_0=0.15$ Mev for I, $\beta x_0=0.30$ Mev for II, and $\beta x_0=0.55$ Mev for III. The data of Ladenburg and Roberts fit well on I (thin target layer), while the data of Bonner and Brubaker fit well[14] on III (relatively thick target layer). In addition to the above, Burhop[15] has given data for extremely low energies (<20 kv) which would be unobservable on Fig. 1, while Döpel[16] has investigated the range of 5 to 150 kv. Over the range in which Döpel's results overlap those of Oliphant, Harteck and Rutherford, they are proportional to the latter, and a factor of about 10^{-3} smaller. For the lower energies, an analytic evaluation of (15) agrees well with both Burhop's and Döpel's results.

It must be emphasized that the excellent agreement between theoretical and experimental relative yields is due primarily to the effect of the Gamow factor, arising from the Coulomb repulsion between incident deuterons, and has very little to do with the details of the remainder of the calculation. Similar calculations of yield have been performed by Dolch.[17] His calculated *absolute* yields agree well with ours (see below), although his relative yields are in much poorer agreement with experiment than ours (compare

[11] Oliphant, Harteck and Rutherford, Proc. Roy. Soc. **A144**, 692 (1934).

[12] Ladenburg and Roberts, Phys. Rev. **50**, 1190 (1936).
[13] Bonner and Brubaker, Phys. Rev. **49**, 19 (1936).
[14] Fig. 1 of reference 13 is printed to such a small scale that the inaccuracy in measuring it is larger than the size of the open circles in our Fig. 2.
[15] Burhop, Proc. Camb. Phil. Soc. **32**, 643 (1936).
[16] Döpel, Ann. d. Physik **28**, 87 (1937).
[17] Dolch, Zeits. f. Physik **100**, 401 (1936).

his Fig. 3 and our Fig. 1), even when the errors in his paper are corrected.[18]

The last point of comparison between theory and experiment is in the matter of absolute yield.[19] Choosing reasonable values for n and β in Eq. (15), obtained by converting α-particle to deuteron ranges,[20] one obtains for the yield at 100 kv from a thick D_3PO_4 target about 3×10^{-4}. The absolute experimental yield from such a target varies with the experimenter over a range of about 10^{-6} to 10^{-9}; thus the theoretical yield is too large by a factor of about 10^3 to 10^5.

In conclusion it is well to repeat that that portion of the theory which concerns itself with the symmetry properties of the situation, leading to Eqs. (11) and (12), is quite rigorous, while the detailed evaluation of the quantities appearing therein is very crude, and serves as little more than an indication of the general nature of the results to be expected. Again, the excellent agreement of relative yields (see Figs. 1 and 2) is due primarily to the Gamow factor, and not to the rest of the theory. Experimental data on absolute cross section as a function of energy, and on angular distribution for higher energies, both obtained with gas targets (to eliminate the effect of penetration into the target), would be very useful at this time.

I wish to express my deep appreciation to Professor Philip M. Morse for his constant encouragement and for his help at many points of the theory. I also wish to thank Professor J. H. Van Vleck for criticizing the manuscript.

[18] Dolch, Zeits. f. Physik **104**, 473 (1937). It is difficult to understand why Dolch's results should deviate so much more from experiment than ours, when both calculations are based on the Gamow factor. In any case, the symmetry properties developed in the present paper, while important for angle distribution, have a small effect on the yield function.

[19] I am indebted to Professor Robley D. Evans for discussion of this point.

[20] Mano, J. de phys. et rad. **5**, 628 (1934).

MAY 15, 1937 PHYSICAL REVIEW VOLUME 51

On the Nuclear Two-, Three- and Four-Body Problems*

WILLIAM RARITA
Columbia University, New York, N. Y.
AND
R. D. PRESENT
Purdue University, Lafayette, Indiana

(Received March 4, 1937)

The simplest nuclear Hamiltonian satisfying all present requirements includes a Majorana-Heisenberg interaction $\{(1-g)P+gPQ\}V(r)$ between unlike particles and an attractive singlet interaction between like particles which is equal to that for unlike particles. The experimental mass defects of H^2 and H^3 together with the cross section σ for slow neutron-proton scattering will determine the range b and depth B of the triplet well and the proportion g of Heisenberg force (we use throughout the potential $Be^{-2r/b}$). An exact analytic expression relating σ, b, B and g is derived for this potential and g is found to be very insensitive to σ. An exact solution of H^2 gives the relation between B and b. The final relation which fixes the parameters is furnished by a Ritz-Hylleraas variational treatment of H^3 with the above Hamiltonian and the wave function:

$$\psi=2^{-\frac{1}{2}}\alpha_1(\alpha_2\beta_3-\alpha_3\beta_2)\phi_1+6^{-\frac{1}{2}}(\alpha_1(\alpha_2\beta_3+\alpha_3\beta_2)-2\beta_1\alpha_2\alpha_3)\phi_2$$

where ϕ_1 and ϕ_2 each represents an exponential times a power series in the interparticle distances of proper symmetry (ϕ_2 is brought in by the Heisenberg term; the Breit-Feenberg operator is used for the small triplet like-particle interaction). The convergence of energies obtained from successive improvements in ψ is rapid and the eigenvalue may be closely estimated. After a relativistic correction is made we obtain: $b=1.73\times10^{-13}$ cm; $B=242\ mc^2$ and $g=0.215$. The binding energy of He^3 is obtained by the same method and the H^3-He^3 difference is found to be $1.48\ mc^2$, agreeing well with experiment. The proton-proton scattering depth is checked to within 1 percent. When applied to He^4, our potential gives approximately 20 percent too much binding energy. Parallel calculations with the Gaussian and Morse curves lead to essentially the same result. No reasonable modification of the experimental data can explain more than a small fraction of the discrepancy.

* The contents of this paper form part of a thesis submitted by William Rarita to the Faculty of Pure Science at Columbia University in partial fulfillment of the requirements for the degree of Doctor of Philosophy.

The Nuclear Hamiltonian

KNOWLEDGE of the nature and magnitude of nuclear forces has undergone rapid development within the past few years. Recent articles by Feenberg and Knipp,[1] Bethe and Bacher[2] and Feenberg and Share[3] have extended our conception of the nuclear Hamiltonian to make it consistent with all the known facts derived from two particle scattering experiments and the binding energies of the hydrogen and helium isotopes. These calculations were of an approximate character, as was justified by the novelty and unreliability of some of the experimental results, and the tentative stage of the theory. However, the agreement between the calculations and experiment was well within the uncertainty of the former. Since a fairly definite formulation of the nuclear Hamiltonian has been arrived at (with the exception that the exact analytic character of the potential functions is not known, but only their general form), the question arises whether the experimental data are now sufficiently accurate to justify a more refined theoretical treatment of these problems. An affirmative answer is given for two reasons: (1) By curiously fortunate circumstances both magnitude and range of the nuclear forces are very insensitive to uncertainties in the experimental data to be used, (2) there exist just enough problems that can be treated in an exact or nearly exact fashion to determine all the essential constants that appear in the Hamiltonian and to verify most of the fundamental assumptions. Taking a definite form for the nuclear Hamiltonian, we have carried out this program and determined the constants in such a way that the probable error arising from both experimental and theoretical uncertainties is of the order of one percent.

The spin-dependence and saturation properties of the neutron-proton forces have been taken as evidence for the mixed Majorana-Heisenberg type of interaction. The existence of an interaction between like particles in the singlet state is established by the experiments on proton-proton scattering[4] and by the failure of neutron-proton forces alone to account for the binding energies of light nuclei.[5] It is consistent with all the experimental evidence to suppose that the non-Coulomb proton-proton forces are identical with the neutron-neutron forces. Breit, Condon and Present have shown that the singlet interaction between two protons, as determined from the experiments of Tuve, Heydenburg and Hafstad,[6] agrees to within one percent with the singlet interaction between neutron and proton as determined from the experiments of Fermi and Amaldi,[7] if the Coulomb force is taken to act at all distances. This reduces the number of arbitrary constants in the nuclear Hamiltonian to four: the radius of interaction and singlet state depth of the potential well for all pairs of particles, the triplet state depth for neutron-proton interaction and the triplet depth for like-particle interaction. Of these constants, only the first three enter effectively into any of the problems under consideration.[8] The triplet depth for like-particle interaction has a small effect on the three and four body calculations which will be discussed later. Two possible forms for this interaction have been proposed, respectively, by Van Vleck[9] and by Breit and Feenberg.[10] An elegant formulation of the nuclear Hamiltonian which is consistent with the facts mentioned above, has been given by Breit and Feenberg. They include the possibility that an ordinary force and a spin exchange force, both small in comparison with unity, may appear in the Hamiltonian. There appears to be no necessity for introducing these modifications at present and in any case they would give rise only to negligible third-order effects in our calculations.[11]

[1] Feenberg and Knipp, Phys. Rev. **48**, 906 (1935).
[2] Bethe and Bacher, Rev. Mod. Phys. **8**, 82 (1936).
[3] Feenberg and Share, Phys. Rev. **50**, 253 (1936).
[4] Breit, Condon and Present, Phys. Rev. **50**, 825 (1936).
[5] Present, Phys. Rev. **50**, 635 (1936).
[6] Tuve, Heydenburg and Hafstad, Phys. Rev. **50**, 806 (1936).
[7] Amaldi and Fermi, Phys. Rev. **50**, 899 (1936). See this paper for complete references to the Italian journals.
[8] The triplet like-particle interaction enters only into the partial waves of odd angular momentum l in the proton-proton scattering, but for the experimental range of energies only the $l=0$ wave is distorted. The ground states of H^3, He^3 and He^4 are all singlet states in the like-particle interaction, if second-order mixing effects due to the Heisenberg operator are neglected.
[9] Van Vleck, Phys. Rev. **48**, 367 (1935).
[10] Breit and Feenberg, Phys. Rev. **50**, 850 (1936).
[11] For the ^3S and ^1S states of H^2, the operator P reduces to unity, whereas in H^3 and He^4 Majorana and ordinary forces give results differing only slightly (because of incomplete saturation of the forces and near symmetry of the Hamiltonian). It is thus a good approximation to

We write the nuclear Hamiltonian in the simplified Breit-Feenberg form using nuclear units (mc^2 for energy, $\hbar(Mm)^{-\frac{1}{2}}c^{-1}=8.97\times10^{-13}$ cm for length):

$$H=\sum_i -\tfrac{1}{2}\nabla_i^2+\sum_{i>j}\{(1-g)P_{ij}+gP_{ij}Q_{ij}\}J(r_{ij}) + \sum_{i_p>j_p}\frac{\kappa}{r_{i_pj_p}}. \quad (1)$$

P_{ij} is a permutation operator exchanging the space coordinates of particles i and j; Q_{ij} exchanges spin coordinates; g is an arbitrary parameter; $J(r)$ is a potential function of the familiar "well" type; and κ is the constant $(\hbar c)^{-1}e^2(M/m)^{\frac{1}{2}}=0.313$. The first summation gives the kinetic energy of all particles; the second summation, taken over all pairs of particles, represents the specific nuclear forces; the last summation, taken over all pairs of protons, gives the Coulomb energy. Throughout the following, we assume that $J(r)=-Be^{-2r/b}$. Previous calculations, together with one to be mentioned subsequently, show that substantially equivalent results are to be expected from the potential $Ae^{-(r/a)^2}$. It is well known from the work of Massey and Mohr,[12] Dolch,[13] and Morse, Fisk, Schiff and Shockley[14] that the properties of the light nuclei are very insensitive to the exact analytic character of the potential.

We propose to determine the parameters b, B and g from exact treatments of the deuteron and of the scattering of slow neutrons in hydrogen, and by a precise variational treatment of H^3. Verification of fundamental assumptions will be obtained by applying the potentials so determined in order to calculate the proton-proton scattering and the Coulomb energy of He^3. Finally a crucial test is provided by the alpha-particle.

replace the ordinary force by a Majorana force and the spin exchange force by a Heisenberg force. More precisely, the near symmetry of the zero-order wave functions for H^3 and He^4 leads to the result that both spin exchange and ordinary forces can produce separate effects only in the third-order approximation of the perturbation theory (cf. reference 10).

[12] Massey and Mohr, Proc. Roy. Soc. **A152**, 693 (1935).

[13] Dolch, Zeits. f. Physik **100**, 401 (1936).

[14] Morse, Fisk and Schiff, Phys. Rev. **50**, 748 (1936); Fisk, Schiff and Shockley, Phys. Rev. **50**, 1090 (1936).

Neutron-Proton Scattering

The known binding energy of the deuteron $(4.35\pm0.10\ mc^2)$[15] determines the triplet neutron-proton depth B in terms of the range b of the forces. For the exponential potential $Be^{-2r/b}$ the relations are: $J_\lambda[b(B)^{\frac{1}{2}}]=0$, $\lambda^2=-b^2E$, $E=$ total energy of H^2 in ground state. Details may be found elsewhere.[2]

The relation between b and the singlet state depth $B'=(1-2g)B$ may be obtained from the scattering of either slow neutrons or fast protons in hydrogen. We choose the former, for which a simple exact relation may be found in the case of the exponential potential. The experiments of Fermi and Amaldi[7] have shown that the cross section for scattering of slow *nonthermal* neutrons on protons is about 13×10^{-24} cm^2, corresponding to a mean free path in paraffin of 1 cm. They have also shown that the large scattering is due to a positive logarithmic derivative of the wave function at the boundary of the well, i.e., that no stable ^1S level exists.

The Schrödinger equation for the relative motion

$$\{d^2/dr^2+E+Ve^{-2r/b}\}u(r)=0$$

is transformed into Bessel's equation by the substitution $y=b(V)^{\frac{1}{2}}e^{-r/b}$. For a positive incident energy E, the general solution is given by

$$u=c_1J_{ip}(y)+c_2J_{-ip}(y),$$

where $p=bk=b(E)^{\frac{1}{2}}$. The boundary condition at $r=0$ requires that

$$c_1J_{ip}[b(V)^{\frac{1}{2}}]+c_2J_{-ip}[b(V)^{\frac{1}{2}}]=0.$$

At infinity the solution is normalized to a sine wave of unit amplitude:

$$\lim_{y=0}\{c_1J_{ip}(y)+c_2J_{-ip}(y)\}=\sin(kr+\delta_0).$$

Imposing the two boundary conditions and allowing E to approach zero (very slow neutrons), one obtains the relation

$$\frac{1}{\alpha}=b\left\{\frac{\pi}{2}\frac{N_0[b(V)^{\frac{1}{2}}]}{J_0[b(V)^{\frac{1}{2}}]}-\log\left[\frac{b(V)^{\frac{1}{2}}}{2}\right]-C\right\}, \quad (2)$$

[15] This value was communicated to us by Professor Bethe at the Ann Arbor summer session. Cf. Feather, Nature **136**, 467 (1935).

where $\alpha=k\cot\delta_0$, $C=0.5772\cdots$ (the Euler constant), and N_0 is the Bessel function of second kind and of order 0 in the notation of Jahnke-Emde. α is approximately equal to the logarithmic derivative of the wave function at the boundary of the well and the sign of α is positive if V gives rise to a "virtual level" and negative if V produces a stable level.[16]

It is interesting to compare the formula (2) with the perturbation formula of reference 4 in order to test the accuracy of the latter.[17] The perturbation formula gives in this case:

$$V-V_0=-\frac{\alpha u^2(\infty)}{\int_0^\infty u^2(r)e^{-2r/b}dr}=-\frac{2\alpha}{b}\frac{1}{J_0^2(bV^{*\frac{1}{2}})+J_1^2(bV^{*\frac{1}{2}})}, \quad (3)$$

where V_0 is the depth that places a stationary level at $E=0$ and V^* is taken in first approximation as V_0 and in second approximation as V. For constants of the proper order of magnitude for the virtual ^1S state, formulas (2) and (3) agree within 3 percent in first and $\frac{1}{2}$ percent in second approximation.

For very slow neutrons ($E=0$, $l=0$), the cross section for elastic scattering is given by:

$$\sigma=\frac{4\pi}{k^2}\sin^2\delta_0=\frac{4\pi}{E+\alpha^2}=\frac{4\pi}{\alpha^2}.$$

The complete cross section, averaged over the two possible orientations of spin, is

$$\sigma^a=\pi(1/\alpha_s^2+3/\alpha_t^2), \quad (4)$$

TABLE I.

TYPE OF TERM	NEUTRON-PROTON POTENTIAL	NEUTRON-NEUTRON POTENTIAL
$(\phi_1\mid V\mid\phi_1)$	$(1-g/2)[J(r_{12})P_{12}+J(r_{13})P_{13}]$	$(1-2g)J(r_{23})$
$(\phi_2\mid V\mid\phi_2)$	$(1-3g/2)[J(r_{12})P_{12}+J(r_{13})P_{13}]$	$-J(r_{23})$*
$(\phi_1\mid V\mid\phi_2)$	$(g\sqrt{3}/2)[J(r_{12})P_{12}-J(r_{13})P_{13}]$	0

* The triplet neutron-neutron interaction given here is that which follows from the Breit-Feenberg form (1) of the nuclear Hamiltonian. The Van Vleck operator would give $-((1-2g)/3)J(r_{23})$ in place of $-J(r_{23})$, i.e., about one-fifth as much repulsion. The arbitrariness involved in this choice is not important since in the first place the entire mixing effect is small and in the second place the interaction is only large at close distances where the wave function is small due to orbital antisymmetry.

[16] The symbol α differs from that used in Bethe and Bacher. In their notation $\alpha\equiv-u'(a)/u(a)\leqq-k\cot\delta_0$ but in our notation $\alpha\equiv k\cot\delta_0\leqq u'(a)/u(a)$ where a is the maximum range of the forces.

[17] Reference 4, formulas (10.3), no. 2.

where α_s and α_t are to be obtained from formula (2) with $V=B'$ (singlet) and $V=B$ (triplet), respectively.[18] We use formula (2) to obtain α_t from B and b, then formula (4) to obtain α_s; finally formula (2) gives $B'=(1-2g)B$ in terms of b. B' is determined with great accuracy by this means, because the scattering is very sensitive to the depth of the well. A ten percent variation in σ^a will produce a variation in B' or g of less than one percent.

THEORY OF THE THREE-BODY PROBLEM

It has been seen that two of the three parameters occurring in the nuclear Hamiltonian can be fixed by exact relations. The three-body problem furnishes the third relation and the desired accuracy may be attained by the use of the Ritz-Hylleraas method. One of the writers[5] has applied this method to the H^3 nucleus, using a Hamiltonian with ordinary forces between unlike particles but with no forces between like particles. Such a model was found to be incompatible with the experimental facts. In the present paper we generalize the previous calculation to take account of the nuclear Hamiltonian discussed in section one. The generalization is threefold: (1) Like-particle forces are included, (2) The matrix elements for unlike particle forces are complicated by the presence of the Majorana operator, (3) The Heisenberg operator causes "mixing effects."

The Majorana-Heisenberg operator $(1-g)P+gPQ$ reduces in first approximation to the effective Majorana operator $(1-g/2)P$. The error introduced by neglecting the second order mixing effect has been estimated by Breit and Feenberg[10] and also by one of the writers.[19] The latter estimate of $0.5\,mc^2$ shows that the correction is by no means negligible. The effect can be treated in a rigorous manner by including in the wave function a term of the "borrowed" symmetry. The possible configurations of the three-particle system include one quartet and two doublet states, and it is readily seen that the operator Q connects

[18] It is worthy of note that a small error would be introduced by using $3/\epsilon_t$ in place of $3/\alpha_t^2$ ($\epsilon_t=4.35\ mc^2$). For our final choice of constants $3/\epsilon_t=0.69$ and $3/\alpha_t^2=1.19$, and the error in the derived value of α_s^2 is 11 percent. However, this would cause an error of only 1 percent in B'.

[19] Present, Phys. Rev. **50**, 870 (1936).

the ground state (doublet with antiparallel neutron spins) only with the other doublet having parallel neutron spins. In terms of the proper spin functions for a total spin angular momentum of $\frac{1}{2}$ in the positive z direction, the complete wave function ψ may be written as (the subscript 1 refers to the proton)

$$\psi = 2^{-\frac{1}{2}}\alpha_1(\alpha_2\beta_3-\alpha_3\beta_2)\phi_1+ 6^{-\frac{1}{2}}(\alpha_1(\alpha_2\beta_3+\alpha_3\beta_2)-2\beta_1\alpha_2\alpha_3)\phi_2,$$

where ϕ_1 is a function to be specified later which is symmetrical in the space coordinates of the two neutrons, and ϕ_2 is similarly antisymmetrical. The only formal complication arising from the presence of ϕ_2 occurs in the potential energy terms which are spin-dependent. The results obtained from summing over spins, are given in Table I.

The nuclear Hamiltonian (1) for H^3 is written in variational form in terms of the elliptic coordinates $s=r_{12}+r_{13}$, $t=r_{12}-r_{13}$, $\rho=r_{23}$. The procedure and the notation are the same as in the previous paper by one of us.[5] The functions ϕ_1 and ϕ_2 are each taken to be an exponential in s multiplied by a power series in s, t, ρ of proper symmetry.

$$\phi_1 = e^{-k_1(s/2)} \sum_{p,\ r,\ \text{even}\ q} C^{(1)}{}_{pqr} s^p t^q \rho^r,$$
$$\phi_2 = e^{-k_2(s/2)} \sum_{p,\ r,\ \text{odd}\ q} C^{(2)}{}_{pqr} s^p t^q \rho^r. \tag{5}$$

For convenience we take $k_1=k_2=k$ and adjust k to make the most important terms of ϕ_1 as good as possible. The summations are to be extended over all positive values of the indices, subject to the above restrictions, and as many terms taken as result in an appreciable lowering of the total energy. It is convenient to make the transformations $s'=ks$, $t'=kt$, $\rho'=k\rho$ (and drop the primes for the remainder of this section). Then the energy matrix element between any terms m and n in the double series is given by:

$$H_{mn}=k^2(P_{mn}+Q_{mn})+L_{mn}(k).$$

The kinetic energy integrals P_{mn}, Q_{mn} and the unity matrix element N_{mn} are different from zero only if m and n are in the same series and in this case they are given by the formulas of reference 5. The matrix elements of potential energy L_{mn} are obtained from the following formulas (Latin subscripts refer to terms in φ_1; Greek subscripts to φ_2).

$$L_{mn} = -(1-g/2)Bl_{mn}{}^{+}-(1-2g)Bl_{mn}{}^{*},$$
$$L_{\mu\nu} = -(1-3g/2)Bl_{\mu\nu}{}^{+}+Bl_{\mu\nu}{}^{*},$$
$$L_{m\nu} = -((g\sqrt{3})/2)Bl_{m\nu}{}^{-},$$

where

$$l_{ij}{}^{\pm}=\int_0^\infty ds\int_0^s d\rho\int_0^\rho dt\rho(s^2-t^2)e^{-s/2}s^{p_i}t^{q_i}\rho^{r_i}\{e^{-\beta(s+t)}P_{12}\pm e^{-\beta(s-t)}P_{13}\}e^{-s/2}s^{p_j}t^{q_j}\rho^{r_j}$$

$$l_{ij}{}^{*}=\int_0^\infty ds\int_0^s d\rho\int_0^\rho dt\rho(s^2-t^2)e^{-s}s^{p_i+p_j}t^{q_i+q_j}\rho^{r_i+r_j}e^{-2\beta\rho},\quad \beta=1/bk.$$

It is readily shown that $l_{ij}{}^{\pm}=l_{ji}{}^{\pm}$. Using the relations

$$P_{12}\begin{Bmatrix}s\\t\\\rho\end{Bmatrix}=\begin{Bmatrix}(s+t)/2+\rho\\(s+t)/2-\rho\\(s-t)/2\end{Bmatrix},\quad P_{12}\begin{Bmatrix}s\\t\\\rho\end{Bmatrix}=\begin{Bmatrix}(s-t)/2+\rho\\-(s-t)/2+\rho\\(s+t)/2\end{Bmatrix},$$

we may evaluate the integrals $l_{ij}{}^{\pm}$ in terms of

$$\begin{matrix}K_{acb}{}^{(12)}\\K_{acb}{}^{(13)}\end{matrix}=\int_0^\infty ds e^{-(\beta+3/4)s}s^a\int_0^s d\rho e^{-\rho/2}\rho^c\int_0^\rho dt e^{\mp(\beta+1/4)t}t^b \tag{6}$$

and $l_{ij}{}^{*}$ in terms of

$$K^{*}{}_{acb}=\int_0^\infty ds e^{-s}s^a\int_0^s d\rho e^{-2\beta\rho}\rho^c\int_0^\rho dt t^b.$$

Details of evaluation of the K's are reserved for the appendix. Using the optimum value of β, tables of K's are calculated for a wide range of the indices. Variation of the constants c_{pqr} determines the lowest energy obtainable from a given combination of the terms in (5) (Ritz-Hylleraas method).

TABLE II. *Coefficients of the H^3 and He^3 wave functions normalized to unity.*

Terms	$H^3(E=-15.880)$	$He^3(E=-14.431)$
[000]	0.450 422	0.433 685
[001]	−0.142 982	−0.135 8180
[002]	0.013 9300	0.012 9308
[003]	−0.000 49357	−0.000 45451
[100]	0.012 1361	0.012 9370
[010]	−0.006 0689	−0.006 29724

DETAILS OF H^3 CALCULATIONS

The range b of the forces must be found which will give the observed binding energy of H^3 (16.55 ± 0.25 mc^2).[15] In preliminary calculations to determine this range approximately we have neglected the second-order mixing effects and also the relativistic correction. Suitable values for k and β must be selected at the outset and this is done by computing the energy given by the single (and most important) term $\varphi_1=e^{-k(\sigma/2)}$.

For a radius $b=0.25$ nuclear unit the best values are $k=6.5$, $\beta=0.61$. At $b=0.20$ the lowest energy of -5.39 mc^2 is obtained for $k=7.4$; with $\beta=0.61$ we would have $k=8.2$ and $E=-5.13$. Since the optimum k increases as b decreases it is satisfactory to use the same β for several nearby radii. If $\beta=0.61$ is used then the energy for $b=0.20$ misses its best value by only 0.26 mc^2 and it is clear that other terms in the wave function will automatically make up for this deficiency. Since the optimum value of k undergoes modification as successive terms in ψ are added, the use of a fixed β is probably within the uncertainty of this method of estimating k. As has been pointed out previously, the use of an unsuitable k or β will not affect the final energy to be obtained from this type of calculation, but may result in a poor convergence of the energy contributions of successive terms. The advantage of a fixed β is that only one set of potential energy integrals need be calculated. The value of $\beta=0.61$ was chosen for the initial computation at $b=0.2508$ and used for subsequent calculations at $b=0.200$ and 0.193.

The previous work by Feenberg and Knipp and by Bethe and Bacher indicated a radius for the Gaussian potential of 2.25×10^{-13} cm. (0.2508 nuclear unit). Our first calculation, made at this radius ($b=0.2508$), gave excellent convergence with six terms in ϕ_1 to an energy of -12.32 mc^2. Clearly a smaller b was required. Repeating this calculation for $b=0.200$, we obtained -15.33 from an eight term function. Before attempting an accurate estimation of b, it was necessary to obtain an approximate idea of the corrections due to the relativistic and mixing effects. We have estimated the former according to the method of Feenberg,[20] for a range of the forces approximately determined from the preceding calculations. A brief calculation, mentioned in the appendix, gives -0.47 mc^2 for the relativistic correction to the kinetic energy. According to one of the writers[19] the mixing effect contributes about -0.5 mc^2 to the energy. Then the proper range of the forces, determined from a calculation with ϕ_1 alone, should lead to an energy of -15.6 mc^2 approximately. It was found that for $b=0.193$ the ϕ_1 series gave energies converging to -15.7.

The final calculation with the complete wave function ψ including ϕ_2, was made at $b=0.193$. Let us designate by $[abc]$ a single term $s^a t^b \rho^c$ in the ϕ_1 or ϕ_2 series. Then the most important terms in ϕ_1 are the following [000], [001], [002], [003], [100] which give in combination an energy of -15.56. When combined with this basic function, the terms [200], [300] and [004] contribute, respectively, 0.05, 0.06, and 0.02 mc^2. All other terms examined including [400], [020], [101] contribute less than 0.01 mc^2, from which it may be concluded that the lowest energy obtainable from a function with the symmetry of ϕ_1 may be less than -15.70 by only a few hundredths of 1 mc^2. This follows from the satisfactory convergence of energy contributions and the completeness of the function system.[20a] The energy is still further decreased by the mixing effect when terms in ϕ_2 are included. The terms investigated were [010], [011], [110] and [012], of which the first two lowered the energy by 0.43 mc^2 when inserted with the eight most important terms of ϕ_1 and the last two were altogether negligible. Then the ground state eigenvalue for the nuclear Hamiltonian (1) with $b=0.193$ may be said to occur at -16.15 mc^2, the difference between this value and the experimental one of -16.55 ± 0.25 mc^2 being accounted for by the relativistic correction.

This determination of the nuclear force constants yields the following results: $b=0.193$ nuclear unit (about 1.73×10^{-13} cm), $B=241.8$ mc^2 (triplet neutron-proton depth), $B'=137.6$ mc^2

[20] Feenberg, Phys. Rev. **50**, 674 (1936).

[20a] The completeness of the Hylleraas function system for the general three-body problem and the convergence of the successive approximations to the energy upon the lowest characteristic value of the differential equation have been proven by H. M. James and A. S. Coolidge in a paper to be published soon.

(singlet depth)[21] and $g=0.215$. The reliability of these results in the light of possible modifications of the experimental data will now be discussed. The cross section for scattering of slow nonthermal neutrons on protons seems to have been determined within a probable error of 10 percent.[7] The uncertainty in B' is then slightly less than 1 percent and this will produce an uncertainty in the calculated H^3 energy of 0.15 mc^2. The H^2 binding energy appears to be subject to an uncertainty of 3 percent and the H^3 binding energy, calculated from the deuteron-deuteron transmutation, has a corresponding uncertainty of 1.5 percent. Now an increase of ϵ in the measured H^2 binding energy would cause an increase of 2ϵ in the experimental H^3 binding energy and an increase of approximately 2ϵ in the calculated value. Hence no reasonable modification of the value 4.35 mc^2 will affect the values of b and B' given above and B will vary by 0.6 percent for a 3 percent modification. In the neighborhood of $b=0.193$ the H^3 binding energy increases by roughly 0.10 mc^2 for a decrease in b of 0.001 nuclear unit.

The wave function for H^3 is readily calculated from the secular determinant evaluated at the energy for which it vanishes.[22] Because of theoretical uncertainties in the nuclear model, there would be no point to evaluating the coefficients c_{pqr} for the best 10 term function, which gives an energy of -16.12 mc^2. However, there exists a simple six-term combination giving only 1.5 percent less binding energy. Coefficients for this function, normalized in the coordinates s', t', ρ' may be found in Table II.[23]

Further Applications

Having completed the calculations for H^3, it was a relatively simple matter to work out the binding energy of He^3. This was done *directly* by computing the matrix elements of the Coulomb energy, adding them to the H^3 matrix elements, and solving the secular equations. The He^3 energy matrix element H_{mn} includes the Coulomb term C_{mn} where

$$H_{mn}=k^2(P_{mn}+Q_{mn})+kC_{mn}+L_{mn}(k),$$
$$C_{mn}=\kappa[J(200)-J(020)].$$

Here κ is the constant of Eq. (1) and $J(abc)$ is the integral defined in reference 5. The matrix elements C_{mn} vanish between m and n of different symmetry. Those ten terms were included in the He^3 wave function which had been found most important for H^3. Their relative weight was the same as before and the convergence of energies was slightly better. Coefficients for the same six-term wave function used with H^3 are to be found in Table II. The ten term function for He^3 gives 14.645 mc^2 for the binding energy as compared with 16.124 mc^2 for H^3 with the same ten terms (with slightly different coefficients of course). The difference of 1.48 mc^2 represents the Coulomb energy of He^3 with great accuracy; since the corrections for convergence, relativistic effect, inaccuracy in experimental data, and uncertainty in the analytic character of the potential would all act as small perturbations affecting the two problems in nearly equal fashion. This value for the Coulomb energy is then somewhat better than the theory behind it. The difference between our value and that obtained by Share[24] (1.37 mc^2) is principally due to the use of quite different radii of interaction for the forces. For the Gaussian analog to our radius (about 0.217 n.u., see below), Share's method would give 1.45 mc^2. As first pointed out by Goldsmith and fully discussed in Bethe and Bacher, the difference in binding energies of H^3 and He^3 is directly measurable as the difference in reaction energies of the two deuteron-deuteron transmutations. Bethe and Bacher give the value 1.49 ± 0.27 mc^2; a later estimate by Bethe, quoted by Share is 1.58 ± 0.18 mc^2. It is seen that our calculated value lies well within the range of error of both estimates; hence we may conclude that the fundamental assumption of the equality of neutron-neutron and non-Coulomb proton-proton forces is verified quantitatively by experiment.

The other explicit assumption used in this work is that the singlet neutron-proton and proton-

[21] For these values of b and B' the "virtual level" comes at 128 kv.

[22] Cf. James and Coolidge, J. Chem. Phys. **1**, 825 (1933).

[23] It is worthy of note that the coefficients of the successive powers of ρ' alternate in sign and diminish rapidly in size. They diminish much more rapidly than would be expected from the exponential function $e^{-\rho'/2}$ or from any simple exponential. From this we may infer that the convergence would not have been much improved by using a symmetrical exponential $e^{-k/2(\alpha+\beta)}$ in φ (Eqs. 5).

[24] Share, Phys. Rev. **50**, 488 (1936).

proton interactions are identical. Confirmation of this assumption is provided by using the proton-proton scattering data of Tuve, Heydenburg and Hafstad to determine the potential depth corresponding to the radius of $b=0.193$ for the simple exponential function. In accordance with the methods described in reference 4, this depth was found to be 135.8 mc^2 as compared with the value of 137.6 mc^2 determined from the neutron-proton scattering. Both figures have a probable error of 1 percent arising from the uncertainties in their experimental determination. As pointed out in reference 4, the excellence of the agreement is seriously impaired if the Coulomb force is taken to act only outside the well. This result is consistent with the agreement of our calculated Coulomb energy for He^3 with experiment, since it was there assumed that the Coulomb potential extended all the way to the origin.

The Alpha-Particle

The triplet neutron-proton potential, determined by our calculation to be $Be^{-2r/b}(B=242\ mc^2, b=0.193$ n.u.), appears to differ considerably from $Ae^{-(r/a)^2}$ ($A=71.5\ mc^2, a=0.250$ n.u.), which is the final potential obtained by Feenberg and Share in agreement with Bethe and Bacher who use the same method. Some calculations mentioned in reference 5 indicated a correspondence of the simple and Gaussian exponentials for $a=b$. The large difference in depths is then partly to be explained by the steeper decline of the simple exponential and partly by a genuine discrepancy in the radii.[25] Feenberg and Share have used nearly the same values of the experimental data as ourselves, except for the ^1S level of the deuteron which they assume to lie at $E=0$. They have made their calculations on H^3 and He^4 with the equivalent two-body method, which is known to give an upper limit to the binding energy and for which they have computed a first-order correction. Both of these facts would tend to explain their greater value for the range of the forces; however, neither is the principal reason for the discrepancy, which is due essentially to the determination of the forces from two different sets of problems. Whereas they have used $H^2(^3S)$, $H^2(^1S)$, H^3 and He^4 to establish the range of the forces, the triplet neutron-proton depth and the singlet neutron-proton and neutron-neutron depths, we have used $H^2(^3S)$, $H^2(^1S)$ and H^3 explicitly and the proton-proton scattering implicitly (through equality of the singlet interactions) in our determination. Therefore the essentially different results appear to imply incompatibility of the three binding energies and two scattering cross sections with the nuclear Hamiltonian in its present form. We consider this possibility further.

The like-particle depth calculated by Feenberg and Share is 41 mc^2 which is to be compared with the value of approximately 36.6 mc^2 determined from the proton-proton scattering for the same radius ($a=0.250$) of the Gaussian potential. This comparison has been taken to indicate satisfactory agreement and general confirmation of the nuclear model. As a matter of fact 41 mc^2 lies far outside the range of error of the scattering depth which is determined to within 1 percent by the present experimental data. Considering the approximations made in the treatments of H^3 and He^4, the discrepancy may be justified.

In order to determine whether the theory agrees with experiment within the limits of error of experiment, we have applied the potential determined in the preceding sections to a calculation of the binding energy of the alpha-particle. A simple variational method gives significant results. If the wave function is assumed as

$$\chi=N\exp\left[-(\nu/2)(r_{12}^2+r_{13}^2+r_{14}^2+r_{23}^2+r_{24}^2+r_{34}^2)\right]$$

then the variational energy to be minimized with respect to ν is given by

$$\begin{aligned} E&=9\nu-(4B^*+2B')F(\sigma),\\ F(\sigma)&=\{[2\sigma^2+1][1-\varphi(\sigma)]e^{\sigma^2}-2\sigma/\pi^{\frac{1}{2}}\}, \end{aligned} \tag{7}$$

where $\sigma=1/(b(2\nu)^{\frac{1}{2}})$, $\varphi(\sigma)$ denotes the error function integral (tabulated in Peirce) and B^* and B' represent the effective neutron-proton depth $B(1-g/2)$ and the singlet like-particle depth $B(1-2g)$, respectively. Minimization of E gives

[25] An experimental determination of the range of nuclear forces can be made by measuring the proton-proton scattering at the lowest energy for which an anomalous scattering is observable (about 100–200 kv) and again at the highest energy available. The energy dependence of the phase shift will determine the proper radius of interaction of the forces.

an energy for He^4 of $-56.5\ mc^2$. The exact energy must certainly lie below this. The experimental value is $-55.2\ mc^2$ which is subject to three corrections before comparison with the calculated value. The Coulomb energy of $1.7\ mc^2$ approximately, the mixing effect correction of the order of $-0.5\ mc^2$, and the relativistic correction of the order of $-1.5\ mc^2$ will produce a mutual cancellation, leaving $-55\ mc^2$ as the value to be compared with theory. It is seen that the simple wave function χ already gives too much binding.

The wave function may be improved by taking a linear combination of functions χ with different values of the parameter ν.[26] The matrix elements are:

$$H_{ii}=9\nu_i-(4B^*+2B')F(\sigma_i), \quad N_{ii}=1,$$

$$H_{ij}=18\nu_i\nu_jN_{ij}/(\nu_i+\nu_j)-(4B^*+2B')N_{ij}F(\sigma_{ij}),$$

$$N_{ij}=16\sqrt{2}(\nu_i\nu_j)^{9/4}/(\nu_i+\nu_j)^{9/2}, \quad \sigma_{ij}=1/(b(\nu_i+\nu_j)^{\frac{1}{2}}).$$

With three terms included the energy is lowered to $-62.2\ mc^2$. In order to estimate the approximate location of the eigenvalue, we apply Feenberg's equivalent two-body method to this problem (see appendix for application of two-body method to H^3 and He^4 with an arbitrary potential function). The resulting energy is $-71.7\ mc^2$ which may be taken as a lower bound. Now Feenberg and Share have shown that if the potential is a function of only even powers of the distance, then a correction can be computed to the two-body method which is approximately twice as large for He^4 as for H^3. It is reasonable to suppose that nearly the same relation will hold for our potential as well, since its general form can be approximated by even power functions. The two-body method gives $-18.2\ mc^2$ for H^3 which is to be compared with $-15.7\ mc^2$, the value obtained previously by the Hylleraas method ignoring mixing effects. Hence the corrected He^4 will have an energy of $-66.7\ mc^2$. If we take this value as the true theoretical energy for He^4 with out potential, the discrepancy is $11.7\ mc^2$ or 20 percent of the experimental value. No sensible modification of the experimental data will suffice to explain so large a difference, since an increase in the range b of 0.001 n.u. causes a decrease in the He^4 binding energy of only 0.25 mc^2 and the uncertainty in the other problems will not justify a much greater increase in b. To explain the binding energy of He^4, it is clear that we should have to go to nearly as wide a radius as that found by Feenberg and Share.

Does this mean that the simple exponential well is not an acceptable analytic form for the nuclear potentials? First it is well to see if the same discrepancies would be encountered with other analytic forms. This will be done in an approximate manner for the Gaussian and Morse potentials. We proceed to fit the experimental data in the same order as previously done with the simple exponential function, using the corrected equivalent two-body method for H^3 and He^4. Neutron-proton scattering, the ^3S level of H^2 and the binding energy of H^3 determine the constants for the Gaussian potential $Ae^{-(r/a)^2}$ with the following values:[27] $a=0.217$ n.u. $(1.945\times10^{-13}$ cm), $A=88.2\ mc^2$ (triplet neutron-proton depth), $A'=49.4\ mc^2$ (singlet depth), $g=0.220$. When these potentials are applied to He^4, the variational method with the function χ gives $-51.5\ mc^2$ and the corrected equivalent method $-63.2\ mc^2$. The discrepancy is 15 percent of the experimental value.

The Morse potential $V(r)=-2Ce^{-2(r-c_1)/c}+Ce^{-4(r-c_1)/c}$, discussed in reference 14, was taken to have an inner repulsive region defined by $c_1=c/2$. It might be expected that the presence of the repulsive region would tend to minimize the discrepancy, since this region would be of more importance for He^4 than for H^3 because of the narrower dimensions of the former nucleus. The neutron-proton scattering and the binding of H^2 are treated by exact relations given in reference 14; the equivalent two-body method (see appendix) is used for H^3 with a correction intermediate between those found for $Be^{-2r/b}$ and $Ae^{-(r/a)^2}$. This results in the following values for the constants: $c=0.150$ n.u., $c_1=0.075$ n.u., $C=100.8\ mc^2$ (triplet neutron-proton), $C'=56.7\ mc^2$ (singlet) and $g=0.218$. The inner repulsive region for the triplet interaction rises to a height of $+197\ mc^2$. A treatment of He^4 with these potentials by the corrected equivalent method gives

[26] This was suggested to us by Dr. Feenberg.

[27] Since the numerical integrations needed in the derivation of A' from the Fermi-Amaldi data are somewhat tedious, we observe that the following relation holds approximately for values of a investigated: $a^3A'=2.33$.

about $-65\ mc^2$, representing an excess binding of 18 percent.

Although the calculations for the Gaussian and Morse potentials involve an uncertain approximation in the treatment of H^3, nevertheless the results are qualitatively significant and indicate that no simple potential well is likely to explain the discrepancy. A potential function falling off more steeply than the simple exponential is almost certainly excluded; on the other hand a function with a large inner repulsive region, giving rise to a predominantly repulsive proton-proton interaction, is excluded by the proton-proton scattering experiments.[4] Although very shallow long-range forces would have an inappreciable effect on the binding, they would lead to phase shifts of higher order in the proton-proton scattering which might destroy the agreement of the singlet interactions and invalidate the calculations of this paper. It is also possible, without contradicting the proton-proton scattering experiments, that an additional force of intermediate range ($<3e^2/mc^2$) or a momentum-dependence unobservable for low energies (<1 Mev) may occur to explain the discrepancy. Another possibility is that the singlet and triplet interactions have different ranges; this would imply that g is a simple function of the distance.[28] Also the binding energy of He^4 may be reduced relative to that of H^3 by the introduction of repulsive many-body forces such as those which would occur in the proposed theory of Gamow and Teller.[29]

As previously mentioned the introduction of small spin exchange and ordinary forces would have only a third-order effect on these calculations and as long as the operator is predominantly Majorana the form of interaction used by us is justified. The success of Feenberg and Wigner,[30] Wigner,[31] and Rose and Bethe [32] in explaining properties of intermediate nuclei, using the Majorana type of interaction, is good evidence for the essential correctness of the latter. Direct but somewhat uncertain evidence for a predominantly Majorana type of interaction between like particles is afforded by the proton-proton scattering experiments which seem to require for their interpretation at small angles a negative phase shift in the p wave and a consequent repulsive triplet interaction.[4] Finally it is possible that either or both of the fundamental assumptions that were verified in these calculations (cf. Section 5) may be partly incorrect. The proton-proton forces may not be identical with the neutron-neutron forces, as was assumed to be true in the H^3 calculation and verified for He^3. Also the agreement between the singlet proton-proton and proton-neutron potentials may be a coincidence; in reality they may have slightly different ranges and depths.

We conclude that it is possible to fit accurately only five out of the six experimental data by means of three constants and two assumptions. Since it is possible to fit all six with a fair degree of approximation,[33] the nuclear model, though incorrect in its present form, may still be of great usefulness. From this point of view our tabulation of H^3 and He^3 wave functions is to be justified.

It is a pleasant obligation to acknowledge the hospitality of the physics department at Ann Arbor, where this work was begun last summer.

Appendix I

Evaluation of the K integrals

Let $K_{a,c,b}^{\lambda,\mu,\nu}=\int_0^\infty ds e^{-\lambda s} s^a \int_0^s d\rho e^{-\mu\rho}\rho^c \int_0^\rho dt e^{-\nu t} t^b$.

Then

$K_{a,c,b}^{(12)}=K_{a,c,b}^{\lambda,\mu,\nu}$ $(\lambda=\beta+3/4,\ \mu=1/2,\ \nu=\beta+1/4)$,
$K_{a,c,b}^{(13)}=K_{a,c,b}^{\lambda,\mu,\nu}$ $(\lambda=\beta+3/4,\ \mu=1/2,\ \nu=-(\beta+1/4))$,
$K_{a,c,b}^{*}=K_{a,c,b}^{\lambda,\mu,\nu}$ $(\lambda=1,\ \mu=2\beta,\ \nu=0)$.

The integrals $K_{a,c,b}^{\lambda,\mu,\nu}$ may be evaluated by means of two recursion formulas:

$$K_{a,c,b}^{\lambda,\mu,\nu}=\frac{1}{\lambda}\{R_{a+c,b}^{\lambda+\mu,\nu}+aK_{a-1,c,b}^{\lambda,\mu,\nu}\} \quad \text{(valid for } a=0\text{)}, \quad (1)$$

[28] The potential function would have the form:

$$\left\{\frac{B+B'e^{-(\Delta a)r}}{2}P+\frac{B-B'e^{-(\Delta a)r}}{2}PQ\right\}e^{-ar}.$$

[29] Gamow and Teller, Phys. Rev. **51**, 289 (1937). This theory appears to be inconsistent with the observed proton-proton scattering at small angles.

[30] Feenberg and Wigner, Phys. Rev. **51**, 95 (1937).

[31] Wigner, Phys. Rev. **51**, 106 (1937).

[32] Rose and Bethe, Phys. Rev. **51**, 205 (1937).

[33] For certain purposes, e.g., approximate calculations on intermediate and heavy nuclei, it may prove useful to have approximate values for the range and depth of the forces. In this case one may distribute the errors of the model more evenly by taking a radius of interaction for the Gaussian potential intermediate between the value of 1.95×10^{-13} cm determined by our method and the value of 2.25×10^{-13} obtained by Feenberg and Share. A suitable set of constants for $Ae^{-(r/a)^2}$ would be: $a=2.1\times10^{-13}$ cm, A (triplet) $=78.3\ mc^2$, A' (singlet) $=42.5\ mc^2$.

$$K_{a,c,b}{}^{\lambda,\mu,\nu}=\frac{1}{\nu}\{bK_{a,c,b-1}{}^{\lambda,\mu,\nu}-R_{a,b+c}{}^{\lambda,\mu+\nu}\}, \tag{2}$$

$$K_{a,c,0}{}^{\lambda,\mu,\nu}=\frac{1}{\nu}\{R_{a,c}{}^{\lambda,\mu}-R_{a,c}{}^{\lambda,\mu+\nu}\},$$

where

$$R_{j,k}{}^{\alpha,\beta}=\int_0^\infty dx e^{-\alpha x}x^j\int_x^\infty dy e^{-\beta y}y^k.$$

The integrals $R_{j,k}{}^{\alpha,\beta}$ are evaluated from the recurrence relations:

$$R_{j,k}{}^{\alpha,\beta}=\frac{1}{\alpha}\{S_{j+k}{}^{\alpha+\beta}+jR_{j-1,k}{}^{\alpha,\beta}\} \quad \text{(valid for } j=0\text{)}, \tag{3}$$

$$R_{j,k}{}^{\alpha,\beta}=\frac{1}{\beta}\{kR_{j,k-1}{}^{\alpha,\beta}-S_{j+k}{}^{\alpha+\beta}\}, \tag{4}$$

$$R_{j,0}{}^{\alpha,\beta}=\frac{1}{\beta}\{S_j{}^{\alpha}-S_j{}^{\alpha+\beta}\},$$

where

$$S_n{}^{\gamma}=\int_0^\infty ds e^{-\gamma s}s^n=\frac{n!}{\gamma^{n+1}}.$$

Appendix II

The relativistic correction for H^3

Using the method of Feenberg,[20] we find for the relativistic first-order correction to the kinetic energy of the three-body problem:

$$\Delta T=-3m/8M\int\psi\Delta_1\Delta_1\psi d\tau_1 d\tau_{23}.$$

Let $\psi=Ne^{-(\nu/2)(r_{12}^2+r_{13}^2+r_{23}^2)}=N'e^{-(\nu/2)(3\rho^2+(3\sigma^2/2))}$,

where $\mathbf{r}=\mathbf{r}_1-(\mathbf{r}_2+\mathbf{r}_3)/2$, $\boldsymbol{\rho}=\mathbf{r}_2-\mathbf{r}_3$.

In these coordinates ΔT is readily evaluated to be

$$\Delta T=-(45m/8M)\nu^2=-0.00305\nu^2.$$

The value of ν may be determined by calculating the variational energy of H^3 with the trial wave function ψ and minimizing with respect to ν. This gives:

$$E=9\nu/2-(2B^*+B')F(\sigma), \quad \sigma=1/[b(3\nu/2)^{\frac{1}{2}}],$$

where $F(\sigma)$ is the function defined in Eq. (7). The value of ν obtained by minimizing E is 12.4 and the relativistic correction is $-0.47\ mc^2$. This is considerably larger than the value $-0.2\ mc^2$ estimated by Feenberg for the Gaussian potential, the difference being due to our use of a narrower interaction radius for the forces.

Appendix III

The equivalent two-body method for an arbitrary potential

Let the potential function be represented by $V(r)=B\varphi(r,\ b,\ b_1)$ where $B=B^*$ (effective neutron-proton depth) or $B=B'$ (singlet like-particle depth) and b is the range of the forces and b_1 any other parameter. Let the same potential function for the equivalent two-body problem have the constants D, d and d_1. Using the Gaussian wave function $Ne^{-\mu\nu^2/2}$ the variational energy of the two-body problem is

$$E=\frac{3}{2}\mu-D\frac{4}{\pi^{\frac{1}{2}}}\int_0^\infty e^{-x^2}\varphi(x/\mu^{\frac{1}{2}},\ d,\ d_1)x^2dx. \tag{1}$$

The Gaussian wave functions for H^3, $Ne^{-(\nu/2)(r_{12}^2+r_{13}^2+r_{23}^2)}$, and for He^4, $Ne^{-(\nu/2)(r_{12}^2+r_{13}^2+r_{14}^2+r_{23}^2+r_{24}^2+r_{34}^2)}$, give the following energy expressions:

$$E(H^3)=\frac{9}{2}\nu-(2B^*+B')\frac{4}{\pi^{\frac{1}{2}}}\int_0^\infty e^{-x^2}\varphi(x/(3\nu/2)^{\frac{1}{2}},\ b,\ b_1)x^2dx, \tag{2}$$

$$E(He^4)=9\nu-(4B^*+2B')\frac{4}{\pi^{\frac{1}{2}}}\int_0^\infty e^{-x^2}\varphi(x/(2\nu)^{\frac{1}{2}},\ b,\ b_1)x^2dx. \tag{3}$$

The equivalent method energy is obtained by solving the two-body problem exactly for the fictitious potential $D(r,\ d,\ d_1)$, where the parameters D, d and d_1 are determined by identifying (1) with (2) or (3). Thus for H^3 we must have:

$$D\equiv 2B^*+B', \quad 3\mu/2\equiv 9\nu/2,$$
$$\varphi(x/\mu^{\frac{1}{2}},\ d,\ d_1)\equiv\varphi(x/(3\nu/2)^{\frac{1}{2}},\ b,\ b_1).$$

Substituting the second identity into the third and transforming back to r, we obtain the correspondence relations for H^3:

$$D\equiv 2B^*+B', \quad \varphi(r/(2)^{\frac{1}{2}},\ d,\ d_1)\equiv\varphi(r,\ b,\ b_1).$$

Similarly for He^4

$$D\equiv 4B^*+2B', \quad \varphi(r/(3)^{\frac{1}{2}},\ d,\ d_1)\equiv\varphi(r,\ b,\ b_1).$$

As an illustration consider the relations for H^3 with the Morse potential: $V(r)=-2Be^{-2(r-b_1)/b}+Be^{-4(r-b_1)/b}$. The two-body constants D, d and d_1 are determined by the conditions $D\equiv 2B^*+B'$ and

$$-2e^{2d_1/d}e^{-2r/d(2)^{\frac{1}{2}}}+e^{4d_1/d}e^{-4r/d(2)^{\frac{1}{2}}}\equiv-2e^{2b_1/b}e^{-2r/b}+e^{4b_1/b}e^{-4r/b}.$$

Hence $d=b/(2)^{\frac{1}{2}}$, $d_1/d=b_1/b$, $d_1=b_1/(2)^{\frac{1}{2}}$.

On the Density of Energy Levels of Heavy Nuclei*

JOHN BARDEEN†
Harvard University, Cambridge, Massachusetts
(Received March 15, 1937)

The present calculation of the density of energy levels of a heavy nucleus is based on the statistical model of Van Vleck. As in Bethe's calculation, the particles are assumed to move in a simple potential hole, but the depth of the hole varies with the velocity of the particle. If exchange forces act, the interaction energy of a given particle with the remainder of the nucleus decreases as the velocity of the particle increases. This results in a lower density of states of the individual particles at the top of the Fermi distribution. Bethe's formula for the density of excited levels of the nucleus as a whole may be applied to the present situation if this change in the density of the individual particle states is taken into account. The spacing between the levels is over a hundred times larger than that found by Bethe, and, if one uses the Gamow value for the radius of a radioactive nucleus ($\sim 9\times 10^{-13}$ cm), is much too large to be reconciled with the frequent occurrence of resonance levels for the capture of slow neutrons. If one uses the new value for the radius suggested by Bethe ($\sim 13\times 10^{-13}$ cm), the present theory gives more reasonable values.

I. INTRODUCTION

AN estimate of the average spacing between the energy levels of heavy nuclei is of interest in explaining the frequency of occurrence of resonance levels for the capture of slow neutrons.[1] Bethe[2] has recently made an approximate calculation which is based on a statistical model in which the particles are assumed to move freely in a simple potential hole (constant potential inside the nucleus). If the interaction between nuclear particles is of the exchange type, the interaction energy between a given particle and the remainder of the nucleus depends on the velocity of the particle, and decreases as the velocity of the particle increases. This effect, which is neglected by Bethe, is here roughly taken into account by using the statistical model of Van Vleck.[3] The particles are again assumed to move in a simple potential hole, but the depth of the hole varies with the velocity of the particle. This causes a lower density of states of the individual particles, and a much lower density of states of the nucleus as a whole.

Let us suppose that a slow neutron is absorbed by a nucleus of mass number $A-1$ and angular momentum I_0. The resonance level[1] of the nucleus of mass number A into which the neutron is captured lies at an energy Q above the ground state. Since the neutron will have no orbital angular momentum ($l=0$), the angular momentum of the excited nucleus will be $I_0\pm\frac{1}{2}$ (the $\frac{1}{2}$ arising from the spin of the neutron). We are therefore interested in computing the number of excited levels $\rho(Q, I)dQ$, of given angular momentum I, which have energies between Q and $Q+dQ$.

The lowest state of the nucleus as a whole is that in which all the lowest states of the individual particles are filled up to some maximum energy, ϵ_m, the remaining states being empty. The excited states are those in which particles are taken from the filled levels into some of the previously unoccupied levels, leaving behind unoccupied states or "holes" in the filled band. The energy required to take a particle from one level to another is equal to the difference in the individual particle energies of the corresponding levels. These energies will depend to some extent on the excitation of the nucleus as a whole, but since this effect is small, we will neglect it in our work. To a first approximation, we will not distinguish between the proton and neutron levels. We then suppose that each level may be occupied by four particles, two protons and two neutrons. The total number of particles A, and the number of protons, Z, are fixed.

Bethe[2] has shown that under these conditions,

* Presented at the American Physical Society, Atlantic City meeting, December 30, 1936.
† Society of Fellows.
[1] The theory of the resonance capture of slow neutrons has been given by Breit and Wigner, Phys. Rev. **49**, 516 (1936). For experimental material, see Goldsmith and Rasetti, Phys. Rev. **50**, 328 (1936); Amaldi and Fermi, Phys. Rev. **50**, 899 (1936) where further references to the literature may be found.
[2] H. A. Bethe, Phys. Rev. **50**, 332 (1936). The equations of Bethe mentioned in the text refer to this paper.
[3] J. H. Van Vleck, Phys. Rev. **48**, 367 (1935). This work is based on that of P. A. M. Dirac, Proc. Camb. Phil. Soc. **26**, 376 (1930).

the density of levels of the nucleus as a whole depends on the density of the levels of the individual particles, and on their mean square angular momentum, $[j(j+1)]_{Av}$. Both refer to energies, ϵ_m, in the neighborhood of the top of the Fermi distribution. His formula, with some minor modifications,[4] may be written

$$\rho(Q, I) = 9(2I+1)[j(j+1)]_{Av}^{-\frac{1}{2}}(\pi^3/216x^2Q)e^x, \quad (1)$$

where $$x = \pi(8N(\epsilon_m)Q/3)^{\frac{1}{2}} \quad (2)$$

and the number of levels of the individual particles between the energies ϵ and $\epsilon+d\epsilon$ is $N(\epsilon)d\epsilon$. This formula applies only to levels of low angular momentum, I.

If, following Bethe, we assume that the particles move freely in a sphere of radius R, so that we need consider only the kinetic energy of the particles, the quantities entering (1) have the following values. The kinetic energy, ζ, of a particle at the top of the Fermi distribution is

$$\zeta = \epsilon_m = (\hbar^2/2M)(9\pi A/8R^3)^{\frac{1}{3}}. \quad (3)$$

It should be noted that if the volume of the nucleus is proportional to the number of particles contained in it, ζ is independent of A. The density of levels, for $\epsilon = \epsilon_m$ is:

$$N_0(\epsilon_m) = (MR^2/\hbar^2)(A/3\pi^2)^{\frac{1}{3}} = 3A/8\zeta. \quad (4)$$

Each such level may be occupied by two protons and two neutrons. We thus have

$$x = \pi(AQ/\zeta)^{\frac{1}{2}}. \quad (5)$$

The mean square angular momentum is (Cf. Bethe, Eq. (44)):

$$[(j+\tfrac{1}{2})^2]_{Av} = (4/5)MR^2\hbar^{-2}\epsilon_m = (3^{4/3}\pi^{\frac{1}{3}}/10)A^{\frac{1}{3}}. \quad (6)$$

Substituting these values in (1), we have

$$\rho(Q, I) = \pi^4 10^{\frac{1}{2}}(2I+1)x^{-4}\zeta^{-1}e^x/216, \quad (7)$$

which should be compared with Bethe's Eq. (49). The numerical factor is slightly different from that given by Bethe.[5]

[4] Cf. Bethe; reference 2, Eq. (41). Bethe does not consider explicitly the general case in which the density of the individual particle states is given arbitrarily, but his method may be extended to yield the result given above.

[5] Bethe does not take the exclusion principle into account in his derivation of $p(M)$ (the probability that a state has the Z component of angular momentum M), given in Eq. (34) and following. The proper correction can be made by dividing his n (Eq. (45)) by $2 \log 2$. There is an error of a factor of $\sqrt{2}$ in passing from Eq. (45) to Eq. (46).

The decrease in the potential energy of a particle as its velocity is increased (considered in the next section) has the effect of decreasing $N(\epsilon_m)$ by a factor of about two. The density of levels of the nucleus as a whole is very sensitive to the density of levels of the individual particles, since this term enters exponentially in (1). For reasonable values of the excitation energy $Q(\sim 8\text{MV})$, x is of the order 20 for a moderately heavy nucleus ($A \sim 100$). Thus a decrease in $N(\epsilon_m)$ by a factor two decreases x by about 6 and $\rho(Q, I)$ by a factor $(1/4)e^6$ or a little over 100. With the Gamow value for the radius of a radioactive nucleus ($R \sim 9\times 10^{-13}$ cm), it is found that the resulting spacing between the levels is too large to be reconciled with the frequent occurrence of resonance levels for the capture of slow neutrons. If, however, one uses the larger value for the radius suggested by Bethe[6] ($\sim 13\times 10^{-13}$ cm) more reasonable values are obtained (Cf. Section 3).

2. Density of States of the Individual Particles

The correct form for the interactions between nuclear particles is still rather uncertain. In the present work we shall assume that the interaction potential between any two nuclear particles is a linear combination of the Majorana and Heisenberg operators,

$$((1-g)P^M + gP^H)J(r). \quad (8)$$

The operator P^M interchanges the space coordinates of the two particles; P^H interchanges both space and spin coordinates; and r is the distance between the particles. The Coulomb repulsion between the protons is neglected.

We assume that the particles have individual wave functions, and that in the lowest level of the nucleus as a whole, each individual state is doubly occupied with like particles having opposite spins. The wave function of the nucleus as a whole is approximated by a product of determinants corresponding to the neutrons and protons. The mean value of the energy under these conditions has been computed by Breit and Feenberg.[7] They find:

[6] H. A. Bethe, Phys. Rev. **50**, 977 (1936).

[7] G. Breit and E. Feenberg, Phys. Rev. **50**, 850 (1936).

$$E=T+(1-\tfrac{1}{2}g)E_{ex}{}^{\nu\nu}+(-\tfrac{1}{2}-\tfrac{1}{2}g)E^{\nu\nu}+(1-\tfrac{1}{2}g)E_{ex}{}^{\pi\pi}+(-\tfrac{1}{2}-\tfrac{1}{2}g)E^{\pi\pi}+(2-g)E_{ex}{}^{\nu\nu}, \quad (9)$$

where T is the kinetic energy, and

$$E^{\alpha\beta}=\tfrac{1}{2}\int\int \rho_\alpha(x)J(x-x')\rho_\beta(x')dxdx', \quad (10)$$

$$E_{ex}{}^{\alpha\beta}=\tfrac{1}{2}\int\int \rho_\alpha(x,x')J(x-x')\rho_\beta(x',x)dxdx',$$

$$\alpha,\beta=\nu \text{ or } \pi; \quad \rho_\alpha(x)=\rho_\alpha(x,x).$$

The index π refers to protons and ν to neutrons. The Dirac density matrix $\rho_\alpha(x,x')$ is obtained by summing over all space states, each doubly occupied state occurring twice.

The individual particle energies are given by:

$$\epsilon_{\alpha i}=\int\psi_{\alpha i}{}^*(x)\left(-\frac{\hbar^2}{2M}\Delta\right)\psi_{\alpha i}(x)dx$$

$$+(1-\tfrac{1}{2}g)\int\int\psi_{\alpha i}{}^*(x)\psi_{\alpha i}(x')J(x-x')\rho_\alpha(x',x)dxdx'$$

$$+(-\tfrac{1}{2}-\tfrac{1}{2}g)\int\int\psi_{\alpha i}{}^*(x)\psi_{\alpha i}(x)J(x-x')\rho_\alpha(x')dxdx'$$

$$+(1-\tfrac{1}{2}g)\int\int\psi_{\alpha i}{}^*(x)\psi_{\alpha i}(x')J(x-x')\rho_\beta(x',x)dxdx'. \quad (11)$$

If a particle is excited from a state i to a state j the excitation energy of the nucleus is given to a first approximation by $\epsilon_j-\epsilon_i$. We neglect the effect of the excitation of the nucleus on the density matrices, and therefore on the individual particle energies. The excitation energy, Q, of a nucleus with several particles excited will then be the sum of the energies of the excited particles minus the sum of the energies of the holes left behind in the filled band. In this approximation states of different multiplicities will have the same energy. However, in counting the number of levels, the only degeneracy we assume is that resulting from the angular momentum of the nucleus.

For the present calculation we use the statistical model[8] of the nucleus; i.e., we take the plane wave functions

$$\psi_{\alpha\mathbf{k}}=V^{-\frac{1}{2}}e^{i\mathbf{k}\cdot\mathbf{x}}, \quad (12)$$

in which V is the volume of the nucleus and $\mathbf{k}$ is the propagation vector. The density of states in k space is then

$$n(\mathbf{k})d\mathbf{k}=(2\pi)^{-3}Vd\mathbf{k}. \quad (13)$$

The density of states in energy, with which we are concerned, is

$$N(\epsilon)d\epsilon=(2\pi^2)^{-1}Vk^2(dk/d\epsilon)d\epsilon \quad (14)$$

if it be assumed that ϵ depends only on the magnitude of $\mathbf{k}$ and not on its direction. Each such state may be occupied by two like particles of opposite spins. The occupied states are assumed to fill a sphere in k space of radius k_α ($\alpha=\nu$ or π), where

$$k_\pi=(9\pi Z/4R^3)^{\frac{1}{3}}; \quad k_\nu=(9\pi N/4R^3)^{\frac{1}{3}}; \quad (15)$$

and Z and N are the numbers of protons and neutrons, respectively. Again, R is the radius of the nucleus. In actual nuclei k_π and k_ν are very nearly equal, and we will later obtain certain simplifications by assuming that they are both equal to:

$$k_m=(9\pi A/8R^3)^{\frac{1}{3}}, \quad (16)$$

where A is the mass number. If the volume of the nucleus is proportional to the mass, k_m will be independent of A.

The Dirac density matrix corresponding to a sphere of particles in k space is:[8]

$$\rho_\alpha(r)=(\sin k_\alpha r-k_\alpha r\cos k_\alpha r)/\pi^2r^3; \quad r=|\mathbf{x}-\mathbf{x}'|. \quad (17)$$

Substitution in (11) gives the following expression for the energy of an individual particle in the statistical model:

$$\epsilon_{\alpha k}=(\hbar^2/2M)k^2+(1-\tfrac{1}{2}g)(\zeta(k,k_\nu)-\zeta(k,k_\pi))-(\tfrac{1}{2}+\tfrac{1}{2}g)(4k_\alpha{}^3/3\pi)\int_0^\infty J(r)r^2dr \quad (18)$$

$$\text{where } \zeta(k,k_\alpha)=\int \exp(i\mathbf{k}\cdot\mathbf{r})J(r)\rho_\alpha(r)d\mathbf{r}. \quad (19)$$

The last term on the right-hand side of (18) is independent of k, and so represents an additive constant which may be neglected for the present considerations.

[8] J. H. Van Vleck, reference 3, or E. Wigner and F. Seitz, Phys. Rev. **43**, 804 (1933).

If we use for $J(r)$ the Gaussian function $A_s e^{-\alpha r^2}$, the integral on the right-hand side of (19) may be evaluated.[9] The result is:

$$\zeta(k, k_a) = A_s\{\text{erf}\,(\omega_+) - \text{erf}\,(\omega_-) + (4\alpha/\pi k^2)^{\frac{1}{2}}(\exp(-\omega_+^2) - \exp(-\omega_-^2))\}, \quad (20)$$

where $\omega_\pm = (k \pm k_a)/2\alpha^{\frac{1}{2}}$

$$\text{erf}\,\omega = 2\pi^{-\frac{1}{2}}\int_0^\omega e^{-x^2}dx.$$

In order to find the density of states in energy, we need to compute $d\epsilon/dk$. With the approximation $k_\nu = k_\pi = k_m$, we have, for $k = k_m$,

$$k_m(d\epsilon/dk)_{k=k_m} = \hbar^2 k_m^2/M - (2-g)A_s(\pi y)^{-\frac{1}{2}}f(y), \quad (21)$$

where $y = k_m^2/\alpha$

and $f(y) = e^{-y}(y+2) + y - 2.$

The first term on the right-hand side of (21) comes from the kinetic energy, the second term from the potential energy, of the particle. Omission of the potential energy term leads to Bethe's formula (7) for the density of levels, $\rho(Q, I)$. This term is, however, of the same order of magnitude as the kinetic energy term. It is convenient to express our result as a ratio of the slope of the total energy (kinetic plus potential) to the slope of the kinetic energy at the top of the Fermi distribution ($k = k_m$). This ratio, which we call γ is equal to the ratio of the density of states (in energy), $N_0(\epsilon_m)$, of the free particle model[10] (kinetic energy only included) to the density of states, $N(\epsilon_m)$, of our statistical model, as follows from (14). We have:

$$\gamma = N_0(\epsilon_m)/N(\epsilon_m) = 1 - (2-g)A_s(\alpha l^2)^{-1}(\pi y^3)^{-\frac{1}{2}}f(y), \quad (22)$$

TABLE I. *Values of* $\gamma = N_0(\epsilon_m)/N(\epsilon_m)$ *for the symmetric potential,* $(0.8P^M + 0.2P^H)A_s e^{-\alpha r^2}$, *as computed from Eq. (22).*

$\alpha^{-\frac{1}{2}}$(cm)	$A_s(mc^2)$ \ R(cm)	γ 9×10^{-13}	11×10^{-13}	13×10^{-13}
2.8×10^{-13}	−53	2.34	2.40	2.35
2.0×10^{-13}	−81	2.07	1.94	1.78
1.6×10^{-13}	−105	1.76	1.60	1.45

[9] C. H. Fay, Phys. Rev. **50**, 560 (1936).
[10] Given by Eq. (4).

where A_s is expressed in units of mc^2 and $l = (\hbar^2/Mmc^2)^{\frac{1}{2}}$ is Feenberg's unit of length (8.97×10^{-13} cm). Values of γ for different values of α and R, computed from (22), are given in Table I. The value $g = 0.2$ was used. The values of A_s for the corresponding values of α were estimated from the work of Feenberg and Share.[11] These values bear out the statement, made earlier, that the dependence of the potential energy of a particle on the velocity of the particle (or on k) reduces the density of states of the individual particles by a factor of about two at the top of the Fermi distribution.

In order to see how the ratio depends on the type of interactions assumed, the corresponding calculations have been carried out with the omission of like-particle interactions. The analysis shows that in this case

$$\gamma = 1 - (1 - \tfrac{1}{2}g)A_{\pi\nu}(\alpha l^2)^{-1}(\pi y^3)^{-\frac{1}{2}}f(y). \quad (23)$$

The values of γ as computed from (23) are given in Table II. The strength of the interaction, $A_{\pi\nu}$, is somewhat larger than the strength for the symmetric potential, A_s, in order to obtain the proper binding energies for the light particles. It is seen that the values of γ are not extremely sensitive to the type of interaction involved. The value of γ would, however, be greatly reduced if the interactions were not of the exchange type.

3. Density of Levels of the Nucleus as a Whole

From the density of states of the individual particles, one can easily obtain the density of levels of the nucleus as a whole from Bethe's expression (1). The value of x is now:

$$x = \pi(AQ/\gamma\zeta)^{\frac{1}{2}} \quad (24)$$

with γ given by (22) or (23) and ζ by (3). The

TABLE II. *Values of* $\gamma = N_0(\epsilon_m)/N(\epsilon_m)$ *for neutron-proton interaction as computed from Eq. (23).*

$\alpha^{-\frac{1}{2}}$(cm)	$A_s(mc^2)$ \ R(cm)	γ 9×10^{-13}	11×10^{-13}	13×10^{-13}
2.8×10^{-13}	−71	1.89	1.93	1.90
2.0×10^{-13}	−108	1.71	1.63	1.52
1.6×10^{-13}	−140	1.51	1.40	1.30

[11] E. Feenberg and S. S. Share, Phys. Rev. **50**, 253 (1936).

TABLE III. *Average spacing,* Δ_0, between nuclear levels of zero angular momentum, for $\gamma=2$.*

R (cm) for $A=230$	ζ (MV) \ QA (MV)	Δ_0 200	400	600	800	1000	1200	1400
9×10^{-13}	21.5	6.7×10^6	1.8×10^6	4.3×10^5	1.3×10^5	5.7×10^4	1.38×10^4	5250
11×10^{-13}	14.4	2.4×10^6	3.2×10^5	4.5×10^4	9000	2100	5200	152
13×10^{-13}	10.3	7.5×10^5	5.3×10^4	5000	660	109	18	3.3

* Units of Δ_0 are ev.

mean value of $(j+\frac{1}{2})^2$ will again be given by (4). We thus have:

$$\rho(Q, I)=10^{\frac{1}{2}}\pi^4(2I+1)x^{-4}(\gamma\zeta)^{-1}e^x/216. \quad (25)$$

The mean spacing between the levels is now:

$$\Delta=1/\rho(Q, I)=\Delta_0/(2I+1) \quad (26)$$

with $$\Delta_0=216\times10^{-\frac{1}{2}}\pi^{-4}\gamma\zeta x^4e^{-x}. \quad (27)$$

Values of Δ_0 computed from Eq. (27) are given in Table III for $\gamma=2$, and for different assumed values of the nuclear radius, R. The values of the nuclear radius listed are for a nucleus of mass number $A=230$; it is assumed that the volumes of all nuclei are proportional to A. The Gamow value is $R=9\times10^{-13}$ cm, while the value recently suggested by Bethe is 13×10^{-13} cm. This table should be compared with Bethe's Table I.

The energy Q set free in the capture of a slow neutron is of the order 7–10 MV. The relevant values of QA thus range from about 800 MV for $A\sim100$ to about 1400 MV for very heavy nuclei ($A\sim200$). From the table, one sees that the mean spacing of levels of zero angular momentum ($I=0$) ranges from 150,000 to 5000 volts if $R=9\times10^{-13}$ cm and from 1000 to 4 volts if $R=13\times10^{-13}$ cm. An average spacing of some tens of thousands of volts seems to be much too large to be reconciled with the frequent occurrence of resonance levels; an average spacing of some hundreds of volts would be more reasonable. The results of the present calculation thus give evidence in favor of the larger radius. A radius as large as 13×10^{-13} cm is not required, however, as the values of Δ_0 listed in Table III for this radius are probably somewhat too small, and they would be even smaller if we had taken into account the decrease of γ with R which is given in Table I.

It is questionable how much one can rely on a calculation of the density of nuclear levels which is based on a statistical model. Actually very few particles are excited. The total number of excited particles and holes is

$$n=\frac{6}{\pi}\left(\frac{AQ}{\gamma\zeta}\right)^{\frac{1}{2}}\log 2,$$

which, for $AQ=1000$ MV, $\zeta=20$ MV and $\gamma=2$ is only 6 or 7. The number is increased to 9 if $\zeta=10$ MV (corresponding to $R=13\times10^{-13}$ cm) for the same values of AQ and γ. The fluctuations in the density of levels among the individual nuclei are probably quite large. The calculation almost certainly leads to a too high density of levels of high angular momenta. If the computed value of the density of levels of low angular momenta is also too high, the conclusion that the frequency of occurrence of resonance levels indicates a larger radius than the Gamow value would not be invalidated.

Regularity Along a Series in the Variation of the Action Cross Section with Energy Discrepancy in Impacts of the Second Kind

O. S. DUFFENDACK AND W. H. GRAN
University of Michigan, Ann Arbor, Michigan
(Received February 25, 1937)

The enhancement of the intensities of lines in the spark spectrum of lead when excited by impacts of the second kind with neon ions relative to their intensities in electron impact excitation was measured. When the values of the enhancements are plotted against the energy discrepancies of the spectral terms in which the lines originate, smooth characteristic curves can be drawn through the points belonging to the same spectral series. The curves for different series, while similar in form, exhibit marked differences in details. Measurements were made on terms of negative as well as on terms of positive energy discrepancy. Maxima appear in the curves on the side of positive energy discrepancy, i.e., on the side where the energy values of the terms are less than the ionization potential of neon. The form of the curves beyond the maxima indicates that they may be of the form $q=A/\sigma^x$ where the value of both A and x vary with the particular series. The terms of the D series are most strongly enhanced. A calculation fixes the cross section for these collisions at approximately 15×10^{-11} cm².

I. INTRODUCTION

THE term "collision of the second kind," since first introduced, has come to have a broader meaning than that given it by Klein and Rosseland. In the present study we are concerned with a special type of such a collision, namely, one in which a normal lead atom collides with a neon ion and, as a result, the lead atom becomes both ionized and excited, while the neon ion returns to its normal state. The reaction may be represented in the following manner:

$$Pb+Ne^+\rightarrow Pb^{+\prime}+Ne+\sigma, \qquad (1)$$

where σ, the energy discrepancy, represents the difference between the initial energy of the Ne ion and that of the final excited state of the Pb ion formed in the collision.

Although collisions may also occur between neon atoms in a metastable state and normal lead atoms, these, as will be shown, will not affect the results obtained.

The probability of an energy transfer as the particles approach each other is measured in terms of an action cross section which may be defined as follows. If we have in unit volume N_1 excited atoms of type A in state E_i and N_2 normal atoms of type B in state F_k, and if their relative velocity is u, then the number of collisions, n, which result in raising the type B atoms to the excited state F_j is given by

$$n=qN_1N_2u, \qquad (2)$$

where q is the action cross section for that particular type of collision. The action cross section may be expressed in terms of the probability of energy transfer, upon approach to a distance r, in the following manner. Let $P(r)$ represent this probability. If, as above, we have N_1 atoms of one kind and N_2 of another per cc, the number of the N_1 kind which approach one of the N_2 atoms to within a distance between r and $r+dr$ will be $N_2u\cdot2\pi rdr$ and the total number of such approaches will be given by $N_1N_2u\cdot2\pi rdr$. Hence the total number of such approaches resulting in energy transfer will be given by

$$n=N_1N_2u\int_0^\infty P(r)2\pi rdr \qquad (3)$$

and, comparing with the above, we have

$$q=\int_0^\infty P(r)2\pi rdr. \qquad (4)$$

Early investigation of collisions of this type were largely of a qualitative nature. Only recently have quantitative results been published[1,2] in which action cross sections were calculated in terms of measured intensities of spectral lines. It has been found that the action cross section in these cases, as well as in those of a related nature, such as the quenching of resonance radiation, diminishes as σ increases and that the probability of an energy transfer is high only when σ is small.

[1] Duffendack and Thomson, Phys. Rev. **43**, 106 (1933).
[2] Duffendack and Manley, Phys. Rev. **47**, 56 (1935).

In these previous studies no attempt was made to determine any relationship between action cross section and energy discrepancy as a function of the different series of energy levels in a colliding atom. The work of Duffendack and Manley[2] on collisions between neon ions and magnesium atoms appeared to indicate that such a relationship did exist and a prediction was made that a definite regularity would be found for any one series, which might differ widely from one series to another. The prediction was based on the relatively small number of levels in each series that could be excited.

It was the purpose of the present investigation to determine whether such regularity exists and, if possible, to determine its nature. To do this it was necessary to observe at least three or four levels of each series and in as many series as possible.

II. Experimental Method

Experimentally the action cross section cannot be determined directly, but has been expressed in the usual manner in terms of an "enhancement" of those energy levels affected by the reaction. The enhancement of the energy level is expressed as the ratio of the intensity of a line originating in that level when excited principally by impacts with Ne ions to the intensity of that line when its initial level has been excited by electron impact. This is quite justified, since the intensity of a line is directly proportional to the number of atoms in a particular state and the number of atoms in that state is directly proportional to the efficiency of the process producing that state. Hence, we may consider:

$$\text{Enhancement} = \frac{\text{Eff. of energy transfer by collision of 2nd kind}}{\text{Eff. of energy transfer by electron impact}} = \frac{\text{Action cross section for collision of 2nd kind}}{\text{Action cross section for electron impact}}. \quad (5)$$

Since the investigation was one to determine series regularities, the first essential was to find a combination of particles such that the one should have many energy levels near the ionization level of the other. The most favorable combination was found to be lead and neon. At least four levels in each of four series for the lead ion are near enough the lowest level for the neon ion to be affected. The lines coming from these levels whose intensities were measured are listed in Table I. Lead had the further favorable properties of relatively low boiling point, making it easy to obtain in vapor state, and the lines involved were within the spectral region where good intensity measurements were possible.

The experimental technique employed was, with slight modification, that used by Duffendack and Manley[2] in the study of collisions between magnesium and neon. The method of excitation was that of the low voltage arc in neon in the presence of lead vapor. For a diagram of the tube see the paper by Duffendack and Manley.[2] The electrode assembly consisted of a quartz crucible, in which the lead was vaporized by means of a spiral heating coil of 12-mil tungsten wire. The crucible was enclosed in a nickel cylinder to reduce radiation losses. A flat, spiral filament of isovolt alloy placed near the mouth of the crucible served as the hot cathode for the arc, while the anode consisted of a nickel hood completely covering the filament and the crucible. The anode was provided with a rectangular side tube about 15 mm long and 2.5×5 mm in cross section, which was placed directly above the heated crucible and about 2 mm in front of the filament. This tube was lined up with the quartz window of the discharge tube and with the slit of the spectrograph. This arrangement greatly reduced the diffusion of the lead vapor and still permitted light from the arc to reach the spectrograph.

The measurements covered a range of wavelengths from about 2400A to 5074.6A. Two spectrographs were used during the course of the investigation. Both were quartz instruments made by Hilger. For the range λ3451.7 to λ5074.6 the type E-1 was used and for the shorter wavelengths, the smaller one, type E-2. Eastman polychrome plates were found quite satisfactory for both instruments.

Excitation by neon ion collisions was readily obtained. Measurements of intensities at a number of neon pressures from 5.5 mm to 1.6 mm indicated that the intensity was independent of the pressure. This would be expected since the low voltage arc, characterized by a neutral space charge, requires a constant concentration of positive ions for a given current.

At least two other methods of excitation were theoretically possible. Excitation by electron impact might be expected to some extent and, to a less extent, excitation due to the fact that the initial levels may be populated by transitions from above. That both of these effects are negligible appears clear from the following observations. The lines could not be obtained at all when the Ne pressure was reduced to a few hundredths of a millimeter. The arc was operated at about 24 volts, only a little above the ionizing potential of neon, and when the Ne pressure was reduced to 0.05 mm a sixteen-hour exposure at 150 volts failed to excite a single one of the lines. Thus the effect of electron impacts must certainly be negligible at the low voltage. Concerning the effect of transitions from above, it appears reasonable to assume that if the levels with which we were concerned could not be measurably excited by electron impacts, those levels still higher were even less likely to be thus excited. No lines from the higher levels were observed and thus the populations of such levels must have been extremely small and transitions from them negligible. We thus assume that the excitation observed is due entirely to collisions of the second kind.

To obtain the normal or electron excitation for comparison, much higher voltages were necessary. A spiral filament of 12-mil tungsten wire was used instead of the isovolt alloy as the latter broke down rapidly under the severe positive ion bombardment at the higher voltages. In order to prevent too rapid diffusion of the lead a small amount of He was admitted into the discharge tube. The He pressure was made such that the mean free path of the electrons was approximately 3 mm, the distance from the filament to the portion of the arc photographed. This required a He pressure of about 0.33 mm.[3] The potential necessary to excite the levels by electron impact was about 450 volts. Under these conditions an exposure of 30 minutes was sufficient to bring out the lines.

That the spark lines thus obtained are purely electron excited may be assumed for the following reasons. They could not have been due to impacts of the second kind with He ions, since the ionizing potential of He is 3 volts above that of Ne. Further, if any were due to such impacts, it would have been evident at the lower voltages. Conceivably it might have been due in part to collisions of the second kind with He metastable atoms whose excitation potential is only one volt below the ionizing potential of Ne. Again, if such effects were present, they would have occurred as well at lower voltages. Measurements also show that the levels in closest resonance with the metastable He were not appreciably enhanced. These facts, together with the high voltage necessary for the excitation, would appear to exclude all possibilities except that of electron impact.

The method of measuring the intensities of the lines was that developed by Thomson and Duffendack[4] in which a step diaphragm was used to place a calibration pattern on each plate that was measured.

TABLE I. *Lines of Pb II whose enhancement by collisions of the second kind with excited neon ions has been measured. Standard for lines λ3117.7 to λ2498.9 = Pb I, λ2476.4.*

Line	Initial Level	Intensity		Enhancement	Energy Discrepancy	
		Ne Impact	Electron		cm	volts
5074.6	7*g*	0.84	0.30	2.8	1879	0.23
5070.7	7*g*	0.91	0.30	3.0	1879	0.23
5042.0	7*d*	0.89	1.60	0.58	19825	2.44
4582.3	8*g*	1.24	.58	2.14	−237	.029
4579.1	8*g*	1.35	.66	2.05	−237	.029
4352.7	8*f*	2.19	.65	3.40	2116	.26
51.5	8*f*					
4296.6	9*g*	.43	.34	1.30	−1688	−.207
4293.8	9*g*	.52	.62	.85	−1688	−.207
4242.5	5*f*	2.12	2.50	.85	21580	2.66
4195.5	11*p*	.48	.12	4.00	1309	.17
3971.3	9*f*	1.02	.35	2.80	−41	−.0055
3785.9	5*f*	2.40	3.00	.80	21580	2.66
3784.0	10*p*	.37	.13	2.90	4258	.525
3718.2	9*s*	1.00	1.00	1.00	12763	1.58
3714.0	8*d*	2.24	2.17	1.03	9919	1.22
3665.6	8*p*	.85	.97	.88	17871	2.20
3451.7	6*f*	2.08	1.29	1.60	11229	1.39
3117.7	9*d*	1.14	.28	4.10	4763	.59
2986.9	10*s*	.067	.039	1.70	6179	.76
2914.5	11*s*	.17	.031	5.50	2535	.31
2887.3	7*f*	.102	.040	2.60	5580	.69
2840.6	10*d*	1.22	.108	11.40	1541	.19
2772.7	9*p*	.067	.045	1.50	9087	1.12
2728.4	12*s*	.110	.021	5.50	197	.024
2717.5	8*p*	.366	1.080	.342	17891	2.20
2693.6	11*s*	.120	.023	5.20	2535	.31
2684.9	11*d*	.322	.065	5.00	−398	−.049
2634.3	10*d*	1.20	.088	13.50	1700	.21
2526.7	7*f*	.96	.370	2.70	5580	.69
2498.9	11*d*	.183	.038	4.90	−357	−.044

[3] K. T. Compton, Phys. Rev. **22**, 338 (1923).

[4] Thomson and Duffendack, J. Opt. Soc. Am. **23**, 101 (1933).

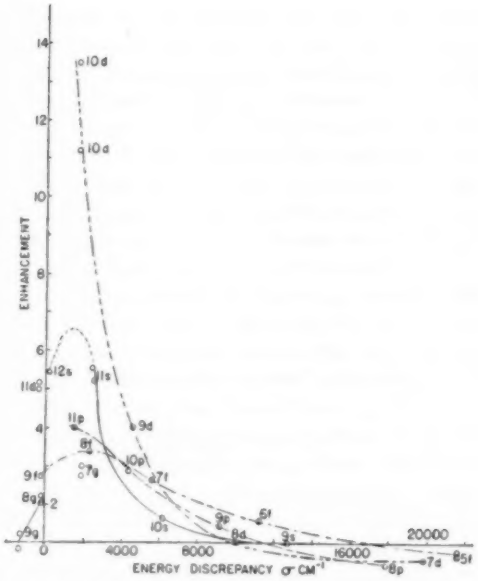

FIG. 1. Variation of enhancement with energy discrepancy.

All intensities were measured in terms of "standards" whose values were assumed to remain the same in the two types of excitation. Two such standards were necessary, one for each spectrograph. In the region of the E-1 spectrograph the line used as the standard was the Pb II line 9S→7P, λ3718.2. Its initial level was about 1.6 volts below the neon ion level and it would, therefore, not be expected to be enhanced by neon ions. The standard for the shorter wavelength region was the Pb I line λ2476.4 and one could be absolutely certain that this one was not affected by neon ions. The smooth curves obtained, when the measurements based upon the two standards were combined, indicate that neither standard was enhanced.

III. Experimental Results

The results of this investigation are presented in Table I and in the curves of Fig. 1.

The measurements given are the average values from a number of plates. In the region of the E-1 spectrograph, the average of four exposures at four different pressures, varying from 5.5 mm to 1.6 mm of Ne, were taken as the Ne impact intensities. These intensities remain constant within the limits of experimental error. In this region two exposures for electron excitation were obtained and two microphotometer tracings made from each, giving again four measurements. In the region of the E-2 spectrograph three good exposures were obtained with each type of excitation. In these measurements the average deviation from the mean in nearly all cases was less than 10 percent. In a very few instances of either very weak or very strong lines it was between 10 percent and 15 percent. In all cases when the error was over 10 percent the levels were far removed from resonance and hence came on the flat portion of the curve.

IV. Discussion

An examination of the curves shows clearly that no regularity whatever exists in the relation between action cross section and energy discrepancy if we consider all the points as a whole. When we consider the levels of any one series, however, marked regularity is shown. Each series shows a decrease in action cross section with energy discrepancy, σ, and three of the series indicate a maximum value of the cross section on the side of positive energy discrepancy; that is, for the case in which the ion has an amount of energy greater than that of the level excited by collision. Such a maximum may also occur in the D series, but we cannot be certain since the two levels, $10D$ and $11D$, nearest resonance are on opposite sides of the zero energy discrepancy axis. These points cannot be joined because of the asymmetry which is present in all of the curves. In the case of the F series the $8f$ and the $9f$ were joined, even though on opposite sides, but only because the curve on the positive side indicated a maximum at about $8f$ and the curves on the two sides are expected to meet at the axis.

A comparison of the relative positions of the points representing $8f$ and $9f$, $7g$ and $8g$, and $10d$ and $11d$ shows clearly the asymmetry of the curves. Thus the cross section for $8f$ on the positive side where $\sigma = 2163$ cm^{-1} is greater than that for $9f$ at $\sigma = -41$ cm^{-1}.

The exact position of the maxima cannot be determined. They cannot be predicted since no theory has been developed for this type of impact. They depend in part upon the inter-

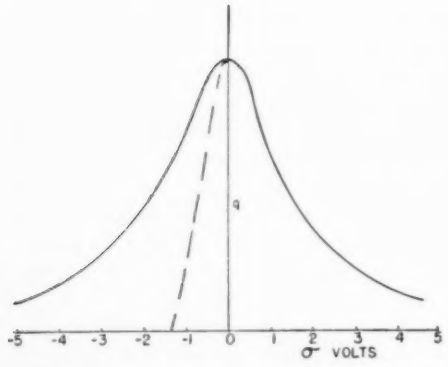

FIG. 2. Showing the relation between cross section and energy discrepancy. Solid curve, according to the theory of Kallmann and Rosen; dashed curve, as modified by taking account of the kinetic energy of the impacting atoms.

action potential curves of the colliding particles and these, at least at present, are outside the range of experimental observation.

The position of the maximum does not occur at the same value of σ for the different series, but in the case of the F series appears to be at about $\sigma = 2000$ cm^{-1} or roughly 0.25 volt. In the case of the S series, the position of the maximum is probably quite well determined, although its magnitude may be considerably in error. No attempt was made to construct a curve for the G series, since only one level, $7g$, was observed for positive values of σ.

As stated above, no theory has been developed for just this type of impact, so only qualitative comparisons are possible between these curves and those theoretically obtained for impacts of a somewhat different type.

In the theoretical treatment of Kallmann and London,[5] an equation is obtained which expresses the action cross section as a function of energy discrepancy for the excitation of *one* state only. In the derivation of the equation it was assumed that an atom had only a normal and one excited state. By neglecting the kinetic energy of the particles and by assuming, further, that, to a first approximation, the atoms upon approaching each other behave as dipoles, the following simple equation was obtained:

$$q\sigma^{\frac{1}{3}} = \text{constant}. \qquad (6)$$

The curve for this equation is symmetrical for values of $+\sigma$ and $-\sigma$ and indicates an infinite cross section for $\sigma = 0$. Since at close resonance the energy transfer proceeds so slowly it is not always completed, the authors, by taking this into account, find a lower limit for the cross section for $\sigma \to 0$. It must be remembered that in this treatment only excitation energy was transferred. There was no ionization and no electron transfer. Beutler and Eisenschimmel[6] show that the reverse reactions in collisions prevent the action cross section from going to infinity for zero energy discrepancy and calculate limiting values of the cross section for various conditions.

Kallmann and Rosen[7] have treated the case in which there was only electron transfer and obtained a curve similar in form to that of Kallmann and London except much broader. Its approximate form is shown in Fig. 2 (solid curve), and it will be noted that it, too, is symmetrical for $+\sigma$ and $-\sigma$.

It was suggested by Tyndall and Powell[8] that an asymmetry would be introduced by taking into account the kinetic energies of the colliding particles. For positive value of σ, there must be a liberation of energy upon impact to the kinetic energies of the particles, and for negative values of σ, energy must be absorbed from the kinetic energy. Thus, in the case of ions of slow speed, we would expect the electron transfer involving a given energy change to be more probable in the case where energy is liberated than where it is absorbed. For very slow speeds, there is no kinetic energy available for absorption and the curve must drop to zero for small negative values of σ. The modified curve would have the form indicated by the dashed curve in Fig. 2.

Morse and Stueckelberg[9] have treated the case where both ionization and excitation occur, but, due to their approximations, obtained values differing materially from those of Kallmann and London only in the region of very close resonance. Within this region, the curves show a maximum cross section for small positive values of σ for the case in which the transition is optically allowed. Since the difference introduced by

[5] Kallmann and London, Zeits. f. physik. Chemie **213**, 220 (1929).

[6] Beutler and Eisenschimmel, Zeits. f. physik. Chemie Abt. **B10**, 89 (1930).

[7] Kallmann and Rosen, Zeits. f. Physik **61**, 61 (1930).

[8] Tyndall and Powell, Proc. Roy. Soc. **A129**, 162 (1930).

[9] Morse and Stueckelberg, Ann. d. Physik **9**, 579 (1931).

Morse and Stueckelberg occurs only for values of σ much smaller than any involved in the present investigation, their curves are of less importance in this case.

A qualitative comparison of the experimental curves with those obtained by Kallmann and London shows that for the region beyond the maximum each of the experimental curves has the same general form as those theoretically obtained. The experimental curves obviously follow an inverse power law, though not as simple a one as that of Kallmann and London. Both the value of the constant and the power of σ must change from series to series, as is evident from the crossing of the curves. The action cross section has a finite value at $\sigma=0$, and the experimental curves are asymmetrical as suggested by Tyndall and Powell.

A striking effect indicated by the curves, but not predicted by the theory, is the marked preference shown for the D levels and a minor preference for the S levels. A tentative explanation of this preference was suggested to us by Dr. Hans Beutler, now at this laboratory. One may assume that at one phase of the impact, the neon ion and the lead atom are bound together into a quasi-molecule. The state of this molecule will be that of an odd spectroscopic term. This molecule dissociates into a normal neon atom and an excited lead ion. Since the normal state of the neon atom is that of an even spectroscopic term, the odd terms, D, S and G series, of the lead ion will be preferred over the even terms, P and F series.

Although it is not possible to calculate accurately the action cross section, one may, by use of Eq. (2), obtain its order of magnitude. Writing the equation as follows: $n=N_eNq_ev\cdots$ (2) where $N_e=$No. of electrons per cc, $N=$No. Pb atoms/cc, we may solve for q_e, the action cross section for electron impact.

Estimating the temperature to be 1300°K and the Pb vapor pressure as 0.02 mm we find $N=1.5\times10^{18}$/cc. N_e may be found from the measure of the arc current, remembering that the current is almost entirely an electron current. From a ratio of the mobility of the positive ions to the electrons and the total current, we may obtain the positive ion current and, from this, the value of n, the number of ionizing collisions per cc per sec. Substituting the values thus obtained we find:

$q_e=6\times10^{-18}$ cm², approximately = action cross section for ionization by electron impact.

Now to find q_{Ne}, the action cross section for Ne ion impact, we must write:

$$\text{Enhancement}=\frac{q_{Ne}N_{Ne}N_{Pb}v_{Ne}}{q_eN_eN_{Pb}V_e}. \qquad (7)$$

From a measure of the currents in the two methods of excitation and from the respective particle velocities, we find that $N_{Ne}/N_e=1/10$. For the Ne^+ excitation, the Pb vapor pressure is estimated to be 0.001 mm, and we thus obtain $N_{Pb}/N_{Pb}'=1/20$. For v_{Ne}/v_e we obtain 1/13000 and substituting these values in Eq. (7) we obtain for an enhancement of 10 the value $q_{Ne}=15\times10^{-11}$ cm². The action cross section for Ne^+ impacts is thus seen to be very large compared to that for electron impacts.

We wish to express our appreciation to Professor S. A. Goudsmit for his interest in discussing with us the theoretical aspects of this research.

Investigation of the Deuteron-Deuteron Reaction[1]

RICHARD B. ROBERTS
Palmer Physical Laboratory, Princeton University, Princeton, N. J.

(Received March 17, 1937)

The excitation curve for the reaction $D^2+D^2\rightarrow He^3+n^1$ has been measured from 40 up to 300 kv. The yield of fast neutrons measured in the forward direction from a thick D_3PO_4 target bombarded by 100 kv deuterons is equivalent to 44 mc of radium-beryllium per microampere. The number of neutrons observed in the forward direction (estimated from the number of recoils produced in air) corresponds to 8.7×10^4 neutrons per second per μa at 100 kv over the entire solid angle if isotropic emission is assumed. However, there is a definite preponderance in the forward direction. The increase of "*C*" neutrons with the increasing thicknesses of paraffin surrounding the neutron source and the neutron detector has been measured for both the D-D neutrons and the Ra-Be neutrons. The two such curves correspond for thicknesses of paraffin greater than 5 cm. With less paraffin, relatively more neutrons are observed from the Ra-Be source. The yield of "*C*" neutrons from a D_3PO_4 target bombarded by 1 μa of 100 kv deuterons is equivalent to that of 15 mC of radium-beryllium, but the yield is very sensitive to the geometrical arrangement of the paraffin surrounding the target. The excitation curve of the reaction $D^2+D^2\rightarrow H^1+H^3$ coincides with that of the alternative reaction for the energy range measured (45–100 kv). The absolute yield of protons, after correcting for the stopping power of the target, is one proton for 6×10^6 deuterons, no correction being made for anisotropy of emission. This agrees within a factor of two within the neutron yield. No resonance was found in either excitation curve.

I. INTRODUCTION

THE disintegraton of deuterium by deuterons (D-D reaction) was shown by Oliphant, Harteck and Rutherford[2] to produce either the emission of a proton and a triterium nucleus or the emission of a neutron and a helium nucleus of mass three. The neutrons were found to be a homogeneous group of 2 Mev energy by Dee.[3] More recently the work of Bonner and Brubaker[4] gives a value of 2.4 Mev energy for the neutrons. The yield of protons for the D-D collisions was estimated by Oliphant, Harteck and Rutherford to be of the order of magnitude of 1 proton for 10^6 incident deuterons at 100 kv. The neutron yield was estimated by them to be of the same order of magnitude.

As this is the simplest reaction for which there are two modes of disintegration, it is important to measure exactly the yield of each and to find out whether the relative probability of the two modes varies with the energy of the bombarding deuterons. Also the high yield reported by Oliphant, Harteck and Rutherford indicated that this reaction might provide an intense source of neutrons of homogeneous energy. It is therefore of practical interest to ascertain what strength neutron source (as compared with a radium-beryllium neutron source) could be realized.

II. APPARATUS

The high voltage used for accelerating the ions was supplied by four 100 kv transformers and rectifier units connected in cascade. The filtering was sufficient to keep the ripple below 1 percent. Two ion sources were used. One was copied from the canal ray discharge tube described by Rutherford and Oliphant,[5] and the other was a low voltage arc similar to that described by Crane, Lauritsen and Soltan.[6] The canal ray source provided an ion beam of 100–200 μa total ion current. Of this current only 2–3 μa of mass two ions were focused on the target which was located 160 cm from the single accelerating gap. In addition light hydrogen could never be eliminated completely from the source and consequently molecular hydrogen ions appeared in the mass two spot. From the current carried by mass one and mass four spots it was estimated that 30 percent of the current in the mass two spot was carried by molecular hydrogen. It was

[1] A summary of the results of this investigation has been published in a letter to the editor, Ladenburg and Roberts, Phys. Rev. **50**, 1190(1936).
[2] Oliphant, Harteck and Rutherford, Proc. Roy. Soc. **A144**, 692 (1934).
[3] Dee, Proc. Roy. Soc. **A148**, 623 (1935).
[4] Bonner and Brubaker, Phys. Rev. **49**, 19 (1936).
[5] Oliphant and Rutherford, Proc. Roy. Soc. **A141**, 259 (1933).
[6] Crane, Lauritsen and Soltan, Phys. Rev. **45**, 507 (1934).

TABLE I. *Composition and energy of ions of different m/e values.*

SPOT	1	2	3	4	5	6	7, 8
Current μa	0.6	1.6	2.4	15	0	3	0
Protons per μc	232	880	412	544	0	292	0
Ions and Energy	H^+, E D^+, $\frac{1}{3}$E DD^+, $\frac{1}{4}$E	HH^+, E D^+, E DD^+, $\frac{1}{2}$E	HD^+, E HHH^+, E DD^+, $\frac{3}{4}$E DDD^+, $\frac{1}{2}$E	DD^+, E HHD^+, E O^+, $\frac{1}{4}$E	HDD^+, E	DDD^+, E C^+, $\frac{1}{2}$E C^{++}, E	O^+, $\frac{1}{4}$E N^{++}, $\frac{1}{4}$E

similarly estimated that atomic and molecular ions were present in equal numbers. The advantage of this type source lies in the high percentage of atomic ions; the disadvantages are the impurity of the mass two ion beam, and the high power and high voltage required for producing the ions.

The low voltage arc was operated under different conditions from those of Crane, Lauritsen and Soltan. A potential of 110 volts was applied between the filament and the anode, and a potential of 3000 volts between the anode and the probe electrode. This source was mounted on a four section accelerating tube and would focus 20 μa of DD^+ ions in a 16 mm spot on the target with 100 kv applied to the tube. A uniform potential distribution along the tube was obtained by wrapping a spiral of 200 10 megohm resistance around it. This was found necessary to stabilize the focusing. The maximum total ion current observed was about 200 μa.

The composition of the ion currents of different e/m from the low voltage arc has been analyzed from the number of disintegrations they produce, counting protons emitted from a D_3PO_4 target bombarded by them. As the tube has four gaps, ions were also found which had been formed by the collision with the gas molecules along the path of the beam and had $\frac{1}{4}$, $\frac{1}{2}$, and $\frac{3}{4}$ of the total voltage E. These ions should be present in approximately equal numbers, as the regions in which ions could be formed which would acquire these fractional voltages are equal. In addition, there may be present multiply charged ions of higher mass.

Table I shows the currents observed for the different spots, the yield of protons produced per microcoulomb (μc), and the possible ions which could be responsible for the spots.

In spite of the complexity of the beam, it becomes apparent that the spot 4 consisted entirely of deuterium molecules. The possible impurities are listed in the table. Since there are no HDD^+ ions the amount of light hydrogen is very small; therefore no HHD^+ ions are contained in spot 4. Neither are there any O^+, $\frac{1}{4}$E ions present, as spot 8 (O^+, $\frac{1}{2}$E) is absent. C^{+++} is very improbable and is for the time assumed absent. Therefore, from the yield of protons per microampere of the spot four, the expected yield of the spot six can be calculated, and is 272. If impurities existed in spot 6, the yield would appear too low. Consequently C^{++} does not exist in spot 6 and C^{+++}, being less probable than C^{++}, does not exist in spot 4. Spot 4 is thereby shown to be pure DD^+ ions. By similar reasoning the composition of the other spots can be determined. This is given in Table II.

The ratio of atoms to molecules (D^+/DD^+) turns out to be 0.08 and the ratio of light to heavy hydrogen present (H/D) is 0.03. The value of D^+/DD^+ is to be expected from Bleakney's measurements.[7] This method of analysis is probably not very accurate, but it does establish the purity of spot 4; therefore this was used for bombarding in the experiments. Incidentally, this analysis shows that the ions formed by collisions between deuterium molecules and 100 kv molecular deuterium ions are mostly atomic.

TABLE II. *Percentage of deuterium ions in the beams of various m/e values.*

Spot	1	2	3	4	5
Ion	D^+, $\frac{1}{4}$E	D^+, E	DD^+, $\frac{1}{2}$E	DD^+, E	DDD^+, E
Percent of current in spot carried by ion listed above	85	70	50	100	100

[7] Bleakney, Phys. Rev. **35**, 1180 (1930).

The voltage was measured with a generating voltmeter and with a high resistance and microammeter, and was additionally checked with a spark gap and by the magnetic analysis of the beam. The generating voltmeter was one built by Harnwell and Van Voorhis.[8] The electrical circuit, however, was changed to a two stage amplifier with a diode rectifier. Provision was made for applying a known field from a potentiometer as a check on the constancy of the amplifier. The generating voltmeter was calibrated by using an alcohol-xylol resistance and a galvanometer. The voltmeter is believed to be accurate to 5 percent in the range 80–300 kv. For greater accuracy in the voltage range up to 200 kv a permanent high resistance voltmeter was constructed of 200 1 watt 10 megohm resistance units. (International Resistance Co. type B-1.) These were wrapped in a spiral around glass rods supported by a textolite cylinder. The change in resistance from heating was negligible up to 250 kv. The accuracy of this method of voltage measurement is believed to be better than 2 percent.

As the current to the target varied somewhat, a current integrator was constructed so that the measurements could be made in terms of neutron (or proton) counts per microcoulomb. A condenser was charged by the ion current to the target, and was periodically discharged through a neon bulb and a resistance. The potential across the resistance operated a thyratron circuit which in turn closed a double pole relay. The relay shorted the condenser and registered on a counter. This integrator was found to be extremely accurate and dependable; its calibration was perfectly linear from 0.1 to 10 μa; and its range could be easily extended to higher or lower currents. Besides this recording device, a microammeter was placed in the ground return for direct reading of the ion current.

The target chamber was designed to avoid errors due to secondary electrons either entering or leaving the Faraday cage surrounding the target. The ion beam was defined by a diaphragm, and screens placed in its "shadow" trapped electrons produced when the ion beam struck this defining diaphragm. As the final check, a small permanent magnet could be placed at the mouth of the Faraday cage; when secondary electrons were present the current to the cage was affected by the magnet. Any measurements made when there was the slightest evidence of any secondary electrons were discarded.

The products of disintegration were detected by use of an ionization chamber, a linear amplifier, and a scale of eight thyraton unit built for this purpose by Dr. J. Giarratana. Four interchangeable ionization chambers were used. One was an air-filled chamber provided with aluminum windows for counting protons; the second was similar, but without windows, for counting neutrons by recoils produced in air; the third has its back surfaces coated with paraffin for counting neutrons by the recoils produced in hydrogen; and the fourth was lined with boron for counting slow neutrons. The resolving time of the counter and amplifier was investigated by Dr. Giarratana, who found that the number of counts missed was negligible for counting rates lower than 3000 per minute.

A standard neutron source of radium bromide mixed with finely powdered beryllium[9] was used both for checking the constancy of the amplifier and counter and as a standard to compare with the yields of neutrons from the deuterium targets. The strength of the source as measured by its gamma-ray activity was 15 millicuries. The neutron activity was within 10 percent of that of a radon-beryllium source of the same gamma-ray activity.

III. Targets

Targets of various deuterium containing substances have been bombarded and their behavior under bombardment as well as the neutron and proton yields observed. KOD targets were prepared by evaporating an excess of 99 percent heavy water onto a piece of clean potassium in a vacuum. The target was then heated in vacuum and the excess water removed. Targets of heavy ammonium salts were prepared by adding heavy water to the normal salt and evaporating the water to leave a crystalline target. Targets of

[8] Harnwell and Van Voorhis, Rev. Sci. Inst. **4**, 540 (1933).

[9] The radium-beryllium source was mixed by Mr. Bilstein of the Radium Chemical Co. under the supervision of Professor Ladenburg.

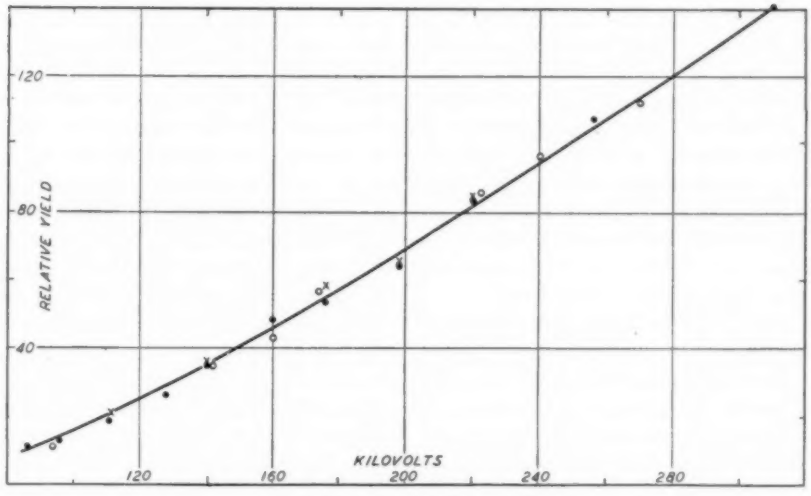

FIG. 1. Fast neutrons from KOD.

D_3PO_4 were prepared by adding 99 percent D_2O to anhydrous P_2O_5.

The behavior of the targets under bombardment varied greatly. A KOD target was bombarded for half an hour with 2 μa of deuterons at 160 kv. In this time the neutron yield fell from 103 counts per minute to 43 per minute. After this initial drop the yield remained within 10 percent of an average value of 45 per minute during a series of measurements lasting five hours. This behavior was typical of all KOD targets used. Targets of ammonium sulphate and chloride were less durable. A thin layer (0.2 mm) of ammonium sulphate was bombarded for half an hour with 6 μa 100 kv deuterons and the yield fell to zero. The target was then examined and it was found that the salt was completely removed in a 16 mm spot where the beam had hit. The D_3PO_4 target was by far the most satisfactory. Several days bombardment had no effect on the yield; it was easy to prepare, and it gave off very little gas for currents up to 12 μa.

IV. FAST NEUTRONS

The variation of the yield of fast neutrons with voltage has been measured from 45 to 300 kv with especial emphasis on the voltages below 100 kv.[10] The yield has also been measured under conditions which permit a calculation of the absolute number of neutrons.

For the voltage variation of the yield from 85 to 300 kv a thick KOD target was bombarded

[10] All voltages refer to the energy of atomic ions.

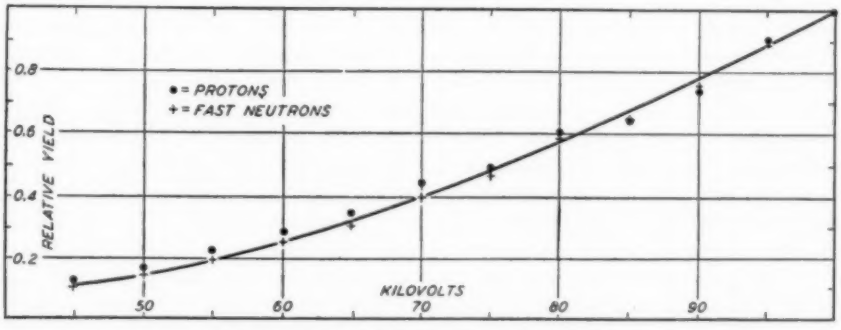

FIG. 2. Protons and fast neutrons from D_3PO_4.

with deuterons from the canal-ray source. The paraffin lined ionization chamber, used to detect the neutrons, was located directly below the target in the direction of the beam. The yield was measured at a standard voltage (160 kv) after every measurement at a different voltage as a check on the constancy of the target. The variation of the yield with the voltage is shown in Fig. 1. The points include values from three different runs on two different KOD targets and each point represents at least 1000 counts.

The yield from a D_3PO_4 target was measured with greater accuracy in the range 45 to 100 kv by use of the molecular ions from the low voltage arc, and by measuring the voltage with a high resistance voltmeter. 100 kv was taken as the standard voltage for these measurements and it might be noted that 16 out of 26 values of the yield at 100 kv fell within 4 percent (the statistical fluctuation) of the mean value. Each point on the graph shown in Fig. 2 represents the mean of several separate measurements.

Measurements of the fast neutrons showed that the number emitted in the forward direction was definitely greater than the number emitted normally to the impinging deuteron beam. The difference was much more than would be expected from consideration of the motion of the center of mass of the two deuterons. This is in accordance with the measurements of Kempton, Browne and Maasdorp.[11] The excitation curve will be influenced by this anisotropy but only insofar as this increases with the energy of the bombarding deuterons. A part of the observed increase with voltage of the number of neutrons emitted in the forward direction must, therefore, be ascribed to the increased concentration of neutrons in that direction, due to the moving center of gravity of the system and to an "abnormal" effect which, according to Kempton, Browne and Maasdorp, is not very sensitive to the velocity of the impinging deuterons. The angular distribution is not determined exactly enough to warrant more than an estimate of the correction involved. This is about 15 percent at 300 kv for the solid angle subtended by the target, and the correction decreases with the voltage.

[11] Kempton, Browne and Maasdorp, Proc. Roy. Soc. **A157**, 396 (1936).

Another point discussed by Kempton, Browne and Maasdorp should also be mentioned, namely the possible error in the excitation curve introduced by the variations in the energy of the neutrons with the energy of the impinging deuterons. They showed that the measured number of recoils in their high pressure helium chamber was quite sensitive to neutron energy. However, this effect is not believed to be as important in the case of a paraffin lined chamber where the selection level was adjusted to count only those protons which traversed the chamber at the end of their range. The main effect in this case would be to shift the layer in which those protons were produced deeper into the paraffin.

The yield of neutrons from different targets was compared with the neutrons from the radium-beryllium source. Four cm of lead was placed between the target and the ionization chamber so that the target could be replaced by the radium-beryllium source with no gamma-ray interference. The target was then bombarded with 100 kv deuterons and the neutrons were counted. Then the Ra-Be source was placed to approximate as closely as possible the position of the target and the neutrons from it were counted. The stray count, subtracted from the DD neutron count, was taken with all the apparatus running but without deflecting the beam to the target. The results in terms of millicuries equivalent per μa are: KOD target, 8.5 mC/μa; D_3PO_4 target, 44 mC/μa. The KOD target had been bombarded until it had reached an equilibrium of about $\frac{1}{2}$ of its original effectiveness.

Counts were also taken with the air-filled chamber located directly below the target. From the number of counts observed and the geometry of the chamber, the number of neutrons passing through the chamber can be estimated by use of Dunning's[12] value for the cross section for scattering. Assuming that every neutron scattered through an angle of 15° or more produces a measurable recoil atom, the number of neutrons traversing the chamber under a solid angle of $4\pi/20$, 8 from a D_3PO_4 target bombarded by 1 μa of 100 kv deuterons is 4.2×10^3 per second. This corresponds to a total of 8.7×10^4 neutrons per

[12] Dunning, Pegram, Fink and Mitchell, Phys. Rev. **48**, 365 (1935).

second over 4π if the neutrons were emitted isotropically.* Correcting for the stopping power of the target by multiplying by the ratio of the number of electrons of a molecule of the target material to the number of deuterium atoms therein, the yield for DD collisions is 1 neutron for 4×10^6 impinging deuterons.

However, the recoil atom must possess a certain minimum energy to produce sufficient ionization in the chamber to actuate the counter. An upper limit of this minimum is determined by the ionization of a proton which is known to actuate the counter, and this corresponds to scattering of the neutrons through an angle of about 90°. If, then, the neutrons are scattered isotropically, the number missed as at most 50 percent of the number scattered through 15° or more. If the minimum number of ion pairs is as low as 1000, the fraction missed will be only 4 percent. The yield calculated above may then be low by as much as a factor of two.

On account of the high ionizing power and the short range of the recoil atoms, very few of those produced in the volume of the chamber were lost by striking the walls before expending their energy in ionizing the gas. Also, very few neutrons were scattered back into the ionization chamber. This was shown by coating the front of the collecting electrode with paraffin. A 10 percent increase in the count was observed as compared with a 400 percent increase when the back of the same plate was coated. A correction for the anisotropy of neutron emission mentioned above might decrease the yield by 30 percent. The effect of disintegration of the aluminum by the fast neutrons is believed to be slight because of the relatively small cross sections for this process.

TABLE III. *Comparison of the relative ease in slowing down neutrons from a radium-beryllium source and from the deuterium on deuterium reaction.*

Thickness of paraffin	Counts/min.	Counts/min. with Cd shield	Counts/min. C neutrons
15 mC Ra-Be Neutron Source			
0.00 cm	30	30	0
1.75	102	37	65
3.50	231	44	187
5.00	432	50	373
8.25	545	49	496
10.75	596	50	546
DD Neutrons per μa			
0.00	13.4	13.5	0.0
1.75	18.7	10.7	8.0
3.50	74.0	20.0	54.0
5.00	156.5	20.8	135.7
8.25	206.5	21.0	185.5
10.75	226.5	20.2	206.3

* An error has been found in the solid angle previously used (Phys. Rev. **50**, 1190 (1936)) for calculation of the neutron yield.

V. Slow Neutrons

The increase of neutrons absorbable by 0.6 mm of cadmium with increasing thicknesses of paraffin cylinders surrounding both the neutron source and the ionization chamber has been measured, both for the DD and the Ra–Be neutrons. Five cylindrical shells of paraffin were cast, each with an inside diameter of 6.5 cm, and a height of 24 cm. At the center was placed a lead cylinder of 6.5 cm diameter and 4 cm height. The neutron source was placed directly above the lead and the boron lined ionization chamber directly below. The sources used were the 15 mC Ra–Be source and a KOD target bombarded by 160 kv deuterons. Measurements were made with and without a 0.6 mm cadmium shield surrounding the ionization chamber.

A KOD target was used which had been bombarded until it had reached an equilibrium; no change in the target was observed during the experiments. The stray count for the DD neutrons was taken with all the apparatus running but without deflecting the beam to the target. The deuteron current was about 2μa. The results corrected for strays are listed in Table III.

The increase of the C neutrons is also plotted in Fig. 3, the two curves being arbitrarily fitted at 8.25 cm. The curve for the Ra-Be neutrons is higher for the thin shells, showing that those neutrons are "easier" to slow down than those from the DD reaction.

With a D_3PO_4 target bombarded by 1 μa of 100 kv deuterons, the yield of slow neutrons produced in 7.5 cm of paraffin was equivalent to that of 15 mC of Ra-Be. The same target gave an equivalent of 44 mC per μa when the fast neutrons were counted. The main reason for this difference and for the difference in the curves (Fig. 3) is probably the higher initial proportion

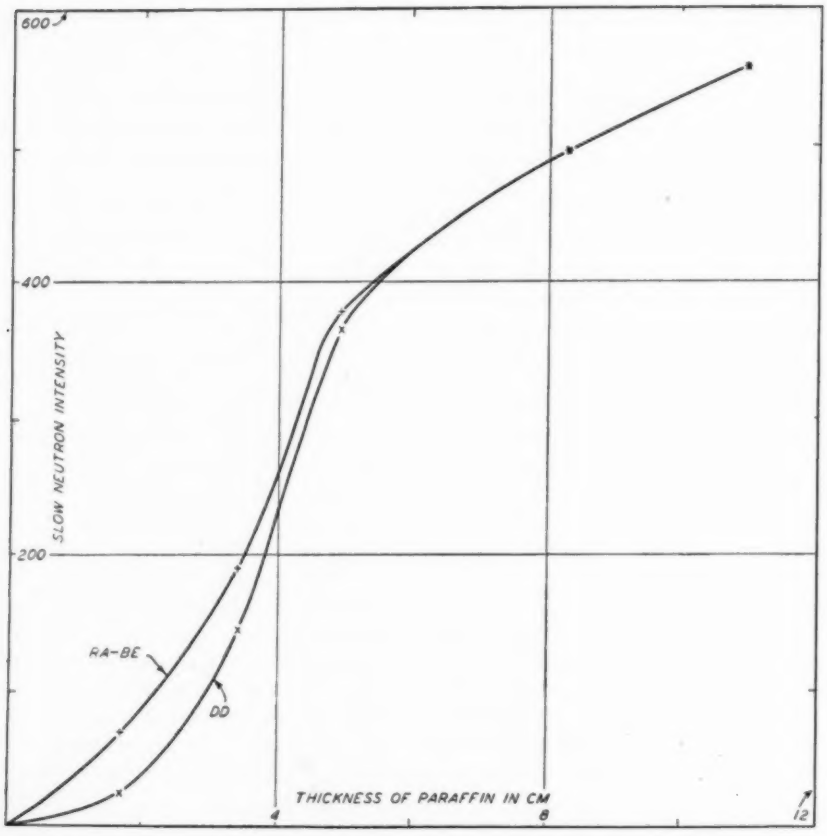

FIG. 3. Increase in number of slow neutrons observed with increasing thickness of paraffin.

of relatively slow neutrons from the Ra-Be, which give no measurable recoils. Also, the anisotropy of the neutron emission from the deuterium accounts partially for the difference, as the fast neutrons were counted in the forward direction whereas the paraffin surrounding the target did not slow down neutrons emitted in that direction.

VI. PROTONS

The yield of protons from various deuterium containing targets has been measured and the variation of the yield with the voltage for a D_3PO_4 target has also been observed. The protons emitted from the target at an angle of 90° to the incident beam passed through an aluminum window 0.0025 cm thick and 0.6 cm in diameter. Immediately outside the window was one of four interchangeable defining diaphragms 1 to 4 mm in diameter which were beveled to a thin edge. The ionization chamber was placed 4 mm in back of the diaphragm. 1.6 cm holes in its shield and high voltage electrode covered with aluminum foil admitted the protons to the chamber. In this way it was insured that the beam of protons was limited only by the one defining diaphragm and that the exact position of the chamber would have no effect on the number of protons counted. The stopping power of the foils and the intervening air spaces was such that a piece of Cellophane of 1.7 cm stopping power could be inserted without affecting the count. The insertion of the Cellophane did, however, increase the size of the pulses of the amplifier. A second Cellophane foil would stop the protons completely so that the last two centimeters of

the proton range were effective in the ionization chamber.

In magnitude the kicks from the protons, as observed on the oscillograph, were about twice the noise level. Consequently, it was possible to vary the bias of the selector tube in the counter from the setting corresponding to a selection level just below the peak of a proton kick to one just above the noise level without affecting the counting rate. As further evidence that the counter was not missing any protons, a visual count of kicks on the oscillograph was compared with the electrical count. The two agreed to the accuracy expected from the visual counting; the electrical count was always a little higher. In addition, counts were taken at different currents and with different diaphragms. All were consistent after the proper correction for solid angle or current had been made.

The procedure in the measurement of the voltage variation of the proton yield was the same as for the fast neutrons. 100 kv was again taken as the standard voltage and the yield at this voltage was checked continually. The yield was measured every five kilovolts from 40 to 100 kv. Each point on the graph shown in Fig. 2 represents the average of several measurements, none of which deviated from the mean by more than 5 percent.

The yield at 100 kv was measured using targets of D_3PO_4, $(ND_4)_2SO_4$ and ND_4Cl. The absolute yields have been calculated from the protons observed at 90° an the assumption of an isotropic emission of the protons. The factor used for correcting for the stopping power of the target is the ratio of the total number of electrons in the molecule of the target material to the number of D atoms. The results are listed in Table IV.

The anisotropy does not affect the excitation curve for the protons as they were observed at 90° to the incident beam. The absolute yield is increased if a correction is made for the anisotropy but not by more than a factor of 1.5.

VII. Discussion

The excitation curves for the neutrons (Fig. 1) agree quite well with the excitation curve given by Oliphant, Harteck and Rutherford between 40 and 140 kv and with the neutron curve of Alexopoulos[13] for the same voltage range. The excitation curves for the protons and neutrons (Fig. 1) from 45 to 100 kv coincide.

The absolute yield of neutrons calculated from the measurements with the air chamber is approximately 1 neutron for 4×10^6 deuterons. The correction for the anisotropy decreases the yield by about 30 percent, but due to the uncertainty of the selection level, the measurement may be low by as much as 50 percent. The neutron yield does not agree with that given by Alexopoulos. His figure (1 neutron for 1.6×10^6 deuterons) is appreciably higher than mine, although it does not include any correction for the composition of the target. On the other hand, the yield found recently by R. Doepel[14] is only 1/120 of mine.

Kikuchi, Aoki and Husimi[15] made an estimate of the yield of neutrons from the D − D reaction as compared with the Ra-Be source by counting slow neutrons. Their results agree approximately

[13] Alexopoulos, Helv. Phys. Acta. **8**, 513, 601 (1935).
[14] Doepel, Ann. d. Physik **28**, 87 (1937).
[15] Kikuchi, Aoki and Husimi, Proc. Phys. Math. Soc. Jap. **18**, 122 (1936).

Table IV. *Yields for 100 kv deuterons on various targets.*

Target	D_3PO_4	$D_3PO_4+D_2O$	ND_4CL	$(ND_4)_2SO_4$	$(ND_4)_2SO_4$
Protons per μ-coulomb observed	1.125	1.32	1.82	1.7	0.48
Total protons per incident deuteron	0.986×10^{-8}	1.115×10^{-8}	1.6×10^{-8}	1.49×10^{-8}	0.42×10^{-8}
D atoms in molecule per total H+D atoms	1	1	0.81	0.87	0.25
Correction factor total electrons per D atom	50/3	46/3	28/3.2	70/7	70/2
Yield for DD collisions	1.64×10^{-7}	1.71×10^{-7}	1.4×10^{-7}	1.49×10^{-7}	1.47×10^{-7}

with mine but they did not analyze their beam magnetically, so that no accurate comparison is possible.

The absolute yield of protons (1 proton for 6×10^6 deuterons) was calculated assuming an isotropic angular distribution of the protons. This yield is smaller than that reported by Oliphant, Harteck and Rutherford who estimated the yield to be of the order of magnitude of 1 proton for 10^6 deuterons when observed at the same angle as in my experiments.

These experiments were done under the direction of Professor Rudolf Ladenburg, to whom I am greatly indebted for his supervision and help. I also wish to express my appreciation to Dr. Giarratana and Mr. Beers for their valuable assistance, to my wife for her help in taking the readings, and to the staff of the Palmer Physical Laboratory for their work in preparing apparatus. Most of the equipment was purchased from a special grant to Professor Ladenburg from the Rockefeller Foundation.

MAY 15, 1937 PHYSICAL REVIEW VOLUME 51

A Wilson Cloud Chamber Investigation of the Alpha-Particles from Uranium

W. M. RAYTON* AND T. R. WILKINS
Department of Physics, University of Rochester, Rochester, New York

(Received February 3, 1937)

The *mean ranges* of the alpha-particles emitted by uranium have been determined in terms of the *mean range* of polonium alpha-particles. The ratios obtained for the *mean ranges* are, for U I/Po, 0.6904 ± 0.0007, and for U II/Po, 0.8357 ± 0.0008. These correspond to *mean air ranges* of 2.63 and 3.18 cm, for the particles from U I and U II, respectively, in dry air at normal pressure and at 15°C, on the basis of the present polonium value of 3.80 cm. The straggling coefficient was determined for the polonium alpha-particles used as the reference range group in the experiment and gave a value considerably closer to theoretical prediction than the usual experimental results. Possible evidence for the existence of a new alpha-emitting isotope of uranium is suggested in the data. The *mean air range* for the new group is believed to be in the vicinity of 2.9 cm. An identification with the actino-uranium isotope of approximately this range suggested by Wilkins as the parent of the actinium series and with Dempster's 235 uranium isotope is proposed.

PRECISE data on the characteristics of the alpha-particles from uranium have been sought for many years. It was of particular importance to the development of the general theory of the disintegration sequence in the uranium family when the alpha-emission from uranium was first definitely resolved by Laurence's[1] data into two range groups. The presence of two isotopes was thus indicated, but a still closer scrutiny of this subject seems worthwhile at the present time.

In the first place it seems advisable to establish the ranges of the alpha-particles from the known isotopes U I and U II with considerably higher precision than has so far been realized. This precision is deemed especially desirable because of the recent advances toward more precise theoretical formulation of the mechanics of alpha emission. Furthermore, this investigation was prompted by the fact that from several independent lines of reasoning the conclusion has been reached that uranium may be more complex than range data have so far indicated and that U I and U II may well have associated with them very small amounts of isotopes whose alpha-rays remain as yet undemonstrated in any direct fashion. These suspected isotopes are believed to be the missing long-lived parent, or parents, of the actinium series of radioelements; and their detection would consequently be a matter of some significance.

The presentation of the arguments which proceed to the conclusion that the parent of the actinium family will be found as an alpha-emitting isotope of uranium, present on earth today only in a small amount, would be too

* Present address, Massachusetts Institute of Technology, Cambridge, Mass.

[1] G. C. Laurence, Phil. Mag. **27**, 690 (1914).

lengthy for this paper, but a brief bibliography of the most important discussions of the topic is appended to this article.

All investigation of uranium alpha-ray ranges is seriously complicated by the extremely slow rate of decay of uranium. This has, in the past, necessitated the use of thick layers of source material to provide a suitable number of emitted particles. The unfortunate consequence was a broadening of the normal straggled distribution of path-lengths to a degree which nearly masked the fact that the radiation from uranium was complex. All work prior to 1910 gave uranium a single range group with a value between 2.9 and 3.4 cm, and subsequent work has realized resolving powers just sufficient to distinguish the two main range groups. The results of the most important range determinations are given in Table I.

Experimental

In the present investigation improved results were hoped for as a consequence of the use of a large area of an extremely thin film of uranium which thereby minimized the disturbing effects of absorption in the source layer itself. Secondly, to accentuate the range differences, this source was used in a relatively large Wilson chamber filled with a low stopping power gas mixture.

The Wilson chamber used was similar in general design to that described by Dahl, Hafstad and Tuve,[2] being of the sylphon bellows type. The chamber proper consisted of a Pyrex annulus some 16 cm in diameter and 5 cm deep, to which was clamped a suitable disk of plate glass which formed the top and viewing window for the chamber. The present outfit was arranged for automatic operation and utilized a motor driven shaft and suitable cams. A useful flexibility in the cycle was obtained through the use of a time-delay relay in the motor circuit. This could be adjusted so as to give a proper rest interval just prior to the expansion. For the track photography, light was supplied by a high intensity arc lamp, located sufficiently distant to prevent serious thermal disturbance at the chamber. The beam was collimated to a rectangular cross section, adapted to the chamber dimensions, and was controlled by a shutter mechanism geared to the main drive shaft of the chamber.

Table I. *Summary of most important range determinations.*

Method	Range in Air @ 15°C 760 mm U I	U II	Investigator	Date
Ionization	2.53 cm	2.91 cm	Geiger-Nuttall[1]	1912
Pleochroic Haloes	2 82	2.91	Gudden[2]	1924
Wilson Chamber	2.73	3.28	Laurence[3]	1927
Scintillations	—	3.23	Rutherford[4]	1927
Wilson Chamber	2.72	3.28	Kurie[5]	1932

[1] H. Geiger, J. Nuttall, Phil. Mag. **23**, 439 (1912).
[2] Gudden, Zeits. f. Physik **26**, 110 (1924).
[3] G. C. Laurence, Phil. Mag. **27**, 690 (1914).
[4] E. Rutherford, Phil. Mag. **4**, 580 (1927).
[5] F. Kurie, Phys. Rev. **41**, 701 (1932).

[2] Dahl, Hafstad, Tuve, Rev. Sci. Inst. **4**, 373 (1933).

The source was prepared by evaporation, in high vacuum, of metallic uranium[3] ribbon. The metallic vapor was condensed on a thin flat plate of rolled nickel, and produced a thin uniform deposit over the entire source area of approximately 30 square centimeters. The deposit weighed 0.09 mg per square centimeter, which is approximately one one-hundredth of the value used by Laurence, and one-twentieth of Kurie's.

In the chamber, a mixture of helium and air was adjusted to give a conveniently low stopping power, with resultant tracks which were approximately twice as long as their normal length in air under standard conditions. The use of helium was dictated by the ease of its retainment, compared with hydrogen, and by the fact that its stopping power relative to air is very close to a constant at all points along the range of a particle.

For several reasons it seemed advisable to refer the present range measurements to some standard range group. The use of polonium suggested itself, inasmuch as all investigations of its alpha-emission have consistently demonstrated its homogeneity. Consequently, a polonium source electrochemically prepared on the tip of a fine nickel wire was attached to one end of the uranium source support and provided one or more suitable reference tracks in every photograph.

Stereoscopic photographs of the tracks were obtained by the use of two Sept cameras with obliquely mounted objectives.[4] The cameras were fastened to a base plate of cast aluminum forming thereby a rigid unit which could be swung into a position such that the cameras looked downward through the top of the chamber. For reprojection,

[3] Purchased from Mackay Chemical Co., New York City.
[4] Glazebrook, *Dictionary of Applied Physics* No. 4, p. 400.

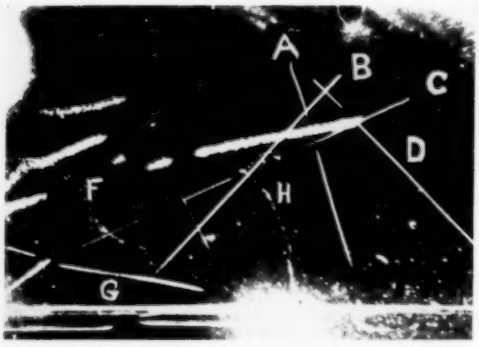

FIG. 1. Reproduction of typical chamber photograph, showing tracks of various types and ages.

the developed negatives were reintroduced into their respective cameras which were equipped with demountable projection illuminators, and the images were projected on a translucent viewing screen, arranged to be conveniently adjustable to any desired plane. Orienting the screen in such a manner that the images of a given track, as projected from the two units, were observed to coincide throughout, reestablished the original position of a track relative to the camera assembly, and a measurement of the true length could be made from the life-sized image so produced. Measurements were made directly by means of millimeter ruled coordinate paper which was waxed to a glass disk, forming thereby a translucent viewing screen which permitted setting and measurement from a position back of the screen. Two foot operated switches in the projection lamp circuits made it possible to flick rapidly from one projector to the other and facilitated accurate settings of the viewing plane, since even slightly incorrect positions were then made manifest by a pronounced flicker or image shifting as one switched rapidly back and forth between projectors. Refractive error, introduced by photography through the chamber top, was balanced out in the customary manner by the insertion of a compensatory glass plate in the projection beam.

With the apparatus as described about 3000 stereophotographs were obtained in the course of a few days, during which time conditions were maintained as constant as possible.

The large area of the source plate made impracticable the use of any shutter arrangements which sharply limited and defined the time during which alpha-particles were traversing the chamber. However, the tracks produced by particles which have passed a trifle prior to the optimum sensitive instant were found to be quite broad and diffuse, while those which came late in the period were characterized by incomplete condensation and a thin, stringy appearance. These characteristics have been shown, especially by the work of Kurie, to be sufficiently pronounced to serve as adequate criteria for the selection of tracks formed during the proper interval. Furthermore, in the present experiment, the duration of the illuminating flash was sufficient to reveal any appreciable falling motion and this provided another check on tracks of doubtful age, since in a track which had just been formed the droplets would be practically motionless. Tracks that showed motion were therefore rejected, as were also any which had passed through, or near, any regions which had been affected by condensations on older tracks in the vicinity. Such regions of prior condensations are locally heated and depleted in condensable vapor to the point that subsequent tracks fail to excite condensation. Moreover, for tracks traversing such regions there is a high probability that the alpha-particle will lose a great deal of energy in a chance journey through a single droplet and its apparent range would be completely altered.

Fig. 1 is a reproduction of a typical photograph and exhibits some of the effects described. The edge of uranium source appears as a white line across the bottom of the photograph, and the wire carrying the polonium is seen at the lower left corner. The broad, fuzzy segments are remnants of tracks of particles which passed so much prior to the sensitive interval that the ions had migrated under the influence of the electric field which was maintained in the chamber almost to the completion of the expansion stroke. Later tracks are seen to be quite sharp and well defined, except in the vicinity of previous condensations as seen in the tracks labeled *A*, *C*, and *D*. Track *C*, from the polonium, occurred quite late in the sensitive period and shows as a thin, threadlike structure. Track *G*, from polonium also, is a trifle old and furthermore ran in so close to the uranium source support that it entered the region of noncondensation which sheathes that object owing

to its high heat capacity. Track *B* is acceptable for measurement, since it had an uneventful and normal career, to all appearance. *F* and *H* are beta-trails which came presumably from the intermediate UX products present on the uranium source.

These standards for track selection reduced the number of usable uranium tracks to about 900. The length distribution obtained is presented in Fig. 2 where the experimental points are shown as small circles; the smooth full-line curves representing Gauss exponential functions which have been fitted to these points.[5] On the theory of probability, it is evident that some alpha-particles will lose more energy than others in traversing a given distance. Consequently there will be differences in the observed ranges of the particles, a phenomenon referred to as "straggling," even though the particles are all ejected with identical speeds for a given radioactive substance. These remarks serve to explain why the observed ranges are to be found grouped around some mean value according to a Gaussian error function, and thus the problem of determining the mean value for a range group involves fitting a curve of this type to the data. This exponential is of the form

$$y=\frac{1}{\alpha_1\sqrt{\pi}}e^{-(x-l)^2/\alpha_1^2}\cdot dx,$$

where y is that fraction of the total number of tracks whose length lies between x and $x+dx$, α_1 is the shape parameter of the distribution, and l the mean path length, or mean range of the group.

To find l and α_1 the method here followed was to determine first an error function which, to the eye, appeared to provide the best fit to the most significant experimental points in the distribution. The fitting of this exponential was carried out by projecting a plot of the experimental points on a screen, and then superposing on this the silhouette of a cardboard error function pattern, projected by means of a point light source. The dimensions of this shadow were thus conveniently adjustable through changes in projection distance, and by rotation of the pattern about its axis of symmetry. By this means it was possible to estimate the approximate shape and extent of a distribution group, and the weighed mean of that distribution gave l, to a zero-order

[5] A. King and W. Rayton, Phys. Rev. **51**, 826 (1937).

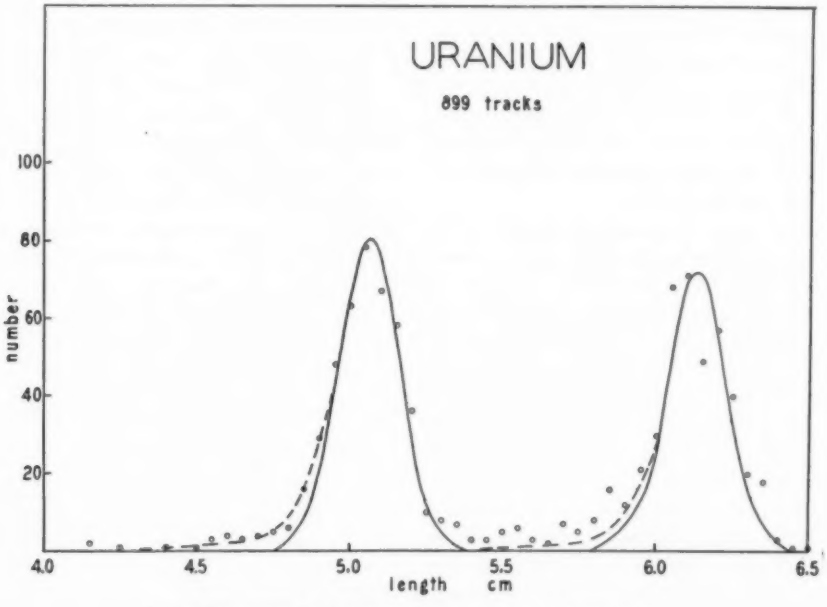

FIG. 2. Track length distribution for uranium alpha-particles.

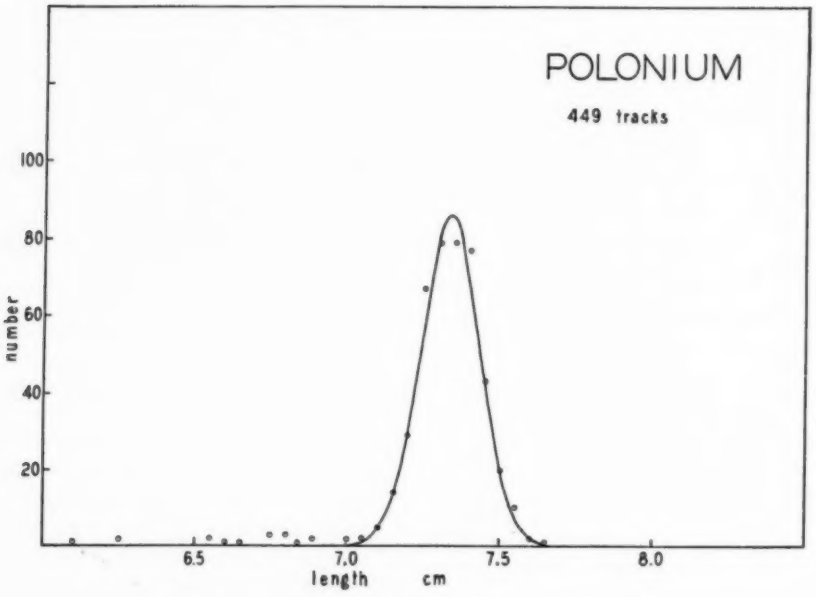

FIG. 3. Track length distribution for polonium alpha-particles.

approximation. The shape parameter α_1 was determined, likewise approximately, from the analytical relation that its square is equal to twice the mean square deviation of the distribution. Having thus found approximate values for the parameters, we proceeded by the method described in the accompanying related paper[5] to the calculation of successively closer approximations as determined by the condition of a least square ordinate deviation between experimental points and the smooth curve.

In the case of the polonium data, the fit of the resulting exponential is quite good even at considerable distances from the mean, as seen in Fig. 3. With the uranium data, however, the situation is complicated by the presence of an appreciable number of tracks whose lengths are such as to place them in the interval between the two main distribution groups. The precision of the results from these data is therefore somewhat inferior to that attained in the polonium case because of the greater uncertainty in determining the proper approximate forms for the component distribution groups. This uncertainty was not thought to be of serious magnitude however, since the long-ranged side of the uranium II group, and the short-ranged side of the uranium I group, provided us with templates which could be applied to the complicated portions of the curves.

The figures thus obtained for the mean values of the distributions came out as in Table II.

The above-mentioned figures cannot be directly compared to establish the ranges of particles from uranium I and uranium II relative to the polonium reference, since the stopping power of the chamber mixture is not quite constant for particles of different energies. However, a comparison of the mean polonium range (7.336 cm) observed in the chamber, with the present accepted value of 3.805 cm[6] for the mean range in air at 15°C and 760 mm pressure sufficed to determine the composition of the chamber mixture,

TABLE II. *Main values of range from distribution curves.*

	Mean values, cm
Polonium	7.336±0.003
Uranium I	5.061±0.003
Uranium II	6.123±0.003

[6] Lewis, Wynn-Williams, Proc. Roy. Soc. **A136**, 349 (1932).

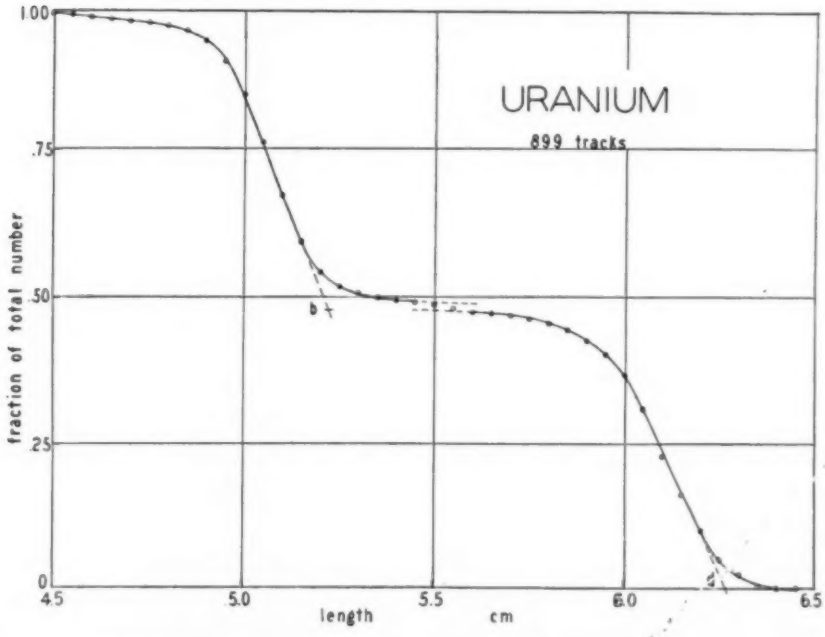

FIG. 4. Integrated number-distance distribution of uranium data.

since Gurney[7] has determined the stopping power of pure helium for polonium alpha-particles. Knowing the chamber mixture, its stopping powers for particles of air range 2.6, 3.2, and 3.8 cm were calculated on the basis of Gurney's data. These stopping powers turned out to be 0.5191, 0.5189, and 0.5187, respectively, and when applied to the chamber data, the mean ranges of uranium I and uranium II, referred to polonium, reduce to the following values:

Uranium I/Polonium $0.6904 \pm 0.0007(5)$
Uranium II/Polonium $0.8357 \pm 0.0008(2)$.

Taking the mean air range for polonium as 3.805 cm leads to mean air ranges for uraniums I and II of 2.63 and 3.18 cm, respectively. The estimated uncertainty in the absolute magnitude of the figure for polonium is stated as being in the vicinity of 0.01, consequently there is small point to quoting further than to the second decimal place in the uranium values here given.

Comparison of the results of this and previous experiments can be made only on a basis of the so-called *extrapolated number-distance*[8] range values. Graphically, these are obtained from a plot in which the number of tracks whose lengths exceed a given value is graphed against length values. An extrapolation of the descending linear portion is commonly used to specify this type of range, by the point of intersection of the line of extrapolation and the horizontal axis. This method of range specification is especially ill-suited to nonhomogeneous cases, as in Fig. 4, owing to uncertainty as to the location of the plateaus which thus renders uncertain the extrapolated values for all except the longest range group.

For purposes of comparison with the earlier results, one may easily compute these extrapolated values, once the mean ranges are known, since the former exceed the latter by the amount $\alpha\sqrt{\pi}/2$, as may be easily shown analytically to be the case for Gaussian functions. In the present instance, the computation yields these values:

Uranium I 2.71 cm @15°C and normal pressure.
Uranium II 3.27 cm

[7] Gurney, Proc. Roy. Soc. **A107**, 340 (1925).

Straggling of Alpha-Particle Ranges

It is clear that the shape of a track length distribution curve will depend upon the precision of the individual measurements of length and thus the constant α_1, previously mentioned as the shape parameter of the distribution, will depend not only on the actual straggling but upon the distribution of errors inherent in the technique of measurement. This dependency can be shown[5] to be of the form,

$$\alpha_1^2=\alpha_0^2+\alpha^2,$$

where α_0 is the modulus of precision related to the measurement process itself, and α is the parameter of the true straggling distribution. In the present case an effort has been made to evaluate α_0 separately, by means of a set of measurements taken on a test object, and thus from the observed α_1, it was possible to determine the α representative of the actual straggling. In the present instance, α_1, was observed as 0.141 cm in the case of the polonium distribution, and α_0 was determined as 0.101 cm, leading to a corrected value of 0.098 cm for α.

Dividing α by l, the mean value of the length distribution, defines a constant known as the *straggling coefficient* and denoted by the letter ρ. As incidental to the present experiment ρ has been determined from the polonium data to have the value 1.34×10^{-2}; a value that is in considerably closer agreement with the results of the Bohr theory[8] of alpha-particle straggling than has usually been observed. The present result is 1.21 times the Bohr value, as contrasted with the more usual discrepancies amounting to factors between 1.4 and 1.5.[9-12]

The inconsistencies between theory and experiment have been large and uniformly in the same direction, but it seems to us probable that they are in large measure to be attributed to the difference between α_1 and α, a distinction which appears to have been overlooked at least in previous Wilson chamber work. To a smaller extent the difficulty is presumably inherent in the limitations of the simple Bohr theory with its simplifying assumptions. The Bethe-Williams[13, 14] wave mechanical treatment is at present the most rigorous discussion of this subject, and the results of this theory are in general about 10 to 15 percent larger than the corresponding Bohr figures. For the present experiment a calculation of the Bethe-Williams straggling coefficient was made, on a basis of mean excitation potential data used by Mano[15] in similar calculations. The result obtained ($\rho=1.19\times10^{-2}$) is exceeded by our experimental value only to the extent of 13 percent. A similar new and close approach to theoretical values has been recently reported by Bennett[16] who used an electrical method to investigate straggling in micas. The results range between 1.1 and 1.2 times the Bohr figure, and lend further strength to the belief that previous determinations have been in error.[17]

Isotopic Composition of Uranium

A comparison of the relative areas included beneath the smooth distributions of the uranium I and uranium II data shown in Fig. 1 is readily made in terms of their definite integrals. The result shows that there are 90.5 percent as many tracks from uranium II as from uranium I. On the basis of the radioactive equilibrium one would expect equal numbers in the two cases, but a definitely smaller angular aperture was available to the longer tracks in the space limitations of the Wilson chamber.

Of particular interest is the appearance of an unexpectedly large number of tracks in the region between the two main groups. (Fig. 2). The dashed portion shown appended to the left side of the uranium II distribution is a transposition, proportionately reduced, of the left side of the uranium I group (observed points—dashed line). This makes possible a rough estimate of the number of "extra" tracks in the vicinity. Plotting this excess leads to the suspicion that there is a

[8] Bohr, Phil. Mag. **25**, 10 (1913); **30**, 581 (1915).
[9] I. Curie, Ann. d. Physik **3**, 320 (1925).
[10] Meitner-Freitag, Zeits. f. Physik **37**, 481 (1926).
[11] Curie, Mercier, J. de phys. **7**, 289 (1926).
[12] Briggs, Proc. Roy. Soc. **A114**, 313 (1927).
[13] H. Bethe, Ann. d. Physik **5**, 325 (1930); Zeits. f. Physik **76**, 293 (1932).
[14] E. J. Williams, Proc. Roy. Soc. **A135**, 108 (1932).
[15] G. Mano, Ann. d. Physik **1**, 407 (1934).
[16] Bennett, Proc. Roy. Soc. **A155**, 419 (1936).
[17] The calculated values of our straggling coefficients are not corrected for the effects due to variation of charge on the alpha-particle during its flight, nor for the influence of the alcohol vapor present in the gas mixture. These two effects are of opposite natures regarding their influence on ρ, and would be of very small magnitude.

small distribution group in the vicinity of 5.55 cm. The same effect appears to be reflected in the integral plot of Fig. 4 as a small but perceptible break in the middle section of the curve. This distribution, if real, corresponds to an alpha-ray group of about 2.9 cm mean air range at 15°C, or an extrapolated range close to 3.0 cm. It may be significant that this value for a range group is in fair agreement with that required by Wilkins[18] in explanation of the observed time shift in the inner rings of the pleochroic haloes in old micas. The magnitude of the observed hump, about 3 percent of the uranium I group, is in accord with most current hypotheses regarding an actinouranium isotope, and it seems especially significant in view of Dempster's[19] recent detection of a uranium isotope of atomic mass 235. It is tempting to identify the source of the alpha-particles here observed with the 235 isotope, which is in all probability the radioactive parent of the actinium family.

Regardless of the existence or nonexistence of a range group at precisely the point suggested, there is definitely an abnormally large number of tracks whose lengths exceed 5.4 cm in the chamber medium, which figure very probably defines the upper limit of the region which can receive contributions from the spread of the uranium I group. Of the total number of measured tracks, 49.7 percent are longer than this in spite of the definite discrimination imposed by the available space in the chamber against the longer tracks. Such an observed result thus seems indicative of the presence of another long range group other than uranium II. Further, since no tracks were observed to be of lengths so great as definitely to place them beyond the normal straggled distribution of uranium II, it can be assumed with some certainty that the mean range of the new group is less than the mean value of that distribution. Further speculation on the point is probably pointless until more data have been secured.

[18] Wilkins, Phys. Rev. **29**, 352 (1927).
[19] Dempster, Proc. Am. Phil. Soc. **75**, 755 (1935).

Conclusion

The mean ranges of the alpha-particles emitted by uranium have been determined in terms of the mean range of polonium alpha-particles. The ratios of these mean ranges are, for uranium I/polonium, 0.6904 ± 0.0007, and for uranium II/polonium, 0.8357 ± 0.0008. These correspond to mean ranges of 2.63 and 3.18 cm in dry air at normal pressure at 15°C for uraniums I and II, respectively. These figures are based on the present polonium value of 3.805 cm, which is believed to be correct in absolute magnitude to within less than 0.01 cm.

The straggling coefficient has been determined for the polonium alpha-particles used as the reference range group in the experiment. The result is in markedly better agreement with theoretical prediction than has been customarily observed.

The distribution of track lengths observed among the alpha-particles emitted from an extremely thin layer of uranium suggests the possibility of a new alpha-emitting isotope of uranium, whose mean range in air has been tentatively placed in the vicinity of 2.9 cm. It seems possible that this may be alpha-particles from Dempster's uranium isotope of mass 235.

Supplementary bibliography on the problem of the radioactive parentage of the actinium series

Piccard, Arch. Sci. Phys. et Nat. **4**, 161 (1917).
Johnstone-Boltwood, Phil. Mag. **40**, 50 (1920).
Wilkins, Nature **117**, 719 (1926); Phys. Rev. **29**, 352 (1927).
Rutherford, Nature **123**, 313 (1929).
A. v. Grosse, Phys. Rev. **42**, 565 (1932); Proc. Roy. Soc. **A150**, 363 (1935).

Ranges and Straggling Coefficients of Alpha-Particles[1]

ALLEN KING* AND W. M. RAYTON†
Department of Physics, University of Rochester, Rochester, New York
(Received February 3, 1937)

A review and evaluation of the analytical and graphical methods customarily applied in range determinations reveals several types of errors that frequently have been overlooked. Of particular importance are the area and error effects. The extrapolated range is shown to be subject to other errors and it is concluded, therefore, that the *mean range* is much the best measure of range. A method of analysis which takes into account these errors is developed and applied to a set of polonium data. The experimental straggling coefficient is only 13 percent greater than the Bethe-Williams theoretical value and 20 percent greater than the Bohr value.

THE ranges of the α-particles from a given radioactive source, as quoted by different observers, frequently exhibit serious discrepancies. Since range values are important not only for the identification of the emitting atoms; but also as a check on theoretical investigations in the fields of natural and induced radioactivity, we believe it desirable to review and evaluate the analytical and graphical methods customarily applied in range determinations. In the course of this discussion we shall point out distinctions and corrections which apply to the concept and measurement of ranges and to the related subject of α-particle straggling.

The range of a homogeneous group of α-particles we define as the most probable distance which an α-particle of the group travels in a given medium before it loses sufficient energy so that it no longer can ionize atoms of that medium. This definition implies that the α-particle emerges from the radioactive atom into the second medium directly without being affected by any neighboring electrons and nuclei of the radioactive source. Strictly, this condition is not always satisfied, so that any residual errors in the final result should be due partly to the presence of source fields. The *mean range* will be taken as the one which most nearly satisfies this definition.

As a group of α-particles penetrates into the surrounding medium, it gradually slows down due to collisions, both near and distant, primarily with electrons of the medium. Since the number of encounters which occur for a single α-particle in a group may differ from the average for all the particles, the path lengths of the particles in a homogeneous group are distributed about a mean value in a manner represented very closely by the Gaussian error function. This effect Darwin[2] termed "straggling," and the ratio of the shape parameter for the function to the mean range was called the *straggling coefficient*.

These two numbers, range and straggling coefficient, which characterize the slowing down process of an α-particle in a given medium, depend upon the homogeneity of the α-ray group; the initial energy associated with the group; the thickness of the source; the atomic density of the medium; the number of electrons per atom; and a characteristic potential for these atoms. We shall confine our attention to a homogeneous bundle of particles which enter into a gaseous medium from a thin source. For thick sources a correction must be applied which increases the uncertainty in the final result.

METHODS OF INVESTIGATION

The earliest range investigations were made with scintillation screens. Counts of the scintillations produced on a zinc sulfide screen, when placed at various positions between the source and observer, were plotted as number-distance distribution curves from which values for the range were obtained. Ranges found in this manner generally are less than those from other methods. One explanation suggests that this result is due to an inability of the observer to

* Now located at Rensselaer Polytechnic Institute, Troy, New York.
† Present address: Massachusetts Institute of Technology, Cambridge, Massachusetts.
[1] To be read in conjunction with the preceding paper "A Wilson Cloud Chamber Investigation of the Alpha-Particles from Uranium."
[2] Darwin, Phil. Mag. **23**, 901 (1912).

count faint flashes in the presence of bright ones. However, in order to obtain a flash the screen must be placed at some distance from the source less than that at which the particle stops ionizing; and this distance will depend upon the energy required to produce detectable triboluminescence. As long as this energy is greater than that necessary to ionize the gaseous medium, any method involving a recording mechanism of this kind will yield ranges less than the true values.

Of the electrical methods, that first used by Bragg has been employed extensively for range measurements. Two parallel metal screens with a potential difference between them are placed at known distances from the source; the ionization produced by the α-particles passing through the space between them is measured. These ionization currents when plotted against distances, yield the well-known Bragg curve which has a maximum near the end and a straight line portion with a negative slope. Marsden and Perkins[3] suggested that the intercept of this linear portion extrapolated to the distance axis would be a reliable and reproducible measure of range. Other investigators, notably Henderson,[4] have improved this apparatus and made many observations over the linear portion and toe of the Bragg curve for various radioactive substances. Since the exact variation of α-particle ionization with distance traveled really is not known, it is difficult to discuss the effect of errors on this extrapolated range. A more serious objection to the use of the extrapolated range is the fact that straightforward analytical methods cannot be used to establish relations between it and related phenomena. Geiger and Nuttall[5] and, later, Geiger[6] used a total ionization method which yielded range values comparable to it. In Fig. 1 are shown several possible measures of range associated with the Bragg ionization curve.

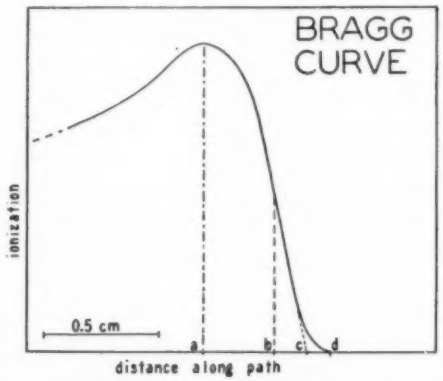

FIG. 1. The Bragg curve near path terminus showing: (*a*) the peak range; (*b*) a characteristic range half-way between maximum and zero ionization; (*c*) the extrapolated ionization range; and (*d*) the maximum range.

The most recent electrical method to be used is that of the differential ionization chamber developed at the Cavendish laboratories.[7] Essentially it measures the position of the maximum rate of change of ionization along the paths of α-particles. The maximum response determines a characteristic range, and the ratio of two such characteristic ranges is assumed to be the same as that of the corresponding true mean ranges. The validity of this assumption should be carefully investigated. Effects of straggling can be followed rather well, so that results from this method are comparable with those obtained by means of the Wilson chamber. It should be noted, however, that the Wilson chamber measures the most probable distance a particle will travel before it stops producing cloud-forming ions.

The Wilson cloud chamber is one of the most direct methods for getting values of ranges and straggling coefficients. A pair of stereoscopic pictures are taken simultaneously of the cloud tracks at a definite instant during the cycle of the chamber. When the developed negatives are projected together on a screen, one may easily measure the lengths of the track images. From the analysis of a number-distance plot of several hundred such tracks one may readily find a mean range and straggling coefficient. In the discussion below, the methods developed will be applied particularly to Wilson chamber data obtained for polonium.

The fine-grained photographic emulsion provides another medium for getting values of mean range. Of course this photographic mean

[3] Marsden and Perkins, Phil. Mag. **27**, 690 (1914).
[4] Henderson, Phil. Mag. **42**, 538 (1921).
[5] Geiger and Nuttall, Phil. Mag. **22**, 613 (1911); **23**, 445 (1912).
[6] Geiger, Zeits. f. Physik **8**, 45 (1921).
[7] Proc. Roy. Soc. **A129**, 211 (1930); **A131**, 684, 391 (1931); **A133**, 351 (1931); **A136**, 349 (1932).

range need not be equal to any of the above ones. Errors in the measurement of the track grains are large enough to mask straggling effects so that this medium is useful primarily as a convenient and simple check on range results from other methods.

The magnetic deflection method is used to measure velocities of α-particles and velocity straggling coefficients. This method proves very useful for straggling investigations. Range values, on the other hand, which are determined from the measured velocities are inexact; since the relation between range and velocity is not known.

In view of the wide variety of possible measures of range, it seems best that one should fix upon a definite standard to which all measurements may be reduced and a standard method by which mean ranges may be compared. In order to satisfy this demand, all measurements should be made relative to a homogeneous standard source, such as freshly prepared polonium films, and then reduced to normal temperature and pressure in dry air. Since the Wilson chamber affords a most direct means of measuring ranges, which very nearly satisfy the above definition, we suggest that it be used wherever possible as a standard method. A careful and detailed investigation of relative mean range values found by each of the above methods should be made in order to find out how such relative values may be reduced to the Wilson chamber standard. In this way, one may find some justification for quoting ranges to *four* significant figures.

Error Effect and Area Effect[8]

As indicated above, a straggling curve for ranges is represented very closely by the Gaussian function. If y is the fraction of the total number of tracks which have path lengths between z and $z+dz$, then

$$y=(1/\pi^{\frac{1}{2}}\alpha)e^{-(z-l)^2/\alpha^2}dz. \tag{1}$$

Here l is the mean range and α is the shape parameter; so that $\rho=\alpha/l$ is the straggling coefficient. We shall discuss the methods by which values of l and α may be determined from observed data.

Actually, due to instrumental and observational errors, the number of tracks of true length z is spread over a small region of observed length values in accordance with the Gaussian error function. That is, superimposed upon the straggling curve is an infinite array of error curves given by the relation

$$y_1=(y/\pi^{\frac{1}{2}}\alpha_0)e^{-(x-z)^2/\alpha_0^2}dx, \tag{2}$$

in which we have assumed the precision parameter, α_0, the same for all values of z. Combining (1) and (2) and integrating over all values of z from $-\infty$ to $+\infty$ one finds that

$$y_1=(1/\pi^{\frac{1}{2}}\alpha_1)e^{-(x-l)^2/\alpha_1^2}dx, \tag{3}$$

in which
$$\alpha_1^2=\alpha^2+\alpha_0^2. \tag{4}$$

It should be noted that the mean range, l, is unaltered by these errors, but, as shown later, that the extrapolated range depends markedly upon them.

In almost all range experiments measurements are made over finite intervals of path length. Thus the ionization chamber cuts out a definite portion of the space through which α-particles are passing; and, on the other hand, the stereoscopic images of fog paths from a Wilson chamber are measured to the nearest half-millimeter.

Experimental points, therefore, should lie on a curve found by plotting

$$1/\pi^{\frac{1}{2}}\alpha_1\int_{x-\Delta x/2}^{x+\Delta x/2}e^{-(x-l)^2/\alpha_1^2}dx \tag{5}$$

against x. The interval of path length, Δx, ordinarily is small enough so that the experimental points may be represented by the function

$$y_2=(\Delta x/\pi^{\frac{1}{2}}\alpha_2)e^{-(x-l)^2/\alpha_2^2}. \tag{6}$$

The relation between α_1 and α_2 is now found by equating (5) and (6). Since the relation is assumed to be good for all values of x, it must be valid for $x=l$ in particular; then

$$P\left(\frac{\Delta x}{2\alpha_1}\right)=\frac{2}{\pi^{\frac{1}{2}}}\int_0^{\Delta x/2\alpha_1}e^{-z^2}dz=\frac{\Delta x}{\pi^{\frac{1}{2}}\alpha_2}. \tag{7}$$

[8] I. Curie, J. de phys. 3, 299 (1925). Mme. Curie discussed the area effect in detail and supplied tables from which correction factors may be obtained. In her analysis, however, Δx is equal to *one-half* the interval used for plotting.

Values of $P(\Delta x/2\alpha_1)$ may be found in tables of values of the probability integral.

As discussed below, this area effect changes the value of the straggling coefficient by approximately 2 percent whereas the error effect described above changes it by nearly 30 percent. Ordinarily the former is neglected and the latter is not even considered.

Evaluation of l and α

Usually the value of l is obtained by making $\sum y_x(x-l)^2$ a minimum;[9] so that

$$l=\sum xy_x, \tag{8}$$

where $\sum y_x=1$. Since the mean square value of $x-l$ is equal to $\alpha^2/2$ one assumes that

$$\alpha^2=2\sum y_x(x-l)^2. \tag{9}$$

These values of l and α will be designated by l_0, α_0 and will be used as zero-order approximations to the best value for a given set of data.

Because the abscissa values are fixed at finite intervals, it would seem preferable to adjust the parameters l and α so as to make $\sum(\Delta y_x)^2$ a minimum. To do this one assumes that $l=l_0+h$ and $\alpha=\alpha_0+k$ in which h and k are small correcting terms to be determined from the minimizing condition. Then the Gaussian function is expanded into a Taylor series about the point l_0, α_0 and the first two terms of the expansion are retained. Thus

$$y=\left\{1+\frac{2z}{\alpha_0}h+\frac{1}{\alpha_0}(2z^2-1)k\right\}pe^{-z^2}, \tag{10}$$

in which $z=(x-l_0)/\alpha_0$ and $p=\Delta x/\pi^{\frac{1}{2}}\alpha_0$. The partial derivatives of $\sum(y_x'-y_x)^2$ with respect to h and k are assumed to vanish; from which one readily finds that

$$2h=\frac{\alpha_0}{p\Delta}\begin{vmatrix}\sum BC & \sum y_x'B-p\sum AB\\ \sum C^2 & \sum y_x'C-p\sum AC\end{vmatrix}, \tag{11a}$$

$$k=\frac{\alpha_0}{p\Delta}\begin{vmatrix}\sum y_x'B-p\sum AB & \sum B^2\\ \sum y_x'C-p\sum AC & \sum BC\end{vmatrix}, \tag{11b}$$

in which $\Delta=(\sum BC)^2-\sum B^2\sum C^2$,

$A=e^{-z^2}$, $B=ze^{-z^2}$, $C=(2z^2-1)e^{-z^2}$, and y_x' represents the experimental values of the ordinates. By use of these relations the correcting terms h, k for l and α are determined. The corrected values of l and α may now be used in place of l_0 and α_0; thus a new set of correcting terms may be found. This operation is repeated as often as desired for higher approximations; but usually one or two applications of it are sufficient. The method may be extended for the case of a more complicated distribution.

[9] The summation, $\sum$, occurs over all values of x.

Application

The number-distance curve obtained by Rayton and Wilkins for the polonium alpha-rays as a reference standard in the study of the alpha-ray isotopes of uranium,[10] has been analyzed by the procedure developed above. Values of the zero, first, and second order approximations of the best values for l and α_2 are given in Table I. The large mean range value is due to the fact that tracks were formed in a mixture of helium and air. We observe that an application of the method of the preceding section to Wilson chamber data does not lead to a significant correction of the values for l and α as obtained by the usual method.

To obtain a value for the precision parameter, α_0',[10a] two artificial tracks, 7.3 cm in length were made from small drill rod and photographed in various angular positions with respect to a plate. The developed negatives were projected on a viewing screen in the same manner as used for the polonium track negatives, and were measured in the same way. An analysis of the data yielded the result $\alpha_0'=0.101$. Finally

$$\alpha=(\alpha_2^2-\alpha_0'^2)^{\frac{1}{2}}. \tag{12}$$

The area effect is automatically taken into account when this equation is applied; so that α is the shape parameter for the straggling curve given by Eq. (1). Then $\rho=\alpha/l=0.0134$ is the straggling coefficient.

If α_2 is corrected for the area effect alone, the value 0.0188 instead of 0.0191 is found for ρ.

[10] W. M. Rayton and T. R. Wilkins, Phys. Rev. this issue.

[10a] α_0' involves the area effect and is related to α_0 by the equation

$$\frac{\Delta x}{\pi^{\frac{1}{2}}\alpha_0'}=P\left(\frac{\Delta x}{2\alpha_0}\right).$$

TABLE I.

	0	1	2
Mean range l	7.337	7.336	7.336
Straggling Coefficient α_2	0.140	0.141	0.141

On the other hand, the error effect reduces it to 0.0134. Thus the area effect changes the value by only 1.4 percent whereas the error effect reduces it by 30 percent. This last value for ρ, although 1.2 times greater than the Bohr theoretical value,[11] is still much less than any previous value obtained with a Wilson chamber. Bennett,[12] from investigations of straggling in mica, obtained a ratio 1.1–1.2. These low values for the ratio indicate that the differences between experiment and theory need not be interpreted in the manner suggested by Briggs.[13]

In Fig. 2 is shown the curve which best fits the experimental points and the curve which is corrected for the area and error effects.

THE INTEGRAL PLOT AND EXTRAPOLATED NUMBER-DISTANCE RANGE

In order to find the integral plot of the number-distance curve, Eq. (3) is integrated from x to $+\infty$, and the results are plotted against the corresponding values of x. Thus there is obtained a curve, as shown in Fig. 3, which is very similar to the end of the Bragg curve. As suggested by Marsden and Perkins, the linear portion may be extrapolated to the distance axis to get a measure of range. This intercept value is related to the mean range by the equation

$$I=l+\pi^{\frac{1}{2}}\alpha_1/2. \qquad (13)$$

When one introduces the area effect, the only change produced is that α_1 is replaced by α_2.

The measured extrapolated range is subject to two errors. In the first place, because of the error effect, it depends seriously upon the experimental errors through α_2. Secondly, any small errors in the ordinate in the neighborhood of the mean range are considerably magnified by the extrapolation so that relatively large errors may occur in the intercept value. Thus in Fig. 3 the intercept occurs at 7.471 cm from which one obtains $\alpha'=0.152$. Since $\alpha_2=0.141$, the difference must be ascribed to the second type of error.

A third error affects many such range values found in the literature. It is due to the fact that the number of tracks with lengths greater than x are plotted against x rather than against $x+\Delta x/2$;[14] or else the number greater than and equal to x are plotted against x rather than $x-\Delta x/2$.[15] In other words, since for Wilson chamber data Δx is usually one-half millimeter, a systematic error of ± 0.025 cm has been introduced into several of the extrapolated number-distance range values.

Because of these various errors, results of different observers are generally in disagreement. On the whole, the mean range, l, seems much the better measure of range.

SUMMARY

(1) The various methods of measuring ranges and straggling coefficients are briefly described

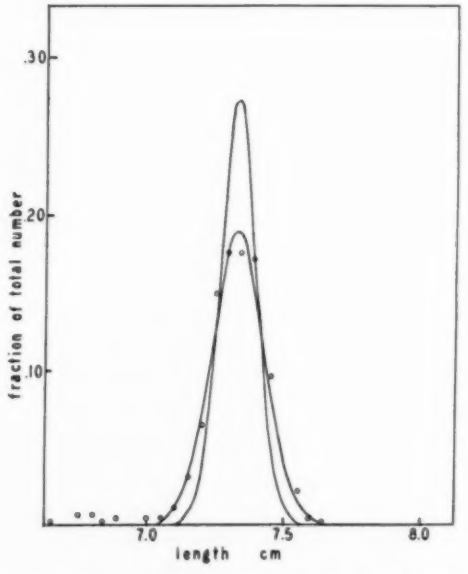

FIG. 2. Track length distribution curve for a set of experimental points, and the corrected curve.

[11] The measured ρ is only 1.1 times greater than the Bethe-Williams theoretical value (see reference 10).
[12] Bennett, Proc. Roy. Soc. **A155**, 419 (1936).
[13] Briggs, Proc. Roy. Soc. **A114**, 313 (1927).
[14] Laurence, Phil. Mag. **5**, 1027 (1928); Kurie, Phys. Rev. **41**, 701 (1932).
[15] Meitner and Freitag, Zeits. f. Physik **37**, 484 (1926); Philipp and Donat, Zeits. f. Physik **52**, 759 (1929).

and the results from these methods are shown to differ from one another.

(2) Range is defined as the most probable distance an α-particle of a homogeneous group will travel in a given medium before it ceases to ionize atoms of the medium.

(3) The mean range from Wilson chamber data is shown to satisfy the above definition, and it is suggested that this method of measurement be used wherever possible. Also all range measurements should be referred to the range of α-particles from a standard homogeneous source such as polonium.

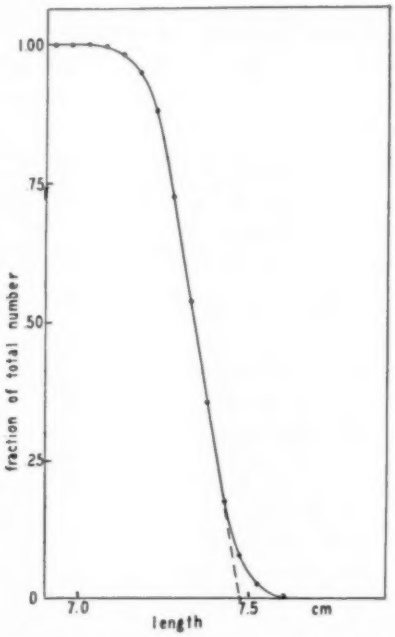

FIG. 3. Integrated number-distance distribution from the data of Fig. 2.

(4) All observations on the straggling of α-particles are shown to be subject to two disturbing factors; (a) the error effect which depends upon the presence of experimental errors and is readily eliminated from Wilson chamber data by measuring artificial track lengths; and (b) the area effect, first analyzed by Irene Curie, is easily taken into account.

(5) Values of l and α may be computed by making $\sum(\Delta y)^2$ rather than $\sum(x-l)^2$ a minimum. Equations are given from which the correction terms may be calculated.

(6) This method of analysis is applied to polonium data and yields a result for the straggling coefficient ρ, which is much less than that from any previously published Wilson chamber data. It is 1.2 times greater than the Bohr theoretical value, a result which agrees with that recently obtained by Bennett.

(7) Finally, the extrapolated number-distance range is shown to be subject to two errors; namely, that due to experimental errors in α, and that due to the magnification of small errors which occur in the neighborhood of $x=l$. A third error appears in much published data due to incorrect plotting.

X-Ray Emission Spectra of Sulphides and Sulphates

JOSEPH VALASEK
University of Minnesota, Minneapolis, Minnesota
(Received March 29, 1937)

A target for exciting x-ray emission spectra of chemical compounds is described. The wave-lengths of the $K\beta$ lines of alkaline earth sulphates and of some semiconducting sulphides are given. Using these results and the wave-lengths of the K absorption edges, the energy gap between the occupied and unoccupied zones in these crystals is obtained. The results for the sulphates are compared with the results previously obtained for the corresponding sulphides. In order to account for the changes in emission wave-lengths from compound to compound, a nonuniform displacement of energy levels is needed in addition to the Madelung energy. A recent article by Slater and Shockley suggests one way in which this may be accomplished.

THE effects of chemical combination on x-ray emission spectra have recently received considerable attention.[1] Since the radiation is emitted by solids in the crystalline state, the results lead to a determination of the relative location of some of the energy levels in these crystals. They supplement the results obtained by studies of ultraviolet absorption and photoelectric effect and contribute to a better understanding of this group of phenomena.

The spectra of the compounds were excited by the general method described by the writer in a previous article.[2] An improvement was effected by water-cooling the clamp which holds the pellet of the material on the target just back of the focal spot. The clamp was made of a loop of thin-walled copper tubing through which water is circulated. In this way the materials are kept much cooler and it is possible to use a greater variety of compounds. A Siegbahn vacuum spectrometer with a calcite crystal was employed. The wave-lengths were determined by comparison with those of Ni $K\alpha$ in the third order.

Table I contains the wave-lengths of the S $K\beta$ lines of various sulphur compounds. The previously published values for the alkaline earth sulphides are given again to facilitate comparison with the new results for the corresponding sulphates. The column K_∞ gives the wave-lengths of the principal K absorption edges as measured by Stelling[3] or Lindh.[4] The next column gives the difference between the $K\beta$ and the K_∞ values in x-ray units (10^{-11} cm). The last column gives this difference in terms of electron volts.

The principal energy bands for the S ions in the alkaline earth sulphides, as inferred from x-ray data, are indicated in Fig. 1. Fine structure, occasionally evidenced by the doublet character of the beta lines and the structure of the K absorption edge is not indicated, the lowest level of each kind being shown. The levels X and above, which belong to the sulphur continuum, are normally vacant, while the sulphur $3p$ band is normally completely filled. The K absorption edge marks the beginning of the removal of a K electron to the X continuum. The $K\beta$ line is emitted when one of the $3p$ electrons drops into the vacancy in the K shell. The last column of

TABLE I. *X-ray wave-lengths of sulphur. (a) Relatively narrow β_1, no β_x; (b) indication of β_x but not measurable; (c) very broad β_{1x}, not resolvable.*

COMPOUND	$SK\beta_1$	$SK\beta_x$	$SK\infty$	DIFF. X.U.	DIFF. VOLTS
MgS	5018.40	(a)	5005.3	13.1	6.44
CaS	5019.00	(a)	5006.6	12.4	6.10
SrS	5019.39	(b)	—	—	—
BaS	5019.74	(b)	5007.5	12.2	6.00
$MgSO_4$	5016.32	(a)	4987.3	29.0	14.3
$CaSO_4$	5017.81	(b)	4987.7	30.1	14.8
$SrSO_4$	5018.55	(b)	4987.3	31.3	15.4
$BaSO_4$	5019.14	5016.0	4987.9	31.2	15.3
Cu_2S	5020.9	5013.1	—	—	—
CuS	5020.8	5013.0	5011.3	9.5 1.8	4.66 0.9
Sb_2S_3	5020.8	5015.5	5009.9	10.9 5.6	5.45 2.8
MoS_2	5019.8	(c)	5009.9	9.9 —	4.86 —
Ag_2S	5024.0	5015.0	5010.1	13.9 4.9	6.82 2.4
Bi_2S_3	5018.5	(c)	5010.3	8.2 —	4.02 —

[1] Faessler, Zeits. f. Physik **72**, 374 (1931); Lundquist, Zeits. f. Physik **89**, 274 (1934); Parratt, Phys. Rev. **49**, 14 (1936); McDonald, Phys. Rev. **50**, 694 (1936); Tazaki, Hiroshima J. Sci. **6**, 299 (1936).

[2] Valasek, Phys. Rev. **47**, 896 (1935).

[3] Stelling, Zeits. f. Physik **50**, 506 (1928).

[4] Lindh, Diss. Lund 1928, or Siegbahn, Spekt. d. R. S. 285 (1931).

Table I gives the gap $X-3p$ in electron volts. This is the internal ionization potential of the sulphur ion in the crystal and should give the threshold of the ultraviolet absorption and the photoelectric effect in the sulphides. In the sulphates, the electrons associated with the oxygen atoms will determine this threshold since they will be more loosely held due to the increased screening.

Because of the similarity in electronic and crystal structure, the energy bands of the alkaline earth sulphides must be similar to those of the alkali halides which have been described by Slater and Shockley.[5] Thus one may imagine the highest occupied $3s$ levels of sulphur to be displaced downward by an amount equal to the Madelung energy Ae^2/r and broadened upward. The location of the original level $3s$ of S^{--} (at very large interionic distances) is determined by the electron affinity of this divalent ion. This has never been directly determined but can be obtained by a quadratic extrapolation of ionization potentials in the isoelectronic sequence of which it is a member.[6] This includes K^+, A, Cl^-, S^{--}, the corresponding ionization potentials being 31.7, 15.7, 3.75. The extrapolation leads to an energy of -4.18 electron volts for the removal of one of the two extra electrons of the divalent sulphur ion. The negative sign indicates that the free divalent ion is unstable. Its existence in crystals is permitted by the increased binding contributed by the surrounding lattice. This is equal to the Madelung energy, Ae^2/r, and is quite large, 15.7 to 19.3 electron volts, in the case of the alkaline earth sulphides.

A comparison of Pauling's ideas in regard to the energy levels of crystals[7] with those of Slater and Shockley reveals striking differences, though for alkali halides the experimental data fit either theory. Referring to Fig. 1 of this paper, the energy difference denoted by E_c is given, according to Pauling, by the average potential, or electron affinity, in the crystal and can be calculated from the diamagnetic susceptibility by a simple semi-empirical formula. The values of E_c thus obtained turn out to be rather large: 5.69[v] for NaCl and 7.01[v] for BaS.

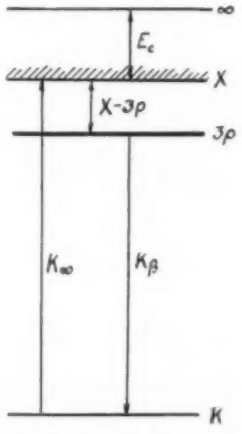

FIG. 1. X-ray levels in a crystal.

This would lead to an enormous difference between the internal and external photoelectric effect. Slater does not make E_c so large, for example, about 2 volts for NaCl, but he does not give a clear cut method for calculating this quantity. Another difference lies in the allocation of the occupied levels of the ions inside the crystal with respect to their positions in the free ions. Pauling displaces these occupied levels by only the Madelung energy, the shift being downward for the negative ions, upward for the positive. This equal shift of all levels preserves the differences between them and thus cannot account for the observed changes in wave-length of the x-ray emission lines, particularly those of the anions. While these changes are small in the alkali halides, they become quite large in the sulphates and sulphides, for example, as shown in Fig. 2. The treatment of the energy bands in crystals by Slater and Shockley suggests a possible solution. They consider the displaced levels to be broadened at the close interionic distances prevailing in the crystal, the broadening being in the opposite direction to the shift due to the Madelung term. In the case of the anion, the upward broadening of the $3p$ band and the higher continuum of their picture give nearly the same difference between the nearest edges of the two bands as one obtains by the formula of Pauling. Though Slater and Shockley's picture makes it possible to understand the changes in position and width of x-ray emission

[5] Slater and Shockley, Phys. Rev. **50**, 705 (1936).
[6] Glockler, Phys. Rev. **46**, 111 (1934).
[7] Pauling, Phys. Rev. **34**, 954 (1929).

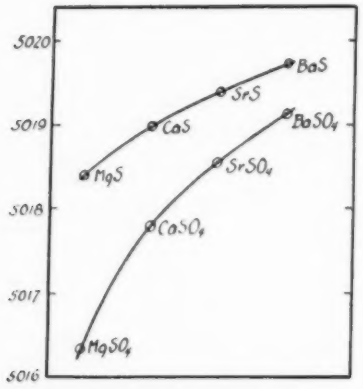

FIG. 2. Wave-lengths of the sulphur $K\beta_1$ lines in compounds.

lines of chemical compounds, the agreement with experiment would be better if the upward turn of the $3p$ band were not accompanied by so much broadening. In the case of NaCl discussed in their paper, the broadening is fully four times that observed.

Molybdenite, MoS_2, argentite, Ag_2S, stibnite, Sb_2S_3, and bismuthinite, Bi_2S_3, are semi-conducting sulphides. Their S $K\beta$ lines are quite broad and consequently difficult to measure accurately. The values given in Table I are probably correct to within 0.4 X.U. while the values for the other sulphides and sulphates are good to 0.15 X.U. Some of the broad lines of the semi-conducting sulphides can be resolved into two lines of approximately the same intensity. The upper level thus obtained is high enough so that its electrons may be raised into the X continuum by visible light. When only one line is observed, it is so broad that the upper edge of its $3p$ band is also close to X.

It is interesting to compare the x-ray spectra of sulphur in the alkaline earth sulphides with the corresponding results for the sulphates. The K absorption edges in the sulphates are harder by about 18.9 X.U. due mainly to the reduced screening resulting from the transfer of electrons from sulphur to the surrounding tetrahedral shell of oxygens. The $K\alpha$ lines are 3.3 X.U. harder in the sulphates.[8] This is an unusually large effect, especially since these are alpha lines. It is rarely surpassed even when the emission is due to a valence electron. On the other hand, the $K\beta$ lines in the sulphates are only 1 X.U. harder, on the average, than in the corresponding sulphides. This is evidence of a rather peculiar deformation.

It is sometimes assumed that sulphur has a valence of plus six in the sulphates. A classical interpretation of this would leave the sulphur with no $3p$ electrons and there would be no ordinary beta line in the x-ray spectrum. The exposure of the $2p$ shell would lead one to expect large shifts in the alpha lines. This agrees with observation, but the beta line appears in nearly its usual place and with fully as great intensity as in the sulphides where the $3p$ group of electrons is completed. It is also interesting that the beta line varies in wave-length from one alkaline earth sulphate to another to even a greater extent than in the corresponding sulphides, as shown in Fig. 2. This is another indication that the outer electron bands of a complex ion belong to the ion as a whole and thus deviate from those of the isolated ion as greatly as the electronic levels of molecules differ from those of the constituent atoms.

The writer is pleased to acknowledge the support of this work by a grant from the graduate school of the University of Minnesota. The author also gives his thanks to Mr. George Welch who assisted him in the laboratory.

[8] Parratt, Phys. Rev. **49**, 14 (1936).

The Excitation of Characteristic X-Rays by Protons

M. Stanley Livingston, Frank Genevese* and E. J. Konopinski†
Department of Physics, Cornell University, Ithaca, New York

(Received February 18, 1937)

A qualitative study of the x-rays produced by protons of 1.76 Mev energy shows that these rays are the characteristic K and L radiations from the targets used. The variation of intensity with proton energy and with atomic number is found to be in agreement with that expected theoretically.

Introduction

In the process of calibration of instruments intended for studies of nuclear disintegrations produced by protons of 2 million electron volts energy, x-radiation was observed to come from several targets in considerable intensity, while other targets showed a much lower intensity. It seemed advisable to make a qualitative study of the properties of this radiation, if only to safeguard interpretations of specifically nuclear phenomena.

Bothe and Franz[1] have shown that under alpha-particle bombardment x-rays characteristic of the target material were produced without the usual continuous background, and that the intensity of the radiation rose rapidly with increasing energy of the alpha-particles. Gerthsen and Reusse,[2] using protons of 150 kilovolts energy and sensitive Geiger counters to detect the radiation, found evidence for the excitation of Al_K, Mg_K and Se_L radiation, but observed no radiation from a target of intermediate atomic weight, Mn. These workers suggested the interpretation which is amplified in the discussion to follow. Henneberg[3] has calculated the probability of excitation of the K radiation from Al as a function of proton energy and his results were found to be in agreement with the observations of Gerthsen and Reusse. Several other observers,[4] using low energy protons, have studied the x-radiation from protons with sensitive detecting instruments and have also concluded that they are characteristic of the target.

The present observations extend the range of proton energies to much higher values and include a wide variety of targets. When the absorption of the x-rays by the air, the target, and other absorbing materials in their path is taken into account the results are found to agree with those predicted from an extension of Henneberg's calculations.

Experimental

The protons were accelerated to high speeds in a small "cyclotron"[5] and directed against targets mounted in the vacuum chamber. For the study of the x-ray intensity as a function of proton energy, aluminum absorbing foils of graded thickness were inserted in the path of the proton beam. Preliminary calibrations of the stopping powers of the foils with alpha-particles insured an accurate knowledge of the reduced energies of the proton beam. The initial energy of the protons was calculated from the resonance conditions and geometry of the cyclotron. The current of protons striking the target (mounted in a shallow Faraday cage) was 5.0 microamperes. For the purpose of measuring relative x-ray intensities an electrometer was used to measure the charge collected in a given time interval on an 8 microfarad condenser connected to the target; various x-ray intensity measurements could then be compared for equal numbers of incident protons.

The target was mounted at an angle of 45° to the direction of the proton beam and to the direction of observation. See Fig. 1. The radiations emerged from the target through a vacuum-tight mica foil, and after passing through lead collimating apertures, entered the ionization

* Now at the Corning Glass Works.
† National Research Fellow.
[1] Bothe and Franz, Zeits. f. Physik **52**, 466 (1928).
[2] Gerthsen and Reusse, Physik. Zeits. **34**, 478 (1933).
[3] Henneberg, Zeits. f. Physik **86**, 592 (1933).
[4] Peter, Ann. d. Physik **27**, 299 (1936); Hoffmann, Physik. Zeits. **37**, 694 (1936).
[5] Livingston, Rev. Sci. Inst. **7**, 55 (1936).

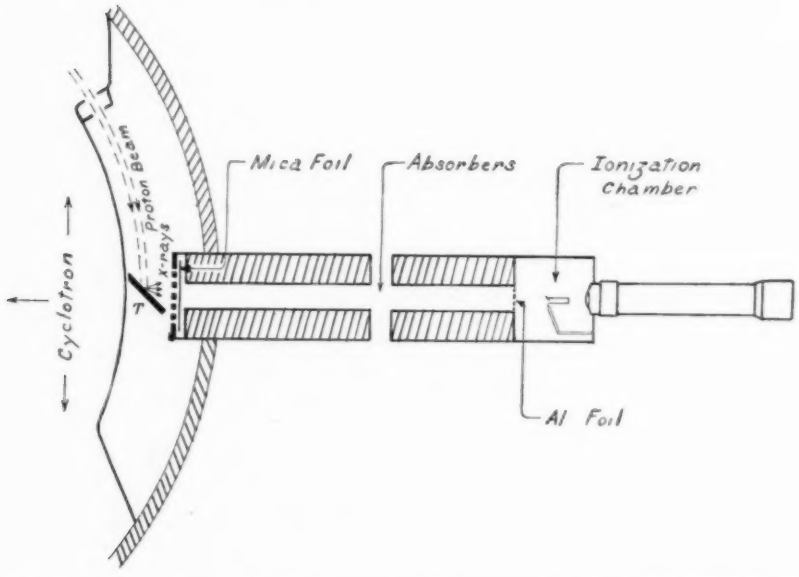

FIG. 1. Schematic diagram of the experimental arrangement for observing x-rays from proton bombardment.

chamber. This was a quartz fiber electroscope, patterned after those developed by Lauritsen,[6] in the form of a thin-walled brass cylinder of 2.5 cm radius and 5 cm length containing air at atmospheric pressure, with a thin Al window 2 cm in diameter over the end. Measurements of the voltage sensitivity together with a roughly computed capacity made it possible to estimate the charge sensitivity and thus absolute intensities.

Before entering the ionization chamber the radiation had to traverse a certain thickness of the target, a mica window of 2×10^{-3} cm thickness (about 20 cm air equivalent absorption for x-rays of $10>\lambda>0.7$A), 18 cm of air path and a thin Al window of 2×10^{-4} cm thickness (about 2.5 cm air equivalent). This served to absorb largely those x-rays of wave-length greater than about 3A, and so led to low intensities for the radiation from light targets.[7] In the discussion to follow this plays an important role in the interpretation of the results.

The identification of the radiation as x-rays was accomplished by studying the absorption in thin aluminum foils placed in front of the electroscope, and by the observation that a crossed magnetic field sufficient to deflect electrons of 100 million volts energy had no effect on the intensities observed in the ionization chamber.

RESULTS

(a) Absorption measurements

A study of the absorption in aluminum foils of the radiation from a Zn target resulted in the data plotted logarithmically in Fig. 2. The absorption coefficient of 42.3 cm²/g of Al deduced from the slope of the straight line indicates a wave-length of 1.47A, and is in good agreement with the mean value of the K lines of Zn, which is 1.43A. The experimental points fall on a well-defined straight line, indicating that the radiation is monochromatic to within 0.1A and that there is no appreciable intensity of continuous radiation, a fact which is expected from theoretical considerations.[8] The L radiation from Zn would

[6] Crane, Lauritsen and Soltan, Phys. Rev. **44**, 514 (1933).
[7] High intensities from a carbon target originally observed were found to be due to the brass target holder.

[8] The intensity of continuous radiation is known to be proportional to $(e^2/Mc^2)^2$, where M is the mass of the emitting particle. For this reason the continuous radiation

be of about 12A, and so would be completely absorbed in the air path. This evidence, combined with the relative intensity measurements to be discussed, makes it seem probable that the radiation in each case is characteristic of the target.

(b) Voltage excitation measurements

The relative intensity of the radiation from Zn as a function of the proton energy is given in Fig. 3. This shows the intensity dropping below the observational limit of this experiment at about 600 kilovolts. The curve was calculated theoretically (cf. "Discussions and Calculations") and fitted to the data at the 1.37 Mev point; the experimental points are found to agree within the limits of error. Similar data taken for other targets (Mg and Mo) show the same features, but with different "slopes" in accordance with the predictions of the theory for the different K wave-lengths.

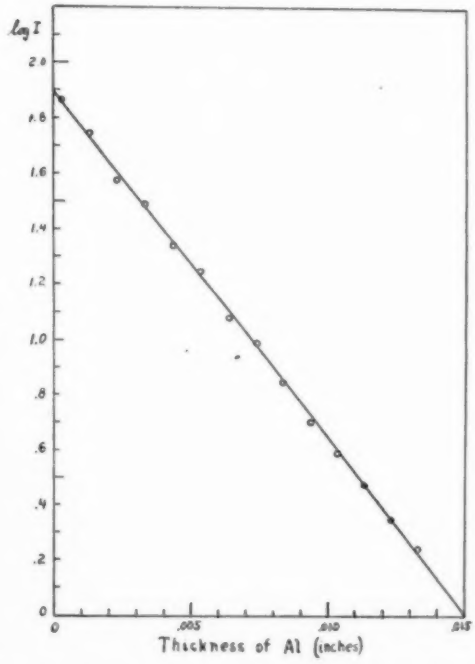

FIG. 2. Absorption in aluminum of the radiation from a zinc target bombarded by 1.76 Mev protons.

(c) Variation with atomic number of the target

The relative intensities from the various targets used, for equal currents of 1.76 Mev protons, are plotted in Fig. 4. These data indicate the existence of two peaks, one near atomic number 26 and another in the rare earths group. These peaks are presumably caused by the K and the L radiations from the respective targets. The steep descent from each peak on the side of the higher atomic numbers is ascribed by the theory to the decreasing probability of excitation of the higher energy K and L radiations from these targets by protons of a given energy. The low intensities on the low atomic number sides of the peaks are due to the exceedingly strong absorption of the air and other absorbing materials for the low energy radiations from these targets. A corrected theoretical curve (cf. "Discussions and Calculations") for the K radiation is fitted to the observed data at Fe, and seems to represent the data adequately. The curve for the L radiation (second peak) was drawn by analogy.

(d) Absolute intensity estimates

In Figs. 3 and 4 the intensities are given in arbitrary units representing the number of scale divisions traversed in a 6 sec. interval by the electroscope fiber—per 1.0 microampere of proton current—incident on the target. From the measured voltage sensitivity and the com-

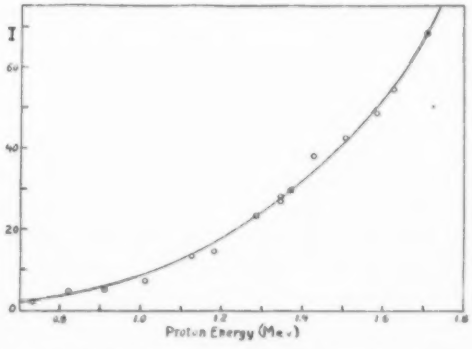

FIG. 3. Variation of x-ray intensity from a zinc target with proton energy. The curve is calculated theoretically and matched to the data at one point.

from protons will be very weak compared to the continuous radiation observed in excitations by electrons. Radiation from the free electrons accelerated by proton impact will have a minimum wave-length of 32A due to conservation laws and so would be unobservable in these experiments.

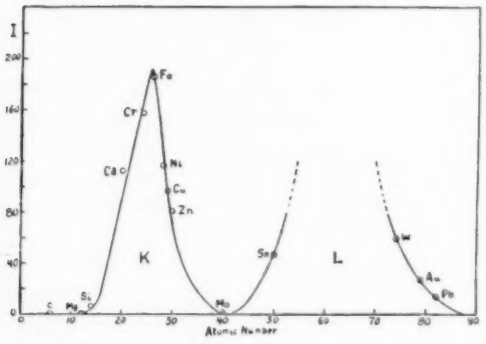

FIG. 4. Variation of x-ray intensity with atomic number of the target. The curve representing the K peak was calculated theoretically and matched to the experimental data at the point for Fe. The L curve is drawn by analogy.

puted capacity of the electroscope a charge sensitivity of about 2×10^{-5} e.s.u./div. was obtained. For the peak intensity on Fig. 4 (Fe) this leads to the value of 5×10^{-4} e.s.u./sec. for each cubic centimeter of the ionization chamber (at a distance of 20 cm from the target) with a proton current of 1.0 microampere. A theoretical estimate of the intensity to be expected, corrected for the special conditions of this experiment, gave roughly 5×10^{-3} e.s.u./cm³ sec. This discrepancy is not entirely surprising in view of the uncertainties in the corrections.

DISCUSSION AND CALCULATIONS

Henneberg[8] gives a graphical representation of the calculated cross section for the excitation of K radiation as a function of proton energy and atomic number, $\varphi(E, Z)$. For small E the dependence is approximately: $\varphi\sim E^4/Z^{12}$. The high absorption of the target for its own K radiation necessitates the superposition of a correction for it upon the thick target correction due to the penetration of the protons. Because of the 45° incidence of the proton beam the x-rays come through a thickness of target equal to the proton penetration, and the intensity of the emergent x-rays is proportional to:

$$\Phi(E_0, Z)=\int_0^{x_0}\varphi(f(x), Z)e^{-\kappa(Z)(x_0-x)}dx, \quad (1)$$

where $E=f(x)$ is the energy range relation for protons[9] in the target ($f(x)\sim x^{\frac{1}{2}}$); x_0 is the maximum penetration of the protons ($E_0=f(x_0)$); $\kappa(Z)$ is the x-ray absorption coefficient of the target material just above the K absorption limit in the wave-length scale. The numerical evaluation of (1) as a function of E_0 with $Z=30$ gave the curve shown in Fig. 3, after a matching with the experimental data at one point. The variation of E_0 from 1.76 Mev to 0.73 Mev is equivalent to a variation of x_0 from 0.0018 cm to 0.0005 cm in Zn.

In order to account for the observed variation of the x-ray intensity with atomic number (Fig. 4) it is necessary to consider the absorption of the various x-ray frequencies by the air, the mica and the Al foils. It is also necessary to correct for the relative sensitivity of the ionization chamber for radiations of various wave-lengths. Consequently, the peaks arise from the following type of function (giving the number of ions collected per second by the electroscope):

$$I=NN_P\Phi(E_0, Z)\cdot(\omega/2)e^{-\tau(\lambda)d}\cdot S. \quad (2)$$

N is the number of atoms per cubic centimeter of the target; N_P is the number of protons incident per second. ω is the fraction of a sphere, centered at the target, subtended by the window of the ionization chamber; it is divided by 2 in order to allow for the fact that the grid at the mica window intercepts half the x-ray beam. $\tau(\lambda)$ is the air absorption coefficient which varies with the wave-length of the radiation, λ. The absorption path for the x-rays in air equivalent cm is given by d. Finally, S is a sensitivity factor for the ionization chamber. If we take into account only the ions created by the photoelectrons (which lose 32.5 volts per ion pair formed[10]), the number of ions collected by the electroscope fiber when n quanta of energy $h\nu$ (in volts) pass through a chamber of length l is:

$$I=nS=n\frac{h\nu-W}{32.5}(1-e^{-\tau(\lambda)l})U. \quad (3)$$

W is the average ionization potential of nitrogen and U is the fraction of the ions recorded.

[9] Mano, Ann. de physique **1**, 407 (1934); Rosenblum, ibid. **9**, 408 (1928).
[10] Gray, Proc. Roy. Soc. **156**, 578 (1936).

The magnitude of U is determined by the amount of recombination which takes place. This was estimated by dividing the electroscope into sections of spherical condensers in each of which there is a uniform distribution of sources of ions and a distribution of sinks proportional to $\alpha n_1 n_2$, where α is the recombination coefficient (1.6×10^{-6} cm³/sec. for air at N. T. P.) and n_1, n_2 the density of positive and negative ions. In this way, S was found to vary by a factor 5 from Ca to Br. It is 0.41 for the peak intensity (Fe).

The function (2) is quite sensitive to S and to the equivalent absorption thickness d; the agreement between theory and experiment as shown by Fig. 4 is as good as could be expected.

I as given by (2), multiplied by the charge on an ion, represents the charge collected by the electroscope per second. The factors $\frac{1}{2}N_P N\Phi$ give the number of quanta emerging from the target per second ("$\frac{1}{2}$" because they may only emerge from one side of the thick target). For Fe this was calculated to be 2×10^{12} quanta per second. Multiplication by $\omega e^{-\tau d}$ gives n, the number of quanta which enter the ionization chamber per second. Then, using (3), we obtain $enS/v=5\times10^{-3}$ e.s.u./cm³ sec. as the charge collected per sec. per cm³ of ionization chamber (volume v), for the Fe radiation.

The evidence for the identification of the first peak of Fig. 4 with the characteristic K radiations is very strong. It seems reasonable that the second peak should be due to L radiation, although no calculations have been attempted and the data are scanty. The curve obtained theoretically for the K radiation is sensitive to the many corrections. Accordingly no strictly quantitative check with the theory can be claimed in this respect. However, qualitatively at least, the agreement is sufficiently satisfactory to justify the interpretation given.

It may be of some significance to x-ray workers that this offers a method for the production of K radiation from light elements without the usual continuous background. The results gain interest also from the fact that the excitation of K radiation by protons plays a part in the determination of the rate at which protons lose energy in passing through matter. The experimental confirmation of the theoretical predictions thus lends support to the use of the theory in determining range-energy relationships.

The authors wish to express their gratitude to Professor H. A. Bethe and Dr. L. G. Parratt for their many suggestions, and to Mr. C. P. Baker for assistance in the experimental work. The experiments were performed with apparatus partially supported by grants from the Grants-in-Aid Committee of the National Research Council.

Damped Electron Waves in Crystals

J. C. SLATER*
Institute for Advanced Study, Princeton, New Jersey
(Received March 24, 1937)

Electrons in solids, as in electron diffraction, suffer inelastic impacts if their energy is great enough to exceed the resonance energy of the atoms of the crystal, resulting in strong damping of the electron beams, with consequent broadening of the reflected peaks about the Bragg scattering angles, and reduction of the reflection coefficient. The problem is discussed mathematically, on the basis of the conventional theory of electron diffraction, by introducing an empirical damping constant in the form of a pure imaginary term in the potential. It is shown that such a constant leads to damped waves of the required sort, and the equations for energy and reflection coefficient are set up. The results are qualitatively of the sort necessary to explain the observations, though no marked asymmetry in the reflected peaks is predicted. Presumably the observed asymmetries arise, as Harding has suggested, from irregular spacings of the atomic planes near the surface. One interesting result of the theory is that the sharp distinction between allowed energy bands and forbidden gaps, which is found in the theory of undamped electrons in periodic lattices, is lost, for all waves are more or less damped.

1. INTRODUCTION

THE conventional theory of solids, developed particularly for metals, assumes as a first approximation that the electrons move in a periodic static potential field. The solution of this problem yields modulated wave functions, whose value is multiplied by a factor $\exp(i\mathbf{k}\cdot\mathbf{R})$ in going from the neighborhood of one atom to a corresponding point in another unit cell, if $\mathbf{R}$ is the vector distance from one point to the other, $\mathbf{k}$ a constant. Such solutions exist for most energies, if the electron is in a high energy level, though there are certain gaps in the energy, in which only damped waves exist as solutions of the problem, one component of the vector $\mathbf{k}$ becoming pure imaginary. On account of these modulated solutions, it is generally supposed that electrons move freely through a crystal lattice, unless they happen to lie in the region of the energy gaps, in which case it is supposed that they are reflected from the crystal, accounting for the Bragg reflection in the problem of electron diffraction.

This naive picture, in which electrons either are freely transmitted or totally reflected, is, of course, far from agreeing with the experimental facts. The most conspicuous difference between electron and x-ray diffraction is the great extinction of electron beams in solids.[1] Furthermore, electrons not only fail to penetrate more than a few atomic layers, but the reflection coefficient at the Bragg angle is only of the order of one percent, instead of unity as the simple theory predicts, and the angular range over which there is reflection is of the order of ten times the range predicted by the simple theory. These are the sort of changes in reflection which would be expected if the electron wave were rapidly extinguished in the crystal. Such extinction is, of course, to be expected on general grounds. An electron moving through atoms in a gas will suffer only elastic collisions, with small loss of energy, if it has an energy smaller than the resonance energy of the atoms of the gas. At higher energies, however, it will suffer inelastic collisions, raising electrons of the gas atoms to higher energy, and losing energy itself. This results in a rapid extinction of beams of electrons of high energy, of a type not met with slow electrons. Of course, the electrons are not lost, only slowed down; but if we are considering only electrons of approximately the incident energy, we shall consider them lost to the beam. In a similar way, the conduction electrons in a metal can have only elastic impacts, losing a little energy to the lattice vibrations, but electrons with more than a few volts energy above the conduction levels can have inelastic impacts, losing part of their energy, raising conduction or x-ray electrons to excited energy levels in the lattice. This is observed experimentally; if electrons of a few hundred or more volts are shot

* On leave from the Massachusetts Institute of Technology, Cambridge, Massachusetts.

[1] For experimental information about electron diffraction, a useful reference is Beeching, *Electron Diffraction* (Methuen, London, 1936).

into a metal, two groups of secondary electrons are emitted: those which have lost a few volts, and happen to have their direction changed so that they emerge from the metal, and slow electrons, which have been raised from conduction levels by the collisions. The theory of such inelastic impacts has recently been discussed by Rudberg and the writer.[2]

A complete treatment of the inelastic damping of excited electron waves, along these lines, would be very complicated. In the present paper, we shall be content with a simpler task. We shall show that an empirical damping constant can be introduced, and that solutions of the wave mechanical problem including this damping give exponentially damped waves, of the sort to be expected intuitively. Furthermore, we shall set up the conditions for electron diffraction in the usual case, and shall show that the decreased reflection coefficient and broadened beam which are found experimentally are adequately described by the theory. We shall also find certain interesting consequences relating to the theory of metals. Thus, the distinction between the allowed and forbidden ranges of energy becomes lost when all waves are damped, and the discontinuities of energy which are such a characteristic feature of the theory with undamped waves become rapidly removed when even a small damping is introduced.

The dynamical theory of electron diffraction has been recently discussed by Harding,[3] using an extension of Darwin's method for x-ray diffraction, in which the scattering from each plane of atoms is considered separately. He attributes most of the broadening to irregularity of spacing of the few planes of atoms near the surface of the crystal, though he also considers absorption. Such an irregularity is undoubtedly responsible for many of the anomalies observed in electron diffraction, in particular for the asymmetry of beams, and Harding's method undoubtedly is the most practicable way of handling it. The object of the present paper is to point out, however, that the absorption can be treated by the conventional theory as well, with tolerably simple results, and to suggest that perhaps it has a more important role than Harding believes. Harding's statement, in particular, that absorption actually decreases the breadth of the beams, seems very questionable; the present theory indicates just the sort of broadening which we should expect on the basis of other types of damped waves with which we are familiar.

[2] E. Rudberg and J. C. Slater, Phys. Rev. **50**, 150 (1936).
[3] J. W. Harding, Phil. Mag. **23**, 271 (1937).

2. Damped Waves in a Region of Constant Potential

A damping constant can be formally introduced into Schrödinger's equation by the device of adding a pure imaginary term to the potential energy, just as in optics a pure imaginary term in the refractive index results in damping. In this section we shall ask how to handle such a term in a region of constant potential. That is, we shall consider the modified Schrödinger equation

$$-\nabla^2\psi+(U-iV)\psi=i\partial\psi/\partial t, \qquad (1)$$

where U is the real potential, $-iV$ the damping term, both constants. The sign of the damping term is chosen so that it will result in disappearance rather than appearance of charge. The units in (1) are atomic units; that is, distances are measured in terms of the radius of the first Bohr orbit of hydrogen, energies in terms of the Rydberg energy, frequencies in terms of 2π times the Rydberg frequency. First we shall show that (1) really leads to a continuous disappearance of charge. To do this, we compute the time rate of change of the charge density $\psi^*\psi$, plus the divergence of the current density, which in these units is $i(\psi \text{ grad } \psi^*-\psi^* \text{ grad } \psi)$, and we shall show that the result is negative, rather than zero as it would be if the equation of continuity held. When we compute this quantity, we substitute from Eq. (1), and from the similar equation for the complex conjugate ψ^*, in which we note that the term iV must appear with positive rather than negative sign, and we find in an entirely conventional way

$$(\partial/\partial t)(\psi^*\psi)+\text{div } i(\psi \text{ grad } \psi^*-\psi^* \text{ grad } \psi) = -2V\psi^*\psi. \qquad (2)$$

That is, the density represented by $\psi^*\psi$ is destroyed at a rate given by $-2V$ times the density itself. We should emphasize again, of course, that as we use the equation we shall be working only with electrons of a given energy, and by their destruction we mean merely their

inelastic scattering to another energy, so that they are removed from the particular energy beam we are considering.

Two types of solution of (1) are particularly important. In the first place, we can find solutions sinusoidal in space, but damped in time. Thus by substitution we see at once that

$$\psi = \exp(-Vt - iEt + i\mathbf{k}\cdot\mathbf{r}) \tag{3}$$

is a solution of the equation, where $\mathbf{k}$ is an arbitrary real vector, $\mathbf{r}$ the radius vector, provided

$$E = k^2 + U, \tag{4}$$

which in these units equals the kinetic energy (k^2, where $\mathbf{k}$ is essentially the momentum) plus the potential energy U. For this type of solution, the divergence of the current in (2) is zero, but if we form $\psi^*\psi$ we have $\exp(-2Vt)$, which obviously satisfies Eq. (2). The quantity $1/2V$ then plays the part of the relaxation time for the charge density, $1/V$ the relaxation time for the wave function. Such a solution would be appropriate, for instance, in a hypothetical problem in which electrons were raised to an excited state all through the interior of the volume by some sudden action, such as a sudden burst of x-rays or other radiation capable of penetrating the volume, and then were allowed to die down. We note that in such a case the damping constant does not affect the function of space at all, but only the time variation of the function.

The second type of solution is the one which concerns us in electron diffraction and similar problems. Here there is a steady state as far as time is concerned. Electrons are being fed into the crystal from the outside at a rate fast enough to balance their loss by inelastic impact, plus their reflection to the outside. We must then look for a solution which is purely exponential in time, but damped in space. Thus

$$\psi = \exp(-iEt - \boldsymbol{\alpha}\cdot\mathbf{r} + i\mathbf{k}\cdot\mathbf{r}), \tag{5}$$

where $\boldsymbol{\alpha}$, $\mathbf{k}$ are arbitrary vectors, is a solution of (1), provided

$$E = k^2 + U - \alpha^2 + 2i(\boldsymbol{\alpha}\cdot\mathbf{k}) - iV, \tag{6}$$

with a real E. Eq. (6) really involves two statements:

$$E = k^2 + U - \alpha^2, \tag{6a}$$

$$2(\boldsymbol{\alpha}\cdot\mathbf{k}) = V. \tag{6b}$$

Eq. (6b) determines the component of the damping vector $\boldsymbol{\alpha}$ in the direction of the propagation vector $\mathbf{k}$, but leaves its component at right angles undetermined, and (6a) determines the energy in terms of $\boldsymbol{\alpha}$ and $\mathbf{k}$. In any problem where a beam of electrons is entering a region over a plane surface, and is being damped inside, the direction of $\boldsymbol{\alpha}$ must of course be chosen normal to the surface, so that the boundary conditions with a beam of constant intensity outside can be satisfied. Equality of energy between the inside and outside beams must also be maintained, as well as equality of the tangential component of $\mathbf{k}$. These provide enough conditions to fix the vectors $\mathbf{k}$ and $\boldsymbol{\alpha}$ within the damping medium. It is to be noticed that even in a non-absorbing medium, $V=0$, we can still have damped waves, as we know by the optical analogy of total reflection, but (6b) tells us that the damping must be at right angles to the propagation vector. Such waves have not been useful in electron theory, because electrons are bent toward the normal on entering a crystal, so that there is no total reflection at the surface between the crystal and air.

3. Damped Waves in a Periodic Potential Field

We now set up the problem of damped waves in a periodic potential field. We assume the same Schrödinger Eq. (1) as before, only now we assume that

$$U = \sum_{\mathbf{K}} W(\mathbf{K}) \exp -i(\mathbf{K}\cdot\mathbf{r}), \tag{7}$$

where the vectors $\mathbf{K}$ are the vectors in the reciprocal lattice corresponding to the crystal in question, and the W's are the Fourier coefficients of the potential. We continue to regard the damping term V as constant; but the results which we find hold without essential change if V is also a periodic function. Now we ask for a solution of (1) with the potential (7), in the form of a sinusoidal function of time, multiplied by a damped modulated function of position. That is, we try to find a solution

$$\psi = \exp(-iEt - \boldsymbol{\alpha}\cdot\mathbf{r} + i\mathbf{k}\cdot\mathbf{r})u(\mathbf{r}), \tag{8}$$

where $u(\mathbf{r})$, a periodic function of position, can

be expanded as

$$u(\mathbf{r})=\sum_{\mathbf{K}}A_{\mathbf{K}}\exp i(\mathbf{K}\cdot\mathbf{r}). \quad (9)$$

When the function (8) is substituted in the differential equation, we find the condition

$$\exp(-iEt-\boldsymbol{\alpha}\cdot\mathbf{r}+i\mathbf{k}\cdot\mathbf{r})\sum_{\mathbf{K}}\exp(i\mathbf{K}\cdot\mathbf{r})\sum_{\mathbf{K}'}C(KK')A_{\mathbf{K}'}=0, \quad (10)$$

where

$$C(KK')=((\mathbf{k}+\mathbf{K})^2-\alpha^2+2i(\boldsymbol{\alpha}\cdot(\mathbf{k}+\mathbf{K}))-iV-E)\delta_{\mathbf{K},\mathbf{K}'}+W(\mathbf{K}'-\mathbf{K}). \quad (11)$$

We can satisfy Eq. (10) by making the last summation equal to zero:

$$\sum_{\mathbf{K}'}C(KK')A_{\mathbf{K}'}=0, \text{ for each value of } \mathbf{K}. \quad (12)$$

In order to satisfy this infinite set of simultaneous homogeneous linear equations, it is necessary as usual to make the determinant of coefficients $C(KK')$ equal to zero:

$$\Delta|C(KK')|=0. \quad (13)$$

Eq. (13) provides a secular equation for E, to be solved subject to the condition that E is real. Just as in the case of constant potential, we have enough constants at our disposal to satisfy both conditions. Thus if $\mathbf{k}$ is determined, and the direction of the damping vector $\boldsymbol{\alpha}$ is fixed, we have two constants, the energy E and the magnitude of $\boldsymbol{\alpha}$, with which to satisfy the secular equation and the additional requirement that E be real. Or if, as in the electron diffraction case, the energy, the two components of $\mathbf{k}$ parallel to the surface of the crystal, and the direction of $\boldsymbol{\alpha}$ are determined, we have the normal component of $\mathbf{k}$ and the magnitude of $\boldsymbol{\alpha}$ at our disposal. In practice, the calculation seems to be simplest when $\mathbf{k}$ and the direction of $\boldsymbol{\alpha}$ are fixed, and E and the magnitude of $\boldsymbol{\alpha}$ are found by the equations.

We shall now consider the solution of the secular Eq. (13) in simple special cases. As in the conventional theory of electron diffraction, we shall assume that far from a Bragg reflection one term of the summation (9) is sufficient, and that near such a reflection two terms must be used. If only one term is to be used, the condition becomes at once

$$(\mathbf{k}+\mathbf{K})^2-\alpha^2+W(0)+2i(\boldsymbol{\alpha}\cdot(\mathbf{k}+\mathbf{K}))-iV-E=0,$$

exactly like Eq. (6) for the case of constant potential, which we have already discussed. We shall then concentrate on the case where two waves are to be used. To fix our attention on a definite problem, we shall take the reflecting planes parallel to the surface of the crystal, the case of regular reflection, though the treatment is carried out in an entirely analogous way in other cases. Then $\mathbf{K}$ is normal to the surface, pointing out of the crystal, and $\boldsymbol{\alpha}$ must be assumed normal, and pointing into the crystal. If $\mathbf{k}_n$ is the normal component of $\mathbf{k}$, pointing into the crystal, the secular equation then becomes

$$\begin{vmatrix} k^2-\alpha^2+W(0)+2i\alpha\mathbf{k}_n-iV-E & W(\mathbf{K}) \\ W(\mathbf{K}) & k^2-\alpha^2+W(0)+2i\alpha\mathbf{k}_n-iV-E-2\mathbf{k}_n|\mathbf{K}|+K^2-2i\alpha|\mathbf{K}| \end{vmatrix}=0, \quad (14)$$

where we have assumed the incident propagation vector to be $\mathbf{k}$, the reflected one $\mathbf{k}+\mathbf{K}$. We shall have Bragg reflection when $\mathbf{k}_n-|\mathbf{K}|/2=0$. Let us then let

$$\mathbf{k}_n-|\mathbf{K}|/2=\delta, \quad (15)$$

where δ is a small quantity vanishing in the Bragg case. Expanding the determinant (14), and solving the quadratic, we then have

$$E=k^2-|\mathbf{K}|\delta+W(0)-\alpha^2+2i\alpha\delta-iV\pm[W^2(\mathbf{K})-\alpha^2K^2+K^2\delta^2+2i\alpha K^2\delta]^{\frac{1}{2}}. \quad (16)$$

In practice, it is more convenient to express this in terms of the glancing angle of incidence θ. Then if $\mathbf{k}_t$ is the tangential component of $\mathbf{k}$, which by the boundary conditions must be equal inside and outside the crystal, we must have

$$E\cos^2\theta=\mathbf{k}_t^2. \quad (17)$$

We then subtract $E\cos^2\theta$ from each side of (16), leaving $E\sin^2\theta$ on the left, and for the first two terms on the right $k^2-|\mathbf{K}|\delta-k_t^2=k_n^2-|\mathbf{K}|\delta=(\mathbf{K}/2)^2+\delta^2$. Eq. (16), with these changes, then becomes an equation for $E\sin^2\theta$. We still must impose the condition that E must be real. The radical in (16) is complex. Its imaginary term

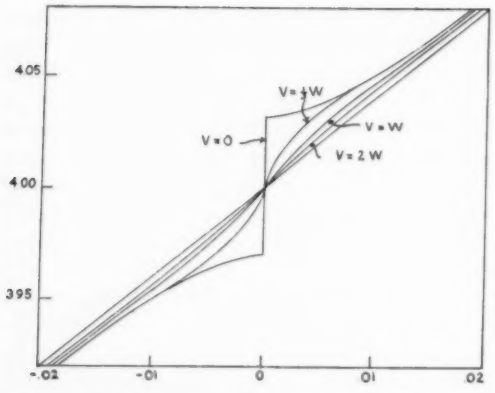

FIG. 1. $E \sin^2\theta$, component of energy normal to surface, as function of δ, component of momentum normal to surface, both in atomic units, for different values of V/W, the ratio of the damping constant to the energy perturbation between incident and reflected beams.

must cancel the other imaginary terms in the equation, and its real term alone is left to contribute to E. Thus we have

$$\pm[W^2(\mathbf{K})-\alpha^2K^2+K^2\delta^2+2i\alpha K^2\delta]^{\frac{1}{2}} = -2i\alpha\delta+iV+f, \quad (18)$$

where f is the real part of the radical. We square both sides of (18), and equate real and imaginary parts separately. From the imaginary part we find

$$f=\alpha K^2\delta/(V-2\alpha\delta). \quad (19)$$

The real part gives a quadratic for α. Its solution is

$$\alpha=-\frac{2\delta V}{K^2-4\delta^2} \pm\left[\frac{W^2+V^2+K^2\delta^2-f^2}{K^2-4\delta^2}+\left\{\frac{2\delta V}{K^2-4\delta^2}\right\}^2\right]^{\frac{1}{2}}. \quad (20)$$

We could eliminate f between (19) and (20) to get an equation for the damping constant α, but the resulting equation is of the fourth degree and cannot be conveniently solved. It is much more practicable to solve Eqs. (19) and (20) simultaneously for f and α by successive approximations, putting a trial value of α in (19), computing a corrected α from this f by (20), and repeating the process until the final value equals the initial one. With a little practice, this calculation proves to be very simple.

We note that Eq. (20) gives two solutions for α. One of these is in general positive and the other negative, and to get a wave which is damped as we go into the crystal we must take the positive root. This determines a single value for f, so that the double valued solution appearing in (16) is not really of physical significance. When we have found the appropriate value of f, we then find for the energy, from (16) and the changes made in that equation,

$$E\sin^2\theta=(K/2)^2+\delta^2+W(0)-\alpha^2+f. \quad (21)$$

Having found the energy, we can now use Eqs. (12) to find the reflection coefficient. Thus if A_0 is the incident amplitude, $A_{\mathbf{K}}$ the reflected amplitude, we have

$$A_0W(\mathbf{K})+A_{\mathbf{K}}(k^2-\alpha^2+W(0)+2i\alpha\mathbf{k}_n -iV-E-2\mathbf{k}_n|\mathbf{K}|+K^2-2i\alpha|\mathbf{K}|)=0. \quad (22)$$

When we substitute for E, this becomes

$$A_0W(\mathbf{K})-A_{\mathbf{K}}(|\mathbf{K}|\delta+f +i(V+\alpha|\mathbf{K}|-2\alpha\delta))=0. \quad (23)$$

From (23) we can then find the ratio $A_{\mathbf{K}}/A_0$ of reflected to incident amplitude, and squaring the magnitude of this we have the reflection coefficient

$$R=W^2(\mathbf{K})/((|\mathbf{K}|\delta+f)^2 +(V+\alpha|\mathbf{K}|-2\alpha\delta)^2). \quad (24)$$

When V is of the same order of magnitude as W, numerical calculations must be made by the method we have sketched. If V^2 is large compared with W^2, however, W^2 can be neglected in the radical in (18), and the expressions simplify greatly. Eq. (18) then becomes

$$\pm|\mathbf{K}|(\delta+i\alpha)=-2i\alpha+iV+f,$$

from which

$$f=\pm|\mathbf{K}|\delta, \quad \alpha=V/(\pm|\mathbf{K}|+2\delta). \quad (25)$$

Eqs. (25) correspond to (19) and (20) in the general case. Since $|\mathbf{K}|$ is a large quantity, δ small, we see that to have α positive we must choose the upper signs. Then the expression for the energy becomes

$$E\sin^2\theta=(|\mathbf{K}|/2+\delta)^2+W(0)-\alpha^2, \quad (26)$$

and the reflection coefficient is

$$R=(W/2)^2/((\mathbf{K}\delta)^2+(V\mathbf{K}/(\mathbf{K}+2\delta))^2). \quad (27)$$

For all ordinary cases, the line is narrow enough so that the ratio $\mathbf{K}/(\mathbf{K}+2\delta)$ can be replaced by unity. Then finally we have

$$R=(W/2)^2/((\mathbf{K}\delta)^2+V^2). \tag{28}$$

The expression (28) is a typical resonance form of curve. The reflection coefficient at the maximum, $\delta=0$, is

$$R_{max}=(W/2V)^2, \tag{29}$$

and the half-breadth, the difference of the two values of δ for which R has half its maximum value, is

$$\delta_2-\delta_1=2V/\mathbf{K}. \tag{30}$$

It is more interesting to compare the breadth with the breadth which the totally reflecting region would have in the theory without damping. To do this, we must use $E\sin^2\theta$ rather than θ as independent variable. We find at once that

$$(E\sin^2\theta)_2-(E\sin^2\theta)_1=2V. \tag{31}$$

The corresponding quantity for the totally reflecting region is $2W$. Hence the half-breadth with damping constant V is (V/W) times the width of this totally reflecting region. If the observed half-breadth is 10 times this theoretical totally reflecting breadth, then V is 10 times W, we are in the region where this approximation is valid, and the maximum reflection coefficient should be $(1/20)^2=1/400$, which is of the order of magnitude of the observed value. One has something of the impression, however, in comparing this theory with published statements of reflection coefficient and breadth, that for a given reflection coefficient the theory gives a somewhat narrower line than is observed. This would fit in with Harding's[3] theory that part of the broadening comes from irregularity of the lattice rather than absorption.

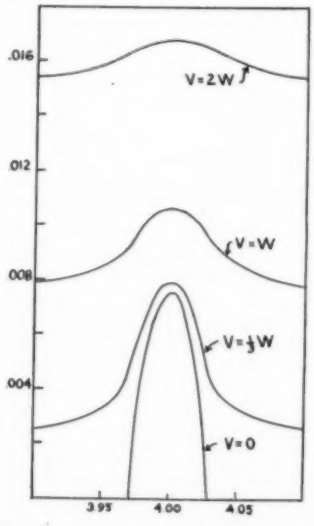

FIG. 2. Total damping constant α, arising from both inelastic and elastic impacts, as function of $E\sin^2\theta$.

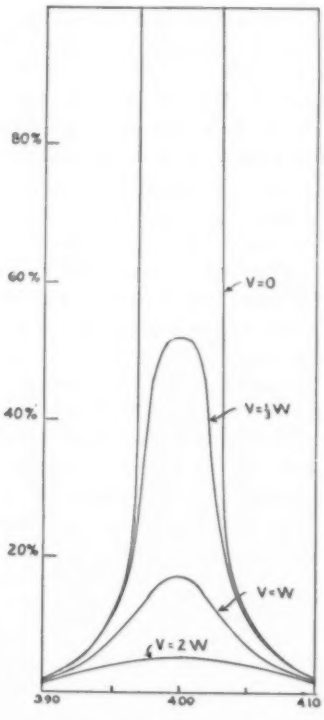

FIG. 3. Reflection coefficient of diffracted beam, as function of $E\sin^2\theta$. $E\sin^2\theta=4$ corresponds to the Bragg angle, $V=0$ corresponds to the case of no inelastic damping.

To show the nature of the solution for smaller values of V/W, for which the approximations are not valid, numerical calculations have been made for a special case, shown in the figures. The values chosen were $K=4$ atomic units, $W=0.03$ atomic units, which are of the order of magnitude of constants actually encountered in the experiments. In Fig. 1 we plot $E\sin^2\theta$ as a function of δ, for several values of V/W. This is the sort of plot often made in the theory of metals, showing essentially the energy (or rather the component

connected with motion normal to the surface) as a function of the component of the **k** vector normal to the surface, in the neighborhood of Bragg reflection. We see that as soon as the damping is introduced, the discontinuity in energy disappears, and is replaced by a gradual transition from one branch of the curve to the other, very rapidly approaching a smooth curve as V/W becomes large. The reason why the energy perturbations become small is clear: they arise from interactions between the incident and diffracted beams, which are of equal magnitude at the Bragg angle in the undamped case. In the damped case, the diffracted beam is of much smaller intensity, and has much less effect on the energy. It is also plain why there is no discontinuity: there is damping for every value of the energy, and the wave functions are no longer separated into two different groups, the damped and the undamped ones. This becomes clear in Fig. 2, where we plot the damping constant α as a function of $E\sin^2\theta$, for various values of V/W. For the case $V=0$, the damping constant goes to zero at the edges of the energy gap, but for $V\neq 0$ the damping merely decreases to a somewhat smaller value as we depart from the conditions for Bragg reflection. Finally in Fig. 3 we plot the reflection coefficient, as a function of $E\sin^2\theta$, for different values of V/W. It will be noted that increasing V, for a given W, always decreases the reflection, but the decrease is so much greater in the middle of the range than at the edges that the effect is to broaden the range. This is entirely analogous to the effect of damping on absorption bands in optics.

In closing, it should be pointed out that damped solutions of the type we have described, while they are appropriate for problems of electron diffraction and other problems in which electrons enter a crystal from outside, would not be suitable for discussing such problems as x-ray absorption, where the electrons are produced within the crystal. In particular, Kronig[4] has discussed the fine structure of x-ray absorption edges in terms of the energy gaps between bands. The present argument does not affect that use of the theory of energy gaps, and it should not be thought that the fact that we find that the gaps disappear indicates a difficulty with Kronig's theory.

[4] R. DeL. Kronig, Zeits. f. Physik **70**, 317 (1931); **15**, 191 (1932); **75**, 468 (1932).

MAY 15, 1937 PHYSICAL REVIEW VOLUME 51

Wave Functions in a Periodic Potential

J. C. SLATER*
Institute for Advanced Study, Princeton, New Jersey
(Received March 24, 1937)

A new method for approximating the solutions of the problem of the motion of an electron in a periodic potential, as a crystal lattice, is suggested. The potential is supposed to be spherically symmetrical within spheres surrounding the atoms, constant outside. The wave function is expanded in spherical harmonics and radial solutions of the wave equation within the spheres, and in plane waves outside the spheres, joining continuously at the surface. A single unperturbed function consists of a single plane wave outside the spheres, together with the necessary spherical functions within the spheres. The matrix components of energy are set up between these unperturbed functions, and the secular equation set up. This equation involves the energy explicitly, and also implicitly through the ratio of the slope of the various radial functions to the functions themselves at the surfaces of the spheres, and must be solved numerically. It is hoped that the method will be useful for comparatively low energy excited electrons, for which the usual method of expansion in plane waves converges too slowly.

INTRODUCTION

THE first step in the solution of the wave mechanical problem of the motions of electrons in a crystal is to replace the other electrons by a static distribution of charge, and to treat the motion of one electron in this static, periodic potential field. The potential is of a particular sort: Near each nucleus, it approaches the potential near the corresponding atom as it would be if isolated from its neighbors, the

* On leave from the Massachusetts Institute of Technology, Cambridge, Massachusetts.

potential energy of an electron becoming negatively infinite as the nucleus is approached. The potential is spherically symmetrical around a nucleus. Between atoms, the potential varies much less rapidly, making a continuous joining with the potentials near the various nuclei. It involves no great inaccuracy to idealize this potential in the following way: we assume spheres surrounding the various nuclei, the sphere around the nth nucleus having a radius R_n (these radii will naturally be equal if the atoms are all alike). We suppose that within each sphere, the potential is spherically symmetrical, so that within the nth sphere it may be taken to be $U_n(|\mathbf{r}-\mathbf{r}_n|)$, where $\mathbf{r}$ is the radius vector to an arbitrary point, $\mathbf{r}_n$ the radius vector to the nth nucleus. Outside all the spheres, we suppose the potential to be constant, and to get continuity of the potential we assume that each of the potentials U_n reduces to this constant value at the radius R_n. In particular, to simplify matters, we shall adjust the zero of potential so that the constant region between atoms is at zero potential. The present paper is devoted to a general formulation of the solution of such a boundary value problem, on the assumption that the atoms are arranged in a regular crystal, and to methods of approximating to the solution.

We seek a solution of energy E. Within any one of the spheres, the wave equation is one of spherical symmetry. Then it can be solved quite rigorously by well-known methods. We separate variables in spherical coordinates with respect to the nucleus. If these coordinates are $|\mathbf{r}-\mathbf{r}_n|$, θ, ϕ, the wave function is

$$\sum_{l=0}^{\infty}\sum_{m=-l}^{l} A_{lm}P_l^{|m|}(\cos\theta)\exp(im\phi)u_{nl}(|\mathbf{r}-\mathbf{r}_n|). \quad (1)$$

Here u_{nl} satisfies the equation

$$-\frac{1}{r^2}\frac{d}{dr}\left(r^2\frac{du_{nl}}{dr}\right)+\left(\frac{l(l+1)}{r^2}+U_n\right)u_{nl}=Eu_{nl}. \quad (2)$$

The radial function u_{nl} of course depends on the energy E as a parameter, but we shall not indicate that in the notation, since it is understood throughout. There are two independent solutions of (2) for any energy value E. Of these, one is regular at the origin, the other regular at infinity, the two coinciding for the characteristic values of E. Since in general we are not dealing with characteristic values of E, and since we are interested in the interior of the sphere, we choose the functions regular at the origin. Then any series of the form (1), with arbitrary coefficients A_{lm}, satisfies the differential equation within the sphere.

Of course, outside the sphere, and up to the shortest distance $|\mathbf{r}-\mathbf{r}_n|$ at which the radius touches the sphere of another atom, so that the problem is still spherically symmetrical, we can still use a solution of type (1). For larger distances than this, however, the problem ceases to be spherically symmetrical, and (1) is no longer a solution. We must then seek a different type of solution which will hold in the region between the spheres. It is known that a general solution of the whole problem is provided by a series of plane waves,

$$\sum_{\mathbf{k}} v(\mathbf{k})\exp(i\mathbf{k}\cdot\mathbf{r}), \quad (3)$$

where only certain discrete wave vectors $\mathbf{k}$ are to be used. These vectors are to be defined as follows. We start with a certain vector $\mathbf{k}_0$, which is arbitrary. Then we may add to this any one of the infinite number of vectors $\mathbf{K}_i$ of the reciprocal lattice.[1] The series (3) is then a solution of the wave equation everywhere, if the $v(\mathbf{k})$'s satisfy the difference equations

$$(\mathbf{k}_0+\mathbf{K}_i)^2v(\mathbf{k}_0+\mathbf{K}_i)+\sum_{\mathbf{K}_j}W(\mathbf{K}_j)v(\mathbf{k}_0+\mathbf{K}_i+\mathbf{K}_j) = Ev(\mathbf{k}_0+\mathbf{K}_i). \quad (4)$$

Here, as elsewhere in this paper, it is assumed that atomic units are used (energies measured in units of the Rydberg energy, distances in terms of the radius of the Bohr hydrogen orbit, so that the energy of a free electron whose wave function is $\exp(i\mathbf{k}\cdot\mathbf{r})$ is k^2). The matrix component $W(\mathbf{K}_j)$ is the matrix component of the potential energy between the wave functions in question, normalized in such a way that $W(0)$ is the average potential energy through the cell,

[1] For references to this and other points, the reader may consult Mott and Jones, *Properties of Metals and Alloys* (Oxford, 1936); Fröhlich, *Elektronentheorie der Metalle* (Berlin, 1936), as well as the older reviews, by Sommerfeld and Bethe, in the *Handbuch der Physik*, second edition, Vol. 24 (1933), and by J. C. Slater, Rev. Mod. Phys. **6**, 209 (1933). Numerous references to special papers can be found in the books and articles mentioned above.

or through the crystal. That is, $W(\mathbf{K}_j)$ is the integral of the potential energy, times

$$\exp\ (i(-\mathbf{k}_0-\mathbf{K}_i+\mathbf{k}_0+\mathbf{K}_i+\mathbf{K}_j)\cdot r)=\exp\ (i\mathbf{K}_j\cdot r),$$

throughout the cell, divided by the volume of the cell. If the volume of the cell is Ω, we then have

$$W(\mathbf{K}_j)=\frac{1}{\Omega}\sum_n \exp\ (i\mathbf{K}_j\cdot r_n)F_n(\mathbf{K}_j), \qquad (5)$$

where the summation is over the atoms of a single cell, and where

$$F_n(\mathbf{K}_j)=\int U_n(|r-r_n|)\exp\ (i\mathbf{K}_j\cdot|r-r_n|)d\tau, \quad (6)$$

where the integral is over the volume of the nth sphere. By expanding the exponential, it can be at once shown that

$$F_n(\mathbf{K}_j)=4\pi\int_0^{R_n} r^2U_n(r)\frac{\sin\ (|\mathbf{K}_j|r)}{|\mathbf{K}_j|r}dr. \quad (7)$$

It has been customary to discuss electron diffraction on the assumption that the matrix component $W(\mathbf{K}_j)$ was the one responsible for the process in which a wave of wave number $\mathbf{k}_0+\mathbf{K}_i$ in the crystal changed over to a wave of wave number $\mathbf{k}_0+\mathbf{K}_i+\mathbf{K}_j$, by Bragg reflection from the planes normal to $\mathbf{K}_j$. The Eq. (5) then expresses this quantity in a way analogous to the x-ray structure factor, and (7) gives the form factor of the nth atom, analogous to the x-ray form factor. The equations (4) are then analogous to the equations in the dynamical theory of x-ray diffraction,[2] and are the ones which must be solved if we wish to set up the whole solution for a diffracted beam.

It might be asked, since (3) gives a complete solution of our present problem, why is it necessary to go further? The answer is that the series (3) converges very slowly. The wave function in the neighborhood of a nucleus corresponds to a rapidly moving electron, and it changes phase in very short distances, corresponding to short wave-lengths. Thus in the series (3), we must have appreciable coefficients of the terms even of very high $\mathbf{k}$ values, such that k^2 for these terms is comparable with the energy of the x-ray terms of the atom. Attempts to solve the difference Eq. (4) directly, made by the writer and Dr. Millman, as well as similar attempts made by others, have convinced us that the use of this series is impractical for obtaining wave functions and energy levels of low energy electrons, valuable though it is for the proof of general theorems and for high energy electrons. In spite of the objections to the use of (3) for practical purposes, still the whole wave function can be expanded in such a series of plane waves, and in particular the part of the function outside the atomic spheres can be so expanded. We shall then assume that the wave function is expanded in series (3) outside the spheres, and in the series (1) inside the spheres. We shall do this in the following way. We set up separate unperturbed functions, each equal to a plane wave outside the spheres, and to a series of type (1) inside the spheres, joining continuously on the surface of the spheres. Then we write the whole solution as a linear combination of such unperturbed functions, determining the coefficients essentially by perturbation theory. But now we may hope that the series represented by this linear combination will converge much more rapidly than the series (3). For the lack of convergence of (3), as we have mentioned, arises from the difficulty of expanding the wave function near the nucleus in plane waves. In our method, the wave function near the nucleus is automatically taken care of, and only the outer part, which really does not depart much from a plane wave anyway, is left to be expanded. Each of our functions can be regarded as an expansion in terms of plane waves, containing all the terms necessary to describe the function near the nucleus, but with correct phase relations so that it reduces to a single plane wave outside the spheres. We shall now proceed with the mathematical formulation of these wâves, and shall set up the matrix components of energy between them and the resulting secular equation for determining the energy.

Mathematical Formulation of the Problem

Let ψ_i be a function which equals $\exp\ (i\mathbf{k}_i\cdot r)$ outside the various spheres, and which joins

[2] See for instance M. von Laue, Ergeb. d. Exakt. Naturwiss. **10**, 133 (1931); also *Die Interferenzen von Röntgen- und Elektronenstrahlen* (Berlin, 1935).

continuously at the surface of each sphere onto a solution of the central field problem, corresponding to the energy E, within that sphere. By a well-known expansion, the exponential $\exp(i\mathbf{k}_i\cdot\mathbf{r})$ can be expanded in spherical coordinates about any point. In particular we expand about the nucleus of the nth atom, at $\mathbf{r}_n$. Then we have

$$\exp(i\mathbf{k}_i\cdot\mathbf{r})=\exp(i\mathbf{k}_i\cdot\mathbf{r}_n)\sum_{l=0}^{\infty}\sum_{m=-l}^{l}(2l+1)i^l \times j_l(k_i|\mathbf{r}-\mathbf{r}_n|)\frac{(l-|m|)!}{(l+|m|)!}P_l^{|m|}(\cos\theta) \times P_l^{|m|}(\cos\theta_i)\exp im(\phi-\phi_i). \quad (8)$$

Here $(|\mathbf{r}-\mathbf{r}_n|)$, θ, ϕ are polar coordinates about $\mathbf{r}_n$ as a pole, and θ_i, ϕ_i are polar coordinates giving the direction of the wave normal $\mathbf{k}_i$. The functions $j_l(kr)$ are spherical Bessel functions,[3] satisfying the differential equation

$$-\frac{1}{r^2}\frac{d}{dr}\left(r^2\frac{dj_l}{dr}\right)+\frac{l(l+1)}{r^2}j_l=k^2j_l. \quad (9)$$

They are finite or zero at the origin, and are so normalized that

$$\lim_{z=0} j_l(z)=\frac{z^l}{1\cdot3\cdot5\cdots(2l+1)}. \quad (10)$$

By comparing terms, we can then at once determine the coefficients A_{lm} of the expansion (1) of the function inside the sphere, so as to make the function continuous at the surface of the sphere. We at once find that inside the sphere we have

$$\psi_i=\exp(i\mathbf{k}_i\cdot\mathbf{r}_n)\sum_{l=0}^{\infty}\sum_{m=-l}^{l}(2l+1)i^l\frac{j_l(k_iR_n)}{u_{nl}(R_n)} \times u_{nl}(|\mathbf{r}-\mathbf{r}_n|)\frac{(l-|m|)!}{(l+|m|)!}P_l^{|m|}(\cos\theta) \times P_l^{|m|}(\cos\theta_i)\exp im(\phi-\phi_i). \quad (11)$$

The value (11) inside the sphere at $\mathbf{r}_n$, together with the expression $\exp(i\mathbf{k}_i\cdot\mathbf{r})$ outside all the spheres, determines the function ψ_i completely.

[3] For a collection of formulas and tables regarding these functions, see P. M. Morse, *Vibration and Sound* (New York, 1936), pp. 246, 247, 335.

Having formulated our various unperturbed wave functions, we must set up the perturbation problem between them. We assume that the exact solution of our problem is expressed as a series

$$\sum_i v_i\psi_i, \quad (12)$$

where the v_i's are constants. Then by the general methods of quantum mechanics the series (12) will be a solution of the problem if the equations

$$\sum_j(H-E)_{ij}v_j=0 \quad (13)$$

are satisfied for all values of i. Here H is the energy operator, E the characteristic energy, and

$$(H-E)_{ij}=\int\psi_i^*(H-E)\psi_j d\tau, \quad (14)$$

the matrix component of the operator $H-E$ between the two states in question. In order to satisfy the Eq. (13), we must as usual have the determinant of coefficients $(H-E)_{ij}$ equal to zero. We now compute these matrix components.

We must notice one point at the outset. Though our function ψ_i is everywhere continuous, its first derivative is in general not continuous at the surfaces of the various spheres, where the functions join. We may regard the object of our perturbation problem to be the setting up of a combination of functions which not only is continuous but has a continuous slope. But now the kinetic energy operator demands special treatment for a function with discontinuous slope. Two forms of integral are often seen for computing the kinetic energy. The more common one is $\int\psi_i^*(-\nabla^2)\psi_j d\tau$, but the other and more fundamental one is $\int \text{grad}\,\psi_i^*\cdot\text{grad}\,\psi_j d\tau$. Ordinarily one can show by integration by parts that one equals the other, but if the function has anywhere a discontinuous slope, they are no longer equal, but differ by a surface integral over the surface of discontinuity. In this case the second, more fundamental form is the correct one, as it is the one which directly enters the variation principle from which Schrödinger's equation is derived. If there is any doubt about this question, it can be easily shown that using the first formula we must add a surface integral, for a discontinuous first derivative amounts to

an infinite second derivative on the surface, and integrates to a finite contribution over the surface. This contribution can be found by a limiting process in which the change of slope occurs in smaller and smaller ranges of variable. We shall use the opposite treatment, however, as being more fundamental, starting with the second integral, but eventually reducing part of our result to a surface integral over the surface of discontinuity.

If U is the potential energy, equal to U_n within the nth sphere, and zero outside the spheres, we then have

$$(H-E)_{ij}=\int (\text{grad}\,\psi_i^*\cdot\text{grad}\,\psi_j + (U-E)\psi_i^*\psi_j)d\tau. \quad (15)$$

We shall carry out the integration in two parts: first over the region outside the spheres, then over the spheres. Outside the spheres, $\psi_i=\exp i(\mathbf{k}_i\cdot r)$, $U=0$. Then $\text{grad}\,\psi_i^*\cdot\text{grad}\,\psi_j=(\mathbf{k}_i\cdot\mathbf{k}_j)\exp i(\mathbf{k}_j-\mathbf{k}_i)\cdot r$. To find the integral outside the spheres, we integrate over the whole space, and subtract the integral over the spheres. It is easily shown that the integral over each cell will be equal, so that we shall carry out all our integrations just over a single cell, which is assumed to be of volume Ω. Furthermore, to get agreement with (5), we shall divide our integrals by Ω, so that they will represent averages over the volume. Now the relation between the vectors $\mathbf{k}_i$ and $\mathbf{k}_j$ is such that $\exp i(\mathbf{k}_j-\mathbf{k}_i)\cdot r$ integrates to zero over the cell unless $i=j$. Thus we have

$$\frac{1}{\Omega}\int_{\text{cell}}(\text{grad}\,\psi_i^*\cdot\psi_j-E\psi_i^*\psi_j)d\tau = (\mathbf{k}_i\cdot\mathbf{k}_j-E)\delta_{ij}, \quad (16)$$

where $\delta_{ij}=1$ if $i=j$, 0 if $i\neq j$. Within the nth sphere, we have the contribution

$$\frac{1}{\Omega}(\mathbf{k}_i\cdot\mathbf{k}_j-E)\exp i(\mathbf{k}_j-\mathbf{k}_i)\cdot r_n \times\int_{\text{sphere}}\exp i(\mathbf{k}_j-\mathbf{k}_i)\cdot(r-r_n)d\tau = (\mathbf{k}_i\cdot\mathbf{k}_j-E)\exp i(\mathbf{k}_j-\mathbf{k}_i)\cdot r_n \times\frac{4\pi R_n^2}{\Omega}\frac{j_1(|\mathbf{k}_j-\mathbf{k}_i|R_n)}{|\mathbf{k}_j-\mathbf{k}_i|}. \quad (17)$$

The terms (17) are to be subtracted from (16) to get the whole contribution to $(H-E)_{ij}$ from the region outside the spheres.

Next we must find the contributions to $(H-E)_{ij}$ from the interiors of the spheres. In this case it is more convenient to integrate (15) by parts according to Green's theorem, obtaining for the nth sphere

$$\frac{1}{\Omega}\int\psi_i^*(-\nabla^2+U_n-E)\psi_j d\tau + \int\psi_i^*(\partial\psi_j/\partial n)dS, \quad (18)$$

where n is the outer normal in the surface integral. The volume integral vanishes on account of (2). For the surface integral, we use the form (11) for the functions, differentiate the radial part of ψ_j with respect to r, and integrate over the angles, obtaining

$$\exp i(\mathbf{k}_j-\mathbf{k}_i)\cdot r_n\frac{4\pi R_n^2}{\Omega}\sum_{l=0}^{\infty}(2l+1)P_l(\cos\theta_{ij}) \times j_l(k_iR_n)j_l(k_jR_n)u_{nl}'(R_n)/u_{nl}(R_n). \quad (19)$$

We must now combine (16), (17), and (19), obtaining

$$(H-E)_{ij}=(\mathbf{k}_i\cdot\mathbf{k}_j-E)\delta_{ij} + \frac{1}{\Omega}\sum_n\exp i(\mathbf{k}_j-\mathbf{k}_i)\cdot r_nF_{nij},$$

where

$$F_{nij}=4\pi R_n^2\Big\{-(\mathbf{k}_i\cdot\mathbf{k}_j-E)\frac{j_1(|\mathbf{k}_j-\mathbf{k}_i|R_n)}{|\mathbf{k}_j-\mathbf{k}_i|} +\sum_{l=0}^{\infty}(2l+1)P_l(\cos\theta_{ij})j_l(k_iR_n)j_l(k_jR_n) \times u_{nl}'(R_n)/u_{nl}(R_n)\Big\}. \quad (20)$$

The resemblance to Eqs. (5) and (6) is plain; F_{nij} plays the part of a form factor in the present theory, in place of the expression $F_n(K_j)$ of (6) and (7).

Having set up the matrix components $(H-E)_{ij}$ in (20), we must next solve the secular equation $\Delta|(H-E)_{ij}|=0$. Of course, we cannot solve this exactly, and we must look for methods of approximation. It is a more difficult secular

equation than one usually meets. In the first place, the functions are not orthogonal, so that as we see from (20) the energy E appears explicitly in the nondiagonal terms. But worse than this, the energy appears implicitly in the expressions $u_{nl}'(R_n)/u_{nl}(R_n)$, which depend on the energy, and which appear both in diagonal and in nondiagonal terms. The only practical method of handling the determinant under the circumstances would seem to be to compute and plot it as a function of E, and find the intersections with the axis graphically. Rather than using the determinant as it stands, it would be more convenient to use a well-known device, and divide all elements of the ith row by the diagonal term $(H-E)_{ii}$. Then the diagonal terms of the new determinant are unity, and the nondiagonal elements are very large for those particular rows for which $(H-E)_{ii}$ is very small, while they are small in other cases. To a first approximation, then, we can consider only the particular rows for which $(H-E)_{ii}$ is small, and the expansion of the determinant becomes very simple. Further approximations can be made by expanding in power series in the small terms. This method amounts to applying a perturbation theory in which we treat the few states whose unperturbed energy is near the energy we are interested in by the perturbation method for degenerate systems, and treat more distant states by the power series method. It should make it possible to get a satisfactory approximation to the whole shape of the curve, and to find its zeros, to a fair approximation, though with considerable labor. The determinant plotted as a function of E will have many intersections with the axis, and may be expected to have roughly the form of a tangent curve, but of course with many local variations. A separate calculation, of course, must be made for each value of the momentum $\mathbf{k}_0$ (that is, at each point of the first or reduced Brillouin zone in $\mathbf{k}$ space). At certain points in this zone there will be symmetry properties which will allow us at once to factor the determinant, so that as with other methods of approximation it will be easier to get the solution in directions having simple symmetry properties than in arbitrary directions.

In conclusion, we may suggest the cases where this method is likely to be particularly useful. These will obviously be the cases where one term of our series is itself a fairly good approximation, so that the correction terms are small. That is, they are the cases where the real wave function outside the spheres is very close to a single plane wave. Such cases are known to exist for the conduction levels of the alkali metals.[4] The method of Wigner and Seitz, as applied by the author to this case, is satisfactory for the conduction levels themselves, but has been shown by Shockley[5] to become very bad for levels even a few volts above the occupied levels. This is natural, for that method assumes an expansion throughout the whole cell in a very few spherical harmonics. But as we see from (8), a whole series of spherical harmonics is needed to expand a plane wave, and the higher terms become important for rather low energies, so that if we break off the series after a few terms, as the earlier method does, the results will be very inaccurate except for very low energies. The present method, however, with its infinite series of spherical harmonics, would not have this difficulty. It is not unlikely that if it were applied to the case of the alkalies, it would show that the excited levels for some distance up are much more like free electrons than the calculations mentioned in reference 4 would indicate, so that it would form a good approximation for this case. It is to be hoped, however, that the present method of approximation will have a wider range of application than this, for it should in principle suffice for finding any energy levels, and the reasons we have suggested in proposing it lead one to hope that it will be practical in its actual application.

---

[4] For application to sodium, see J. C. Slater, Phys. Rev. **45**, 794 (1934).
[5] W. Shockley, Phys. Rev. **51**, 379 (1937).

A New Method for the Measurement of the Bohr Magneton

OTTO STERN
Research Laboratory of Molecular Physics, Carnegie Institute of Technology, Pittsburgh, Pennsylvania
(Received March 8, 1937)

A molecular ray method for the measurement of forces acting on molecules is discussed in which these forces are compensated by the force of gravity (molecular balance).

IN the following paper a method is discussed in which, by employing a molecular ray, the acceleration given to a molecule by an external field (magnetic, electric) is compared directly with the acceleration produced by gravity. The experiments now under way in this laboratory attempt to employ this method for an exact determination of the Bohr magneton.[1] However, the method should be useful also for many other problems.

THE MEASUREMENT OF THE FREE FALL OF MOLECULES

The free fall of molecules in the gravitational field of the earth could be easily observed by the following experiment with molecular rays.

A molecular ray, Cs in our case, is produced by the ovenslit A (Fig. 1) and the collimating slit B. The detector C is a heated tungsten wire. Both slits and the detecting wire are horizontal. The Cs atoms striking the surface of the wire are ionized. The ion current between the wire and a negatively charged cylinder gives directly the number of impinging atoms per second (Langmuir-Taylor method[2]). The dotted lines in Fig. 1 give the paths of some Cs atoms with different velocities. We shall find a deflected beam with an intensity distribution corresponding to Maxwell's law.

NUMERICAL EXAMPLE

We assume the distance $AB=BC=l$. Then in our arrangement the distance of free fall s_α for the atoms with the most probable velocity α is

$$s_\alpha=gl^2/\alpha^2=gl^2M/2RT \quad (\text{since } \tfrac{1}{2}M\alpha^2=RT). \qquad (1)$$

With $l=100$ cm we have

$$s_\alpha=\tfrac{3}{5}\times(M/T)\text{ mm}. \qquad (1a)$$

For Cs ($M=132.9$; $T=450°$K): $s_\alpha=0.177$ mm. Fig. 3 gives the distribution of the intensity in the vertical direction for a beam of 0.04 mm width (beam without half-shadow, detecting wire very thin). s is the distance from the center of the beam, i/i_0 the ratio of the ion current i at the position s to i_0 for the undeflected beam, that is, the straight beam of atoms not influenced by any force.

The available intensity J_0 is in a very rough approximation given by

$$J_0=\frac{2\times10^{-5}}{(MT)^{\frac{1}{2}}}\frac{h}{r^2}\frac{\text{mol}}{\text{cm}^2\text{ sec.}},^{3}$$

where $r=2l$ is the length of the beam and h the height of the ovenslit (in this case h is horizontal).[4] With $M=132.9$; $T=450°$K; $2l=r=2\times10^2$ cm, $h=0.2$ cm:

$$J_0=4\times10^{-13}(\text{mol/cm}^2\text{ sec.}).$$

If the diameter of the detecting wire is 4×10^{-3} cm and the effective length 2×10^{-1} cm, J_0 corresponds to an ion current $i_0=3\times10^{-11}$ amp.

[1] Specially interesting with regard to the present inconsistencies in the numerical values of the fundamental constants. By measuring the Bohr magneton per mole we get essentially a numerical value for h/m. h/m combined with the Rydberg constant gives directly (after a remark of Niels Bohr) the fine structure constant α and a check on Eddington's hypothesis $\alpha=1/137$.

[2] John B. Taylor, Zeits. f. Physik **57**, 242 (1929); U.z.M. 14 (U.z.M., Untersuchungen zur Molekularstrahlmethode, refers to a series of papers concerning the molecular ray method.)

[3] O. Stern, Zeits. f. Physik **39**, 755 (1926); U.z.M. 1.

[4] J_0 depends also on the product of the width b of the ovenslit and the pressure p in the oven. But because of the condition that the mean free path λ in the oven should not be smaller than b, this product is constant. In the above equation it is assumed that for all substances in the first approximation $\lambda=1/10$ mm for $p=1/10$ mm.

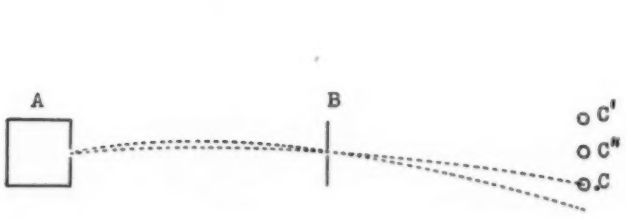

FIG. 1.

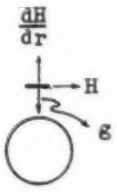

FIG. 2.

COMPENSATION OF THE FORCE OF GRAVITY BY A MAGNETIC FIELD

The magnetic field may be produced by a current I flowing through a wire underneath and parallel to the beam. Led d be the distance between the center of the beam and the center of the wire. Then at the place of the beam the field strength H is $2I/d$ and the inhomogeneity $dH/dr=-2I/d^2$. H is horizontally, dH/dr vertically directed (Fig. 2). The magnetic force $F_m=\mu(dH/dr)$ exerted on a magnetic dipole has also the vertical direction. Thereby μ is the component of the magnetic moment of the dipole in the direction of H (horizontal in our case).[5] For alkali atoms in a strong field μ has only the two values $+\mu_0$ and $-\mu_0$ (μ_0 Bohr magneton). In our case we have to deal with a very weak field where we have many more components. But this does not make any difference in the essential point as we shall see later. So let us assume for the moment that we have only the two components $+\mu_0$ and $-\mu_0$.[6] Then for one-half of the atoms the magnetic force has the same direction as the force of gravity, for the other half of the atoms the opposite direction. For these atoms it will be possible to choose $|dH/dr|=2I_0/d^2$ so that the magnetic force just cancels the force of gravity. These atoms will get no acceleration at all and move strictly in straight lines. I_0 is determined by the equation

$$mg=\mu_0|dH/dr|=\mu_0(2I_0/d^2). \qquad (2)$$

To find I_0 we can employ different methods. The most straightforward procedure seems to be the following one: We place the detecting wire a short distance above the straight beam (Fig. 1, C') and let I increase. As long as $I<I_0$ all atoms are deflected downward, no atom strikes the wire and we have no ion current. The instant I becomes larger than I_0, half of the atoms regardless of their velocity are deflected upwards and some atoms strike the wire. Since the amount of the deflection depends on the velocity, the slowest atoms strike the wire first, then with increasing $I-I_0$ the faster ones. No matter how far above the beam we set the detecting wire, we shall get an ion current as soon as I becomes larger than I_0. The intensity of this ion current, however, depends of course on the distance between the beam and the detector. It can be easily calculated as a function of $I-I_0$ by using Maxwell's law of the velocity distribution.

At this point we can see at once why the splitting of the beam into many components, 16 for Cs, by a weak field does not matter. The component with the largest value of μ has always

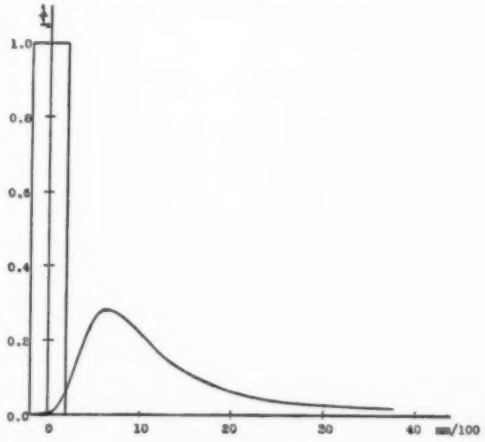

FIG. 3.

[5] In the usual arrangement H and dH/dr are parallel. The validity of $F_m=\mu(dH/dr)$ for the present case follows directly from the consideration of the energy or from considering the forces and taking into account curl $H=0$.

[6] This case could be realized experimentally by superimposing a strong homogeneous field.

the moment μ_0.[7] But this component is the only one we are concerned with because only for this one the deflection has an upward direction as long as $I-I_0$ does not become too large (till about $I-I_0<\frac{1}{3}I_0$).

Another method to determine I_0 would be to place the detecting wire directly in the path of the straight beam (Fig. 1, C'') and measure i as a function of I. Then i should have a maximum for $I=I_0$ because if I is larger or smaller than I_0 we deflect atoms upward or downward and diminish the intensity.[8] The other components do not disturb us in this case either because they give no maximum of i for $I=I_0$ but only a monotonic increase of i with I. Of course, also here i can be easily calculated as a function of I.

It seems that I_0 could be determined very accurately by either one of these methods. This should make possible a very exact measurement of $N\mu_0$. Eq. (2) gives:

$$\mu_0=mgd^2/2I_0 \quad \text{or} \quad N\mu_0=\mathrm{M}_0=Mgd^2/2I_0$$

(N Avogadro's number, M molecular weight).

Since M and g are well known the accuracy of the result will probably depend mainly on the accuracy of d, that is of the alignment of the arrangement.

To calculate numerical values we write (2) in the form

$$|dH/dr|=(\mathrm{M}/\mathrm{M}_0)g=2I_0/d^2. \qquad (2a)$$

For Cs we have

$$|dH/dr|=(132.9/5550)\times 980=23.5 \quad \text{gauss/cm}$$

and for $d=1$ cm

$$I_0=\tfrac{1}{2}\times 23.5 \text{ e.m.u.}=117.5 \text{ amp.}$$

Corrections for the finite height h of the beam and the magnetic field of the earth are small (quadratic terms) and can easily be taken into account. Furthermore, the beam must be placed in the north-south direction. In this case the Coriolis force produced by the rotation of the earth has no vertical component. Otherwise this force amounts to some tenths of one percent of the force of gravity even for the atoms with the velocity α.

Nuclear Moments

It is quite interesting to consider the numerical values for a similar experiment with H_2 molecules. For the deflection by gravity Eq. (1a) gives

$$s_\alpha=\frac{3}{5}\times\frac{M}{T}=\frac{3}{5}\times\frac{2}{60}=\frac{1}{50} \text{ mm}$$

if we take $T=60°$K. For the compensating inhomogeneity we get from Eq. (2a) taking $N\mu$ equal to 5 nuclear magnetons per mole

$$\left|\frac{dH}{dr}\right|=\frac{M}{N\mu}g=\frac{2}{15}\times 980=131\ \frac{\text{gauss}}{\text{cm}},$$

still quite a convenient value for a wire field.

But in this case it will be necessary to take into account the diffraction of the de Broglie waves for the interpretation of the measurements. The wave-length λ_α of a molecule with the velocity α is

$$\lambda_\alpha=\frac{h}{m\alpha}=\frac{Nh}{(2RTM)^{\frac{1}{2}}}=\frac{30.7}{(TM)^{\frac{1}{2}}}10^{-8} \text{ cm.}$$

For this wave-length the distance s_d of the first diffraction maximum from the beam at the place of the detector is

$$s_d=l\frac{\lambda_\alpha}{b}=\frac{l}{b}\times\frac{30.7}{(MT)^{\frac{1}{2}}}\times 10^{-8} \text{ cm,}$$

where b is the width of the collimating slit and l the distance between the collimating slit and the detector. For H_2 at 60°K we get:

$\lambda_\alpha=2.8\times10^{-8}$ cm and with $b=1/100$ mm,
$s_d=2.8\times10^{-3}$ cm

compared with $s_\alpha=2\times10^{-3}$ cm. For Cs, however, we have

$\lambda_\alpha=0.125\times10^{-8}$ cm and with $b=2\times10^{-3}$ cm,

$s_d=0.62\times10^{-4}$ cm. Consequently the diffraction will require at most a small correction.

It is self-evident that, employing the same method, we can use also other forces to compensate the force of gravity.

[7] Exactly, $\mu_0\pm$magnetic moment of the nucleus. Since this moment is of the order of magnitude $10^{-3}\mu_0$ it has to be known only very roughly. On the other hand it may be possible in the future to determine nuclear moments in this way.

[8] This is analogous to the method used by Rabi and his fellow-workers (see for instance, Phys. Rev. **50**, 472 (1930)) compensating deflections by sending the beam through a weak and afterwards a strong field. They also were the first ones to employ wire fields in actual experiments. On the other hand the whole method has a certain analogy with Millikan's experiments for the determination of e.

On the Convergence of the Hylleraas Variational Method

ALBERT SPRAGUE COOLIDGE AND HUBERT M. JAMES
Harvard University and Purdue University

(Received March 22, 1937)

The result of Bartlett, Gibbons and Dunn, that the wave function for He cannot be expressed as a power series in the particle separations r_1, r_2, r_{12}, is discussed in relation to the validity of the Hylleraas variational attack. By a simple analogous example, it is shown that this result does not establish the impossibility of using polynomials in these variables to represent the function as closely as desired. It is further shown that if a formal solution of the wave equation for He exists, then the energy given by the Hylleraas method will converge upon the correct energy and the function will converge in the mean upon the correct function. Even if there exists no formal solution of the wave equation, there is a lower bound to the energy which can be computed with any function, and upon this bound the Hylleraas method will converge. In either case, therefore, the method is justified.

IN a recent article by Bartlett, Gibbons and Dunn,[1] doubt is expressed whether the limit approached by a variational attack upon the helium problem carried out with comparison functions of the Hylleraas type is necessarily identical with the absolute minimum of the energy computed with any function whatever. Expressing the wave function as

$$\psi = \sum_{lmn} a_{lmn} r_1^l r_2^m r_{12}^n,$$

they apply the operator $(H-E)$ to this series term by term. By rearranging terms they then express the wave equation as

$$(H-E)\psi = \sum_{lmn} F_{lmn} r_1^l r_2^m r_{12}^n = 0,$$

the F's being linear combinations of the as yet undetermined a's. If the wave equation is to be satisfied identically at every point, each of the coefficients F must vanish. This condition, however, is found to impose relations among the a's which cannot be satisfied by any set of finite numbers. (It is readily shown that precisely similar results are obtained if one takes ψ in the Hylleraas form,

$$\psi = \sum_{lmn} a_{lmn} r_1^l r_2^m r_{12}^n e^{-\delta(r_1+r_2)}.)$$

Since it is thus shown to be impossible for any Hylleraas series to be a formal solution of the wave equation, Bartlett, Gibbons and Dunn conclude that other forms of trial function in the variational process might give lower results.

The inadequacy of this treatment may be shown by a simple example. Consider the equation

$$y' + (\tfrac{1}{2} - 1/x)y = e^{-x/2}; \quad 0 \leqq x < \infty.$$

If we attempt to find a solution by assuming that

$$y = e^{-x/2} \sum a_n x^n$$

and substituting in the equation, we obtain an impossible condition on the coefficients, namely

$$\sum n a_{n+1} x^n = 1.$$

Yet it is possible to find a series of the form stated which will approximate the desired solution at every point within an arbitrarily small error. For, with the aid of the Laguerre orthogonal functions

$$\varphi_n(x) = (1/n!) e^{-x/2} L_n(x)$$

we can find the uniformly convergent series[2]

$$x \ln x e^{-x/2} = (1-C)\varphi_0 + (C-2)\varphi_1 + \varphi_2/1\cdot 2 + \varphi_3/2\cdot 3 + \cdots,$$

both sides of which satisfy the equation. Now, given any small error ϵ, we know that there is a finite number t of terms of the series which will represent the left side everywhere within ϵ, and these t terms can be rearranged into the form of the exponential times a polynomial in x of degree t. The reason why we may not regard this latter as a true expansion is that, as t is increased to improve the accuracy, the coefficients all increase without limit, instead of staying constant or approaching limits. However, this would not prevent us from determining the best t term approximation S_t by a suitable variation method, as, for example, minimizing $\int_0^\infty (y - S_t)^2 dx$.

In this case the reason why we cannot get a true expansion as a power series times an exponential is clearly because y' becomes infinite at the origin. We could, therefore, not safely use the "improper" expansion obtained above in any process involving differentiation. However, when we examine the helium function from the point of view suggested by this analogy, and identify the derivatives whose be-

[1] J. H. Bartlett, Jr., J. J. Gibbons, Jr., and C. G. Dunn, Phys. Rev. **47**, 697 (1935).

[2] The case satisfies the conditions stated in Madelung, *Die Mathematischen Hilfsmittel der Physiker*, third edition, p. 31.

havior is responsible for the failure of the expansion in a power series, we find that none of the derivatives which occur in the energy integral need be infinite at any point, but that two of them must have finite discontinuities at the origin. There seems to be nothing in this situation which need interfere with the setting up of "improper" expansions which can be used to calculate the integral as closely as desired.

To obtain the result just stated, we assume that an acceptable solution of the wave equation exists, and express it as a function of the variables r_1, r_2, r_{12}. The domain of these variables is bounded in part by three edges, along each of which one of the variables vanishes while the other two are equal to each other. The physical situation at such an edge is similar to that at the origin in the problem of two particles, and the wave function should be analytic in the vanishing coordinate, which corresponds to the radius vector in a local set of spherical coordinates. (The other coordinates should not give any trouble.) We therefore try the assumption that in the neighborhood of any point on an edge, with the possible exception of the origin, we may expand ψ in a multiple Taylor's series. Thus, if the point be $r_1=0$, $r_2=r_{12}=c$, and if the values at this point of ψ, $\partial\psi/\partial r_1$, $\partial\psi/\partial r_{12}$, $\partial^2\psi/\partial r_1^2$, $\partial^2\psi/\partial r_1\partial r_2$ be denoted respectively by ψ^0, $\psi_1{}^0$, $\psi_{12}{}^0$, $\psi^0{}_{1,\,1}$, $\psi^0{}_{1,\,2}$, etc., we have

$$\psi=\psi^0+\psi_1{}^0r_1+\psi_2{}^0(r_2-c)+\psi_{12}{}^0(r_{12}-c)+\tfrac{1}{2}\psi^0{}_{1,\,1}r_1^2+\cdots,$$

$$\partial\psi/\partial r_1=\psi_1=\psi_1{}^0+\psi^0{}_{1,\,1}r_1+\psi^0{}_{1,\,2}(r_2-c)+\psi^0{}_{1,\,12}(r_{12}-c)+\tfrac{1}{2}\psi^0{}_{1,\,1,\,1}r_1^2+\cdots,\text{ etc.}$$

The wave equation which ψ must satisfy is

$$0=-(H-E)\psi=\psi_{1,\,1}+\psi_{2,\,2}+2\psi_{12,\,12}+E\psi+[\psi+2\psi_1]/r_1+[\psi+2\psi_2]/r_2+[-\psi/2+4\psi_{12}]/r_{12}+[r_1^2-r_2^2+r_{12}^2]\psi_{1,\,12}/r_1r_{12}+[r_2^2-r_1^2+r_{12}^2]\psi_{2,\,12}/r_2r_{12}.$$

It is advantageous to introduce the new variables defined by the equations

$$r_1=u,\qquad r_2=c+v,\qquad r_{12}=c+v+\beta u\qquad(\beta^2\leqq 1),$$

thereby explicitly taking account of the limitation on the magnitude of r_2-r_1. The substitutions are made wherever r_1, r_2, r_{12} occur explicitly, but not in the derivatives. Then upon expanding $1/r_2$ and $1/r_{12}$ in positive powers of v and β and collecting terms, we find

$$\psi=\psi^0+\psi_1{}^0u+(\psi_2{}^0+\psi_{12}{}^0)v+\tfrac{1}{2}\psi^0{}_{1,\,1}u^2+(\psi^0{}_{1,\,12}+\psi^0{}_{1,\,2})uv+\psi_{12}{}^0u\beta+\cdots,$$

$$0=-(H-E)\psi=[\psi+2\psi_1]/u+\psi_{1,\,1}+\psi_{2,\,2}+2\psi_{12,\,12}+2\psi_{2,\,12}+E\psi+[\psi+4\psi_2+8\psi_{12}]/2c+2\psi_{1,\,12}\beta+\psi_{1,\,12}u/c-[\psi+4\psi_2+8\psi_{12}]/2c^2v+\cdots.$$

Upon inserting into the last equation the expansions of ψ and its derivatives, and again collecting terms, we obtain an expression which can vanish identically only if the coefficient of each combination of powers of u, v, β, vanishes separately. Thus, the term in u^{-1} gives $\psi^0+2\psi_1{}^0=0$, while that in β gives $\psi_{12}{}^0+4\psi^0{}_{1,\,12}=0$. There is no difficulty in finding finite values of ψ^0 and its derivatives which satisfy all the relations found in this way. If, now, we investigate the edge $r_{12}=0$, $r_1=r_2$, and remember that the function must be symmetrical with respect to r_1 and r_2, we obtain, among other relations, $\psi^0-8\psi^0{}_{12}=0$ and $\psi_1{}^0-8\psi^0{}_{1,\,12}=0$; and again all relations can be satisfied. When, however, we consider the origin, where the edges intersect, we find it impossible to satisfy both sets of relations at once. Thus, if we assign to ψ a given value ψ^0 at the origin, and assume that its first derivatives are everywhere continuous, then, as we approach the origin along the edge $r_1=0$, it must be that $\partial^2\psi/\partial r_1\partial r_{12}$ approaches the limit $-\frac{1}{32}\psi^0$, whereas if the approach is along the edge $r_{12}=0$ the limiting value is $-\frac{1}{16}\psi^0$. Symmetry requires the same behavior of $\partial^2\psi/\partial r_2\partial r_{12}$. Further examination shows that no other inconsistencies relating to the second derivatives are involved, and since the higher derivatives do not occur in $H\psi$ it is unnecessary to determine their behavior.

While this argument removes the objection raised against the Hylleraas method by Bartlett, Gibbons and Dunn, it does not, of course, establish the validity of that method. We shall now prove that if ψ is any piece-wise continuous single-valued function of r_1, r_2, and r_{12} such that

$$\int\psi^2d\tau=8\pi^2\int_0^\infty dr_1\int_0^\infty dr_2\int_{|r_1-r_2|}^{r_1+r_2}dr_{12}r_1r_2r_{12}\psi^2=1,$$

and if S_t is a sum of t terms in the form

$$S_t=\sum_{lmn}a_{lmn}r_1{}^lr_2{}^mr_{12}{}^ne^{-\delta(r_1+r_2)},$$

then, given any small positive number, ϵ, we can find a finite number t, and a set of finite coefficients a_{lmn}, such that

$$\int(\psi-S_t)^2d\tau<\epsilon.$$

Furthermore, if the Hermitian condition is satisfied ($\int\psi Hfd\tau=\int fH\psi d\tau$ for each term f in the Hylleraas series), then

$$\int(\psi H\psi-S_tHS_t)d\tau<\epsilon.$$

If a formal solution of the wave equation exists, it will (as we shall show) satisfy the Hermitian condition, and the Hylleraas process is therefore justified. We shall finally discuss the significance of the fact that we have no proof of the existence of such a formal solution.

In the simplest form of multiple expansion theory, we have a function $w(x, y, z)$ such that

$$\int_{G_x}dx\int_{G_y}dy\int_{G_z}dzw^2=1,$$

the domains G_x, G_y, G_z, being independent of each other. We can then get a root-mean-square expansion of w in products of the functions of

any three sets which are, respectively, complete normal orthogonal sets in x, y, and z, over the given domains. The problem of expanding ψ in a Hylleraas series is complicated by three circumstances—the terms in the series are neither normal nor orthogonal, the domains of the variables are not independent, and the normalizing condition contains an additional factor $r_1r_2r_{12}$. The first two considerations are easily handled, but the third is more troublesome.

If the form of the problem were not already fixed by the fact that we wish to justify a process which has been actually used, we might seek to avoid this difficulty by absorbing the troublesome factor in the function itself, just as we treat the one-electron problem by considering the radial function to be $r\psi$ instead of ψ. However, if we attempt to expand $\psi(r_1r_2r_{12})^{\frac{1}{2}}$ in a Hylleraas series and then find ψ by dividing out the radical, we obtain an expression which will not permit term-by-term evaluation of the energy integral, because the integrals of the separate terms diverge.

We may surmount the difficulty by using the following theorem: Let φ_n be the general example of a set of functions (of one or more variables) which are complete, normal, and orthogonal with respect to the integration $\int d\tau$. And let ρ be some function, defined within the domain of the φ's, which is nowhere negative and which has an upper bound R. Then, with respect to the integration $\int \rho d\tau$ the set of φ's is complete, though neither normal nor orthogonal. That is to say, given any piece-wise continuous function ψ such that $\int \psi^2 \rho d\tau$ converges, and given any small positive number ϵ, it is possible to set up S, a linear combination of a finite number of φ's, such that $\int (\psi - S)^2 \rho d\tau < \epsilon$.

To prove this, we choose some number η, such that $0 < \eta < R$, and divide the domain into two regions G and H, such that within G, $0 \leqq \rho \leqq \eta$, while within H, $\eta < \rho \leqq R$. Construct the function $\psi(\eta)$, which is equal to ψ in H, and to zero in G. Then

$$\int_{G+H} \psi^2(\eta) d\tau = \int_H \psi^2 d\tau$$

must converge, and $\psi(\eta)$ can be expanded in the φ's. That is, we can always find a finite number $p(\eta)$ such that

$$\int_{G+H}{}' [\psi(\eta) - \sum_{n=0}^{p(\eta)} a_n(\eta)\varphi_n]^2 d\tau < \epsilon/4R,$$

and the a's will be the Fourier coefficients. We abbreviate the sum to $\sum(\eta)$. Then

$$\int_{G+H} [\psi(\eta) - \sum(\eta)]^2 \rho d\tau = \int_G [\sum(\eta)]^2 \rho d\tau + \int_H [\psi - \sum(\eta)]^2 \rho d\tau < \epsilon/4,$$

and this limit holds for each of the two integrals separately. Now, in order to obtain the integral

$$I(\eta) = \int_{G+H} [\psi - \sum(\eta)]^2 \rho d\tau,$$

we have to add the terms

$$\int_G \psi^2 \rho d\tau - 2\int_G \psi \sum(\eta) \rho d\tau.$$

By taking η small enough, but still not zero, we can always secure that the first of these terms will be less than $\epsilon/4$ (since $\int_{G+H} \psi^2 \rho d\tau$ is assumed to converge). By the Schwartz inequality, the absolute value of the second term cannot exceed $\epsilon/2$. Therefore $I(\eta) < \epsilon$, which is the desired proof of completeness of the φ's with respect to $\int \rho d\tau$. Note, however, that they are neither normal nor orthogonal for this integration, and the coefficients $a_n(\eta)$ are not the new Fourier coefficients. As the approximation is improved by taking η smaller and increasing the number of terms, the $a_n(\eta)$ will all change, and may even tend to infinity. This behavior can, of course, be rectified by transforming to the normal orthogonal combinations of the φ_n's, which can always be set up.

Returning to the He problem, we introduce new coordinates

$$x = \delta(r_1 + r_2 - r_{12}),$$
$$y = \delta(r_2 + r_{12} - r_1),$$
$$z = \delta(r_{12} + r_1 - r_2).$$

The normalizing condition satisfied by ψ is then

$$\int \psi^2 d\tau = (\pi^2/4\delta^6) \int_0^\infty \int_0^\infty \int_0^\infty \psi^2 (x+y) \times (y+z)(z+x) dx dy dz$$
$$= (\pi^2/4\delta^6) \int_0^\infty \int_0^\infty \int_0^\infty [\psi e^{\gamma(2x+y+z)}]^2 \times (x+y)(y+z)(z+x) e^{-2\gamma(2x+y+z)} dx dy dz = 1.$$

The conditions for applying our theorem are now satisfied if we take $0<\gamma<\frac{1}{2}$ and identify ρ with $(x+y)(y+z)(z+x)e^{-2\gamma(2x+y+z)}$, and we can obtain a root-mean-square expansion of $\psi e^{\gamma(2x+y+z)}$ in terms of any system of functions which are complete with respect to the integration $\int_0^\infty\int_0^\infty\int_0^\infty dxdydz$. Now, such a set can be constructed in the form $\xi_{pqr}=\varphi_p(2x(1-2\gamma))\varphi_q(y(1-2\gamma))\varphi_r(z(1-2\gamma))$, the φ's being Laguerre orthogonal functions. Hence

$$\int_0^\infty\int_0^\infty\int_0^\infty[\psi e^{\gamma(2x+y+z)}-\sum c_{pqr}\xi_{pqr}]^2 \times(x+y)(y+z)(z+x)e^{-2\gamma(2x+y+z)}dxdydz$$
$$=\int_0^\infty\int_0^\infty\int_0^\infty[\psi-\sum k_{fgh}x^fy^gz^he^{-(2x+y+z)/2}]^2 \times(x+y)(y+z)(z+x)dxdydz<\epsilon,$$

where all the coefficients are finite and the sums are all over a finite number of terms. On going back to the coordinates r_1, r_2, r_{12}, we obtain just the desired completeness relation for the functions of the Hylleraas approximation.

Upon introducing the normal orthogonal combinations of these functions, ζ_n (where n stands for a set of three numbers), we can proceed to a discussion of the energy integral along familiar lines. For any two quadratically integrable functions f and g, with expansion coefficients f_n and g_n, we have the usual form of the completeness relation:

$$\int fgd\tau=\sum_{n=0}^{\infty}f_ng_n,\quad f_n=\int f\zeta_nd\tau,\quad g_n=\int g\zeta_nd\tau.$$

Letting $f=\psi$, $g=H\psi$, $H_{nm}=\int\zeta_nH\zeta_md\tau$, we easily obtain the result

$$\int\psi H\psi d\tau=\sum_{m,\,n=0}^{\infty}\psi_m\psi_nH_{mn},$$

provided that $\int\zeta_nH\psi d\tau=\int\psi H\zeta_nd\tau$.

This condition will certainly be satisfied for the whole operator H, if it is satisfied by each Laplacian separately. Let us consider electron 2 fixed, and designate by $d\tau_1$ integration over all positions of electron 1. Then, by Green's theorem,

$$\int[\zeta_n\nabla_1^2\psi-\psi\nabla_1^2\zeta_n]d\tau_1=\lim_{r_1\to0}\int_{-1}^{+1}d\cos\theta_1\int_0^{2\pi}d\varphi_1 \times r_1^2[\zeta_n\partial\psi/\partial r_1-\psi\partial\zeta_n/\partial r_1]=\lim_{r_1\to0}\int_{-1}^{+1}d\cos\theta_1\int_0^{2\pi}d\varphi_1 \times[r_1\zeta_n\partial(r_1\psi)/\partial r_1-r_1\psi\partial(r_1\zeta_n)/\partial r_1].$$

Now, if ψ be taken as the "unperturbed" function $\psi_0=e^{-2(r_1+r_2)}$, each term in the integrand is found to vanish, for $r_1\psi_0$ and $r_1\zeta_n$ tend to zero with r_1 and their derivatives remain bounded. To get the true function ψ we must alter ψ_0 in such a way as to reduce as much as possible the contribution which the electronic repulsion makes to the energy integral, while producing the minimum disturbance in ψ_0, which already minimizes the remaining contributions. Clearly this will be accomplished by reducing the value of ψ_0 in those parts of configuration space where r_{12} is small, while normalization is preserved by a compensating increase in regions where r_{12} is large. Consequently, for a given small value of r_2, the value of ψ will be less than that of ψ_0 in the region of small r_1, and no matter how peculiar the behavior of ψ may be near the origin, $r_1\psi$ will tend to zero and its derivative remain bounded. For large r_2 it may be that $\psi>\psi_0$, but in this case the essential nature of the singularity cannot be affected. The integrand thus remains zero, and in the final integral $\int[\zeta_nH\psi-\psi H\zeta_n]d\tau$ the contribution from the Laplacian of each electron vanishes upon integration over the coordinates of that electron alone.

The existence of a satisfactory series in the ζ's having been established (always assuming that the function itself exists), we must show that the variation method will actually converge upon this series. It is quite possible that, when a finite number of terms is taken, the variation method will produce a set of coefficients giving a lower energy integral than if the same number of true expansion coefficients had been used. It cannot lead to a higher result, since it must find the lowest result possible. But no such result can be lower than the correct energy E, which is an absolute minimum for all normalized functions. The variation result is therefore constrained to lie between E and a quantity which converges upon E as the approximation is improved, and must itself converge upon E. This conclusion also holds when the Hylleraas functions are used directly, for only operations with finite numbers of terms are considered in the analysis. Now, the ground state function, being nondegenerate, uniquely determines a set of expansion coefficients in the ζ's, and these must be the coefficients upon which the variation process converges, since no others could give a result converging upon E. However, the coefficients of the nonorthogonal Hylleraas terms need

not converge upon any finite limits (as was brought out in discussing the analogy of $x \ln xe^{-x/2}$). There is thus no inconsistency between the present treatment and that of Bartlett, Gibbons and Dunn. Indeed, the behavior of the coefficients obtained in actual computations is in complete harmony with this analysis.

It is important to notice, however, that we may not conclude that the value of the wave function at any point can be computed with arbitrary accuracy by evaluating a finite number of terms of the series. There may be points at which the sum of the series (if it exists) differs from the function by an amount which is not zero, but which contributes nothing to the integrals. In particular, the regions where two particles coincide might be such points. Therefore, we should regard with suspicion such attempts as were made in a previous paper[3] to draw conclusions about the nature of the function at the singularities. Such questions are, however, of no physical significance. Physical properties correspond to integrals over wave functions (or, at least, over finite portions of them), and to the physicist a discussion about a point in configuration-space which contributes nothing to the integrals is as impertinent as the traditional theological discussion about the point of a pin.

Indeed, from this point of view, it is not even pertinent to enquire whether there exists any function which satisfies the wave equation at every point. Suppose we know only that there must exist some number E such that $\int \psi H \psi d\tau$ can never be less than E for any normalized function ψ which satisfies the proper boundary and continuity conditions, but that permissible comparison functions can be constructed such as to make the integral exceed E by as small an amount as desired. (Such a number E must exist unless the integral can decrease without limit.) If, now, we have a trial series of a form which can give an arbitrarily good root-mean-square approximation to every such permissible comparison function, and to its energy integral, it is shown by Courant and Hilbert[4] that the Ritz method, applied to such trial series, must converge upon E. We have shown that the Hylleraas trial series meets these requirements. (The argument about the Hermitian condition can evidently be applied to any suitable comparison function.) That some limit E exists is certain, since the energy integral cannot be as low as the known lowest solution of the problem obtained by omitting the electronic repulsion. Therefore, the Hylleraas method must be capable of giving the correct energy.

Some further discussion of the significance of the coefficients in this case appears to be needed. It should be possible to show, without assuming the existence of an actual minimizing function, that where the state is not degenerate a unique set of coefficients will emerge from the variation process (using, of course, the orthogonalized trial functions), and that for all physical purposes these coefficients are all that is required. The difficulty is in formulating and proving non-degeneracy without referring to the actual wave function. We hope to discuss this matter in a later communication.

We wish to express our gratitude to Professor Edwin C. Kemble for much helpful discussion of this problem.

[3] H. M. James and A. S. Coolidge, J. Chem. Phys. **1**, 825 (1933). The H_2 problem is similar to the He problem in this respect.

[4] R. Courant and D. Hilbert, *Methoden der Mathematischen Physik I*, p. 157.

Criteria of Goodness for Approximate Wave Functions

HUBERT M. JAMES AND ALBERT SPRAGUE COOLIDGE
Purdue University and Harvard University

(Received March 22, 1937)

The relations between the root-mean-square error of an approximate ground state wave function, the energy error, and the root-mean-square local energy deviation are exhibited and discussed. Computations of these quantities for helium wave functions containing errors of different character and magnitude are presented, and are shown to indicate that the errors in wave functions of the Hylleraas type are of increasingly short range character as these functions are made more flexible. The form of variational process which will give a wave function most satisfactory for a given purpose is discussed with illustrative computations relating to the diamagnetic susceptibility of He. It is found that the energy error associated with a wave function may be a comparatively unsatisfactory criterion of goodness.

IN this note we wish to discuss the three simplest criteria for the goodness of an approximate ground state wave function, and their relation to the most desirable type of variational procedure for obtaining such a function.

Let ψ_1 be the correct wave function for the ground state of a system, and let $\psi_2, \psi_3 \cdots$ be the correct wave functions for the other states of the system with the same fundamental symmetry characteristics (e.g., in the case of He, the other singlet S states, if spin energy is neglected). The corresponding energies we will denote by $E_1 < E_2 < E_3 < \cdots$.

Let ψ be the approximate normalized wave function for the ground state, associated with the energy $E = \int \psi^* H \psi d\tau$. The variational principle assures us that $E \geqslant E_1$. We now define ψ_x, a normalized function characterizing the nature of the error in ψ, by

$$\psi_x = (1-a_1^2)^{-\frac{1}{2}}(\psi - a_1\psi_1) \tag{1}$$

where $$a_1 = \int \psi_1^* \psi d\tau.$$

This integral will exist provided only that ψ_1 and ψ are quadratically integrable, as we have assumed, and the resulting ψ_x will be a well-behaved function orthogonal to ψ_1. Then

$$\psi = a_1\psi_1 + a_x\psi_x, \tag{2}$$

$a_x = (1-a_1^2)^{\frac{1}{2}}$ measuring the amount of the deviation function ψ_x appearing in ψ.

As practical measures of the inaccuracy of ψ we take: q, the root-mean-square error in ψ,

$$q = [\int (\psi - \psi_1)^2 d\tau]^{\frac{1}{2}} \tag{3}$$

ϵ, the energy error $\epsilon = E - E_1$ (4)

δ, the root-mean-square local energy deviation

$$\delta = [\int \{(H-E)\psi\}^2 d\tau]^{\frac{1}{2}}. \tag{5}$$

All these quantities exist for trial functions of the sort most commonly used and, of course, must vanish as $\psi \to \psi_1$, $E \to E_1$.

We can also characterize ψ_x by means of similar quantities:

$$\begin{gathered} E_x = \int \psi_x^* H \psi_x d\tau, \quad \epsilon_x = E_x - E_1, \\ \delta_x^2 = \int [(H-E)\psi_x]^2 d\tau. \end{gathered} \tag{6}$$

The significance of these quantities may be illustrated by supposing ψ to be expanded in terms of the correct eigenfunctions:

$$\psi = a_1\psi_1 + a_2\psi_2 + \cdots \tag{7}$$

and $$\psi_x = (\sum_{n=2}^{\infty} a_n^2)^{-\frac{1}{2}}(a_2\psi_2 + \cdots + a_n\psi_n + \cdots).$$

Then $$\epsilon_x = \sum_{n=2}^{\infty} a_n^2 (E_n - E_1) / \sum_{n=2}^{\infty} a_n^2 \tag{8}$$

is an average value of $E_n - E_1$ weighted with the squares of the coefficients of the higher states in the expansion of ψ, while

$$\delta_x^2 = \sum_{n=2}^{\infty} a_n^2 (E_n - E)^2 / \sum_{n=2}^{\infty} a_n^2 \tag{9}$$

is a similarly weighted average of $(E_n - E)^2$.

Since ψ_x is orthogonal to ψ_1, the variation principle assures us that

$$\epsilon_x \geqslant E_2 - E_1. \tag{10}$$

From $\int[(H-E)\psi_x-(E_x-E)\psi_x]^2 d\tau \geqslant 0$, we find also that

$$\delta_x \geqslant E_x - E = \epsilon_x - \epsilon. \tag{11}$$

It is obvious from Eqs. (8) and (9) that $\kappa=\delta_x/(\epsilon_x-\epsilon)\geqslant 1$ will be larger the broader the range of energies for which there are important terms in the expansion (7).

Inserting into (3), (4), (5) expression (2) for ψ, and assuming that $\int\psi^* H\psi_1 d\tau = \{\int\psi_1^* H\psi d\tau\}^*$, (for a discussion of this assumption, which is clearly less severe than the usual expansion in series, see our preceding paper on the Hylleraas method) we find:

$$q^2 = 2-2a_1 = 2-2(1-a_x^2)^{\frac{1}{2}}, \tag{12}$$

$$\epsilon = a_x^2\epsilon_x, \tag{13}$$

$$\delta^2 = \epsilon^2 + a_x^2(\delta_x^2-\epsilon^2). \tag{14}$$

Eliminating a_x between (12) and (13) we get

$$q^2 - \tfrac{1}{4}q^4 = a_x^2 = \epsilon/\epsilon_x \tag{15}$$

or, if ψ is a fairly good approximation to ψ_1,[1]

$$q^2 \leqq \epsilon/\epsilon_x. \tag{16}$$

Eliminating a_x between (13) and (14) we obtain

$$\delta^2 = \epsilon[\epsilon + (\delta_x^2-\epsilon^2)/\epsilon_x] \tag{17}$$

whence $\quad \delta^2/\delta_x^2 \leqq \epsilon/\epsilon_x \quad$ or $\quad \delta^2 \leqq \epsilon\epsilon_x\kappa^2$. (18)

From (15) and (17) we obtain finally,

$$q^2 \leqq (\epsilon^2/\delta^2)\kappa^2. \tag{19}$$

In a concrete problem we know ψ, E_1 and E_2, and can compute E, ϵ and δ. For the other quantities we can fix limits by use of the above equations.

$$\begin{gathered} E_2-E_1 < \epsilon_x < (\delta^2+\epsilon^2)/\epsilon, \\ 1 < \kappa^2 < \delta^2/\epsilon(E_2-E_1-2\epsilon), \\ \epsilon^2/(\delta^2+\epsilon^2) < q^2 - \tfrac{1}{4}q^4 < \epsilon/(E_2-E_1). \end{gathered} \tag{20}$$

As an illustration of the usefulness of this analysis, we now present results of calculations on three approximations to the ground state function for the helium atom (Table I). With r_1, r_2 and r_{12} representing the distances of electron 1 and 2 from the nucleus, and their mutual separation, respectively, the functions are

$$\psi_A = Ce^{-2(r_1+r_2)},$$

$$\psi_B = Ce^{-2(r_1+r_2)}[1+c(r_1-r_2)^2],$$

$$\psi_C = e^{-2(r_1+r_2)}[c_0+c_1r_{12}+c_2(r_1-r_2)^2 + c_3(r_1+r_2)+c_4(r_1+r_2)^2+c_5r_{12}^2].$$

In making the computations E_1 was taken as the apparent limit of convergence of the non-relativistic treatment as obtained by subtracting the relativity correction[2] from the observed term value. The first excited singlet level of the system is observed to be 20.51 ev higher.

The most striking characteristic of these results is the slow decrease of δ as the function is improved, compared with that of ϵ. Eq. (19) shows that this must occur in general if the "improvement" of the function involves a reduction of the root-mean-square error.[3] Associated with this is the increase in $\kappa^2\epsilon_x$ which is easily understood as follows: The error in the wave functions may be roughly divided into two parts; long range errors arising from the use of poor effective shielding constants in the construction of the function (as in the case of ψ_A) or of comparatively inflexible functions of any sort, and short range errors associated with the singularities in the energy when the particles are close together. In the neighborhood of these singularities the curvature of the correct wave function will be large and change rapidly. Unless the approximate functions are especially designed to be good in these regions, an increase in flexibility by the introduction of parameters such as appear in ψ_c will only slowly reduce the error here. Thus as the function is improved ψ_x will become more

TABLE I. *Approximations to the ground state function for the helium atom.*

Function	ϵ, ev	δ, ev	$\kappa^2\epsilon_x$, ev	κ	δ_x, ev	q
A	4.2	28.4[1]	190.	<3.1	61. <	0.15 <q<0.47
B	0.72	14.2[1]	280.	<3.7	76. <	0.051 <q<0.19
C	0.019	3.5[2]	660.	<5.7	116. <	0.0054 <q<0.031

[1] From data of D. H. Weinstein, Phys. Rev. **41**, 839 (1932).
[2] J. H. Bartlett, Jr., J. J. Gibbons, Jr., and C. G. Dunn. Phys. Rev. **47**, 679 (1935).

[1] Equations involving the sign $\sim$ have an approximate validity when ϵ is small as compared with E_2-E_1.

[2] H. Bethe, *Handbuch der Physik*, Vol. 24, p. 384.

[3] Possible decreases in κ which might lead to a contrary behavior are limited by the inequality $\kappa<1$, and are in any case unlikely to occur, as is indicated by the argument to follow immediately.

and more concentrated in the small regions where the particles are close together. By analogy with the Fourier expansion in one dimension of a function which vanishes except in a small region, we can see how the expansion as in Eq. (7) of ψ_z will be modified as this process goes on. Thus we will expect that the most important terms will tend to be those of higher and higher energy, so that ϵ_z will rise, while at the same time the range in energy of the important high energy terms will increase, giving larger κ and δ_z. Long range errors are clearly important in ψ_A and ψ_B, and should be fairly well eliminated from ψ_c.

According to Eq. (20) we have $q^2 \gtrsim \epsilon/(E_2-E_1)$, a relation given by Eckart.[4] Thus we can place on q an upper limit which decreases with $\sqrt{\epsilon}$; that q is actually considerably smaller than this limit and decreases more rapidly with decreasing ϵ is indicated by the considerations of the preceding paragraph concerning the behavior of E_z, which we have replaced by E_2 in deriving this equation. A check on optimism in this respect is provided, however, by our lower limit for q.

Through δ may be interpreted as the root-mean-square value of a "local energy error," its value must not be confused with the error in the computed energy, which is necessarily a much smaller quantity if ψ is at all a good function (cf. Eqs. (18), (19)).

From the foregoing analysis we can draw some conclusions concerning the form of variational process which will give a wave function most satisfactory for a given purpose. In the computation of such properties of an atom as radial charge density or diamagnetic susceptibility what we have termed long range errors will be very important, while short range errors will tend to cancel out. On the other hand, in the computation of hyperfine structure constants long range errors will be of little importance if only the wave function is correct when the electrons are near the nucleus. Thus it may be advantageous to adjust the parameters in a function of given form in different ways, depending on the use to which this wave function is to be put. Now ϵ, δ^2, $\epsilon^{1+|K|}/\delta^2$, etc., are all positive quantities which approach zero as ψ approaches ψ_1; thus minimization of each one will give a variational procedure yielding a function useful for a given purpose.[5] Eq. (18) shows that minimization of δ^2 tends to give a function with small values of ϵ_z and κ, in preference to a value of ϵ which is as small as possible. This process then picks out a function which has a comparatively large root-mean-square error, (Eq. (16)), but one in which the short range errors are reduced at the expense of an increase in long range errors. Such a function should thus be particularly suitable for computations of hyperfine structures. On the other hand, minimization of $\epsilon^{1+|K|}/\delta^2$ is a process tending to give particularly large values of ϵ_z and thus small long range errors.

[4] C. Eckart, Phys. Rev. **36**, 878 (1930).

TABLE II. *Results obtained for the helium atom by minimizing* δ^2, ϵ, ϵ/δ^2.

	Minimize δ^2	Minimize ϵ	Minimize ϵ/δ^2
α	1.804	1.6875	1.647
ϵ, ev	1.88	1.52	1.56
δ, ev	24.7	25.6	26.3
$\kappa^2\epsilon_z$, ev	320.	430.	450.
q	$0.076<q<0.30$	$0.060<q<0.28$	$0.059<q<0.28$
$(r_1^2)_{Av}+(r_2^2)_{Av}$	1.84	2.11	2.21

As an illustration of the varying results given by these processes we consider again the helium atom. The assumed wave function is of the simple type constructed from hydrogenic orbitals with adjustable effective shielding, the space part being, for the ground state,

$$\psi=(\alpha^3/\pi)e^{-\alpha(r_1+r_2)}.$$

Elementary computations give

$$E=(2\alpha^2-6\tfrac{3}{4}\alpha)Rh,$$
$$\delta^2=(8\alpha^4-30\alpha^3+(29+5/48)\alpha^2)(Rh)^2.$$

The results obtained by minimizing δ^2, ϵ, ϵ/δ^2 are summarized in Table II. (Minimization of ϵ/δ^2 cannot be shown in general to lead one toward the ground state function, but with the particular type of variation available here it is a method of getting a larger value of δ with little increase in ϵ, as is clear from Table II.) Included in the table are computed values of $(r_1^2)_{Av}+(r_2^2)_{Av}$, which enters the computation of the diamagnetic

[5] When a quantity other than ϵ is to be minimized caution must be used. Thus δ^2 approaches zero also if $\psi\rightarrow\psi_2$; a wave function of inappropriate form might give, on minimization of δ^2 a function approximately that for some other state than the one to be treated. The corresponding value of ϵ must thus be computed as a check on which state is described by the function. Minimization of $\epsilon^{1+|K|}/\delta^2$ requires the use of a value for the correct energy, presumably obtained from experiment; it is thus a procedure interesting only in connection with the determination of wave functions.

susceptibility. The value computed for this quantity using Hylleraas' function, ψ_C,[6] is 2.46, a value which may be accepted as nearly correct. Since in computing this quantity it is desired to minimize long range errors the most reliable results should be obtained, according to our argument, by minimizing ϵ/δ^2, the least reliable by minimizing δ^2. Actually the deviations from the correct answer have the corresponding order.

[6] The radial charge distribution corresponding to this function is given by Bethe, Zeits. f. Physik **55**, 431 (1929).

It is interesting to compare these results with those for ψ_B. The low value of $\kappa^2\epsilon_z$ given by ψ_B indicates that the low value of ϵ compared to the values given in Table II, is due to reduction of short range errors. (ψ_B takes some account of the relative positions of the electrons, whereas ψ_A and the above functions do not.) Despite the smaller energy error, therefore, this is not a favorable function for the computation of $(r_1^2)_{Av}+(r_2^2)_{Av}$; actually, it gives the value 1.76, lower than any other computed.

MAY 15, 1937 PHYSICAL REVIEW VOLUME 51

Magnetic Analysis of Evaporated Bi Deposits

C. T. LANE
Sloane Physics Laboratory, Yale University, New Haven, Connecticut
(Received February 1, 1937)

The magnetic susceptibility of evaporated bismuth films ranging in thickness from 0.1μ to 4μ has been measured by a compensated Gouy method in conjunction with a Sartorius microbalance. Films above 0.5μ are found to have a susceptibility, independent of film thickness, whose value agrees well with that of a single crystal with trigonal axis parallel to the field. Below 0.5μ the susceptibility decreases as the film thickness is reduced. It is suggested that films below 0.5μ possess a microcrystalline fiber structure which merges into a phase of macrocrystalline structure above this thickness. If films less than 0.5μ were aged for long periods in vacuum an increase in the susceptibility was noted, whereas no such effect was observed when thicker films were similarly treated, the effect being ascribed to a recrystallization process. The susceptibility of thick films (>0.5μ) was found to be identical when deposited, respectively, on glass, Au, Cu and Sn. The nature of the crystalline aggregate, as determined from the susceptibility, was found to be dependent on the amount of residual gas present in the apparatus when the films were deposited. As the gas pressure, during deposition, was increased from about 10^{-5} mm of Hg the susceptibility measured with the field parallel to the film normal was greater than the same quantity measured in films produced in high vacuum. The susceptibility measured when the field was perpendicular to the film normal, on the other hand, remained approximately the same in the two cases. At relatively large gas pressures (*ca.*10^{-2} mm) the resulting films possessed a susceptibility which was independent of the angle between the film normal and the magnetic field. The bearing of these results on the structure of the deposits is briefly discussed.

INTRODUCTION

THE question as to whether metallic condensates possess crystalline structure or are amorphous aggregates of atoms has, for some years, been a matter of considerable controversy. Such layers as are produced, for instance, by evaporating metal onto a cold surface in vacuum possess a number of abnormal properties as compared with bulk metal. Among these may be mentioned their very high specific resistance, and the fact that it has often been difficult or impossible to obtain from them sharply defined x-ray patterns.

In recent years such layers have been the object of renewed investigation by electron diffraction.[1] A number of such investigations have shown that evaporated films possess a crystalline structure, even down to thicknesses of a few atomic layers, the lattice spacing being identical with that of the bulk material. Kirschner found that such layers often possessed preferred orientation and that the films appeared to be composed of individual crystallites with linear dimensions, for very thin films, of the order of 10A, the particle size increasing as the thickness of the layer increased. Heating the films tended to sharpen up the diffraction lines, that is to say, the crystal

[1] F. Kirschner, Zeits. f. Physik **76**, 576 (1932).

grains increased in size or became more perfectly arranged, or both.

Recently the production of films with electron diffraction pattern like that of a single crystal, has been reported.[2, 3] These layers, up to the limiting thickness produced, 0.1μ, consist of large numbers of crystals (average size from 0.001μ to 0.01μ) all orientated alike. The resulting films are therefore really mosaic monocrystals. Furthermore the investigators have shown that the temperature of the surface upon which the vapor is condensed determines whether one gets such a single crystal or not. In general there is a pseudo-critical temperature, characteristic of the metal, below which it is not possible for form a "single crystal" film.

In the particular case of bismuth no observations have been reported by Lassen and Bruck but new observations on the crystalline nature of this metal have been published recently by Goetz, Stierstadt and Focke.[4] These authors have investigated thick Bi layers (>0.1 mm) by an optical method. If a section of the deposit taken perpendicular to the backing surface be examined under a high power microscope two distinct layers are seen. The first, starting at the backing surface and extending out for about 100μ, has grains, if any, so small as to appear "amorphous" and the second layer rooted in this one appears as a conglomerate of fine parallel needles, each obviously a single crystal. The transition between the two layers is very abrupt. The "amorphous" layer remains virtually unresolved even up to the highest magnification employed (some 1500 diameters). On the basis of these observations the authors conclude that the "amorphous" layer consists of crystalline Bi of extremely small particle size (microcrystalline layer). The second layer on the other hand consists of large orientated crystals (macrocrystalline layer). From what has been said previously about electron diffraction experiments it is apparent that this explanation is qualitatively plausible. The fact that this microcrystalline layer extends to thicknesses of as much as 100μ is, however, very surprising, since as has been mentioned the particle size increases as the film thickness is increased, even far below this thickness. Very small particles are associated with very thin films and on this scale of measurement films greater than about 1μ must be regarded as "thick."

It seemed desirable, therefore, to examine this problem by a third method, entirely different from those mentioned above. It appeared that absolute measurements of the magnetic susceptibility of Bi films would provide considerable information about these matters. For one thing, the susceptibility of Bi varies with crystal orientation and the nature of this variation is well known, so that preferred orientation of microcrystals might be quantitatively estimated. Again there is good evidence in support of the fact that microcrystalline Bi has a smaller susceptibility than macrocrystalline.[5] Bismuth particles less than about 1μ have a susceptibility less than the bulk material, as the particle size is decreased below this limit the susceptibility decreases roughly proportionally. This makes it possible to follow changes in mean particle size at very small sizes. And finally amorphous Bi should have a susceptibility some 20 times less than the regulus material, so that if any considerable fraction of the film were amorphous the fact could not escape notice. In general an interpretation of the crystalline nature (or otherwise) based on susceptibility measurements should be unambiguous.

Technique

The bismuth used in this work was supplied by Eimer and Amend and had a stated purity of 99.98 percent without, however, an analysis showing the amounts of individual impurities. This stock metal was, however, subjected to magnetic tests, discussed later, which showed it to be highly pure from a magnetic point of view. The films were produced in high vacuum by evaporation from a small furnace, through a series of collimating slits. The actual design of this equipment will not be further discussed here since similar apparatus containing all the essential features has already been described.[6] Particular pains were taken to insure that all films

[2] H. Lassen and L. Brück, Ann. d. Physik **22**, 65 (1935).
[3] L. Brück, Ann. d. Physik **26**, 233 (1936).
[4] A. Goetz, O. Stierstadt and A. B. Focke, Zeits. f. Physik **98**, 118 (1936).
[5] S. Rao, Ind. J. Phys. **6**, 251 (1931); **7**, 38 (1932).
[6] C. T. Lane, Phys. Rev. **48**, 193 (1935).

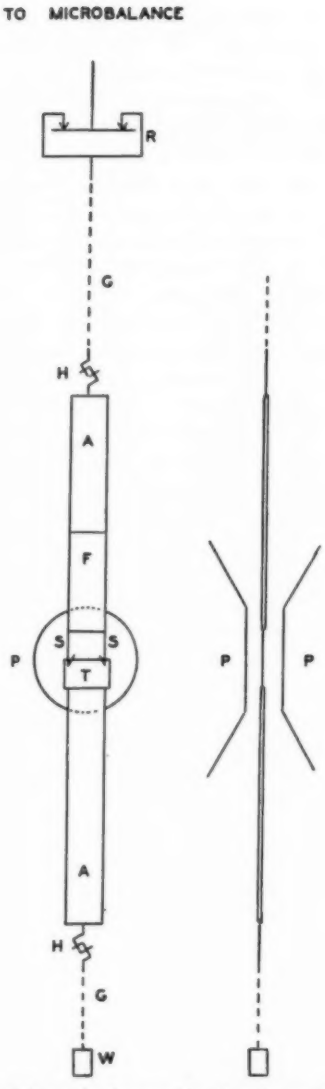

FIG. 1. Schematic diagram showing the method of measuring the susceptibility of thin films.

were produced under as nearly identical conditions as possible. Furnace temperature and residual hydrogen pressure in the apparatus were rigorously controlled and the films were "aged" by filling the apparatus with hydrogen at atmospheric pressure as soon as the evaporating process was complete. It has been mentioned previously that an absolute measurement of the susceptibility was desirable and of the several methods available for such measurement the Gouy method is by far the simplest and most reliable. This method consists in measuring the logitudinal force on a long prism of the substance, one end of which is in a strong magnetic field, the other end being in a field of much lower intensity. In the case of a thin film two special difficulties present themselves. The first, and least important of these, is that, since the amount of matter of which the film is composed is very small, the resultant force on it in the strongest available magnetic fields will likewise be very small. This trouble was overcome by using a Sartorius microbalance which would measure 2×10^{-6} g as a lower limit. This balance also conveniently measured the total weight of the film. The second difficulty lies in the fact that any substance upon which it is practical to deposit the film will itself experience in a magnetic field a force some hundreds of times larger than that upon the film itself. In order, then, to measure the film susceptibility with any degree of accuracy it is apparent that its backing must be magnetically compensated to a high degree. That is to say, the effective susceptibility of the backing must be reduced to as low a figure as possible. Fig. 1 indicates in a schematic manner the way in which this was brought about. *AA* are two glass microscope cover slips approximately 10 cm long, 2 cm wide and 0.01 cm thick. One of these slips has three glass hooks *S*, *S*, *H*, fused directly on to it. The other has a glass trapeze *T* at one end and a hook *H* at the other. This "glass blowing" was done with a gas flame a few mm long. This system is suspended from a small rotation head *R* which in turn is suspended from one arm of the microbalance. By means of *R* the film normal can be set at any desired angle to the magnetic field. A small gold weight *W* is used to keep the glasses straight. *G* is a very fine gold chain. The positions of the magnet pole pieces are indicated in the sketch (*P*). Evidently this system will have an effective susceptibility of zero provided the two glasses *AA* are alike in dimensions and in susceptibility in the parts extending beyond the uniform field at the center, supposed to extend over the hooks and trapeze, and provided further that the field intensities at the upper end of *A* and at the lower end of *A** are zero. In actual practice, small differences in the two glasses, asymmetry in the

magnetic field, etc., resulted in the system having a small effective susceptibility. This was corrected by depositing a film of gold on one or other of the glasses depending on whether the net susceptibility was positive or negative, the appropriate thickness of this gold deposit being determined empirically. The Bi film (F) was then deposited on the other glass. It is evident that small traces of ferromagnetic impurity at any part of the system would completely upset its compensation and hence very considerable care had to be exercised in the choice of materials. Only very pure diamagnetic materials were used and each piece was inspected magnetically before being selected for use.

The hooks made it possible to remove the system and replace it in virtually its original position in the magnetic field. The system used in the final measurements was acted upon by a residual force, in a field of maximum intensity about 28,000 gauss of the order of 5×10^{-6} g (equivalent susceptibility, 10^{-9}) and it was found possible to repeat its compensation to within this limit when the glass strips were removed and replaced. In carrying out an actual measurement the following procedure was followed. The system was set up, compensated, removed, and a Bi film deposited upon one of the glasses. After measuring the force on the film in the maximum field allowed by the set-up the system was again removed, the bismuth film was dissolved away in dilute HNO_3, the system replaced, and the compensation rechecked. If any significant change was found to have occurred this set of data was thrown out. In about 5 percent of the actual trials it was found that the compensation had changed. The most frequent source of such changes was probably incomplete demagnetization of the magnet, which varies the change in pull upon remagnetizing to the measured maximum intensity.

The majority of the measurements was made with the plane of the film perpendicular to the field since in this case the magnet air-gap was least, giving highest field and greatest sensitivity. When it was necessary to investigate the variation of susceptibility with angle between film normal and field a wider gap had to be employed. In this case significant measurements could only be made on relatively thick films. In using a balance of high sensitivity the control of the temperature is naturally of great importance. In the present case triple shielding was resorted to. The system was suspended with its center 50 cm below the balance arm in a narrow rectangular trough made of three vertical strips of brass. Surrounding this and also enclosing the pole pieces was a base made of plywood. Surrounding the whole water-cooled magnet was a third casing of beaver board. A heavy slate shelf, which supported the microbalance, served as the roof of this last mentioned housing. The microbalance itself was shielded by heavy cardboard. Finally, when measurements were being made, the temperature of the whole room (a small one) was kept as constant as possible.

In order to arrive at an absolute value for the susceptibility it is of course necessary to know the field strength at each end of the film. To measure this ballistically in a region where the field gradient is large (as it is at the end of the film not in the magnet air-gap) presents considerable difficulties. It appeared better to measure the desired function of the magnetic field intensities by the force on a substance of known susceptibility. To this end some extruded polycrystalline wires, about 0.5 mm in diameter, were made of the stock bismuth. Since the principal susceptibilities of a single crystal of this material had been determined, the susceptibility for a polycrystalline was calculable.

A film of thickness about 0.001μ was now deposited and a number of the extruded wires, of the same length as the film, were tacked down upon this film with drops of collodion so as to form an artificial "film" of known susceptibility. The magnetic forces on the 0.001μ evaporated film were, of course, negligible in comparison with those on the wires. The film merely marked the proper location for the latter.

Results

In Fig. 2 a curve has been plotted showing the diamagnetic susceptibility as a function of film thickness, and, for comparison, the susceptibility of a single crystal (dotted line) placed in the field (H) with [111] parallel to H, and therefore perpendicular to the axis of the crystal rod. In passing we may mention that the single crystal value is determined from a crystal grown from

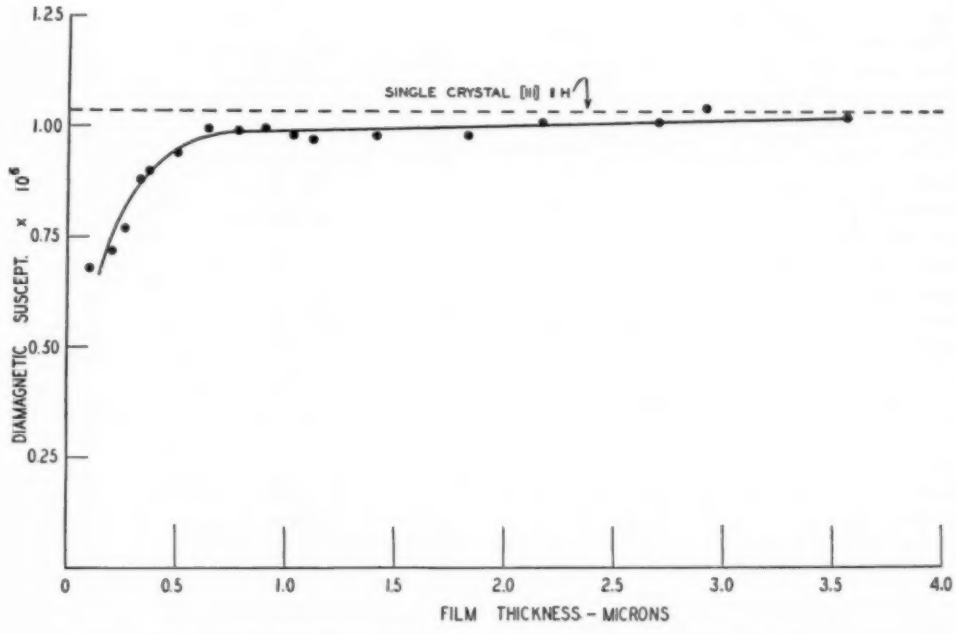

FIG. 2. Curve showing the relation between susceptibility and film thickness.

the same stock material as was used to produce the films, at a fast rate of speed (4 mm per minute) in order to insure that any possible impurities present in the stock material would be distributed uniformly throughout the resulting crystal.

It will be noticed that for thicknesses from about 0.5μ upwards the susceptibility is practically independent of the film thickness and very close to the value for a single crystal for the orientation mentioned above. It is true that the curve does rise somewhat in this region apparently approaching the single crystal value more closely as the film becomes thicker. However, the effect is small and it is rather doubtful whether the accuracy of the experiment is sufficient to warrant a definite conclusion on this point. Below 0.5μ, however, and down to 0.1μ, where the method begins to be seriously inaccurate, the susceptibility definitely decreases as the film thickness is reduced. It may also be mentioned that the susceptibility in this region is smaller than that which is found in massive Bi whether mono- or polycrystalline.

In order to study the effect of the rate of deposition on the structure of the deposits, a number of films of approximately the same thickness (1μ) but produced by widely different rates of evaporation were studied. It was found that the rate of deposition, within wide limits, (30 to 3000 seconds for deposit) had no effect upon the susceptibility nor, by inference, upon film structure.

The effect of the backing substance on the film structure was also investigated. To do this a thick film ($>10\mu$) of another metal was deposited by evaporation on the glass and on top of this layer was condensed the Bi film, the susceptibility of which was to be found. The backing layer was of course compensated by a similar layer on the other glass. No significant difference could be detected in the susceptibility of Bi when deposited respectively on glass, gold, copper and tin. Since glass is amorphous, gold and copper cubic, and tin tetragonal, the structure of the Bi layer is, to this extent, at least, independent of the backing material. Indeed it was found possible to deposit a visible layer of gold on top of the Bi film without appreciably destroying the structure of the film as judged by its suscep-

tibility. The effect of aging the films was also tried. For those thicker than 0.5μ no effect was observed when the films were left in high vacuum for many hours at room temperature. For films below this thickness, however, it was found that the absolute value of the susceptibility tended to increase and approach that of a thick film, especially for films about 0.1μ thick. A similar effect has been found for the electrical resistivity and it is reasonably ascribed to a recrystallization process.

The presence of gas H_2 in amounts from 0.01 to 0.001 mm was found to produce a considerable effect on the structure of the films. The effect of poor vacuum tended to be somewhat irregular but roughly speaking the more gas was present the more nearly the film tended to behave like a random polycrystalline aggregate. In order to study this effect more closely the dependence of the susceptibility on the angle between the film normal and the magnetic field was measured. The results of this are shown in Fig. 3, the notation being such that at zero degrees abscissa the film normal is parallel to the field. Curve D is for a film approximately 2μ thick produced in high vacuum (at between 10^{-5} and 10^{-6} mm Hg). This film possessed a parallel susceptibility (i.e., film normal parallel to H) of $x_{\parallel}=1\times10^{-6}$ and an anisotropy $x_{\perp}/x_{\parallel}=1.33$. These are fairly close to the values for a single crystal with [111] parallel to H (dotted curve C, $x_{\perp}/x_{\parallel}=1.404$). It must be noticed here that in order to make measurements on the susceptibility at 90° to the normal it was obviously necessary to employ a wide air-gap, with a corresponding reduction in the magnetic field strength and in the sensitivity. As a consequence, the accuracy of the points plotted at either side of the figure is least. Curve B is that for a film produced with a residual pressure of hydrogen of about 10^{-3} mm of Hg. It will be seen that this curve departs from the single crystal type much more noticeably. The anisotropy is now reduced to 1.25, and, what is more important, the relatively accurately determined parallel susceptibility has increased to 1.17×10^{-6}.

Curve A is that for a film produced with a still higher pressure of gas in the chamber. This film is apparently a random polycrystal, its susceptibility, 1.30×10^{-6}, being close to the suceptibility of the polycrystalline bulk metal (1.33×10^{-6}).

Discussion

Before proceeding with a review of the results obtained in this work it is in order to make some comparison with previous results. As far as the writer is aware the only other determination of the susceptibility of a nonferromagnetic film is the author's own work[7] published in 1932. This experiment differed in two important respects from the present one. First, no absolute measurement of the susceptibility was attempted; the ratio of the susceptibilities of presumably comparable films was measured. Second, the arrangement of the apparatus was such that the film normal was always perpendicular to the magnetic field. Again the measurements were carried out in vacuum and the thickness of a film could only be rather roughly estimated from the time of exposure to the molecular beam under standard conditions. These experiments showed that, within an estimated error of 10–15 percent, no difference in the perpendicular susceptibility occurred between thicknesses of 0.2μ film and 15μ.

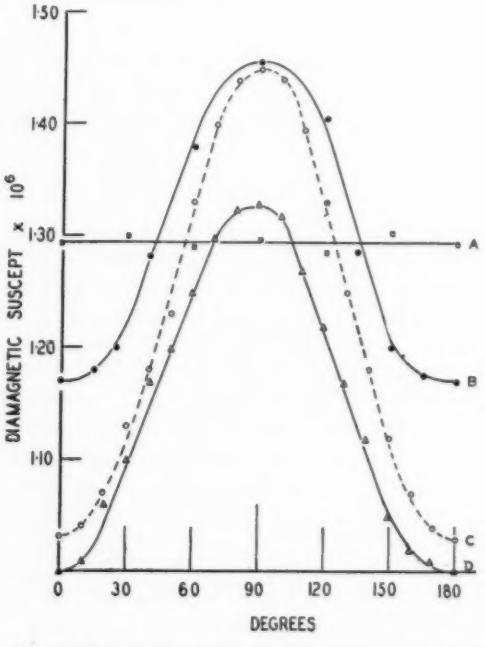

Fig. 3. Curves showing the relation between susceptibility and angle between film normal and magnetic field for various films.

[7] C. T. Lane, Nature **130**, 999 (1932).

From what has been said it is clear that no direct comparison can be made with the present experiments. However, it seems strange that the perpendicular susceptibility, $x_\perp$, should behave so differently from the parallel susceptibility, $x_{\parallel}$. Referring to Fig. 2, however, it is seen that, for the perpendicular setting, the susceptibility of a film 0.3μ thick differs from that for a 3μ film by only 18 percent which is not far from the possible experimental error in the earlier work. Further we now know that thin films tend to increase susceptibility when left in high vacuum. Hence some legitimate doubt may be cast on the validity of the earlier work, although as has been emphasized, no direct comparison is possible. The accuracy of the present work should be about 3–4 percent.

That the effect found cannot be ascribed to impurities in the original bismuth metal is apparent when we consider the anisotropy ratio $(x_\perp/x_{\parallel})$ of the single crystal. For our material this ratio, which of course can be measured with great accuracy, turns out to be 1.404 as against 1.406 by Goetz *et al.* and 1.393 by Schoenberg.[8] As Goetz and his co-workers have shown, this ratio is very sensitive to impurities. We must conclude therefore that the rise in susceptibility shown by films less than about 0.5μ is due to a transition from a microcyrstalline to a macrocrystalline structure, completed at about this thickness. As has been mentioned the dependence of susceptibility on particle size seems to be well established experimentally, at least for graphite and bismuth, although the theoretical reasons for this are still somewhat osbcure.[9] Again since the susceptibility for films below 0.5μ is less than the smallest value ever obtained in bulk material $(x_{\parallel})$ it is most likely that the fiber structure with (111) parallel to the surface of deposition is maintained as we pass through the transition point. This, of course, is in agreement with the electron diffraction experiments. The work is in disagreement with Goetz, Stierstadt and Focke as to the thickness of the microcrystalline layer by a factor of about 200. The writer feels that purely microscopical observations have to be interpreted with very great care if dependable conclusions are to be reached.

With regard to the effect of gas in the apparatus curve B in Fig. 3 is of special interest. It may readily be shown that the apparent susceptibility x for a monocrystal rod is given by

$$x = x_\perp \sin^2\theta + (x_\perp \cos^2\phi + x_{\parallel} \sin^2\phi)\cos^2\theta,$$

where in θ, and ϕ are, respectively, the angles between the trigonal axis and the magnetic field and between the trigonal axis and the (axial) direction of the measured force. For the single crystal (curve C) we have $\phi = 90°$. If now in a film $\phi < 90°$, the perpendicular susceptibility ($\theta = 90°$) will be the same as before; the pseudo-parallel susceptibility ($\theta = 0$) will, however, be greater than previously found for the single crystal. Thus the presence of approximately 10^{-3} mm of gas in the apparatus disturbs the normal crystalline growth of the films. The trigonal axis of the crystallites composing the film are not now accurately perpendicular to the surface of deposition but rather scatter about the normal to this surface. The presence of still more gas in the apparatus tends to accentuate this effect until a pressure is finally reached wherein the crystal structure of the film is "destroyed," i.e., the film is now composed of crystallites orientated at random with respect to the backing surface (curve A).

In conclusion I should like to express my gratitude to Professor L. W. McKeehan for his interest in this work and also to Dr. A. B. Focke of Brown University for his generous gift of some single crystal bismuth seeds.

[8] Cf. reference 4, page 125.

[9] The effect has recently been found for quartz. Y. Shimizu and N. Takatori, Sci. Rep. Tohoku Imperial Univ., Honda Anniversary Volume, p. 306 (1936).

Powder Patterns on Ferromagnetic Crystals

K. J. SIXTUS
General Electric Company, Schenectady, New York
(Received March 5, 1937)

The regular patterns which, as Bitter has found, form on ferromagnetic single crystals from a suspension of magnetic iron oxide have been studied on large crystals of 3.5 percent silicon-iron. Three different types of patterns were observed at low, medium, and high fields, respectively. The direction of Type I and Type II patterns is determined by the crystal orientation; that of Type III is always nearly normal to the applied field. Type I patterns were found only after polishing or otherwise straining an annealed sample, and the line spacing stayed constant (except at $H=0$) as the field was increased. We conclude that surface strains are essential in producing this type of pattern. Type II patterns were little affected by stress, and the lines multiplied when the longitudinal or normal field component was increased. Certain dissymmetries of the lines and their behavior near a hole in the sample were studied. It is concluded that the Type II lines are formed at the intersections of magnetic "sheets," lying in dodecahedral (110) planes, with the surface. Type III patterns form near surface inhomogeneities where the magnetic flux is forced to cross the surface and where the magnetization accordingly has a normal component.

FOR the study[1] of "Bitter" patterns[2] a suspension of iron oxide ($\gamma-Fe_2O_3$) with a particle size of 0.5×10^{-4} cm in Nujol—a viscous mineral oil—was used. Here the particles do not have the mobility exhibited by colloidal particles such as used by L. W. McKeehan and W. C. Elmore.[3] Once a pattern has formed, it stays nearly fixed under changed external conditions; it has to be stirred or replaced for a new pattern to develop.

The crystals were prepared in the form of disks or strips by recrystallization from silicon iron strips with 3.5 percent Si. The results on only three out of a total of ten studied are given here. The patterns on these three appeared more clearly than on the rest and it can be seen from Table I which gives their orientation that in all of them a (100) plane lies nearly in the surface.

The field was produced by an electromagnet for the short samples, by a coil for the long ones. The values of field strength given below are not corrected for demagnetization. The fact that the pattern remained "fixed" after its development in the field allowed the removal of the sample from the coil and its observation under the microscope.

[1] Most of the experiments described here were reported at a meeting of the American Physical Society in February, 1934. An abstract of that paper appeared in Phys. Rev. **45**, 565 (1934). A few experiments were made shortly after this meeting. Since a continuation of the work appears not possible in the near future, the data forming the original paper are given here together with some additional results.

[2] F. Bitter, Phys. Rev. **38**, 1903 (1931); **41**, 507 (1932).

[3] L. W. McKeehan and W. C. Elmore, Phys. Rev. **46**, 226 (1934); **46**, 529 (1934).

Direction of Patterns

It was found independently by S. Kaya[4] and by the author[1] that three different types of patterns existed in the different ranges of the magnetization curve, and that these types had different directions. On the first steep part of the magnetization curve patterns (Type I) form along intersections between the surface and those (100) planes most nearly perpendicular to the surface (Fig. 1). If the surface also lies nearly in a (100) plane as in our case there are two possible line directions. It depends on the polishing and field direction which set will appear; in some cases both are observed together. Between the first bend of the magnetization curve and the bend at reaching saturation, lines (Type II, Fig. 3a, c) form at intersections between (110) planes and the surface. Ordinarily only that set

TABLE I. *Orientation of the crystal axes with respect to a coördinate system in the crystal surface. The suffixes y and x refer to the angles with the y and x axes, which lie in the sample surface at right angles to each other; the field is always applied parallel to the y axis.*

Dimensions: Crystal No. 1. $1.55\times0.050\times2.4$ cm³; crystal No. 70. $1.35\times0.056\times5.0$ cm³; crystal No. 7N. $1.55\times0.054\times25.0$ cm³.

Crystal No.	[001] axis		[010] axis		[100] axis	
	α_y	α_z	β_y	β_z	γ_y	γ_z
1	−85	−74	31	62	−60	33
70	88	79	−10	−80	79	−15
7N	86	−68	−26	−71	−71	30

[4] S. Kaya, Zeits. f. Physik **89**, 796 (1934); **90**, 551 (1934).

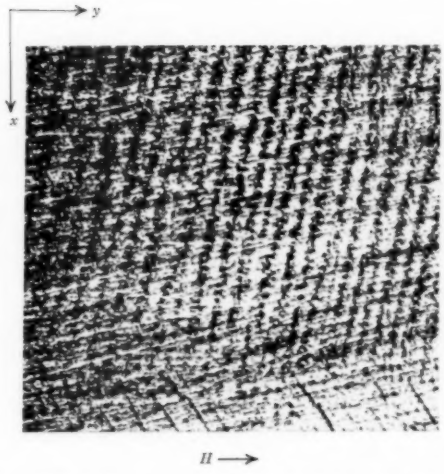

FIG. 1. Type I pattern on crystal No. 70 at 5 oe. Due to inhomogeneous field distribution, several Type II lines appear on the lower part of the figure. The white lines are polishing scratches. (Magnification 15×).

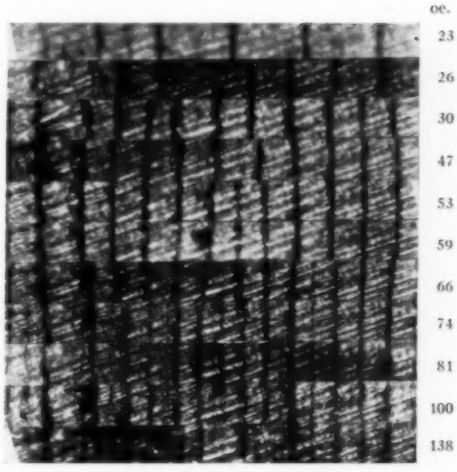

FIG. 2. Type II patterns taken at the same place on crystal No. 1 after successive increases in field. (Magnification 48×.) The Type II pattern on crystal No. 1 was observed in a field range between 20 and 160 oe.

of lines appears whose direction is given by the (110) plane most nearly perpendicular to the field. Beyond the saturation bend we observe bands of irregular length and appearance whose direction is very closely perpendicular to the applied field (Type III, Fig. 3b).

SPACING

The spacing of the Type I pattern was fairly constant in different places on any one sample and it stayed constant over the Type I field range except in 0 field where the number of lines doubled (cf. McKeehan and Elmore[3]). On different samples the range of spacings found lay between 5 and 30×10^{-3} cm. This spacing is considerably higher than that observed by McKeehan and Elmore which was about 2×10^{-4} cm; it is probable that such a fine structure can only be detected with extremely fine suspensions.

Some remarkable properties were observed with the Type II pattern. Bitter[2] has shown that on nickel crystals the lines obviously multiply by splitting. The division of a line into two new ones at certain field values rather than the development of new lines appears to be the mode of multiplication in our case also, but the process is somewhat different from that observed on nickel. On the Fe-Si crystals the lines show a strong tendency to have, at any field, a uniform spacing. Thus Fig. 2 shows clearly in several instances how the addition of a new line "pushes" the neighboring line away in order to equalize the line spacing.

Bitter has also pointed out[2] that on reapplication of a given field the lines appear in new places. We found in addition that the entire process of line multiplication is irreversible. If the field is reduced from any value in the Type II range, the number of lines does not change until this pattern disappears at the first bend. Another effect which illustrates the irreversibility of the process of line production is the following. If a field value in the Type II range is reached by increasing the field from the Type I range, many of the lines extend over a large part of the surface, as indicated by the photograph (Fig. 3a). If, however, the same field value is reached by a field reduction from the Type III range (Fig. 3b), the lines are short and less uniform in direction (Fig. 3c).

The magnetization curve of the long crystal No. 7N is given in Fig. 4, together with the spacing-field dependence of the Type II pattern. The magnetization curve seems to contain several sharp "kinks," connected by straight lines. These were first reported by W. Gerlach, and have later been either confirmed or doubted by

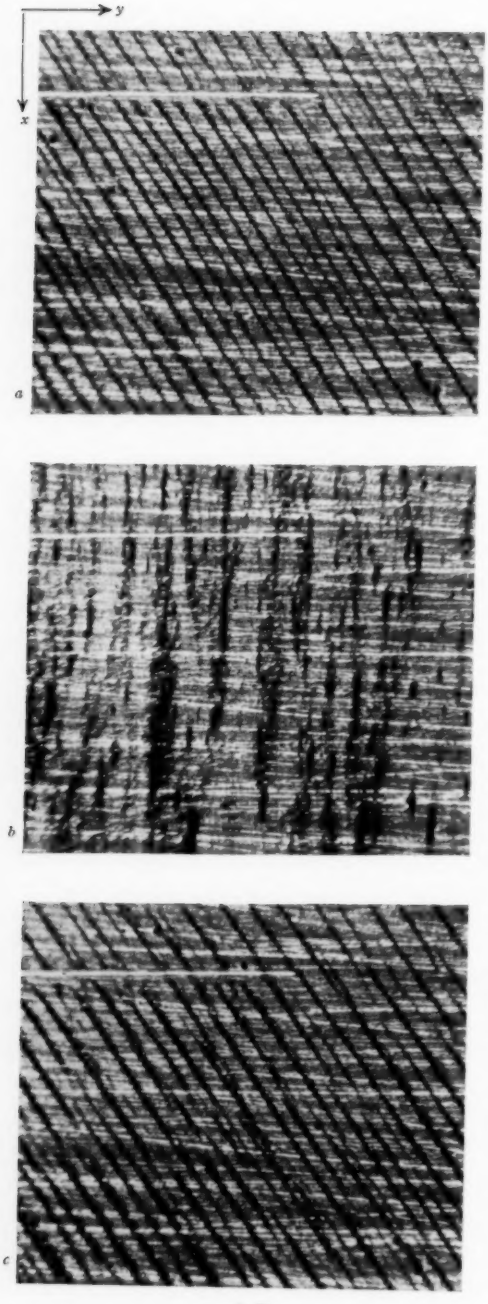

FIG. 3. *a;* Pattern (Type II) on crystal No. 70 at 36 oe. *b;* Pattern (Type III) after the field was raised to 90 oe. *c;* Pattern (Type II) after field reduction from 90 to 35 oe. (Magnification 15×.) The Type II field range on crystal No. 70 lay between 8 and 80 oe.

other workers.[5] The field dependence of the line spacing is definitely a discontinuous curve, indicating that line multiplication takes place at certain critical field values. The relation between the sudden slope changes in the magnetization curve and the changes in line spacing is here merely suggested, because the accuracy of the present measurements does not allow definite conclusions. There is additional evidence for the suggested relation in that the descending branch of the magnetization curve, though lying very close to the ascending one, has no breaks, while the line spacing during field reduction stays constant.

Effect of Strain

Some preliminary tests were made on crystal No. 70 which was subjected to bending so that the upper surface could be put either under tension or compression. The Type I lines, which under compression ($\epsilon = -5\times10^{-4}$) and also with zero strain formed at an angle of $-80°$ with the field direction, switched to the other possible direction, at $+10°$ from the field direction, when tension ($\epsilon = 5\times10^{-4}$) was applied.[6] The line spacing became more irregular with stress but was of the same general order (15×10^{-3} cm). The direction of the Type II pattern was the same ($+56°$) in all three cases; the spacing, at a given field, showed a variation only in the case of compression (from 20 to 7×10^{-3} cm). It has to be added that with the Type I pattern the line changes were reversible when the stress was applied or removed, which, however, was not the case with Type II pattern. On application of pressure the lines multiplied; if now the stress was released without changing the field, the lines (after replacing the powder suspension) stayed in the same place although they were weaker than before. Only after the field had been reduced to 0 and returned to the previous value would the spacing return to its old value. The Type III pattern was not affected by stress.

The experiments were repeated using the long crystal No. 7N under pure tension, which offered two advantages. The strain could be determined

[5] See discussion by L. W. McKeehan, Trans. A.S.M.E. **111**, 11 (1934).

[6] A similar effect was observed by N. Akulov and S. Raewsky, Ann. d. Physik [5] **20**, 113 (1934).

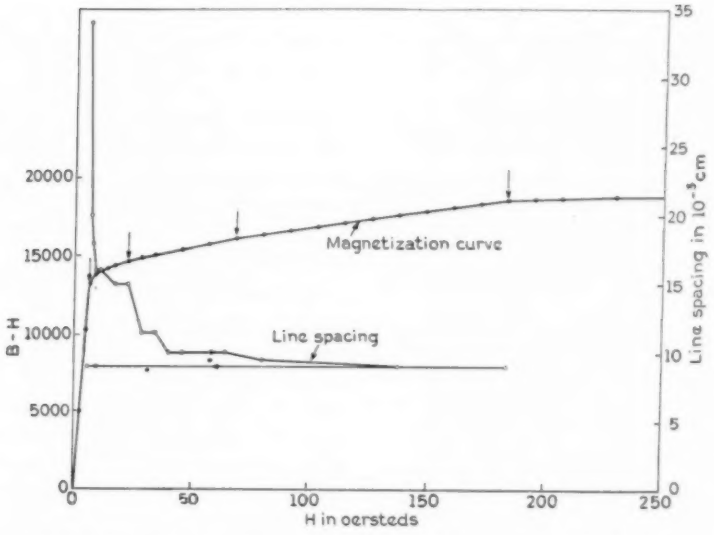

FIG. 4. Magnetization curve of crystal No. 7N (not corrected for demagnetizing effect) and line spacing (Type II) *vs.* field relation. The vertical arrows point to sharp breaks in the magnetization curve.

more accurately, and a magnetization curve with a definite relation to the pattern could be obtained. The corresponding compression case was not investigated. Fig. 5 shows that only the steep part of the magnetization curve of crystal No. 7N is affected by tension. It should be added that a previous curve was retraced when the tension was released to the old value, indicating that the strain had been elastic. Judging from the magnetization curves, we should expect the most profound changes in the Type I pattern. This was confirmed, for with a stress of 100 kg cm^{-2} the lines which ordinarily formed at $+70°$ had already switched their direction to an angle of $-24°$. Tension also affected the time interval between application of powder suspension and completion of the pattern. With 100 kg cm^{-2}, the lines could be seen clearly after less than 10 minutes, whereas it took more than one-half hour for them to appear without applied stress. The strain corresponding to 100 kg cm^{-2} was measured roughly and found to be about 8×10^{-5}. The tension was kept below 250 kg cm^{-2} to avoid plastic deformation, and at that value the pattern was as clear as at lower values.

The Type II pattern throughout the range of stress did not change materially, except that it became a little less clear at higher tension. It was observed, in addition, that under tension the Type II pattern did, with increasing field, appear already below the first bend in the magnetization curve, contrary to the behavior without stress.

Considering the decisive effect which elastic tension has on the Type I pattern, it is not surprising that the direction and manner of polishing

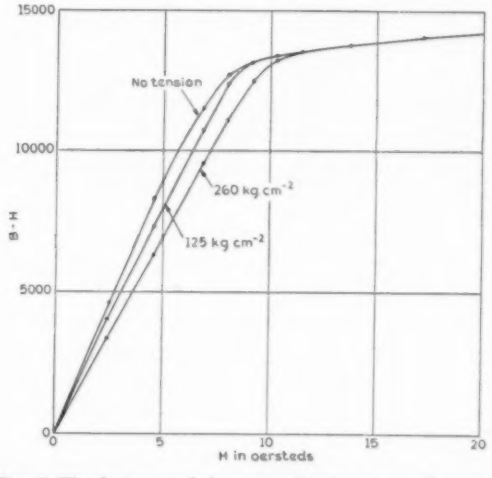

FIG. 5. The first part of the magnetization curve of crystal No. 7N with different values of tension.

should also influence this pattern. Kaya[4] has already given proof of this influence in very painstaking experiments and we give only a short account of our corroborating evidence. The long crystal No. 7N was polished with emery paper (000) and then annealed for one hour at 850°C in pure dry hydrogen. There was practically no change in the reflecting power of the surface before and after the anneal, indicating that surface contamination, if there was any, could only be very slight. The crystal after this treatment showed no Type I pattern, whereas Types II and III appeared as clear as ever. Half of the strip was polished with (000) emery paper parallel to the long axis of the sample and then a set of clear +70° Type I lines could be produced on the polished part.

Polishing affects a surface in two ways, both of which are possible causes for the formation of a pattern. It removes surface material and also introduces cold work effects in the outer layers of the remaining material, consisting in crystal reorientation and strains. If the first effect were the essential one, etching, which will remove any possible surface contamination, would also result in pattern formation. A solution of picric acid in alchol and also a mixture of hydrochloric and nitric acids were applied in different places on the unpolished part, but no pattern would form there. If, however, strains were introduced by subjecting the crystal to tension, the +70° lines appeared at about 100 kg cm^{-2} on the unpolished section, persisted at higher tension, and vanished again below 100 kg cm^{-2}.

The unavoidable conclusion to be drawn from our experiments seems to be that surface strains, as caused by polishing or by applied tension, are a necessary condition for the formation of a Type I pattern. We observed no effect of polishing in the case of Type II and Type III patterns. This had to be expected from the absence of an effect of elastic tension on these patterns.

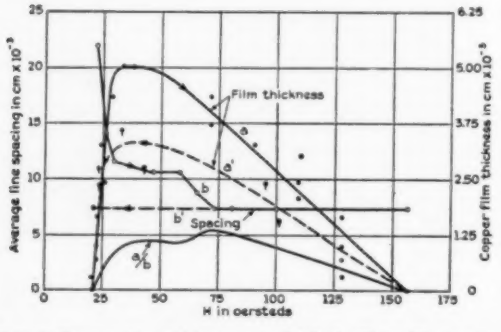

FIG. 6. Copper film thickness, at which the Type II pattern disappears, and spacing on crystal No. 1.

INCIDENTAL OBSERVATIONS

The cause for the formation of powder lines is the presence of poles in the surface. The following tests were undertaken to obtain more information about their strength in the Type II range. An indirect, qualitative method was employed. The crystal was covered with nonmagnetic material in successive layers and at intervals the range of field strength was determined in which the pattern could be observed. Copper was selected as nonmagnetic material because it could easily and uniformly be applied by an electroplating process and its thickness found from the increase in weight. The points on Fig. 6 were obtained in the following way: After plating to a certain thickness, which is plotted as ordinate, the sample was subjected to a magnetic field. The field strength was raised in successive steps, allowing sufficient time at any step for the powder to settle, and the minimum and maximum field values were noted at which a pattern could just be discerned. The experimental points were connected by the line a in Fig. 6. The result shows that the poles which formed at the boundary surface between Si-Fe and Cu, for example, in a field of 100 oersteds were not strong enough to attract powder in distances greater than 2.7×10^{-3} cm above that surface. The dashed line a' connects the experimental points determined at decreasing field values.

The pole density per unit area, σ, which is proportional to the component of magnetization normal to the surface may be roughly calculated with the data of Fig. 6. The force F acting on a pole m in distance a from a line of poles of line density ρ is $F=2\rho m/a$. Now $\sigma=\rho/b$ where b is the line spacing and therefore $\sigma=aF/2mb$. F is constant at the threshold and m is approximately constant along curve a which makes $\sigma\sim a/b$. Fig. 6 shows that the lines multiply as long as this ratio rises, a process which, however, is not reversible.

Two phenomena were in most cases associated with the Type II pattern which, on account of their appearance, we shall name "fringes" and "beards." The former can be clearly seen on Fig. 3a, where each line shows a sharp straight boundary towards the left and is jagged towards the right. The direction of these "fringes" is fixed with regard to the crystal; it is the same all over the surface and stays the same when the field direction is reversed. On the opposite face of the crystal the fringes point in the opposite direction. Incidentally, the fringes can also be seen on some of Kaya's photographs.[4] They assumed a definite direction with respect to that dodecahedral plane whose intercept with the surface determined the line direction, forming on that side of a line where the dodecahedral plane made the smaller angle with the surface (Fig. 8). No fringe was observed on crystal No. 1, where the (110) plane made a right angle with the surface.

"Beards" were first observed on small holes drilled through the crystal. Fig. 7a shows that in the neighborhood of such a disturbance the Type II pattern forms quite unsymmetrically as regards line spacing. On one side of the hole the spacing is the same as on the rest of the crystal, but on the other side the line spacing is smaller and the total amount of powder deposited is much greater. On the reverse face of the crystal the beard pointed always in the opposite direction. At first it was thought that a local distortion might have caused this asymmetry, but it soon became evident that, like the fringes, it was related to the crystal orientation of the sample. In comparing four different crystals, it was found that the direction of the beard was dependent on the angle which the [001] axis made with the axis of the hole. The beard formed on that side of a hole away from which the [001] axis through the hole was inclined, as shown in Fig. 8. The beard persisted in a field range where ordinarily only the bands of Type III would appear. Fig. 7b, taken in a high field, shows besides the beard a heavy symmetrical deposit. The latter was the clue for the explanation of Type III patterns which will be discussed later. The hole caused no disturbance in the Type I pattern.

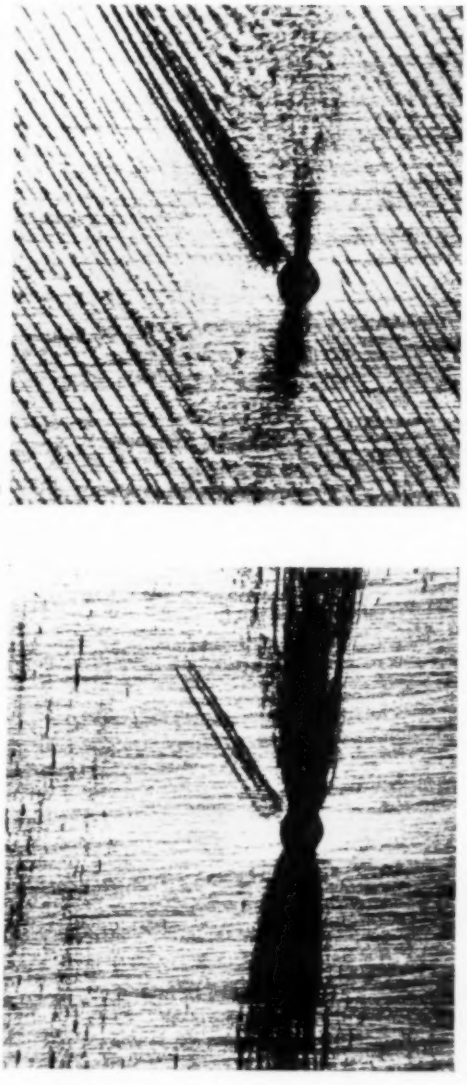

FIG. 7. Patterns near a hole on crystal No. 70. *a;* in medium field. *b;* in high field. (Magnification 15×.)

DISCUSSION

It appears as if the powder patterns could give us valuable information about the actual process of magnetization in crystals supplementing the picture derived from the statistical theory of this process given by Akulov and others. The patterns seem to furnish visible evidence for the existence of elementary magnetic districts made audible in

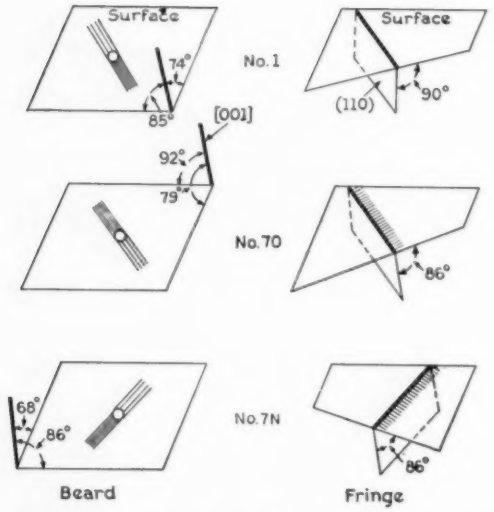

FIG. 8. The direction of "beards" caused by a hole and of "fringes" forming on lines, for different crystals.

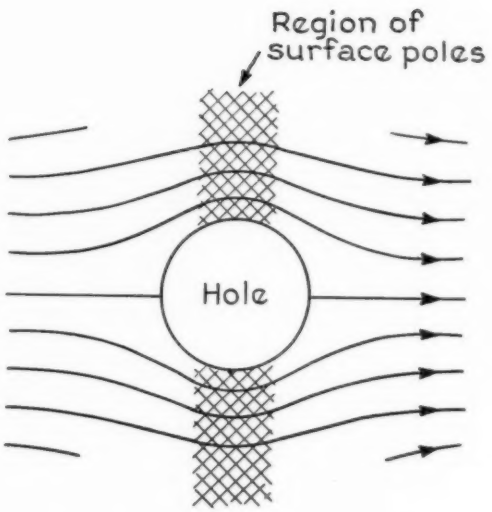

FIG. 9. Explanation for the Type III pattern.

the Barkhausen effect. The evidence, however, is confined to the surface of the material, which—especially as regards magnetic properties—may behave entirely different from the bulk.

The Type I pattern, according to our results, is due to a strain condition at the surface. The ordering effect of applied tension or of polishing is needed to make the magnetic districts line up in a block structure suggested by the Type I pattern. In the case of applied tension, this structure may, of course, extend through the whole crystal. It appears likely that the fine structure pattern as observed by McKeehan and Elmore which has been found so far only on highly polished surfaces can be classed together with our Type I pattern.

The Type II pattern has a definite relation to the normal component of induction which appears at the bend of the magnetization curve and vanishes at saturation. The line spacing decreases, though irreversibly, as this component increases. This component has not been actually measured, but our contention is borne out by conclusions drawn from several experiments: 1. If a field normal to the surface is applied, the number of lines increases. 2. If a sample in a longitudinal field is compressed, the number of lines increases. Since the magnetostriction is positive in the Type II range, compression will result in an increase in the normal component of magnetization. 3. The increase in line number on one side of a hole (beard in Fig. 7a) is due to an increase in the vertical field component on that side. 4. The lines multiply as long as σ (see above) rises. The Type II pattern may be only a surface phenomenon but its independence of surface conditions makes it likely that it reveals a condition present throughout the crystal. The observed pattern is in accord with the assumption that the regions magnetized at large angles to the surface are localized within the crystal in "sheets" parallel to (110) planes. This was also demonstrated in a model made of a razor blade held between two brass blocks. In a suitable field a line with fringe formed along the edge of the blade which was very similar in appearance to a Type II line.

The explanation for the Type III pattern was first reported in February, 1934 and has independently been indicated in Kaya's paper. It becomes evident in a sample in which a small hole has been drilled (Fig. 7). At and near saturation the local magnetization throughout the sample is practically parallel to the total magnetization, or, in different terms, the lines of force are parallel to H as long as the material is homogeneous. If, however, an obstacle such as a hole is present, the lines of force which can

not be "compressed" any more will mainly be "pushed" away in a horizontal plane. Some are "pushed" upward and cross the iron-air boundary near the hole, forming poles on the surface along a line which goes through the hole and is perpendicular to the induction (Fig. 9). A rigorous mathematical solution of this problem is not possible on account of the dependence of permeability on magnetization.[7] The "obstacle" need not be a hole; it may be represented by any region in which the permeability is lower than in the rest of the material, such as inclusions or regions with high local strains in or near the surface. It is evident that the Type III lines are not confined to single crystal samples. Polycrystalline material will exhibit them, particularly if it is subjected to a uniform stress which creates a direction of preferred orientation. Thus the bands, which were observed on stressed and twisted wires[8] and which were found to lie approximately perpendicular to the direction of induction, are another form of Type III lines.

Discussions with Dr. I. Langmuir and Dr. L. Tonks have been of great help to the author in the progress of this work.

[7] R. Richter, Elektrotechnik. u. Maschinenbau **51**, 285 (1933).

[8] K. J. Sixtus, Phys. Rev. **44**, 46 (1933).

MAY 15, 1937 PHYSICAL REVIEW VOLUME 51

The Damping of Torsional Oscillations in Quartz Fibers

G. A. DOWNSBROUGH*
Rutgers University, New Brunswick, New Jersey
(Received September 21, 1936)

The results obtained by previous workers have been qualitatively confirmed, but it was demonstrated that many of the perplexing features were characteristic of the material used to mount the quartz fibers, and not of the fibers themselves. When fused quartz joints were substituted, these features were eliminated, and in addition the damping became very much smaller than in any previous work. As a result, it was also necessary to investigate energy losses hitherto unimportant; several were found capable of affecting the results, but in the final arrangement they were all insignificant. On the assumption that the damping is a purely viscous phenomenon, it is shown that the product of the period of oscillation and the logarithmic decrement should be a constant of the material. This was experimentally verified over a small range of periods; the value obtained was 1.3×10^{-5}. The coefficient of viscosity for quartz, derived from this, is 2.2×10^{8} g/cm sec.

INTRODUCTION

LET a body whose moment of inertia is I execute torsional oscillations about the axis of a quartz fiber whose moment of torsion is T. If the oscillations are damped by a resisting couple proportional to the angular velocity, the equation of motion is

$$I(d^2\theta/dt^2)+b(d\theta/dt)+T\theta=0 \qquad (1)$$

with the solution

$$\theta=\theta_0 e^{-bt/2I}\sin(2\pi t/P), \qquad (2)$$

where P is the period. Since b is very small for quartz, P is given to a high degree of approximation by

$$P=2\pi(I/T)^{\frac{1}{2}}. \qquad (3)$$

The damping of this oscillatory motion is most conveniently measured by the logarithmic decrement δ, defined as the natural logarithm of the ratio of successive amplitudes; thus

$$\delta=\frac{bP}{2I}=\frac{1}{n}\log_e\left[\frac{\theta_0}{\theta_n}\right]=\frac{P}{t_n}\log_e\left[\frac{\theta_0}{\theta_n}\right], \qquad (4)$$

where t_n is the time for the amplitude to change from θ_0 to θ_n. Experimentally it is much simpler to measure t_n than to count n, the number of oscillations.

If we assume that the force dissipating energy

* Now with the Research Laboratories of Johns-Manville Corporation, Manville, N. J.

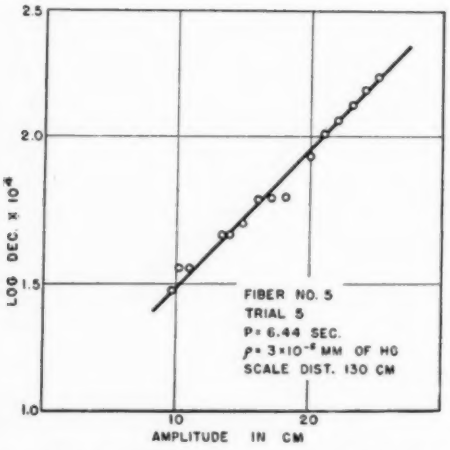

FIG. 1. Showing the variation in δ with amplitude of a fiber mounted with glyptal. (Trial 5 should read Trial *D*.)

is viscous in nature, we may formally define a viscosity, μ, by the equation

$$f/A = -\mu(\partial V/\partial Z), \tag{5}$$

where f/A is the force per unit area called into play by the velocity gradient $\partial V/\partial Z$. K. Honda[1, 2] has shown that

$$b = \mu(\pi r^4/2l), \tag{6}$$

where r is the radius and l the length of the fiber. Combining this with the well-known equation

$$T = \eta(\pi r^4/2l), \tag{7}$$

where η is the coefficient of rigidity, and using (3) and (4), we have

$$\mu/\eta = P\delta/2\pi^2. \tag{8}$$

[1] K. Honda and S. Konno, Phil. Mag. **42**, 115 (1921).
[2] K. Iokibe and S. Sakai, Phil. Mag. **42**, 414 (1921).

Therefore, so long as μ and η are constants,[3] $P\delta$ is a constant of the material. It is not necessary that the quartz fiber should be uniform for Eq. (8) to hold, because the integrations which produced Eqs. (6) and (7) both involve r and l in the same way.

PRELIMINARY RESULTS

An examination of the data on the damping of torsional oscillations in quartz fibers[4–10] shows great discrepancies in the order of magnitude of the damping, even after one had allowed for the variations in the periods. In addition, whenever the logarithmic decrement was carefully studied, it was found, first that the damping of any one fiber depended on its thermal history; second, that the quantity δ defined formally by Eq. (4) was a function of the amplitude of the oscillation so that Eq. (1) and the assumptions on which it was based were invalid.

These two conclusions were qualitatively confirmed by the preliminary work of the present investigation. A quartz fiber was fastened to a support and to a suspended mass by glyptal[11] and

[3] O. Reinkoper has shown (Physik. Zeits. **33**, 32 (1932)) that the coefficient of rigidity is independent of the dimensions for quartz fibers with a diameter greater than 4×10^{-3} cm.
[4] F. Horton, Phil. Trans. Roy. Soc. **A204**, 407 (1905).
[5] J. L. Hogg, Proc. Am. Acad. Arts & Sci. **45**, 1 (1909).
[6] G. E. Guye and M. Einhorn, Arch. d. Sci. Phys. & Nat. (4)**41**, 287, 377, 457 (1916).
[7] G. E. Guye and A. Morein, Arch. d. Sci. Phys. & Nat. (5)**2**, 351 (1920).
[8] G. E. Guye and A. Pazziani, Arch. d. Sci. Phys. & Nat. (5)**6**, 47, 89 (1924).
[9] E. Bolton-King, Proc. Phys. Soc. Lond. **38**, 80 (1925).
[10] G. A. Tomlinson, Phil. Mag. **9**, 913 (1930).
[11] C. Ellis, *The Chemistry of Synthetic Resins*, Vol. II (Reinhold, N. Y. C., 1935), p. 955.

TABLE I. *Preliminary results.*

TRIAL	FIBER	APPROX. LENGTH (cm)	MOMENT OF TORSION	PERIOD IN SECONDS	JOINTS	GENERAL NOTES	MEAN LOG. DEC.	VARIATION	AMPLITUDE
A	5′	10	87	8.2	Glyptal		1.23×10^{-3}	− 7%	26−10
B	5″	9	91	8.1	Glyptal		3.4×10^{-4}	−	24−22
C	5	10	94	6.42	Glyptal	(a)	3.8×10^{-4}	−41%	25− 5
D	5	10	94	6.44	Glyptal	(b)	1.9×10^{-4}	−32%	25− 9
E	5	10	94	6.44	Glyptal	(c)	4.1×10^{-4}	−16%	25−16
F	5	10	94	6.44	Glyptal	(c)	6.3×10^{-4}	−	24−17
G	10	6	19	0.88	Graded Seals	(d)	5.5×10^{-5}	−	25−23
H	10	6	19	1.17	Mirror Glyptaled	(e)	6.6×10^{-5}	− 7%	25− 5
K	11	9	24	1.56	Graded Seals	(f)	8.23×10^{-6}	0	22−18

(a) Pressure 2×10^{-4} mm of Hg.
(b) Pressure 3×10^{-5} mm of Hg; fiber remounted with new mirror and system rebaked.
(c) Apparatus rebaked all other conditions remaining unchanged.
(d) Moment of inertia of mirror is 47 percent of the total moment of inertia.
(e) Moment of inertia of mirror is 70 percent of the total moment of inertia.
(f) The suspended mass serves as mirror so that no glyptal is required for the mirror.

mounted in a vacuum. Table I gives a summary of the most significant results; a great many observations made with other fibers have been omitted. Trials *C–F* show the manner in which the logarithmic decrement varied with the same fiber after heat treatments. The variation of δ with the amplitude in a single run is shown in more detail by Fig. 1 which is a typical curve obtained from the data summarized in trial *D*.

Since the maximum angle of shear must have been far below the elastic limit for quartz and since the baking never took the quartz above 450°C, it seemed that the quartz could hardly be responsible for the peculiar variation in δ.

The material used to mount the fiber seemed to be the most likely source of error, and, it was therefore eliminated by use of quartz-to-Pyrex seals, to be described later, in trials *G* and *H*. The marked decrease in the logarithmic decrement for these cases, the much reduced dependence of the logarithmic decrement on the amplitude, and the increase of δ with the increase in the moment of inertia of the mirror which was still attached by a small amount of glyptal, indicated that the glyptal was the main disturbing feature and must be eliminated still more thoroughly. For this reason the suspended mass was finally made of black Pyrex, so that it could itself serve as the mirror. Glyptal was now used only to attach a minute piece of iron wire to the back of the mass, in order to start the oscillations. The value of δ dropped again (trial *K*), to a value which careful experimentation has failed to reduce further.

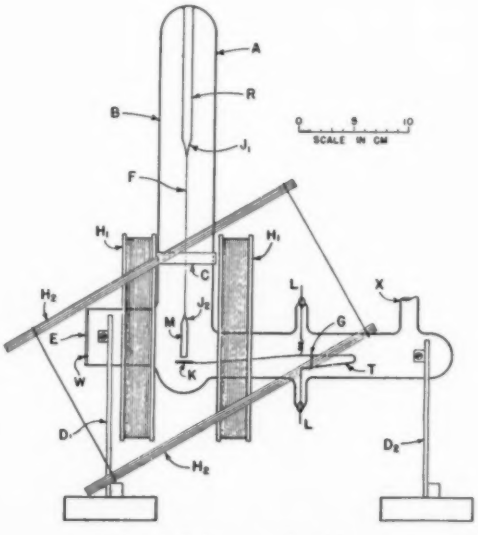

FIG. 2. Apparatus side view.

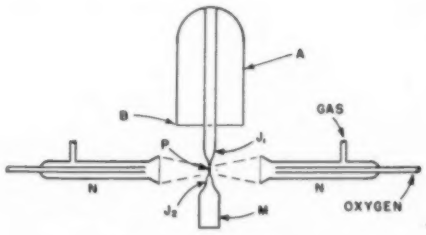

FIG. 3. Drawing fiber.

FINAL EXPERIMENTAL ARRANGEMENT

The arrangement finally adopted is shown in Fig. 2, which is drawn to scale. The tube was made of Pyrex, and the window *W* was fused on, so that the apparatus could be baked out. The suspended mass *M* was a piece of black Pyrex with the front face ground and polished to serve as the mirror. It was joined by the quartz-to-Pyrex graded seal J_2 to a quartz rod from which the fiber *F* was drawn. The other end of this rod, at the top of the fiber, was joined by the quartz-to-Pyrex seal J_1 to a Pyrex capillary *R* of one mm bore and 8 mm thickness which was sealed to the top of the tube *A*. The quartz-to-Pyrex seals J_1 and J_2 were made from a graded mixture of finely ground quartz and Pyrex powders. These seals, five mm in length and three mm in diameter, were thoroughly worked in an oxyhydrogen flame. During all of the work of drawing fibers the heat cracked a seal once, and in this case it was carefully reworked and the crack healed.

The method of drawing the fibers is indicated in Fig. 3. A forked carbon rod, not shown in the diagram, was held in the hands to support *M* while the flames from the torches *N* were on. This arrangement allowed one to work the quartz at *P* so that it was a particular length and diameter; then the carbon holder was dropped and the flames cut off nearly simultaneously by a foot control, permitting *M* to draw the fiber under the action of gravity. With practice one could adjust the length and diameter of the rod at *P* so that fibers of approximately a predetermined length and period could be produced. The center of

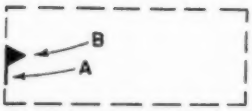

FIG. 4. Amplitude mark.

gravity of M appeared to be directly in line with the fiber, and the polished surface, which acted as the mirror, hung vertically. After the fiber had been drawn, the entire top A was sealed to the tube at B.

Connection was made at X (Fig. 2) to the pumps and ionization manometer through two liquid-air traps, one of which contained charcoal.

It was found necessary to have some method of damping out vibrations which arose from the preliminary work of baking out, and adjusting the liquid air. A very satisfactory arrangement was made by attaching a microscope cover glass K to a bimetallic strip T by means of a somewhat flexible metal arm. A current passed through the bimetallic strip by means of the leads L caused it to warm up and unbend, thus raising the cover glass under the mirror. When the current was cut off the bimetallic strip cooled slowly and the mirror was left hanging motionless in its natural position of rest. The iron guard ring G was adjusted to prevent too great an expansion of the bimetallic strip during the process of baking out the apparatus.

To start the oscillations, the mirror was rotated by the action of the Helmholtz coils, H_1, on a very small piece of soft iron on the back of M. The coils H_2 neutralized the earth's field (see below).

In order to determine the logarithmic decrement, the image of a straight filament lamp was reflected from the mirror M and focused by the lens E on a scale 130 cm distant. The scale was an exposed and developed photographic plate upon which thin lines (slits) were marked at convenient distances with a ruling machine.

For the preliminary work, where the damping and period were relatively large, the following method of determining the time t_n (Eq. (4)) was convenient. A ground glass screen was placed behind the slits and observations made behind the screen. As long as the image of the filament was moving past any one slit, one flash was seen as it passed that slit on the way out and another as it passed after turning. When the turning point was very near the slit only one long flash was seen; accordingly, the flashes were watched until they became single, and the time was taken from the third single flash at one slit to the third single flash at the next.

For the final results, where the damping constant was very small, and the period short, the torsion pendulum had several hundred turning points which produced long flashes; it was thus difficult to determine accurately, by the above method, the time required for the amplitude to drop from one slit to the next. The following method was adopted as the most satisfactory. A white card, represented by the dotted line in Fig. 4, was inked as shown as A and B. The left-hand edge was carefully set on one slit of the plate and observations made from the front of the scale. The black parts absorbed practically all of the light, so that the image of the filament was visible only when it appeared on a white section of the card. The black mark A was 0.3 mm wide, while the bright section of the filament image was about 0.5 mm wide. With the point of B toward larger amplitudes, time was measured from the first swing in which the bright image of the filament failed to appear over the edge A at one slit to the corresponding swing at the next slit. The internal consistency showed this method to be reliable. For instance, trial A in Table II is the mean of the first six determinations with this new method, and the maximum variation from the mean was 3.4 percent. Later work with a more intense source showed more consistent results, as is evidenced by the three runs, taken at widely different times, that were averaged for

TABLE II. *Experimental results. Fiber No. 11, fused joints, $T=20°C$, $p=5\times10^{-6}$ mm, $P=1.56$ sec., $T=21.5$ dyne-cm.*

TRIAL	LOG DEC. $\times10^6$	CURRENT J IN AMP.	GENERAL NOTES
A	8.23	0	
B	8.24	0	Rebaked as check on A
C	8.24	0	Stops D_1 and D_2 in use
D	8.96	+2.00	
E	10.00	−2.00	
F	9.44	+1.80	
G	8.28	+0.85	
H	8.20	+0.45	Amplitude = 20 cm
K	8.29	0.00	
L	8.20	+0.45	Amplitude = 10 cm
M	8.26	+0.85	Screw removed from C
N	8.33	0.00	H_2 individually shorted

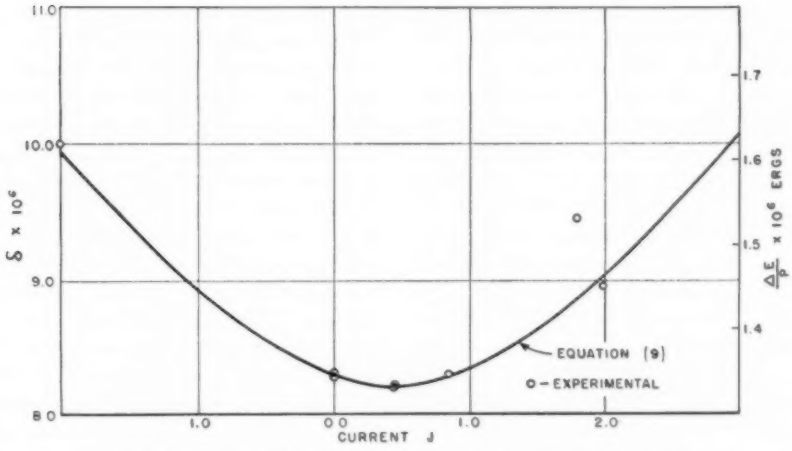

FIG. 5. Showing the changes in δ produced by hysteresis energy loss.

trial L of Table II. The greatest variation from the mean was now 0.5 percent.

RESULTS

The data obtained are summarized in Tables II and III. Trials A and B show that there is now no variation of the logarithmic decrement of the same suspension when the apparatus was rebaked. This conclusion was further supported by the general nature of the remaining data. These data also show that the logarithmic decrement is independent of the amplitude. Trial A is an average of six determinations within a range of four centimeters; the variations from the mean were small and distributed at random. This conclusion was further supported by trials H and L which were taken at 20 and 10 cm amplitudes, respectively.

This work showed that the greatest part of the energy loss in the preliminary work was in the glyptal joints, and it seemed reasonable to believe that this also was the case with the previously reported work. The logarithmic decrement and the properties previously assigned to it therefore, were characteristic of the joints and not of the quartz.

TABLE III. *Log decrement for five fibers and the values of the product $P\delta$.*

FIBER	LOG DEC. $\times 10^6$	PERIOD P	$P\times\delta\times 10^6$
11	8.2	1.560	12.8
12	13.4	1.059	14.2
13	6.7	1.990	13.3
14	8.4	1.625	13.6
15	8.7	1.523	13.2

The energy-loss per period was now so small that it was necessary to investigate various agents which might be dissipating energy in addition to the fiber. It is easily seen that

$$\delta=\Delta E/2E,$$

where ΔE is the change, per period, in the total energy E. Putting $T=24$ and taking the amplitude as 10/130 radians, we have $\Delta E=1.34\times10^{-6}$ ergs per period, or about 1/5 of the energy of a single slow α-particle. Losses of this magnitude might occur in a considerable number of ways.

The first factor considered was a possible twisting of the whole tube, which would have produced inelastic displacements in the asbestos padding that separated it from the clamp C. To test this, the tube was clamped by the heavy supports D_1 and D_2. (Fig. 2). In Table II, trial C differs from B only in this respect, and it is evident that there was no appreciable loss due to inelastic displacements at the supports.

The soft iron on the back of the mirror was rotating in the earth's field and going through a hysteresis cycle each swing. For the second possible external factor dissipating energy, the loss in magnetic hysteresis per cycle per cubic centimeter $\oint Hd\mathfrak{I}$, was considered. The quantities involved (the component of the earth's field strength H, the intensity of magnetization $\mathfrak{I}$, and

the volume of the iron) were all very small, but the loss was just appreciable, as was shown in trials D–L of Table II. These readings were obtained by passing a current J through the coils H_2 (which caused no detectable change in the period or in the zero position), and measuring the corresponding δ. They are plotted in Fig. 5, where δ, part of which is now proportional to the hysteresis energy loss, is plotted against the current J. The magnetic hysteresis loss will be zero, corresponding to the minimum of Fig. 5, when the current J balances the earth's field. The minimum occurs at $J=0.45$ ampere. The total field H acting on the iron is thus proportional to $(J-0.45)$. Neglecting the point at $J=1.80$ (trial F) the equation

$$\delta=8.20\times10^{-6}+0.38(J-0.45)^{1.74} \qquad (9)$$

represents the observations well. For the small fields involved H is very nearly proportional to the magnetic induction B, we can write Eq. (9) in the form

$$\delta=8.20\times10^{-6}+KB^{1.74}. \qquad (10)$$

Subtracting 8.20×10^{-6}, the damping due to the quartz fiber, from both sides, we can write

$$\Delta E=KB^{1.74}, \qquad (11)$$

where ΔE is the energy loss per cycle per unit volume due to magnetic hysteresis, and K is a constant.

Eq. (11) is in good agreement with the empirical formula

$$\Delta E=nB^{c} \qquad (12)$$

given by Steinmetz,[12] where $c=1.66$ to 1.70 and n is a constant of the material.

It appears that magnetic hysteresis is capable of causing appreciable energy-losses, but that the effect will be negligible if the earth's field is balanced. It is not necessary to have the balance exact, since the curve shows that in the present case a 66 percent error in J will produce only a 0.7 percent error in the experimental determination of δ. With a larger piece of iron more care would, of course, be necessary.

The third possible external damping agent consisted of the induced currents in closed circuits near the rotating iron, which possessed some residual magnetism. Since the coils H_1 were only used to start the oscillation, and were always on open circuit during a run, the most likely circuits to be investigated were the clamp C and the coils H_2. In order to test the first of these possibilities, an improvised support was made from D_1 and D_2, and the screw was removed from the clamp C so that it became an open circuit. The results are given in trial M, and when compared with the corresponding trial G show no appreciable energy loss due to induced currents in C. The second possibility in this respect was tested by shorting each of the H_2 coils individually. This required the run to be taken with $J=0$; therefore it must be compared with A, B, C and K. There is perhaps a small divergence, which may be due to currents induced in the coils H_2; for this reason, N is not plotted in Fig. 5. When H_2 were actually in use, the error must have been much smaller, since they were used with 30 ohms in series, while their own resistance was only 0.1 ohm.

As a fourth possible disturbing factor the damping due to residual gases was considered. The general nature of the results indicated that this was negligible. This was confirmed by calculations and by a direct experiment performed as follows.

A fiber was mounted and the logarithmic decrement determined after the ionization gauge and charcoal were baked. The run was made with liquid air on the mercury trap but none on the charcoal. Then the tube as well as the gauge and charcoal was baked, and a run was taken with the liquid air on the charcoal and on the mercury trap. The first results gave δ only 31 percent greater than the second case. The pressure in the first case was not determined, since the ionization gauge could not be degassed at this high pressure. It seems safe to assume, however, that the pressure must have been at least 100 times greater than the 4×10^{-6} mm obtained in the second case. Since the energy loss due to the gas present must be proportional to the pressure, the δ at the low pressure was probably less than 0.3 percent in error because of the residual gases. The calculated energy loss per period due to residual gas is 2×10^{-7} erg at 4×10^{-4} mm.

The fifth spurious energy dissipator considered was inelastic displacements in the glyptal which

[12] C. P. Steinmetz, Electrician **26**, 261 (1891); **28**, 245 (1892).

held the small piece of iron on the back of M. For the work summarized in Table II, a piece of soft iron wire 5 mm long and 10 mg in mass was used. For the results of Table III (other than fiber No. 11) a piece of the same wire was rolled flat and 2.2 mg were used. The surface in contact with M was now 1.8×2.5 mm², which is considerably larger than for the case of the wire. To test for losses due to the yielding of the glyptal, a piece of platinum, of 31 mg mass, was then placed on the back of M in addition to the iron. The logarithmic decrement increased by 11 percent. Since the platinum had approximately the same area in contact with the mirror, and (except for its greater thickness), was the same shape as the flat piece of iron, it seems reasonable to assume that the loss would be approximately proportional to the mass. With this assumption the measurements of fibers 12–15 in Table III are too large by 0.8 percent. (It had been planned to use fiber 11 for this test, but a vacuum accident destroyed the fiber and No. 15 was used.) The loss might have been expected to be larger with the round wire, but Table II, which is also summarized in the first entry in Table III, shows no sign of this. Probably the loss was too small to be detected in both cases.

Table III is a final summary of the data for the five fibers investigated by the method that has been developed. The dimensions were varied somewhat, but on account of the very small damping it was not practicable to vary the periods much. The lengths could also not easily be made much more than 10 cm; but one or two were effectively somewhat shorter. In each case, except No. 14, the figure given is the average of a large number of very consistent determinations, and represents several days' swinging of the torsion pendulum.

Two special notes are to be made regarding this table. First, the orientation of fiber No. 12 was such that the intensity of the light was low; therefore the accuracy was not as high as for the other fibers. Second, the logarithmic decrement given for No. 14 was a minimum value obtained soon after mounting. The value gradually increased as the swinging continued. This was undoubtedly due to a bad crack in the graded joint at M which occurred during the production of No. 14. The crack was healed and No. 15 was made. This last fiber, like all previous ones except No. 14, showed a constant value for δ.

These data show that within an accuracy of about 3 percent $P\delta$ is a characteristic of the material, as predicted by Eq. (8), on the assumption that μ and η are constants.

The differences between different fibers are considerably larger than the variations for any one fiber; since the damping was logarithmic for each fiber, it seems most likely that the actual properties of the quartz (μ or η or both) varied somewhat, due to differences in the amount of working when the fibers were drawn.

Unless some unsuspected source of damping is still present, the viscosity of quartz, as defined in Eq. (5) is also determined by these results, using Eq. (8). Taking Reinkoper's[3] value of the coefficient of rigidity, 3.33×10^{11}, we have

$$\mu=\eta P\delta/2\pi^2=2.2\times10^5 \text{ g/cm sec.} \qquad (13)$$

This is the viscosity tending to damp out, in solid fuzed quartz, shearing strains that keep well within the elastic limit. The dynamical situation is apparently fully described, as far as the quartz itself is concerned, by the specification of a rigidity and a viscosity, and even with the very small damping now obtained, the viscosity is very much higher than for liquid quartz.

In conclusion the writer wishes to express his appreciation to the members of the physics department at Rutgers University for their continued interest and helpful discussions, and in particular to Dr. Robert d'E. Atkinson under whose direction this work was done.

Note on the Nature of Cosmic-Ray Particles

SETH H. NEDDERMEYER AND CARL D. ANDERSON
California Institute of Technology, Pasadena, California

(Received March 30, 1937)

MEASUREMENTS[1] of the energy loss of particles occurring in the cosmic-ray showers have shown that this loss is proportional to the incident energy and within the range of the measurements, up to about 400 Mev, is in approximate agreement with values calculated theoretically for electrons by Bethe and Heitler. These measurements were taken using a thin plate of lead (0.35 cm), and the observed individual losses were found to vary from an amount below experimental detection up to the whole initial energy of the particle, with a mean fractional loss of about 0.5. If these measurements are correct it is evident that in a much thicker layer of heavy material multiple losses should become much more important, and the probability of observing a particle loss less than a large fraction of its initial energy should be very small. For the purpose of testing this inference and also for checking our previous measurements[2] which had shown the presence of some particles less massive than protons but more penetrating than electrons obeying the Bethe-Heitler theory, we have taken about 6000 counter-tripped photographs with a 1 cm plate of platinum placed across the center of the cloud chamber. This plate is equivalent in electron thickness to 1.96 cm of lead, and to 1.86 cm of lead for a Z^2 absorption. The results of 55 measurements on particles in the range below 500 Mev are given in Fig. 1, and in Fig. 2 the distribution of particles is shown as a function of the fraction of energy lost. The shaded part of the diagram represents particles which either enter the chamber accompanied by other particles or else themselves produce showers in the bar of platinum. It is clear that the particles separate themselves into two rather well-defined groups, the one consisting largely of shower particles and exhibiting a high absorbability, the other consisting of particles entering singly which in general lose a relatively small fraction of their initial energy, although there are four cases in which the loss is more than 60 percent. A considerable part of the spread on the negative abscissa can be accounted for by errors; it seems likely, however, that the case plotted at the extreme left represents a particle moving upward. Particles of both signs are distributed over the whole diagram, and moreover, the initial energies of the particles of each group are distributed over the whole measured range.

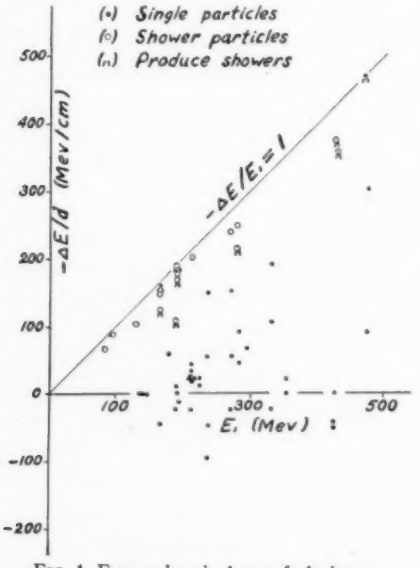

FIG. 1. Energy loss in 1 cm of platinum.

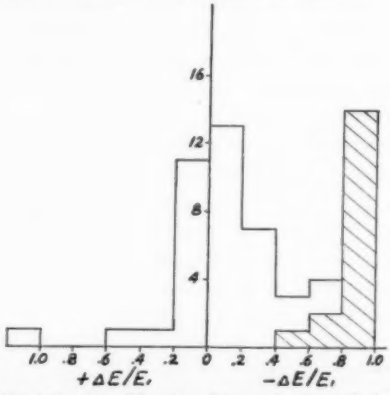

FIG. 2. Distribution of fractional losses in 1 cm of platinum.

[1] Anderson and Neddermeyer, Phys. Rev. **50**, 263 (1936).
[2] Anderson and Neddermeyer, Report of London Conference, Vol. 1 (1934), p. 179.

The chief source of error in these experiments lies not in the curvature measurements themselves, but in the track distortions produced by irregular motions of the gas in the chamber. The distortions are much larger when a thick plate is inside the chamber than when it is left unobstructed. These distortions are not sufficient to alter essentially the distribution of observed losses for the nonpenetrating group, but they could have a very serious effect in the part of the distribution representing small losses. This is especially true inasmuch as this group represents a small percentage of the total number of tracks, selected solely on the basis that they should exhibit a measurable curvature and at the same time be free from obvious distortion. The problem of measuring small energy losses is then evidently an extremely difficult one compared to that of measuring energy distributions in an unobstructed chamber. While it is possible in many cases to distinguish a distortion as such when a magnetic field is present, it is necessary to obtain independent criteria as to the reliability of the measurements; it is not a satisfactory procedure to try to do this simply by measuring curvatures of tracks taken with no field and comparing the curvature distribution thus found with the one obtained when the field is present. Observations made with no magnetic field indicate that serious distortions occur on about 5 percent of the photographs, and show that they are by no means a uniform function of the orientation and position of the track in the chamber. It is therefore not possible to correct for distortion in individual cases. When large distortions do occur, however, they are likely to obey one or both of the following correlations: (*a*) a curvature concave upward when the track makes a considerable angle with the vertical; (*b*) a curvature concave toward the center of the chamber. The observed percentages of measured single tracks obeying the correlations (*a*) and (*b*) are compared in Table I with the percentages expected if the observed curvatures have no relation to the positions and orientations of the tracks. If the 11 cases of apparent gains in energy are left out of consideration the observed percentages are brought somewhat closer to the expected values as shown in the last column.

TABLE I. *Correlations between track curvatures and positions and orientations of tracks.*

Designation (See text)	Percentage correlation		
	Observed	Expected	Observed (excluding apparent gains)
(*a*)	52	50	55
(*b*)	67	50	55
(*a*) and (*b*)	33	25	27
neither	15	25	18

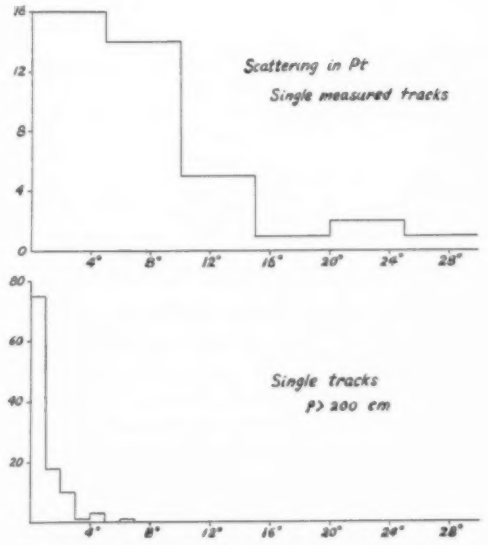

FIG. 3. Scattering distributions in 1 cm of platinum.

A second independent check on the validity of the measurements can be obtained by measuring the scattering of the particles which show apparent curvatures, and comparing this with the scattering exhibited by those single tracks whose curvatures are just outside the range of measurability. In Fig. 3 are shown the distributions of scattering angles (the angles projected on the plane of the chamber) for the measured single tracks and for single tracks with a radius of curvature, $\rho \gtrsim 200$ cm (475 Mev). As it is scarcely conceivable that distortions could influence the scattering measurements by as much as 5°, these distributions constitute strong independent evidence that the measured tracks actually lie in the energy range indicated by the curvature determinations.

It has been known for a long time that there exist particles of both penetrating and nonpenetrating types. Crussard and Leprince-Ringuet[3] have recently made measurements of

[3] Crussard and Leprince-Ringuet, C. R. **204**, 240 (1937).

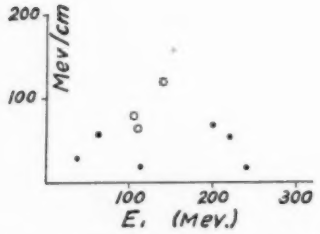

FIG. 4. Early measurements of energy loss in 0.7–1.5 cm of Pb. Dots indicate single particles; circles, shower particles.

energy loss in a range mainly above that covered in our experiments. They have concluded from their data that either the absorption law changes with energy or else that there is a difference in character among the particles. This same conclusion has already been twice stated by the writers.[4, 5] The present data appear to constitute the first experimental evidence for the existence of particles of both penetrating and nonpenetrating character in the energy range extending below 500 Mev. Moreover, the penetrating particles in this range do not ionize perceptibly more than the nonpenetrating ones, and cannot therefore be assumed to be of protonic mass. The lowest $H\rho$ among the penetrating group is 4.5×10^5 gauss cm. A proton of this curvature would ionize at least 25 times as strongly as a fast electron. It is interesting that our early measurements[2] of the energy loss in thicknesses of lead from 0.7 to 1.5 cm show a similar tendency to separate into two groups. They are reproduced in Fig. 4. If reinterpreted in the light of our present data they provide no evidence against high absorbability for electrons.

The nonpenetrating particles are readily interpreted as free positive and negative electrons. Interpretations of the penetrating ones encounter very great difficulties, but at present appear to be limited to the following hypotheses: (*a*) that an electron (+ or −) can possess some property other than its charge and mass which is capable of accounting for the absence of numerous large radiative losses in a heavy element; or (*b*) that there exist particles of unit charge, but with a mass (which may not have a unique value) larger than that of a normal free electron[6] and much smaller than that of a proton; this assumption would also account for the absence of numerous large radiative losses, as well as for the observed ionization. Inasmuch as charge and mass are the only parameters which characterize the electron in the quantum theory, assumption (*b*) seems to be the better working hypothesis. If the penetrating particles are to be distinguished from free electrons by a greater mass, and since no evidence for their existence in ordinary matter obtains, it seems likely that there must exist some very effective process for removing them.

The experimental fact that penetrating particles occur both with positive and negative charges suggests that they might be created in pairs by photons, and that they might be represented as higher mass states of ordinary electrons.

Independent evidence indicating the existence of particles of a new type has already been found, based on range, curvature and ionization relations; for example, Figs. 12 and 13 of our previous publication.[1] In particular the strongly ionizing particle of Fig. 13 cannot readily be explained except in terms of a particle of e/m greater than that of a proton. The large value of e/m apparently is not due to an e greater than the electronic charge since above the plate the particle ionizes imperceptibly differently from a fast electron, whereas below the plate its ionization definitely exceeds that of an electron of the same curvature in the magnetic field; the effects, however, are understandable on the assumption that the particle's mass is greater than that of a free electron. We should like to suggest, merely as a possibility, that the strongly ionizing particles of the type of Fig. 13, although they occur predominantly with positive charge, may be related with the penetrating group above.

We wish to express our gratitude to Professor Millikan for his helpful discussions and encouragement. These experiments have been made possible by the Baker Company, who very generously loaned us the bar of platinum; and by funds supplied by the Carnegie Institution of Washington.

Note added in proof: Excellent experimental evidence showing the existence of particles less massive than protons, but more penetrating than electrons obeying the Bethe-Heitler theory has just been reported by Street and Stevenson, Abstract no. 40, Meeting of American Physical Society, Apr. 29, 1937.

[4] Reference 2, p. 182.
[5] Reference 1, p. 268.
[6] The energies referred to throughout are, of course, calculated on the assumption of electronic mass. For a mass $m\lesssim50m_e$ the actual energy is very roughly $E=E_{el}-mc^2$ in the range of curvature here considered.

LETTERS TO THE EDITOR

Prompt publication of brief reports of important discoveries in physics may be secured by addressing them to this department. Closing dates for this department are, for the first issue of the month, the eighteenth of the preceding month, for the second issue, the third of the month. Because of the late closing dates for the section no proof can be shown to authors. The Board of Editors does not hold itself responsible for the opinions expressed by the correspondents.

Communications should not in general exceed 600 words in length.

A New Precision Determination of e/m for Electrons

In a recent* issue of this journal, I presented a preliminary account of a study which had been made to develop a new focusing criteria for electrons in superimposed electric and magnetic fields, in connection with a precision determination of e/m. Since this account was published, it has been possible experimentally to demonstrate the validity and great precision of both the magnetic and the electrostatic focusing methods. In this way means are provided for the elimination of the uncertainties due to contact potential difference in the accelerating field. It is, in fact, interesting to note, that in the measurement of e/m for electrons by this method, the ultimate precision attainable appears to be limited only by the mechanical accuracy of the present apparatus.

The constants of the magnetic field and the geometrical constants of the apparatus have been rechecked carefully and e/m computed from the best set of observations to be

$$e/m_0 = (1.7571 \pm 0.0013) \times 10^7 \text{ e.m.u.},$$

where 0.0013 is the probable error derived from a least squares solution applied to a set of 14 observations on e/m for various electric field intensities. Other sets differed from this by less than 1 : 5000.

As already stated, the accuracy of the measurement of the geometrical dimensions of the present apparatus sets an upper limit on the ultimate accuracy, but the error due to this cause is less than the probable error. A full account of the complete determination will be published shortly.

A. E. SHAW

Ryerson Physical Laboratory,
University of Chicago,
Chicago, Illinois,
April 17, 1937.

* Shaw, Phys. Rev. **51**, 58 (1937).

Note on the Sign of the Magnetic Moment of the K^{39} Nucleus

Observations on the hyperfine structure splitting of the $4s\ ^2S$ state of K^{39} made by Jackson and Kuhn[1] using spectroscopic methods and by Millman,[2] Fox and Rabi,[3] and Torrey[4] using the magnetic deflection methods are in good agreement so far as the magnitude of the splitting is concerned but in contradiction in regard to the sign of the nuclear magnetic moment. Jackson and Kuhn conclude from the relative intensities of the doublet into which each of the potassium resonance lines is split that the hyperfine levels are inverted and that the magnetic moment of the nucleus of K^{39} therefore is negative. Torrey finds the moment to be positive as determined by the method of nonadiabatic transitions in an atomic beam. The contradiction has been attributed by Bethe and Bacher[5] to reversal effects in Jackson and Kuhn's lines which were obtained by absorption in an atomic beam.

Recently I have observed structure in the resonance lines of potassium produced in emission. The excitation is accomplished by projecting an atomic beam of potassium into a space in which an electrodeless discharge is maintained in argon, the argon being at such a pressure that the mean free path for collisions between atoms is several centimeters. Electron impacts alone then produce the excitation of the potassium. This source gives lines having a half intensity width of less than 0.010 cm^{-1}. That the source is free from absorption and reversal effects is demonstrated by the fact that the hyperfine structure components of the resonance lines of sodium produced by it show the 5 : 3 intensity ratio with good accuracy.

The potassium resonance lines produced by this source show a doublet structure with a separation of 0.016 cm^{-1} between the two components. The weaker of the two components unquestionably lies on the side of lower frequency. This is substantially the structure observed by Jackson and Kuhn in absorption. It therefore confirms their observation of the inversion of the hyperfine multiplet and indicates a negative nuclear magnetic moment for K^{39}.

The components were not here sufficiently separated to permit an accurate quantitative comparison of their intensities. I hope that further refinements of the source may make this possible.

The resolving element used in these observations was a Fabry-Perot interferometer with an 11 centimeter invar spacer. The temperature of the interferometer was held constant within 0.02°C during exposures.

RUSSELL A. FISHER

Department of Physics,
Northwestern University,
Evanston, Illinois,
April 20, 1937.

[1] Jackson and Kuhn, Nature **137**, 107 (1936).
[2] Millman, Phys. Rev. **47**, 739 (1935).
[3] Fox and Rabi, Phys. Rev. **48**, 746 (1935).
[4] Torrey, Phys. Rev. **51**, 501 (1937).
[5] Bethe and Bacher, Rev. Mod. Phys. **8**, 82 (1936).

Evidence for the Instability of He^5

Recently Kempton, Browne and Maasdorp[1] have made a search for homogeneous groups of particles from the proposed reaction

$$_3Li^7 + _1H^2 \rightarrow _2He^5 + _2He^4. \quad (1)$$

If He^5 were stable the He^4 group would have a greater energy than the continuous energy distribution of α-particles from

$$_3Li^7 + _1H^2 \rightarrow _2He^4 + _2He^4 + _0n^1, \quad (2)$$

which has been investigated by Oliphant, Kempton and Rutherford.[2] The former authors' interpretation of their experimental results was that if (1) occurs at all it must be less than one percent of (2).

With the 275 kv transformer-kenetron apparatus previously described[3] we have made a study of the numbers *vs.* range distribution of α-particles resulting from (2). Deuterons magnetically separated from the constant energy ion beam impinged on targets of LiOH or LiCl fused on steel disks. These targets were rotated to present a fresh surface after each reading of approximately two minutes duration. The disintegration products were observed at $90 \pm 5°$ to the direction of the ion beam with a modified Dunning[4] ionization chamber and linear amplifier after passing through an adjustable pressure absorption tube. The residual range of the mica windows and ionization chamber was calibrated with α-particles from a Th C+C′ source replacing the Li target.

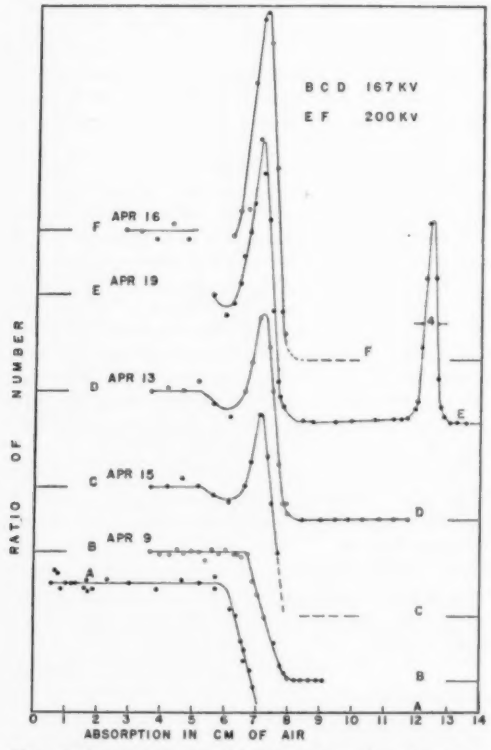

Fig. 1. Ratio of number of particles detected at a given absorption to the number at the minimum absorption. The lettered scale marks on the left are unity and the corresponding marks on the right are zero. Curve *A* is from Oliphant, Kempton and Rutherford. Increasing peak height at a given voltage is evidence of increasing differentiality of detecting apparatus.

Curves of numbers of particles *vs.* absorbing material in cm of air at 15°C are shown in Fig. 1. The scale of numbers is the ratio of numbers observed at a given amount of absorbing material to the number at minimum absorbing material. Numbers at the minimum absorption were repeated every third reading and served to check the constancy of our deuterium concentration, target condition and amplifier gain. This procedure served to minimize the "capricious fluctuations" reported by others and observed by us in less controlled experiments.

The curves show the existence of a homogeneous group superimposed on the background of (2). The yield in this group is small compared to the yield from (2) and only becomes detectable with increasing differentiality of the ionization chamber and amplifier. The number of particles detected for minimum absorption per arbitrary unit of deuterium charge is a rough measure of the inverse of the differentiality. When the detecting apparatus is "semi-differential," curve (*B*), the results compare favorably with those of Oliphant, Kempton and Rutherford[2] who selected oscillograph kicks greater than one cm, curve (*A*).

The ionizing power of the particles in the homogeneous group compared to those at 3.5 cm range was tested by continuing to increase the negative bias of our counter until no particles were recorded. No significant difference was found in the ratio of the counts at the peak to counts at the control range. We conclude that the homogeneous group is due to α-particles.

Assuming the peak of 7.10 cm mean range to be α-

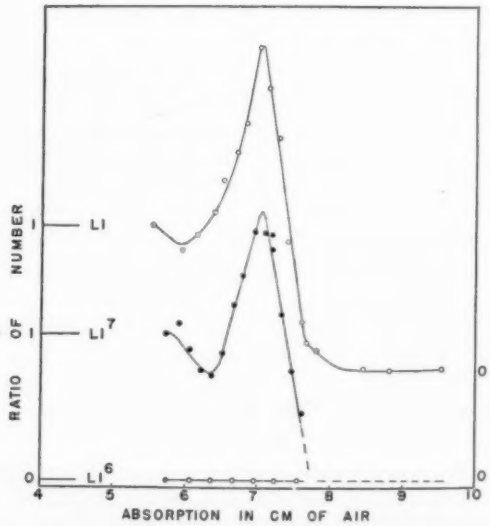

Fig. 2. Ratio of number of particles detected at a given absorption to the number at the minimum absorption for targets of natural Li in LiOH and separated isotopes of Li^7 and Li^6.

particles from (1), the expected range of He^5 is 4.35 cm on reasonable assumptions for the range-energy distribution for He^5 as compared to He^4. The mass of He^5 is then 5.0140 which is unstable by 0.93 Mev. There is no evidence for such a homogeneous group from our results shown in Fig. 1.

The other alternative is to assume the homogeneous group is He^5 from (1) which leads to the prediction of an α-particle group of equal intensity at 11.68 cm. There is no evidence for this group on the low energy side of the homogeneous group of α-particles from

$$_3Li^6 + {}_1H^2 \rightarrow {}_2He^4 + {}_2He^4, \qquad (3)$$

which have a range of 12.70 ± 0.05 cm at a bombarding potential of 190 kv.[2]

If the homogeneous group observed at 7.10 cm is due to α-particles from (1) a possible interpretation is that He^5 exists only long enough to give He^4 a definite energy before it disintegrates into He^4 and a neutron. A somewhat equivalent interpretation is that the observed group is a preferential mode of disintegration (2). The former interpretation leads to a continuous energy distribution of α-particles and neutrons, the α-particle continuum extending from 1.85 cm to 6.26 cm range.

The origin of the observed group was established by observations on targets of the separated isotopes of Li kindly supplied by Dr. L. H. Rumbaugh of the Bartol Research Foundation. The definite indications of Fig. 2 also eliminate any possibility of the group originating from a contamination of the target. A further measurement showed that the yield of the group increased regularly relative to the yield from (2) in the range 140 to 210 kv.

We wish to express our appreciation to Professor E. L. Hill for his constant interest and stimulating discussion and to Professor John T. Tate for his encouragement and support. The research was supported in part by a grant from the Graduate School.

J. H. Williams
W. G. Shepherd
R. O. Haxby

University of Minnesota,
Minneapolis, Minnesota,
April 20, 1937.

[1] Kempton, Browne and Maasdorp, Proc. Roy. Soc. **A157**, 372 (1936).
[2] Oliphant, Kempton and Rutherford, Proc. Roy. Soc. **A149**, 406 (1935).
[3] Williams, Wells, Tate and Hill, Phys. Rev. **51**, 434 (1937).
[4] Dunning, Rev. Sci. Inst. **5**, 387 (1934).

Neutron-Proton Interactions

Measurements of Harkins[1] and co-workers on the scattering of Po-Be neutrons by protons have shown that there is a marked anisotropy in the system where the center of gravity is at rest. These results have recently been augmented by investigations of the scattering of D-D neutrons by protons, (1) by Lampson, Mueller, and Barton[2] using a photographic emulsion method of detection, and (2) by Kruger, Shoupp, and Stallman[3] with a cloud chamber. The general forms of the scattering curves agree, so that we have evidence for a preferred backward scattering of neutrons already at about 2 Mev.

The writer has attempted to fit the experimental curves by assuming that a single rectangular potential well[4] is effective. This would necessitate a radius of about 5.5×10^{-13} cm, provided that the depth be adjusted to give the observed mass defect of the deuteron, whereas the radius of a Gaussian well necessary to fit the observed binding energies of H^3, He^3, and He^4 is 2.25×10^{-13} cm, so that the disagreement is considerable. Furthermore, the theoretical scattering curve deviates rather badly from the observed one at large proton recoil angles (110°–130°).

Current theories provide for four types of interaction between neutron and proton, one being an ordinary force, and the other three of an exchange nature. As a consequence, the states of the deuteron may be classified as symmetric or antisymmetric in the spins, and as even or odd, so that there will be four force laws between a proton and a neutron.[5] Let us denote them generically by ^1S, ^3S, ^1P, and ^3P. In a discussion with the writer, Dr. Feenberg[6] pointed out that it is only the ^1S and ^3S interactions which are used for calculations of the binding energies of H^3, He^3, and He^4, and that one is still free to choose the ^1P and ^3P interactions.

For a preliminary investigation, it seems to be sufficiently accurate not to distinguish between singlets and triplets, and to regard the incident wave function as a sum of two parts, one with even l and the other with odd l. The even part is to be matched with wave functions of the "S" well, and the odd part with wave functions of the "P" well. Phase shifts for $l > 1$ will be supposed negligible, as is usually so. Only two phases, δ_0 and δ_1 will enter the problem, and there is now no connection between them because each has its own potential well. Therefore, one needs only to fit the experimental scattering curve (e.g. system) by a quadratic expression in $\cos\theta$ where θ = angle of neutron scattering, and to determine δ_0 and δ_1 from the relations between the coefficients. This was done for the data of Kruger, Shoupp, and Stallman, and the resulting phases were $\delta_0 = 133°\ 40'$ and $\delta_1 = 16°\ 10'$. (These are not to be regarded as very accurate, owing to the statistical fluctuations. However, the only result which we use is δ_0, which will not become appreciably smaller by fitting differently.) If now, we use this value of δ_0, together with the binding energy of the deuteron, we find 1.7×10^{-13} as the radius of the rectangular potential well, so that the scattering results seem to be in good agreement with the theoretical expectations. From the value of δ_1, we may determine the radius of the "P" well as a function of its depth, which, however, is not known. Measurements for neutrons of other velocities, if made accurately, should yield this knowledge.

I wish to thank Dr. Feenberg for the discussion above mentioned, and Messrs. Shoupp and Lampson for informing me of their results before publication.

James H. Bartlett, Jr.

University of Illinois,
(Temporarily at Institute for Advanced Study),
April 17, 1937.

[1] Harkins, Kamen, Newsom and Gans, Phys. Rev. **50**, 980 (1936).
[2] Lampson, Mueller and Barton, Bull. Wash. meeting No. 121 (1937).
[3] Kruger, Shoupp and Stallman, Bull. Wash. meeting No. 122 (1937).
[4] Massey and Mohr, Proc. Roy. Soc. **148**, 206 (1935). Cf. also Fisk and Morse, Phys. Rev. **51**, 54 (1934).
[5] Cf. Cassen and Condon, Phys. Rev. **50**, 846 (1936).
[6] See also Feenberg, Phys. Rev. **51**, 775 (1937).

Radioactivity Due to Neutron Ejection Produced by Fast Neutrons

The disintegration of beryllium[1] and deuterium[2] by gamma-ray bombardment has been reported by Szilard and Chalmers and by Chadwick and Goldhaber. Bothe and Gentner[3] and Heyn[4] have more recently reported similar activation of heavier elements. Since the cyclotron yields intense gamma-radiation as well as fast neutrons this subject is investigated further. Deuterons of 6.3 Mev were allowed to fall on various targets and the radiation from these targets in turn made to activate other elements shielded completely from the deuteron beam. It was at once observed that these secondary targets were strongly activated in a quite different way than when activated directly by deuterons or by slow neutrons. Elements which in the usual way by neutron capture yield a certain number of radioactive isotopes as revealed by the half-life periods, now have one of the ordinary periods either completely lacking or suppressed. In addition there appears a new period which is radio-positive. This is as expected if, in this disintegration, neutrons are ejected from, rather than added to the nuclei by the exciting radiation. The question then arises whether the fast neutrons or the gamma-rays or both are the exciting agents.

To answer this question experiments of two types have been carried out. In one method the secondary target was placed 4.5 cm from the primary target and bricks of lead or paraffin could be interposed between the two and the change in activation of the secondary target observed. In another the activation of a given secondary target was observed as the primary target was changed so as to give neutrons and gamma-rays of different known energies. From both of these experiments the conclusion is that for the most part, if not completely, the activation of the secondary target is due to fast neutrons. Table I shows in resumé the results when secondary targets of nitrogen, oxygen, silver and copper are each used with primary targets of lithium, boron, beryllium and copper. Secondary oxygen targets of several forms were employed, namely as metallic oxides, ammonium nitrate and water. The energies of the neutrons emitted from lithium, boron and beryllium under deuteron bombardment have been measured and have values reaching up to 14, 13 and 4.6 Mev, respectively.[5] The energies of the neutrons from copper are not known. To these energy values must be added a large portion of the impinging 6.3 Mev deuteron energy.

The neutron radiation from the beryllium and copper primary targets appears to be inadequate to activate the 10 min. period of copper and the 26 min. period of silver, yet adequate to activate the oxygen period. This is perhaps surprising since from the energy balance an incident energy of about 15 Mev or more should be necessary.

TABLE I. *Relative activation (approximate I_0) of secondary targets under high energy neutron bombardment.*

Neutrons from	N^{13} 11 min.	O^{19} 2.1 min.	Ag^{108} 26 min.	Ag^{109} 2.3 min.	Cu^{62} 10 min.	Cu^{64} 12 hr.	Cu^{66} 5 min.
Li	100	60	100	50	100	6	0
B	27	15	42	43	73	4	0
Be	0	72	0	28	0	3	14
Cu	18	100	0	3	0	2	4

As is evident from the table high energy neutrons form Cu^{62} and Cu^{64} from the two stable Cu^{63} and Cu^{65} isotopes. For slow neutrons Cu^{64} and Cu^{66} are formed from the same two stable isotopes. A similar relation holds for the two stable Ag^{107} and Ag^{109} isotopes.

Investigation of other elements is being continued. Most all the elements, so far bombarded with these high energy neutrons, have yielded new or previously known artificial radioactive periods. Br, Sn, In, Zn and Cd have been found to be particularly easy to activate. For slow neutron bombardment, as was shown by Fermi, the bombarded nucleus most frequently increases in mass number by one. For high energy neutron bombardment the bombarded nucleus, in every case so far investigated, apparently decreases in mass number. It is therefore apparent that for elements with two or more isotopes the assignment of radioactive periods may now in many cases be made more easily and certain.

This work has been made possible by a grant from the Horace H. Rackham Fund.

M. L. POOL*
J. M. CORK
R. L. THORNTON

Department of Physics,
University of Michigan,
April 27, 1937.

[1] Szilard and Chalmers, Nature **134**, 494 (1934).
[2] J. Chadwick and M. Goldhaber, Proc. Roy. Soc. **A151**, 479 (1935).
[3] W. Bothe and W. Gentner, Naturwiss. **25**, 90 (1937); **25**, 191 (1937).
[4] F. A. Heyn, Physica **4**, 160 (1937).
[5] Bonner and Brubaker, Phys. Rev. **48**, 742 (1935); **50**, 308 (1936).
* Elizabeth Clay Howald Scholar.

Critical Frequencies of Low Ionosphere Layers*

The comparatively well-known layers of the ionosphere which have been studied by the pulse method lie between virtual heights of approximately 100 and 500 kilometers. Layers much below 100 kilometers have been reported by several observers[1-3] during the past two years. In all of these cases such high frequencies were used that the low layers were penetrated by the same emissions for which reflections are reported to have been obtained. Therefore these experimenters have not determined the critical frequencies or maximum ionization densities of the lower layers, and have offered no means of studying variations of these properties. It would seem that the low layer reflections reported may have been of the nature of "sporadic"[4] or partial reflections from a sharp boundary, but were certainly not total reflections such as are obtained from the normal E, F_1 and F_2 layers for frequencies below the critical frequencies. The mechanism producing the partial reflections can hardly be that envisaged by the Eccles-Larmor theory of refraction.

The critical frequency of at least one of these lower layers has been observed by us by the method of continuous automatic field intensity recording, and this layer has

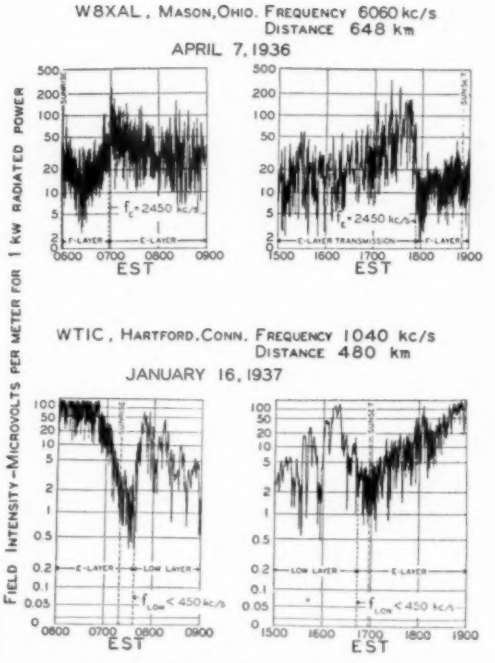

FIG. 1. Change of layer effect for high and low frequency transmission. (1) Upper record, E layer critical frequency = 6060 kc/s at time of change of layer. This corresponds to a normal incidence E layer critical frequency of 2450 kc/s. (2) Lower record, low layer critical frequency = 1040 kc/s at time of change of layer. This corresponds to a normal incidence low layer critical frequency of less than 450 kc/s.

been observed to provide regular radio transmission by the same refracting process as the well-known higher layers. This is in contrast to the behavior of the "nondeviating" low region postulated by other workers. The evidence we present is therefore the first proof of the existence of a truly refracting layer below the E layer.

Continuous records of high frequency field intensity, when compared with simultaneous ionosphere measurements, have demonstrated that the phenomenon of change of layer in the morning and afternoon can be recognized (see Fig. 1 top record). The lower record of Fig. 1 shows a similar effect in the broadcast frequency band. A comparison of the broadcast records with regular ionosphere measurements has shown that this effect cannot be a change between F and E layer transmission but must be a change between the E layer and a lower layer. Therefore this phenomenon marks a critical frequency of a low layer of low maximum ionization density. This critical frequency, for the distance given, is 1040 kc/s at the time of the change of layer; this corresponds to a normal incidence critical frequency of less than 450 kc/s and an equivalent electron density of less than 2.5×10^3 per cm^3. Critical frequencies and equivalent electron densities of these low layers have not previously been reported.

With the method of field intensity recording it is possible to determine virtual heights and normal incidence critical frequencies of this or other low layers by simultaneous measurements at different frequencies and distances. Automatic field intensity recording thus avoids some of the difficulties encountered in the application of the usual group velocity methods of ionosphere measurements to the determination of the critical frequencies and other properties of these low layers of low ionization density. It is therefore suggested as an effective method for such determinations.

N. SMITH
S. S. KIRBY

National Bureau of Standards,
Washington, D. C.,
March 16, 1937.

* Publication approved by the Director of the National Bureau of Standards of the U. S. Department of Commerce.

[1] S. K. Mitra and P. Syam, Nature **135**, 953 (1935).
[2] R. C. Colwell and A. W. Friend, Nature **137**, 782 (1936).
[3] R. A. Watson Watt, L. K. Bainbridge Bell, A. F. Wilkins and E. G. Bown, Nature **137**, 866 (1936).
[4] S. S. Kirby and E. B. Judson, Nat. Bur. Stand. J. Research **14**, 469 (1935); Proc. I. R. E. **23**, 733 (1935).

892